İSTANBUL TECHNICAL UNIVERSITY ★ INSTITUTE OF SCIENCE AND TECHNOLOGY

THE CONCEPT AND THE MODELING OF SUBSTRATE STORAGE IN THE BIODEGRADATION OF TANNERY WASTEWATER

Ph.D.Thesis by
Gülseda DİZDAROĞLU RİŞVANOĞLU, M.Sc.
(501942013)

Date of submission : 23 September 2002
Date of defence examination: 03 March 2003

Supervisor (Chairman): **Prof.Dr. Derin ORHON**

Members of the Examining Committee
Prof.Dr. İzzet Öztürk (İTÜ)
Prof.Dr. Seval SÖZEN (İTÜ)
Prof.Dr. Orhan YENİGÜN (BÜ)
Assoc. Prof.Dr. Beyza ÜSTÜN (YTÜ)

MARCH 2003

PREFACE

I would like to express my profound thanks and gratitude to Prof. Dr. Derin ORHON, who has in the first place, granted me the honor by accepting me as Ph.D. student under his supervision. Furthermore, I am pleased to express that I am extremely indebted to him for his enormous support, patience, encouragement, inspiring comments, recommendations, and his magnificent supervision.

I would like to extend my genuine gratitude to Prof. Dr. Mark C. M. van LOOSDRECHT, who has granted me the honor to study under his supervision in Delft University of Technology by paying particular personal attention to my thesis. I am deeply grateful for his invaluable support, inspiring remarks and recommendations, and exceptional supervision, anytime under all conditions.

My sincere gratitude to Prof. Dr. Öner HORTAÇSU for the initiation of this study with his gentle concern. I am particularly grateful to Prof. Dr. İlhan TALINLI for his invaluable support and generous interest during all phases of my study. I would like to express my sincere thanks to Prof. Dr. Cumali KINACI for his valuable support with kind concern.

I would like to acknowledge everybody in Kluyver Labotatory for Biotechnology at Delft University of Technology.

I am greatly indebted to dearest exceptional friend and colleague in true sense of the word bright young scientist Özlem KARAHAN, for her remarkable support, utmost help and friendship during the completion of this study. I will always remember the wonderful times we shared in T.U. Delft and I.T.U. My particular thanks to dear Devrim DEMİRAY, who has so patiently assisted me to type the thesis in extreme efficiency and perfection.

I am eternally grateful to my dearest friends Magda J. van der WIEL-WOLTING, and Cees H. van der WIEL and my remarkable lawyer Jos J. P. M. BENDERS for their genuine friendship, generous interest, invaluable help and support which enabled me to complete this study during the most difficult times of my life. I am greatly thankful to Dr. Bülent ERDOĞAN for his valuable medical treatment.

This study is dedicated to my dear mother Süheyla DİZDAROĞLU, my dear father Dr. Vahap DİZDAROĞLU and my dear brother Mehmet S. DİZDAROĞLU who have not spared their ultimate support and encouragement with fabulous love during all phases of my life. I would like to extend the dedication of this study to my beloved son Mehmet Tufan and my beloved daughter Nurseda.

September, 2003 Gülseda DİZDAROĞLU

CONTENTS iii

LIST OF TABLES

LIST OF FIGURES

LIST OF SYMBOLS

b_A : Endogenous Decay Rate for Autotrophic Biomass [1/T]
b_H : Endogenous Decay Rate for Heterotrophic Biomass [1/T]
b_H' : Rate of Viability Loss for Heterotrophic Biomass [1/T]
b_{STO} : Endogenous Decay Rate for Stored Polymer [1/T]
C : Concentration [M COD/L^3]
C_I : Initial Total Inert COD Concentration [M COD/L^3]
C_S : Initial Total Biodegradable COD Concentration [M COD/L^3]
C_T : Initial Total COD Concentration [M COD/L^3]
$(C_T)_1$: Final Total COD Concentration of Raw Wastewater Reactor [M COD/L^3]
$(C_T)_2$: Final Total COD Concentration of Filtered Wastewater Reactor [M COD/L^3]
f_a : Activity Coefficient for Active Biomass
f_E : The Fraction of Total Inert COD Generated in Biomass Decay
f_{ES} : The Fraction of Soluble Inert COD Generated in Biomass Decay
f_{EX} : The Fraction of Particulate Inert COD Generated in Biomass Decay
f_I : The Particulate Inert Fraction of COD Generated in Biomass Decay
f_P : The Particulate Inert Fraction of COD Generated in Biomass Decay
f_{PS} : Inert Fraction of the Endogenous Soluble Matter
f_{PX} : Inert Fraction of the Endogenous Particulate Matter
f_{SI} : The Inert Fraction of COD Generated in Biomass Hydrolysis
f_{SS} : Readily Biodegradable Fraction of Total Influent COD
$i_{N,SI}$: N content of S_I [M N/M TOC_{SI}]
$i_{N,SS}$: N content of S_S [M N/M TOC_{SS}]
$i_{N,XI}$: N content of X_I [M N/M TOC_{XI}]
$i_{N,XS}$: N content of X_S [M N/M TOC_{XS}]
$i_{N,BM}$: N content of biomass, X_H, X_A [M N/M TOC_{XBM}]
$i_{SS,XI}$: SS to TOC ratio for X_I [M SS/M TOC_{XI}]
$i_{SS,XS}$: SS to TOC ratio for X_S [M SS/M TOC_{XS}]
$i_{SS,BM}$: SS to TOC ratio for biomass, X_H, X_A [M SS/M TOC_{XBM}]
K_C : Equilibrium Constant
k : Reaction Rate Coefficient
k_d : Decay Coefficient [1/T]
k_h : Maximum Specific Hydrolysis Rate Coefficient of First Degree [M COD/M Cell COD.T]
K_h : Maximum Specific Hydrolysis Rate Coefficient of First Degree [M COD/M Cell COD.T]
k_H : Maximum Specific Hydrolysis Rate Coefficient for Slowly Hydrolyzable COD [M COD/M Cell COD.T]
k_{HS} : Maximum Specific Hydrolysis Rate Coefficient for Rapidly Hydrolyzable COD [M COD/M Cell COD.T]

k_{hx} : Maximum Specific Hydrolysis Rate Coefficient for Slowly Hydrolyzable COD [M COD/M Cell COD.T]

K_{NH} : Half Saturation Constant for Ammonia [M/L^3]

K_{NO} : Half Saturation Constant for Nitrate [M/L^3]

$K_{O,A}$: Half Saturation Constant for Oxygen Limitation of Autotrophic Biomass [M/L^3]

$K_{O,H}$: Half Saturation Constant for Oxygen Limitation of Heterotrophic Biomass [M/L^3]

K_S : Half Saturation Constant [M/L^3]

K_{STO} : Half Saturation Constant for Stored Polymer [M/L^3]

k_{STO} : Maximum Specific Rate of Storage [1/T]

k_{XSTO} : Maximum Specific Rate of Consumption of Stored Products [1/T]

K_X : Half Saturation Constant for the Hydrolysis Rate of Slowly Hydrolyzable COD [M COD/M Cell COD.T]

K_{XS} : Half Saturation Constant for the Hydrolysis Rate of Rapidly Hydrolyzable COD [M COD/M Cell COD.T]

K_{XX} : Half Saturation Constant for the Hydrolysis Rate of Slowly Hydrolyzable COD [M COD/M Cell COD.T]

OUR : Oxygen Utilization Rate [$M/L^3.T$]

Q : Flow Rate [L^3/T]

q : Specific Substrate Removal Rate [$M/L^3.T$]

q_S : Maximum Specific Substrate Uptake Rate [$M/L^3.T$]

r : Rate of reaction [$M/L^3.T$]

R : Conversion rate [$M/L^3.T$]

$r_{O,C}$: Rate of Consumption of Oxygen [$M/L^3.T$]

r_S : Substrate Uptake Rate [$M/L^3.T$]

$r_{S,C}$: Rate of Consumption of Readily Biodegradable COD [$M/L^3.T$]

$r_{S,P}$: Rate of Production of Readily Biodegradable COD by Hydrolysis [$M/L^3.T$]

r_{STO} : Storage Rate [$M/L^3.T$]

$r_{STO,C}$: Rate of Consumption of Stored Polymers [$M/L^3.T$]

$r_{STO,P}$: Rate of Production of Stored Polymers [$M/L^3.T$]

r_X : Growth Rate [$M/L^3.T$]

$r_{X,C}$: Rate of Consumption of Active Biomass [$M/L^3.T$]

$r_{X,P1}$: Rate of Production of Active Biomass over Substrate [$M/L^3.T$]

$r_{X,P2}$: Rate of Production of Active Biomass over Stored Polymers [$M/L^3.T$]

R_S : Substrate conversion rate [$M/L^3.T$]

R_{STO} : Storage Polymer conversion rate [$M/L^3.T$]

R_X : Biomass conversion rate [$M/L^3.T$]

R_{O2} : Oxygen conversion rate [$M/L^3.T$]

$R_{STO,P}$: Conversion rate for the Production of Storage Polymer [$M/L^3.T$]

$R_{STO,C}$: Conversion rate for the Consumption of Storage Polymer [$M/L^3.T$]

$R_{X,P1}$: Conversion rate for the Production of Active Biomass over Substrate [$M/L^3.T$]

$R_{X,P2}$: Conversion rate for the Production of Active Biomass over Stored Polymer [$M/L^3.T$]

S : Substrate Concentration [M COD/L^3]

S_{ALK} : Alkalinity Concentration [M/L^3]

S_{G1} : Initial COD Concentration of Glucose Reactor [M COD/L^3]

$(S_G)_1$: Final Soluble COD Concentration of Glucose Reactor [M COD/L^3]
S_H : Rapidly Hydrolyzable COD Concentration [M COD/L^3]
S_I : Soluble Inert COD Concentration [M COD/L^3]
S_{N2} : Dinitrogen Concentration [M/L^3]
S_{ND} : Entrapped Organics Concentration [M/L^3]
S_{NH} : Ammonium Nitrogen Concentration [M/L^3]
S_{NO} : Nitrate Concentration [M COD/L^3]
S_O : Dissolved Oxygen Concentration [M COD/L^3]
S_P : Soluble Inert Microbial Products Concentration [M COD/L^3]
$(S_P)_G$: Residual Soluble Microbial Products Generated in the Glucose Reactor [M COD/L^3]
$(S_P)_2$: Residual Soluble Microbial Products Generated in the Filtered Wastewater Reactor [M COD/L^3]
S_R : Total Residual COD Concentration [M COD/L^3]
S_S : Readily Biodegradable COD Concentration [M COD/L^3]
S_T : Initial Total Soluble COD Concentration [M COD/L^3]
$(S_T)_1$: Final Soluble COD Concentration of Raw Wastewater Reactor [M COD/L^3]
$(S_T)_2$: Final Soluble COD Concentration of Filtered Wastewater Reactor [M COD/L^3]
X : Biomass Concentration [M/L^3]
X_A : Active Autotrophic Biomass Concentration [M/L^3]
X_H : Active Heterotrophic Biomass Concentration [M/L^3]
X_I : Particulate Inert COD Concentration [M COD/L^3]
X_{ND} : Entrapped Organic Nitrogen Concentration [M/L^3]
X_P : Particulate Inert Microbial Products Concentration [M COD/L^3]
$(X_P)_1$: Residual Particulate Microbial Products Concentration Generated in the Raw Wastewater Reactor [M COD/L^3]
$(X_P)_2$: Residual Particulate Microbial Products Concentration Generated in the Filtered Wastewater Reactor [M COD/L^3]
X_S : Slowly Hydrolyzable COD [M COD/L^3]
X_{STO} : Storage Polymer COD Concentration [M COD/L^3]
X_{TS} : Total Particulate COD [M COD/L^3]
Y : Stoichiometric Coefficient [M COD/ M COD]
Y_H : Heterotrophic Yield Coefficient [M COD/ M COD]
$Y_{H,O2}$: Aerobic Heterotrophic Yield Coefficient [M COD/ M COD]
$Y_{H,NO}$: Anoxic Heterotrophic Yield Coefficient [M COD/ M COD]
Y_{H1} : Heterotrophic Yield Coefficient for Direct Growth [M COD/ M COD]
Y_{H2} : Heterotrophic Yield Coefficient for Growth on Stored Polymers [M COD/ M COD]
Y_{NH} : Net Yield Coefficient [M COD/ M COD]
Y_{SP} : Fraction of Biodegradable COD Converted into Soluble Inert Microbial Products [M COD/ M COD]
Y_{STO} : Storage Yield Coefficient [M COD/ M COD]
Y_{XP} : Fraction of Biodegradable COD Converted into Particulate Inert Microbial Products [M COD/ M COD]
α_D : Growth Associated Soluble Inert Product Formation Coefficient for the Endogenous Decay Model

α_R : Growth Associated Soluble Inert Product Formation Coefficient for the Death Regeneration Model

η_g : Anoxic Conversion Factor for Growth

η_h : Anoxic Conversion Factor for Hydrolysis

μ : Spesific Growth Rate [1/T]

$\hat{\mu}$: Maximum Spesific Growth Rate [1/T]

$\hat{\mu}_H$: Maximum Spesific Growth Rate for Heterotrophs [1/T]

$\hat{\mu}_{H1}$: Maximum Spesific Growth Rate for Direct Growth [1/T]

$\hat{\mu}_{H2}$: Maximum Spesific Growth Rate Growth on Stored Polymers [1/T]

ρ : Process Rate

θ_X : Sludge Age [T]

DERİ ATIKSUYUNUN BAKTERİLERLE AYRIŞMASINDA SUBSTRAT DEPOLAMA KAVRAMI VE MODELLEMESİ

ÖZET

Aktif çamur proseslerin simulasyonu için, IAWQ Çalışma Grubu, Activated Sludge Model No.1 (ASM1) modelini (Henze ve diğ., 1987) oluşturmuştur. ASM1 modeli, aktif çamur sistemlerinde organik madde giderimi, biyolojik nitrifikasyon ve denitrifikasyon proseslerine ait tasarım ve simulasyonlarının yapılmasını sağlamaktadır. Daha sonra, ASM1 modeli biyolojik fosfor giderimini de içerecek şekilde değiştirilerek ASM2 ve ASM2d modelleri geliştirilmiştir (Henze ve diğ., 1995; 1999). IAWQ Çalışma Grubu tarafından önerilen en son model olan ASM3 (Gujer ve diğ., 2000), ASM1'den farklı olarak kolay ayrışan substratın (S_S) depolama ürünlerine (X_{STO}) dönüştükten sonra heterotrofik biyokütle (X_H) tarafından tüketildiğini varsayan depolama kavramını esas almaktadır. Ancak bu varsayım gerçeği tam olarak yansıtmamaktadır. Daha gerçekçi bir yaklaşım, van Aalst (1997) tarafından ele alınmıştır; bu yaklaşıma göre S_S'in bir kısmı direkt olarak X_H tarafından tüketilirken, geri kalan kısım öncelikle depolama polimerlerine dönüşerek X_H tarafından tüketilmeye hazır hale gelmektedir. Bu yaklaşım, metabolik yolizi (metabolic pathways) terminolojisini kullandığı için literatürde metabolik modelleme olarak adlandırılmaktadır, ancak bu çalışmada sisteme giren substrat ve depolanan polimer üzerinden simultane çoğalma ve depolama olarak isimlendirilmiştir. Diğer önemli nokta ise kolay ayrışan (S_S) ve yavaş ayrışan (X_S) KOİ bileşenlerinin ASM3'teki tanımlarının farklı olmasıdır; ASM3 modelinde 0.45 μm gözenek çaplı membran filtre kullanılarak yapılan süzme işleminden sonra sadece filtre üzerinde kalan fraksiyonun yavaş ayrışan KOİ (X_S) olduğu, süzüntüdeki ayrışabilir fraksiyonunun ise (S_S) olduğu kabulü yapılmıştır.

Bu çalışmanın amacı, deri atıksuyu için farklı aktif çamur modellerinin incelenmesidir. Çalışma kapsamında deri atıksuyu için ASM1, ASM3 ve simultane çoğalma ve depolama modelleri kıyaslanmıştır. Literatürde, özellikle ASM3'ün deneysel değerlendirmesi ve ASM3 modifikasyonları ile ilgili çok az araştırma mevcuttur. Mevcut deneysel çalışmalar asetat, glikoz ve evsel atıksular ile yapılmıştır. Bu çalışmada çok karmaşık bir atıksu olan deri atıksuyunda depolama kavramının etkisi irdelenmiştir. Modelleme çalışmalarında kullanılmak üzere ham ve süzülmüş atıksu için üretilen deneysel veriler değerlendirilmiştir.

Simulasyonlar ASM1, ASM3 ve simultane çoğalma ve depolama modelinin üç farklı alternatifi olan; a) substrat alım hızının (r_S) ve depolama hızının (r_{STO}) belirlenerek, çoğalma hızının (r_X) hesaplandığı, b) r_X ve r_{STO} hızlarının belirlenerek, r_S hızının hesaplandığı ve c) r_S ve r_X hızlarının belirlenerek, r_{STO} hızının hesaplandığı, durumlar için yapılmıştır. Deri atıksuyuna uyarlanan matrisler hazırlanarak Aquasim bilgisayar programı ile simulasyon çalışmaları yapıldıktan sonra her model için elde edilen simulasyon sonuçları, deneysel verilerle kıyaslanmıştır.

Bu simulasyon çalışmalarının sonuçları, farklı aktif çamur modellerinin kavramsal değerlendirmesine örnek olarak ve deri atıksuyuna uyarlanabilecek bütünsel ve bölümsel (structured and unstructured) modellerin kinetik ve stokiyometrik katsayıları için veri tabanı oluşturulmasına hizmet etmek amacıyla sunulmuştur. Değerlendirilen veriler gelecekteki deneysel çalışmalara ve modelleme uygulamalarına esas teşkil edecek niteliktedir.

Aktif çamur sistemleri için çeşitli model yapıları önerilmişse de, bu modellerin endüstriyel atıksular için kalibrasyonu hala irdelenmemiş bir konu olarak durmaktadır. Bu çalışmada, deri atıksuyu için ASM1 ve ASM3 modelleri kullanılarak yapılan simulasyon uygulamaları ve modelleme sonuçları kıyaslanarak değerlendirilmiştir. Bunlara dışında ASM3 modeli, simultane çoğalma ve depolama kavramına uyarlanarak deri atıksuyuna uygulanacak hale getirilmiştir. Literatürde, simultane çoğalma ve depolama yaklaşımının ele alındığı çalışmalar asetat ve glikoz için yapılmıştır. Yukarıda sözü edilen bölümsel modellerin deri atıksuyuna uygulandığı modelleme çalışmaları literatürde yer almamaktadır. Bundan dolayı bu çalışmada deri atıksuyu için elde edilen sonuçların karşılaştırmalı olarak değerlendirmesi yapılmış ve farklı bölümsel modellerin endüstriyel atıksulara uygulanabilmesi için gerekli olan kavramsal yaklaşımlar irdelenmiştir.

Bu çalışmada elde edilip literatür ile kıyaslanarak değerlendirilen modelleme sonuçları, her bir spesifik atıksu için model parametrelerinin doğru belirlenmesine duyulan gereksinimi vurgulamaktadır. Yürütülen simulasyon çalışmalarında, deri atıksuyu için literatürde verilen değerler kullanılmıştır. Bu kapsamda, tüm model simulasyonları deney başlangıç koşulları olarak, aynı içsel solunum hızı ve aktif biyokütle konsantrasyonları esas alınarak gerçekleştirilmiştir.

Başlangıç atıksu KOİ fraksiyonları ASM1 ve ASM3 modellerindeki tanımlar esas alınarak hesaplandığında ASM1 modeli simulasyon sonuçlarının literatürde verilen değerler ile uyumlu olduğu görülmüştür. ASM3 model sonuçlarının ASM1 sonuçları ile karşılaştırıldığında, dinamik şartlar altındaki oksijen tüketim hızı (OTH) tepkisini daha iyi tanımladığı saptanmıştır. Bu sonuç, atıksuyun yüksek uçucu yağ asitleri (UYA) içeriği ve kesikli deneylerdeki dinamik koşullar ile uyumludur.

ASM3 simulasyon sonuçları literatür verileri ile karşılaştırıldığında, deri atıksuyu proses hızlarının, biyolojik olarak daha kolay ayrışabilen farklı substratlar için rapor edilen değerlerden daha düşük olduğu görülmektedir. Bu durum, ele alınan mikroorganizma topluluğunun kompozisyonundaki muhtemel farklılıkların sonucu olarak yorumlanabilir.

Bu çalışmada, IAWQ Çalışma Grubu tarafından önerilen ASM1 ve ASM3 modellerinin deri atıksuyuna uyarlanması ve dinamik şartlar altında gözlenen simultane çoğalma ve depolama modeli uygulamaları incelenmiştir.

İncelenen beş farklı modelin sonuçları karşılaştırıldığında, gerçek durumu daha iyi tanımlayan modellerin daha detaylı modeller olduğu sonucuna varılmaktadır. Sonuçlar hidroliz prosesinin kesikli deneylerde düşük F/M oranlarında daha az etkin olduğunu, ancak yüksek F/M oranlarındaki model kalibrasyonlarının, S_S tanımının çok doğru olmadığını vurguladığını göstermiştir. Bunlara ek olarak sonuçlar, yavaş ayrışan substratın çözünmüş fraksiyonunun ihmal edilmesi durumunun, depolama polimerleri üzerindeki çoğalma tepkisinin birinci derece reaksiyon kinetiği üzerinden tanımlanması ile telafi edilebildiğini göstermektedir.

Dinamik koşullar altında, deri endüstrisi atıksuları için elde edilen OTH tepkilerinin en iyi bölümsel modeller ile ifade edildiği dikkat çekmektedir. Bununla birlikte, karmaşık substrat kompozisyonları söz konusu olduğunda, tüm depolama ürünlerinin deneysel olarak belirlenmesinin zorluğu ya da imkansızlığı nedeniyle, model katsayılarının doğru saptanması mümkün olamamaktadır. Bundan dolayı model parametrelerinin deneysel olarak belirlenmesi gerektiğinde, uyarlanan modellerden, substrat alım hızını ana proses olarak dikkate alan modelin (MODEL C), depolama ürünlerinin ölçümünü gerektirmemesi nedeniyle en uygun model olduğu sonucuna varılabilir.

Deri atıksularında bölümsel modellerin spesifik parametrelerinin belirlenebilmesi için daha fazla araştırma yapılması gereklidir. Kolay ayrışabilen substratın tanımlanması, halen daha fazla deneysel çalışma gerektiren bir konu olarak gündemdeki yerini korumaktadır. Giriş KOİ kompozisonundaki kolay ayrışabilen fraksiyonun tanımı son derece önemlidir ve bu tanımın seçimi endüstriyel atıksuların modelleme uygulamalarındaki amaç göz önünde tutularak dikkatle yapılmalıdır.

THE CONCEPT AND THE MODELING OF SUBSTRATE STORAGE IN THE BIODEGRADATION OF TANNERY WASTEWATER

SUMMARY

The IAWQ Task Group on mathematical modeling for design and operation of wastewater treatment processes introduced ASM1 for the simulation of activated sludge processes (Henze *et al.*, 1987). ASM1 allows organic matter removal and nitrification and denitrification simulations in activated sludge systems. Later, ASM1 was expanded and improved for the biological phosphorus removal to evaluate ASM2 and ASM2d (Henze *et al.*, 1995 and 1999). Recently IAWQ introduced ASM3 (Gujer *et al.*, 2000) which is different from ASM1 in many cases, i.e. ASM3 is based upon storage concept that assumes readily biodegradable substrate (S_S) is firstly converted to storage polymer (X_{STO}) and then used by heterotrophic biomass (X_H). This assumption is far away from reality. A much more realistic approach was studied by van Aalst-van Leeuwen *et al.* (1997): a part of S_S is directly used by the active biomass while the rest of it is firstly converted to storage polymers, then consumed by X_H. This approach is named as metabolic modeling in literature because of using metabolic pathways in terminology. However in this study it can be renamed as simultaneous growth and storage concept on external substrate and stored polymers. Another major difference is in the definition of S_S and slowly biodegradable substrate (X_S) components as in ASM3, X_S is assumed to be only the particular fraction and all of the filtrate (soluble fraction) is composed of S_S when 0.45 μm membrane filter is used.

The aim of this study is to investigate different activated sludge models for tannery wastewaters. ASM1, ASM3 and simultaneous growth and storage models were compared for tannery wastewater in this study. In literature, scarce information is available, especially on the basis of experimental evaluation for ASM3 and simulateneous growth and storage models. Very few experimental studies were carried out with acetate, glucose and domestic wastewater. In this study tannery wastewater was handled which is a very complicated type and since there is no experimental study on the effect of the storage phenomena for tannery wastewaters. Experimental data were evaluated for both raw and filtered wastewater in order to be used for modeling studies.

The simulations were performed for ASM1, ASM3 and three different alternatives of simultaneous growth and storage models: a) firstly fixing substrate uptake rate (r_S) and storage rate (r_{STO}) for calculating the growth rate (r_X); b) secondly fixing r_X and r_{STO}, calculating r_S; and c) lastly fixing r_S and r_X in order to calculate r_{STO}. For tannery wastewater relevant matrices were prepared and loaded into Aquasim. The obtained simulation results for each of the models were compared with experimental data.

These simulation studies present an example for the conceptual evaluation of different activated sludge models and serve as data base for kinetic and

stoichiometric coefficients of unstructured and structured models for tannery wastewater. Evaluated data can be used as default values in further experiments and simulations.

In spite of a variety of model structures proposed for activated sludge systems, calibration of these models for industrial wastewaters still stands untouched. In this study, application and comparison of modeling studies using ASM1 and ASM3 for tannery wastewater. Additionally, ASM3 was extended and adapted for tannery effluent according to the simultaneous growth and storage concept. In literature, simultaneous growth and storage models were applied for acetate and glucose. There is no available research for the application of above-mentioned structured models for tannery wastewater. Therefore, comparison and evaluation of the results obtained for tannery wastewater in this study presents a conceptual framework for the application of different structured models for industrial wastewaters.

The modeling results obtained in this study, in comparison with literature, highlight the need for reliable estimation of model parameters with respect to each specific wastewater of concern. Model simulations conducted in this study were based on previous literature data obtained for tannery effluents. In this context, all the model simulations were based on the same endogenous decay rate and active heterotrophic biomass concentrations as one of the initial experimental conditions. The initial wastewater COD fractions were calculated based on the definitions in ASM1 and ASM3. Model simulation results for ASM1 were quite consistent with those given in literature.

ASM3 modeling results yielded a better description of the dynamic OUR response compared to ASM1. This result is obviously a consequence of the high amount of VFA content and prevailing transient conditions in batch experiments. When ASM3 simulation results are compared with the set of model coefficients reported in literature, it can be stated that lower process rates are estimated for tannery wastewaters, than those reported for different substrates, which are more biodegradable than tannery effluent. This result is interpreted as a consequence of the possible differences in the composition of studied microbial communities.

In addition to IAWQ Task Group Models ASM1 and ASM3 modified versions of ASM3 involving simultaneous growth and storage under dynamic conditions have also been investigated in the scope of this study.

When the simulation results of five different models are compared, it can be concluded that the possibility of describing the real case increases as the model gets more detailed. The results have shown that the hydrolysis process is less effective when batch tests with low F/M ratios are concerned but the calibration studies at high F/M ratios clearly emphasize the challenge in the definition of readily biodegradable COD. The results also point out that, the neglected OUR response due to the hydrolysis of soluble slowly biodegradable substrate can be compensated when first order kinetics is chosen to describe the growth response on storage polymers.

Although structured models can generally be regarded as the best interpretation to describe the dynamic behavior observed for tannery effluents, the insufficiency experienced in the experimental determination of all the storage products when complex substrate compositions are concerned, hinders the correct determination of model coefficients. Thus, when the case of experimental determination of model parameters are concerned the adapted model considering substrate uptake could be

used more effectively since this model does not need the measurement of storage polymers.

Further research should be conducted on the assessment of specific parameters of structured models for industrial wastewaters. The description of readily biodegradable substrate still needs additional experimental studies and the choice of definition on the readily biodegradable fraction of influent COD should be dealt with significant care and this choice should be made meticulously depending on the purpose of modeling application for industrial wastewaters.

SECTION 1 INTRODUCTION

1.1 Relevance of the Subject

In order to understand the mechanistical behaviour of the processes in activated sludge systems, different hypothesis have been postulated. The validity of the hypothesis can be tested experimentally and/or via computer modeling, design and simulation. Measured environmental data (i.e. collective parameters: OUR, COD, *etc.*) mostly can not be directly used to evaluate the postulated hypothesis.

Utilizing the advantage of contemporary computer programs, i.e., computer modeling for design and simulation of the system, the evaluation of the hypothesis will be faster. Different mathematical can be applied into computer programming and various hypothesis can be verified. This procedure leads to the determination of the model(s) that give the best fit (result) for relevant experimental data. The flexibility of mathematical modeling gives the possibility to expand the model for different types of wastewater especially for complex wastewater compositions such as industrial wastewaters like tannery effluents. Industrial wastewaters,with variable characteristics, can have quite different kinetic and stoichiometric coefficients and rate expressions.

The importance of storage concept in activated sludge systems has been emphasized in recent modeling approaches. In activated sludge modeling, storage polymers have been neglected, without considering that they might have a significant role. The significance of the storage polymers have been reported and this study also highlights the role of storage for the biological treatment of tannery wastewaters.

1.2 Aim and Scope of the Study

The aim of this study is to investigate different activated sludge models for tannery wastewaters. ASM1, ASM3 and simultaneous growth and storage models were compared for tannery wastewater in this study. In literature, scarce information is available, especially on the basis of experimental evaluation for ASM3 and

simulateneous growth and storage models. A very few experimental studies were carried out with acetate, glucose and domestic wastewater. Tannery wastewater was handled which is a very complicated type and since there is no experimental study on the effect of the storage phenomena for tannery wastewaters. Experimental data were evaluated for both raw and filtered wastewater in order to be used for modeling studies.

The simulations were performed for ASM1, ASM3 and three different alternatives of simultaneous growth and storage models: firstly fixing substrate uptake rate (r_S) and storage rate (r_{STO}) for calculating the growth rate (r_X); secondly fixing r_X and r_{STO}, calculating r_S; and lastly fixing r_S and r_X in order to calculate r_{STO}. For tannery wastewater relevant matrices were prepared and loaded into Aquasim. The obtained simulation results for each of the models were compared with experimental data.

These simulation studies present an example for the conceptual evaluation of different activated sludge models and serve as data base for kinetic and stoichiometric coefficients of unstructured and structured models for tannery wastewater. Evaluated data can be used as default values in further experiments and simulations.

SECTION 2 ACTIVATED SLUDGE MODELING

2.1 Biological Processes

The objectives of the biological treatment of wastewater are to coagulate and remove the nonsettleable colloidal solids and to stabilize the organic matter. For domestic wastewater, the major objective is to reduce the organic content and also the nutrients such as nitrogen and phosphorus. For all kinds of industrial wastewaters, the objective is to remove or reduce the concentration of organic and inorganic compounds. As a summary, almost all wastewaters can be treated biologically with proper analysis and environmental control. The removal of organic matter is achieved biologically using a variety of microorganisms, principally bacteria.

2.2 Basic Concepts In Activated Sludge Modeling

Activated sludge models provide a reliable basis for the design and operation of activated sludge systems. The aim is to identify a rational mechanistic description of the process in order to define and predict system performance. These models offer the basic relationships between process components, kinetics, stoichiometric characteristics and basic system parameters.

2.2.1 Wastewater Characterization

Wastewaters contain a great variety of organics, which cannot be uniquely identified by simple techniques. For this reason, collective substrate parameters like biochemical oxygen demand (BOD_5), chemical oxygen demand (COD) and total organic carbon (TOC) are traditionally used for the characterization of organic content. TOC represents the total organic carbon in wastewaters but it has to be used carefully since the oxidation level of not all the carbon molecules is the same in different organic compounds. BOD_5 is still used in some cases but it is inadequate for proper characterization of the wastewater and can hardly serve as a model parameter in the reactor kinetics of activated sludge systems. The problem of using the BOD_5

parameter is that, it does not fit with the mass balance concept; in other words, BOD_5 values measured in different points and conditions cannot be used directly in modelling in mass balances for electron equivalence (Orhon and Artan, 1994).

COD parameter reflects only the degree of oxidation and can be used as the stoichiometric equivalent of organic substrate in biochemical reactions. However, COD parameter measures the non-biodegradable (inert) portion of the organic matter together with the biodegradable part. This interference is largely overcome by the help of new respirometric techniques (Orhon and Ubay Çokgör, 1997).

2.2.1.1 Multicomponent Approach in Wastewater Characterization

The classical activated sludge modeling approach is limited using only one substrate and biomass component for modeling. Since new concepts have been developed, this approach is no more useful. The introduction of multicomponent approach has presented new dimensions and should be used for proper understanding of wastewater characterization and activated sludge processes.

COD parameter contains different forms of organic carbon that needs to be classified carefully with respect to its biodegradability characteristics. Total influent COD (C_{T0}), is divided into two fractions as; total biodegradable COD (C_{S0}) and total inert COD (C_{I0}). Total inert COD has also two components as soluble inert COD (S_{I0}) and particulate inert COD (X_{I0}). Influent soluble inert COD concentration does not go through biochemical reactions in the reactor and leaves the system unchanged while particulate inert COD accumulates within the sludge and leaves the system with excess sludge.

According to the model proposed by Dold and Marais (1986) total biodegradable COD (C_{S0}), can be defined in two major fractions as readily biodegradable COD (S_{S0}) and slowly biodegradable or hydrolyzable COD (X_{S0}). Both of the fractions contain many compounds of different biodegradation rates (Dold *et al.*, 1980). The readily biodegradable COD can be directly absorbed for synthesis but the slowly biodegradable portion cannot pass through the cell wall and needs to undergo hydrolysis before absorption. The hydrolysis of slowly biodegradable COD component is the limiting step for the rate of utilization of the slowly biodegradable organic matter. It is also difficult to characterize this fraction by a single hydrolysis rate, since a significant variation of compounds in the wastewater is present.

Therefore, this hydrolyzable group may be divided into further fractions as rapidly hydrolyzable COD (S_{H0}) and slowly hydrolyzable COD (X_{S0}) (Henze, 1992).

2.2.1.2 Multicomponent Approach in Effluent Characterization

The process effluent has a different COD structure than the wastewater. The soluble COD (S_T), includes the nonbiodegradable organics originating from the wastewater and leaving the reactor unchanged (S_I), a small portion of the biodegradable COD remaining after biological oxidation and soluble inert COD generated as metabolic products (S_P). Consequently, the effluent stream generally contains more soluble inert COD than the wastewater because the entire residual COD of effluent (S_R), includes both the unchanged influent soluble inert COD and soluble inert microbial products.

Similarly the particulate COD in the effluent stream has four fractions. The major component is the active biomass (X_H) that is sustained in the reactor using the biodegradable COD as the energy and carbon source. The other component is a small fraction of the particulate slowly hydrolyzable organics (X_S), remaining after hydrolysis and subsequent utilization. The effluent also contains particulate inert COD of wastewater origin (X_I), that is entrapped in the biomass while accumulating in the reactor and particulate inert organic products (X_P), generating as a result of microbial metabolic activity during the endogenous decay or the death-regeneration phase, depending on the model adopted.

2.2.2 Process Stoichiometry of Aerobic Activated Sludge Systems

In activated sludge systems removal of substrate is accomplished by the generation biomass and the consumption of dissolved oxygen. For the stability of treatment, generated biomass must be withdrawn from the system as excess sludge. The calculation of excess sludge and estimation of the amount of oxygen utilization is equally important as substrate removal. The concept of yield is one of the major modeling tools used for the correct assessment of excess biomass generation and oxygen utilization in relation to substrate removal. It defines the amount of biomass formed per unit amount of organic matter removed in aerobic systems.

The yield concept is used as two different coefficients in process modeling and design: net yield (Y_{NH}) and true yield (Y_H). True yield relates only to the growth

mechanism. But the generated biomass is always lower than the given value by true yield. This is known as net yield, which can be expressed as the combined effect of growth and endogenous decay. The value of the yield coefficient depends upon parameters, such as COD, BOD_5, VSS or TOC, selected to define substrate and biomass (Orhon, 1999). The true yield can be expressed in terms of COD as follows:

$$Y_H = \frac{\text{COD of generated biomass}}{\text{COD of removed substrate}} \qquad (2.1)$$

The net yield can be calculated by the help of true yield and is defined as a variable function of sludge age. The net yield, Y_{NH}, is decreased and oxygen utilization is increased as sludge age increases (Orhon, 1999).

2.2.3. Process Kinetics of Aerobic Activated Sludge Systems

There are two main processes as microbial growth and microbial decay in activated sludge systems.

2.2.3.1. Microbial Growth

In the activated sludge process, a microorganism culture grows in a wastewater including both organic and inorganic substrates. In this case an empirical deduction from pure culture studies gives the appropriate growth rate for microbial growth, known as Monod expression. μ is specific growth rate, $\hat{\mu}$ is maximum specific growth rate, S is the growth limiting substrate concentration and K_S is half saturation constant in this equation:

$$\mu = \hat{\mu}\frac{S}{K_S + S} \qquad (2.2)$$

Monod expression states that small half saturation constants increases the sensitivity of specific growth rate for the changes observed in lower levels of substrate concentrations. High half saturation coefficients result in high growth rates independent from the substrate concentration.

Microbial growth is commonly defined by means of a differential equation where X is the biomass concentration and μ is the specific growth rate:

$$\frac{dX}{dt} = \mu X \tag{2.3}$$

Equations (2.2) and (2.3) are combined and expression (2.4) is obtained for biomass growth.

$$\frac{dX}{dt} = \hat{\mu}\frac{S}{K_S + S}X \tag{2.4}$$

The growth expression, when combined with the equation defining the yield relationship between bacterial growth and substrate removal equation (2.5) is formed defining the correlation between the amount of biomass generated and the amount of substrate consumed:

$$\frac{dX}{dt} = -Y\frac{dS}{dt} \tag{2.5}$$

The specific substrate removal rate, q, is related to substrate removal with the following equation:

$$-\frac{dS}{dt} = qX \tag{2.6}$$

The specific substrate removal rate, q, may also be expressed in terms of the specific growth rate and yield coefficient:

$$q = \frac{\mu}{Y} \tag{2.7}$$

Expression (2.8) is formed by combining (2.6) and (2.7).

$$-\frac{dS}{dt} = \frac{\mu}{Y}X \tag{2.8}$$

Microbial growth expression (2.9) can be written as follows by the combination of (2.2) and (2.8):

$$-\frac{dS}{dt} = \frac{\hat{\mu}}{Y}\frac{S}{K_S + S}X \tag{2.9}$$

Collective analytical parameters such as BOD_5 and COD are generally used to reflect the total organics in wastewaters, do not correspond to the real system variable, i.e. the growth limiting substrate. COD is estimated to be a more useful parameter but it cannot identify the growth limiting components directly related to the corresponding process rate expressions, especially in complex media. In new models, slowly biodegradable particulate matter is advocated as the major rate limiting process component in microbial heterotrophic growth and this growth is controlled alone by the readily biodegradable substrate, which is either present in the wastewater, or generated through the hydrolysis of slowly biodegradable organic matter. The initial readily biodegradable COD, S_S, is a relatively small fraction of the total COD content of wastewaters, therefore biological treatment systems are not controlled by the depletion of the readily biodegradable organics, but by hydrolysis of slowly biodegradable organics, a much slower process compared with heterotrophic growth (Orhon and Ubay Çokgör, 1997).

2.2.3.2 Microbial Decay

The process of microbial decay is used to define the loss of biomass. The basic mechanism explaining microbial decay is the degradation of biomass for the generation of maintenance energy. Accurate description of the decay process is restricted by the limitations of the traditional VSS (volatile suspended solids) parameter used to define the concentration of microorganisms in the mixed liquor. It cannot differentiate a series of other mechanisms responsible for the loss of biomass, such as microbial death, cell lysis and interactions between predators and bacteria (Orhon and Artan, 1994). Microbial decay is defined by a first order rate expression with respect to the biomass concentration:

$$-\frac{dX}{dt} = k_d.X \qquad (2.10)$$

where, k_d is the decay coefficient of biomass. There are three different modeling approaches are present with regard to microbial decay:

- traditional model
- death regeneration model
- endogenous decay model

2.3 Different Approaches In Activated Sludge Modeling

2.3.1 Traditional Modeling

The traditional model focuses on defining carbon removal in activated sludge systems. Thus, reaction kinetics is evaluated by means of a two-component system. Overall substrate parameter, S, reflects all biodegradable organic compounds in terms of BOD_5 or COD parameters and overall biomass parameter, X, covers all the fractions that may be measured in the form of VSS or cell COD. This classical approach, although useful especially for conventional activated sludge practice for carbon removal, has two main inadequacies for a more fundamental understanding and interpretation of the process. Firstly, there are only two components aside from dissolved oxygen, as told above. Difficulties associated with the correct assessment of organic substrate and biomass causes much confusion in modeling. The collective analytical parameters (VSS, COD, BOD_5) do not correspond to real system variables like biomass and growth limiting substrate. Secondly, the two traditional processes of growth and endogenous decay do not provide a complete description of the complex relationships and conversions among real process components. This concept states that the rate limiting substrate concentration in the effluent of an activated sludge reactor is independent of the influent concentration. It is necessary that additional process components are evaluated for a more accurate modeling approach.

2.3.2 Death Regeneration Model

In this model it is accepted that, death or loss of viability of microorganisms occur without the utilization of any electron acceptor. Also no loss of COD is involved while decay acts to convert biomass to a combination of particulate products and slowly biodegradable substrate. A major part of the decaying biomass is converted into slowly biodegradable substrate (X_S), and a small portion is associated with the formation of inert endogenous mass (X_P). The slowly biodegradable substrate formed, is then hydrolyzed, releasing an equivalent amount of readily biodegradable COD (S_S), and passes through the same growth cycle as its counterpart in the influent. The only step using an electron acceptor is the consumption of regenerated S_S. No oxygen is consumed in the death phase directly, but there is an indirect consumption of oxygen by the end product of decay, S_S (Henze *et al.*, 1987).

Death or loss of viability of the biomass can be shown by the following equation where b_H' is the rate of viability loss for heterotrophic biomass.

$$-\frac{dX_H}{dt} = b_H' X_H \tag{2.11}$$

Most of the nonviable biomass becomes available as slowly biodegradable substrate:

$$\frac{dX_S}{dt} = (1-f_{PX}) b_H' X_H \tag{2.12}$$

A little part of this nonviable portion remains as inert endogenous mass, X_P:

$$\frac{dX_P}{dt} = f_{PX} b_H' X_H \tag{2.13}$$

The term f_{PX}, in these expressions symbolizes the inert fraction of the endogenous particulate matter.

In the death regeneration model, S_S, is included in the wastewater but also generated by hydrolysis of slowly biodegradable organic matter:

$$\frac{dS_S}{dt} = -\frac{\hat{\mu}}{Y_H}\frac{S_S}{K_S + S_S} X_H + K_h X_S \tag{2.14}$$

Soluble inert microbial product formation has two steps reflecting both the growth associated product generation and decay associated mechanism as shown in equation (2.15).

$$\frac{dS_P}{dt} = \alpha_R \hat{\mu}_H \frac{S_S}{K_S + S_S} X_H + f_{PS} K_h X_S \tag{2.15}$$

α_R is growth associated soluble inert product formation coefficient for the death regeneration model and f_{PS} is the fraction of endogenous particulate matter converted into soluble microbial products.

There are some inadequacies in death-regeneration model like that it cannot differentiate between particulate slowly biodegradable substrate of influent origin

and its counterpart generated as a part of nonviable biomass. The model based upon the death regeneration concept is illustrated in Table 2.1.

2.3.3. Endogenous Decay Model

Endogenous decay model has at least seven or eight components aside from dissolved oxygen. In this model, only readily biodegradable substrate can be used directly by viable heterotrophic biomass; particulate slowly biodegradable substrate goes through hydrolysis first, and then becomes ready for direct use. Readily biodegradable substrate is converted into soluble inert microbial products (S_P) with soluble inert product formation coefficient (α_D). Similarly, a fraction (f_{ES}) of the endogenous biomass is not oxidized and converted into soluble inert products (S_P). The decay of active biomass is coupled with the generation of particulate inert organic products (X_P). During endogenous respiration, a fraction (f_{EX}) of the active biomass does not undergo any further reaction and accumulates in the activated sludge. This fraction is removed from the system by excess sludge.

Readily biodegradable substrate is only affected by the growth process and its utilization rate is directly related to the growth of heterotrophic biomass by means of the yield coefficient:

$$-\frac{dS_S}{dt} = \frac{\hat{\mu}_H}{Y_H}\frac{S_S}{K_S + S_S}X_H \qquad (2.16)$$

The conversion of slowly biodegradable substrate (X_S) to readily biodegradable substrate through hydrolysis is given in (2.17) as a first order equation; K_h symbolizes the first order hydrolysis rate coefficient.

$$-\frac{dX_S}{dt} = K_h X_S \qquad (2.17)$$

The growth associated soluble inert products form by the below equation, where α_D is growth-associated soluble inert product formation coefficient for the endogenous decay model:

$$\frac{dS_P}{dt} = \alpha_D \hat{\mu}_H \frac{S_S}{K_S + S_S}X_H \qquad (2.18)$$

Table 2.1 Process Kinetics and Stoichiometry for Carbon Removal Involving Two Hydrolyzable Components for Death-Regeneration

Component→	1	2	3	4	5	6	7	8	9	Process Rate
Process↓	S_S	X_H	X_P	S_P	S_I	X_I	X_{SE}	X_S	S_O	$ML^{-3}T^{-1}$
Growth	$-\frac{1}{Y_H}$	1		α_R					$-\frac{1-\alpha_R Y_H - Y_H}{Y_H}$	$\hat{\mu}_H \frac{S_S}{(K_S + S_S)} X_H$
Death		-1	f_{PX}				$1-f_{PX}$			$b_H' X_H$
Hydrolysis of particulate slowly biodegradable organic matter of endogenous nature	$1-f_{PS}$			f_{PS}			-1			$K_{hE} X_{SE}$
Hydrolysis of particulate slowly biodegradable organic matter	1							-1		$k_{hX} \frac{X_S/X_H}{(K_{XX} + X_S/X_H)} X_H$
Parameters, ML^{-3}	COD	Cell COD	COD	COD	COD	COD	COD	COD	O_2	

According to the endogenous respiration the decrease of active heterotrophic biomass can be described by a first order rate expression where b_H shows the endogenous decay coefficient for active biomass.

$$-\frac{dX_H}{dt} = b_H X_H \tag{2.19}$$

The formation of soluble inert and particulate inert compounds are given by equations (2.20) and (2.21); f_{EX} is inert fraction of the biomass and f_{ES} is the fraction of endogenous biomass converted into soluble inert products.

$$\frac{dS_P}{dt} = f_{ES} b_H X_H \tag{2.20}$$

$$\frac{dX_P}{dt} = f_{EX} b_H X_H \tag{2.21}$$

Table 2.2 gives the matrix representation of the process kinetics and the stoichiometry of a model based upon the concept of endogenous decay.

2.4 Activated Sludge Models

2.4.1 Activated Sludge Model No.1 (ASM1)

Development of mathematical modeling for the design and operation of an activated sludge system achieving simultaneous carbon and nitrogen removal, has lead to the evolution of ASM1 proposed by IAWQPRC Task Group (Henze *et al.*, 1987). There is a large number of reactions between a large number of components in activated sludge systems. Especially if carbon oxidation, nitrification and denitrification are all together in a system, quantity of reactions increases a lot. Simulation of the systems can be made by models. A qualified model should contain both the kinetics and the stoichiometry of each process in order to define the rate-concentration dependence and the relationship between the components in a reaction. The most important thing in developing a mathematical model is to define the processes and select the appropriate kinetic and stoichiometric expressions for these.

Table 2.2 Process Kinetics and Stoichiometry for Carbon Removal Involving Two Hydrolyzable Components for Endogenous Decay

Component→	1	2	3	4	5	6	7	8	9	Process Rate
Process↓	S_S	X_H	X_P	S_P	S_I	X_I	S_H	X_S	S_O	$ML^{-3}T^{-1}$
Growth	$-\frac{1}{Y_H}$	1		α_D					$-\frac{1-\alpha_D Y_H - Y_H}{Y_H}$	$\hat{\mu}_H \frac{S_S}{(K_S + S_S)} X_H$
Death		-1	f_{EX}	f_{ES}					$-(1-f_{EX}-f_{ES})$	$b_H X_H$
Hydrolysis of soluble slowly biodegradable organic matter	1						-1			$k_{hS} \frac{S_H/X_H}{(K_{XS} + S_H/X_H)} X_H$
Hydrolysis of particulate slowly biodegradable organic matter	1							-1		$k_{hX} \frac{X_S/X_H}{(K_{XX} + X_S/X_H)} X_H$
Parameters, ML^{-3}	COD	Cell COD	COD	COD	COD	COD	COD	COD	O_2	

Simply, two fundamental processes occur in activated sludge systems: the biomass increases by cell growth and decreases by decay. As a result of these reactions oxygen utilization and substrate removal also occur but they are not considered to be fundamental. In ASM1, processes like aerobic and anoxic growth of heterotrophs, aerobic growth of autotrophs, decay of heterotrophs and autotrophs, ammonification and hydrolysis of organic carbon and organic nitrogen are all together involved. Also biomass and substrate are subdivided into a number of categories. Primary consideration was given to the prediction of activated sludge concentrations and estimation of electron acceptor requirements as to select the proper process stoichiometry and rate expressions. Processes that are essential in a realistic approach and rate expressions that have simplified solutions are selected for decreasing the complexity of the model. COD is used for expressing the concentrations of all organic matter, including biomass.

Components of the model: Soluble inert and particulate inert organic matters are involved in the matrix for only their important effect to the performance of the system. Soluble inert organic matter contributes to the effluent COD, while particulate inert organic matter accumulates in the system as a part of biomass. They are not involved in any conversion processes so their columns in the matrix do not contain stoichiometric coefficients. Readily biodegradable substrate is present in the influent or formed by the hydrolysis of slowly biodegradable substrate. Slowly biodegradable substrate is removed by hydrolysis but on the other hand, formed by the decay of biomass. Heterotrophic biomass, $X_{B,H}$ is formed by growth under either aerobic or anoxic conditions, while autotrophic bacteria, $X_{B,A}$ needs strictly aerobic environment. Particulate inert microbial products form by the decay of heterotrophic or autotrophic bacteria. This component shows the inactive part of the biomass in an activated sludge system. As a result the volatile solids concentration, in terms of COD, is the sum of five particulate terms: $X_{B,H}$, $X_{B,A}$, X_S, X_I and X_P. Appropriate conversion factors can be used to convert them from COD units to VSS units.

Oxygen utilization is only accomplished by the growth of heterotrophs or autotrophs. Decay is not effective in oxygen utilization, it is estimated as a slowly biodegradable organic matter releaser; then this slowly biodegradable part is recycled back to soluble substrate and used for more cell growth. This means, the oxygen utilization

normally associated directly with decay is calculated as if it occurs indirectly from the growth of new biomass on released substrate (Dold *et al.*, 1980).

Processes of the Model: Growth of biomass, decay of biomass, hydrolysis of slowly biodegradable organic matter and ammonification of organic nitrogen are the four major processes considered for this model. It is accepted that readily biodegradable organic matter is the only substrate used in growth process while slowly biodegradable organic matter from influent accumulates within the biomass. Active biomass is converted to slowly biodegradable organic matter and particulate inert organic matter by decay process. Slowly biodegradable substrate re-enters the hydrolysis cycle and again readily biodegradable substrate forms so growth continues on this material.

Both the concentrations of readily biodegradable substrate and dissolved oxygen are limiting factors for the rate of aerobic growth of the heterotrophic organisms. Storage of readily biodegradable substrate is not considered because there are only a few substrates as monosaccharides and acetate that can go through storage process. Thus, removal of soluble substrate becomes proportional to growth. On the other hand, substrate removal may be accomplished without biomass growth as a result of the entrapment of slowly biodegradable organic matter in the biofloc.

In order to decrease the complexity of mass balance equations, a pragmatic approach is adopted for modeling the decay of heterotrophs and autotrophs depending upon the death-regeneration concept (Dold et. al., 1980). According to that concept death or loss of viability of microorganisms occur without any utilization of electron acceptor, thus it does not matter whether aerobic, anoxic or anaerobic conditions are dominant in the system and no loss of COD is involved. The original ASM1 matrix is represented in Table 2.3.

Default values for the parameters and effects of environmental factors: Stoichiometric and kinetic coefficients suggested are listed in Table 2.4 for two different temperatures. These values are typical for neutral pH and domestic wastewater. It should be emphasized that many parameter values are influenced by environmental conditions. Most important factors are specific stimulators or inhibitors in the wastewater, pH and temperature. Neutral pH is needed for the proper growth conditions for biomass, also it is effective on nitrification-denitrification

processes. An increase in temperature generally results in an increase in the value of a rate coefficient like μ, b or k_h. Half saturation constants are also affected but some decrease, some increase and some remain unchanged. Kinetic coefficients always change when the temperature decreases or increases. This suggests that their values should be determined at the temperature, which will impose the most critical condition in the full-scale facility or correction factor for temperature must be used.

Process rates for ASM1

Aerobic growth of heterotrophs is given by the following equation:

$$\rho_1 = \mu_H \frac{S_S}{K_S + S_S} \frac{S_O}{K_{O,H} + S_O} X_H \qquad (2.22)$$

Anoxic growth of heterotrophs is given by equation (2.23).

$$\rho_2 = \mu_H \frac{S_S}{K_S + S_S} \frac{K_{O,H}}{K_{O,H} + S_O} \frac{S_{NO}}{K_{NO} + S_{NO}} \eta_g X_H \qquad (2.23)$$

Aerobic growth of autotrophs can be expressed as below:

$$\rho_3 = \mu_A \frac{S_{NH}}{K_{NH} + S_{NH}} \frac{S_O}{K_{O,A} + S_O} X_A \qquad (2.24)$$

Decay of heterotrophs and decay of autotrophs can be calculated by the following equations:

$$\rho_4 = b_H X_H \qquad (2.25)$$

$$\rho_5 = b_A X_A \qquad (2.26)$$

Ammonification of soluble organic nitrogen and hydrolysis of entrapped organics and entrapped organic nitrogen are calculated by expressions (2.27), (2.28) and (2.29) respectively:

$$\rho_6 = k_a S_{ND} X_H \qquad (2.27)$$

$$\rho_7 = k_h \frac{X_S/X_H}{K_X + (X_S/X_H)} \left(\frac{S_O}{K_{O,H} + S_O} + \eta_h \frac{K_{O,H}}{K_{O,H} + S_O} \frac{S_{NO}}{K_{NO} + S_{NO}} \right) X_H \qquad (2.28)$$

$$\rho_8 = \rho_7 (X_{ND}/X_S) \qquad (2.29)$$

Table 2.3. Process Stoichiometry for Carbon Oxidation, Nitrification and Denitrification (Henze *et al.*, 1987)

Component→	1	2	3	4	5	6	7	8	9	10	11	12
Process↓	S_S	X_H	X_A	X_P	S_I	X_I	X_S	S_O	S_{NO}	S_{NH}	S_{ND}	X_{ND}
Aerobic growth of heterotrophs	$-\frac{1}{Y_H}$	1						$-\frac{1-Y_H}{Y_H}$		$-i_{XB}$		
Anoxic growth of heterotrophs	$-\frac{1}{Y_H}$	1							$-\frac{1-Y_H}{2.86\,Y_H}$	$-i_{XB}$		
Aerobic growth of autotrophs			1					$-\frac{4.57-Y_A}{Y_A}$	$\frac{1}{Y_A}$	$-i_{XB}-\frac{1}{Y_A}$		
Decay of heterotrophs		-1		f_P			$1-f_P$					$i_{XB}-f_P i_{XP}$
Decay of autotrophs			-1	f_P			$1-f_P$					$i_{XB}-f_P i_{XP}$
Ammonification of soluble organic nitrogen										1	-1	
Hydrolysis of entrapped organics	1						-1					
Hydrolysis of entrapped organic nitrogen											1	-1
Parameters, ML^{-3}	COD	Cell COD	Cell COD	COD	COD	COD	COD	O_2	NO_3-N	NH_3-N	N_2	N_2

Table 2.4 Typical parameter values at neutral pH (Henze *et al.*, 1987)

Symbol	Unit	Value at 20°C	Value at 10°C
	Stoichiometric parameters		
Y_A	g cell COD formed (g N oxidized)$^{-1}$	0.24	0.24
Y_H	g cell COD formed (g COD oxidized)$^{-1}$	0.67	0.67
f_P	g inert COD formed (g COD oxidized)$^{-1}$	0.08	0.08
i_{XB}	g N (g COD)$^{-1}$ in biomass	0.086	0.086
i_{XE}	g N (g COD)$^{-1}$ in endogenous mass	0.06	0.06
	Kinetic parameters		
μ_H	day^{-1}	6.0	3.0
K_S	g COD m^{-3}	20.0	20.0
$K_{O,H}$	g O_2 m^{-3}	0.20	0.20
K_{NO}	g NO_3-N m^{-3}	0.50	0.50
b_H	day^{-1}	0.62	0.20
η_g		0.8	0.8
η_h		0.4	0.4
k_h	g slowly biodegradable COD (g cell COD.day)$^{-1}$	3.0	1.0
K_X	g slowly biodegradable COD (g cell COD)$^{-1}$	0.03	0.01
μ_A	day^{-1}	0.80	0.3
K_{NH}	g NH_3-N m^{-3}	1.0	1.0
$K_{O,A}$	g O_2 m^{-3}	0.4	0.4
k_a	m^3 (gCOD.day)$^{-1}$	0.08	0.04

2.4.2 Activated Sludge Model No.3 (ASM3)

ASM3 has been proposed by IAWQ Task group to establish new concepts in activated sludge modeling (Gujer *et al.*, 2000). ASM3 can be used in the estimation of oxygen consumption, sludge production, nitrification and denitrification of activated sludge systems. The model aims to correct some defects of ASM1. The components and processes are similar to ASM1 but ASM3 has some additional components like cell internal storage products and processes like storage. ASM3 includes nitrogen and alkalinity limitations for the growth of organisms, which were not taken into account in ASM1. Biodegradable soluble and particulate organic nitrogen model components in ASM1 have been eliminated in the new model. Thus, the deficiency of ASM1 for the proper description of ammonification kinetics was defeated by assuming a constant N to COD ratio.

It was not possible to differentiate the inert particulate organic material depending on its origin, influent or biomass decay as in ASM1, therefore a single particulate inert COD component has been used in ASM3. The hydrolysis process has been very important in predicting the electron acceptor consumption under aerobic and anoxic conditions but the quantification of the kinetic parameters for this process was also difficult. ASM3 has only one process to represent a simplified hydrolysis process, independent of the electron acceptor conditions. In ASM1, the lysis combined with

hydrolysis and growth was used for the decay mechanism which lead to difficulties in the evaluation of kinetic parameters. These problems have been eliminated by describing the decay process with endogenous decay. The differences between the COD flows of ASM1 and ASM3 are schematically shown in Figure 2.1.

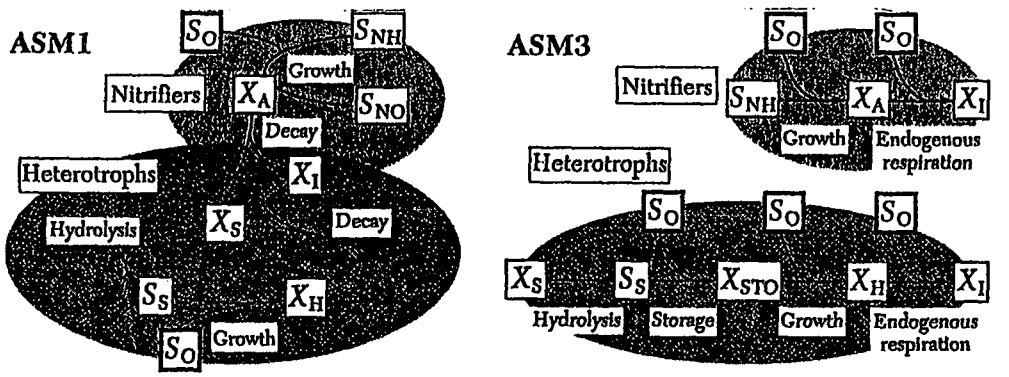

Figure 2.1 COD flow in ASM1 and ASM3

Components and processes of the model: ASM3 differentiates soluble and particulate components by 0.45 μm membrane filtration whereas a significant fraction of X_S would be contained in the filtrate in ASM1. Seven soluble and six particulate components are used to characterize the wastewater and activated sludge in ASM3.

Dissolved oxygen (S_O) is the first component, which can be directly measured and is subject to gas exchange. Inert soluble organic material (S_I) is a part of influent and may be produced by the hydrolysis of X_S. Readily biodegradable organic substrates (S_S) have special importance in ASM3 because they are first taken up by heterotrophic organisms and stored as X_{STO}, then used for growth. S_S and S_I are approximately equal to the total soluble COD determined by filtration from 0.45 μm membrane filters. There are three fractions of nitrogen as ammonium plus ammonia nitrogen (S_{NH}), dinitrogen (S_{N2}) and nitrite plus nitrate nitrogen (S_{NO}). Alkalinity of the wastewater (S_{ALK}) is used to approximate the conservation of ionic charge in biological reactions.

Inert particulate organic matter (X_I) is a part of influent and also may be produced as a result of biomass decay. Slowly biodegradable substrates (X_S) must undergo hydrolysis before they are used by the biomass because they are high molecular weight, colloidal and particulate organic substrates that cannot be directly used. The products of the hydrolysis are assumed to be readily biodegradable or soluble inert

substrates. It must be reminded that all X_S is contained in the influent and not involved in the filtrate of 0.45 μm membrane filter in ASM3. Heterotrophic organisms (X_H) may grow both aerobically and anoxically. Cell external hydrolysis in ASM3 does not consume any electron acceptor. Active biomass is responsible for the hydrolysis of X_S and storage process. Cell internal storage products (X_{STO}) consists of PHA, glycogen etc., which is only defined as a functional component required for modeling but is not directly identifiable chemically. X_A represents autotrophic organisms responsible for nitrification. They oxidize the ammonium directly to nitrate, nitrite is not considered in ASM3. Last component considered in the model is the total suspended solids, X_{TS}. It may be used for the modeling of volatile suspended solids by some special ratios. There are twelve processes considered in ASM3.

Hydrolysis: All of the slowly biodegradable substrates in the influent are converted to available soluble substrates by hydrolysis. This process is independent from electron acceptor and therefore is different when compared to ASM1.

Aerobic storage of readily biodegradable substrate: It is assumed that all readily biodegradable substrate is first converted to storage products (X_{STO}), and then becomes available for the usage of biomass. Required energy for this conversion is compensated by aerobic respiration.

Anoxic storage of readily biodegradable substrate: This process is identical with aerobic storage process, but required energy is gained from anoxic respiration. The process rate is naturally smaller than aerobic storage rate because of the lower amount of denitrifiers.

Aerobic growth of heterotrophs: Heterotrophs use the storage products as substrate.

Anoxic growth of heterotrophs: It is based on anoxic respiration.

Aerobic endogenous respiration: The decay process is defined as all forms of biomass loss and energy requirements not associated with growth. The process considers all related respiration under aerobic conditions: decay, maintenance, endogenous respiration, lysis, predation, motility and death.

Anoxic endogenous respiration: This process is similar to aerobic endogenous respiration, but occurs at a slower rate. Especially protozoa predation is considerably less active under anoxic conditions then under aerobic conditions.

Aerobic respiration of storage products: Like endogenous respiration, X_{STO} decays together with biomass.

Anoxic respiration of storage products: Denitrifiying conditions are applied for the analogous process of aerobic respiration of storage products.

Aerobic growth of autotrophs: Nitrifiers oxidize ammonium directly to nitrate, nitrite as an intermediate component, is not considered.

Aerobic endogenous respiration for autotrophs: Similar to aerobic endogenous respiration, but is described for nitrifiers.

Anoxic endogenous respiration for autotrophs: Analogous to aerobic endogenous respiration for autotrophs, but at a slower rate.

Process stoichiometry: The net true yield of heterotrophic biomass produced per unit of substrate removed is calculated as the product of storage yield and growth yield because growth process completely depends on the storage process. Firstly storage is completed, and then stored products are used for growth so the total yield is the combination of yields of these processes.

$$Y_{net,O2} = Y_{STO,O2} \cdot Y_{H,O2} \quad (2.30)$$

$$Y_{net,NOX} = Y_{STO,NOX} \cdot Y_{H,NOX} \quad (2.31)$$

The stoichiometric matrix of ASM3 is given in Table 2.5 and the COD transformations are summarized in Figures 2.2-2.13.

1. Hydrolysis: Hydrolysis of slowly biodegradable substrate, X_S, is illustrated in Figure 2.2

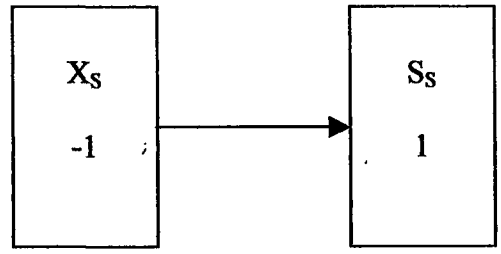

Figure 2.2 COD transformation in hydrolysis

f_{SI}: 0, x_1: 1

y_1: 0.01: $(i_{NXS}-X_I\, i_{NSS})$: i_{NSI}

z_1: 0.001: $y_1/14$: $i_{NSI}/14$

Table 2.5 Process stoichiometry for ASM3 (Gujer *et al.*, 2000)

	Compound $i \rightarrow$	1	2	3	4	5	6	7	8	9	10	11	12	13
j	Process	S_{O_2}	S_I	S_S	S_{NH_4}	S_{N_2}	S_{NOX}	S_{ALK}	X_I	X_S	X_H	X_{STO}	X_A	X_{SS}
↓	Expressed as →	O_2	COD	COD	N	N	N	Mole	COD	COD	COD	COD	COD	SS
1	Hydrolysis		f_{S_I}	x_1	y_1			z_1		−1				$-i_{X_S}$
Heterotrophic organisms, aerobic and denitrifying activity														
2	Aerobic storage of S_S	x_2		−1	y_2			z_2				Y_{STO,O_2}		i_2
3	Anoxic storage of S_S			−1	y_3	$-x_3$	x_3	z_3				$Y_{STO,NOX}$		i_3
4	Aerobic growth of X_H	x_4			y_4			z_4			1	$-1/Y_{H,O_2}$		i_4
5	Anoxic growth (denitrific.)				y_4	$-x_5$	x_5	z_5			1	$-1/Y_{H,NOX}$		i_5
6	Aerobic endog. respiration	x_6			y_6			z_6	f_I		−1			i_6
7	Anoxic endog. respiration				y_7	$-x_7$	x_7	z_7	f_I		−1			i_7
8	Aerobic respiration of X_{STO}	x_8										−1		i_8
9	Anoxic respiration of X_{STO}					$-x_9$	x_9	z_9				−1		i_9
Autotrophic organisms, nitrifying activity														
10	Aerobic growth of X_A	x_{10}			y_{10}		$1/Y_A$	z_{10}					1	i_{10}
11	Aerobic endog. respiration	x_{11}			y_{11}			z_{11}	f_I				−1	i_{11}
12	Anoxic endog. respiration				y_{12}	$-x_{12}$	x_{12}	z_{12}	f_I				−1	i_{12}
Composition matrix $i_{k,j}$														
k	*Conservatives*													
1	ThOD	g ThOD	−1	1	1		−1.71	−4.57		1	1	1	1	1	
2	Nitrogen	g N		i_{N,S_I}	i_{N,S_S}	1	1	1		i_{N,X_I}	i_{N,X_S}	$i_{N,BM}$		$i_{N,BM}$	
3	Ionic charge	Mole +				1/14		−1/14	−1						
	Observables														
4	SS	g SS								i_{SS,X_I}	i_{SS,X_S}	$i_{SS,BM}$	0.60	$i_{SS,BM}$	

2. Aerobic Storage of S_S. Storage polymers are produced from readily biodegradable COD as shown in Figure 2.3.

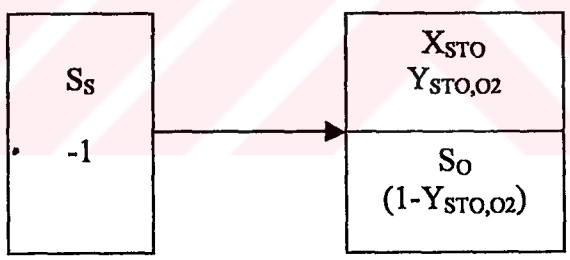

Figure 2.3 COD transformation in aerobic storage

$Y_{STO,O2}$: 0.85 g X_{STO}/gS_S

x_2: -0.15: -(1-$Y_{STO,O2}$)

y_2: 0.03: i_{NSS}

z_2: 0.002: y_2/14: i_{NSS}/14

3. Anoxic Storage of S_S. Storage polymers are also produced under anoxic conditions (Figure 2.4).

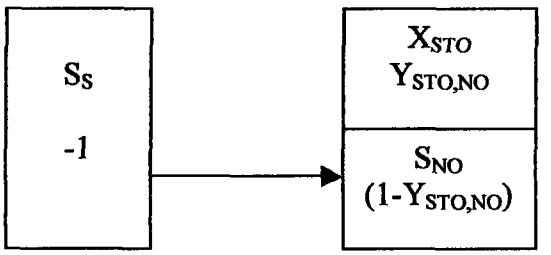

Figure 2.4 COD transformation in Anoxic storage

$Y_{STO,NO}$: 0.80 g X_{STO}/gS_S

x_3: -0.07: $-(1-Y_{STO,NO})/2.86$

y_3: 0.03: i_{NSS}

z_3: 0.007: $(-x_3+y_3)/14$

4. Aerobic Growth of Heterotrophs: Heterotrophic biomass grows on the stored polymers and utilizes oxygen during this process (Figure 2.5).

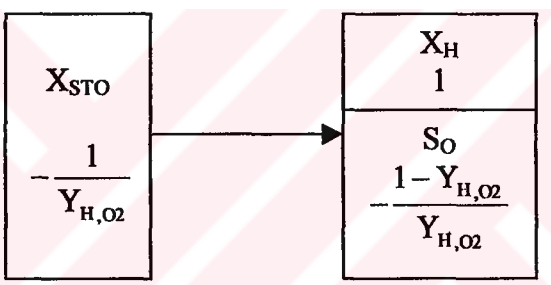

Figure 2.5 COD transformation in aerobic growth

$Y_{H,O2}$: 0.63 g $X_H/g\ X_{STO}$

x_4: -0.60: $-(1-Y_{H,O2})/Y_{H,O2}$

y_4: -0.07: $-i_{NBM}$

z_4: -0.005: $y_4/14$: $i_{NBM}/14$

5. Anoxic Growth of Heterotrophs: Same with process 4, but anoxic conditions are dominant as illustrated in Figure 2.6.

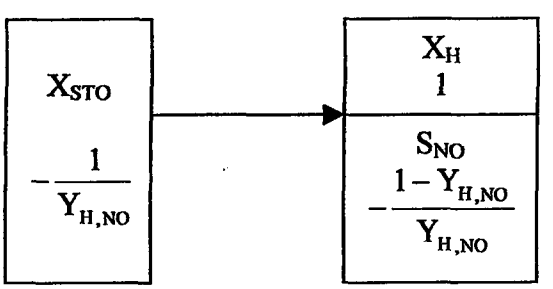

Figure 2.6 COD transformation in anoxic growth

$Y_{H,NO}$: 0.54 g X_H/g X_{STO}

x_5: -0.30: $-(1-Y_{H,NO})/2.86Y_{H,NO}$

y_5: -0.07: $-i_{NBM}$

z_5: 0.016: $(-x_5+y_4)/14$

6. Aerobic Endogenous Respiration: Figure 2.7 represents the stoichiometry.

f_I: 0.20

x_6: -0.80: $-(1-f_I)$

y_6: 0.066: $(i_{NBM}-f_I.i_{NXI})$

z_6: 0.005: $y_6/14$: $(i_{NBM}-f_I.i_{NXI})/14$

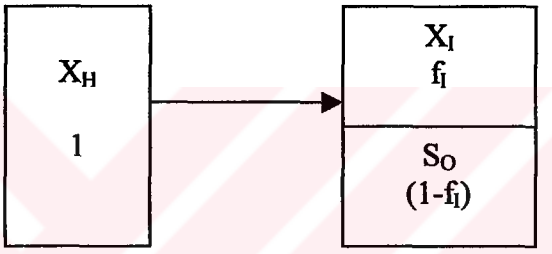

Figure 2.7 COD transformation in aerobic endogenous respiration

7. Anoxic Endogenous Respiration: Endogenous respiration occurring under anoxic conditions is given in Figure 2.8.

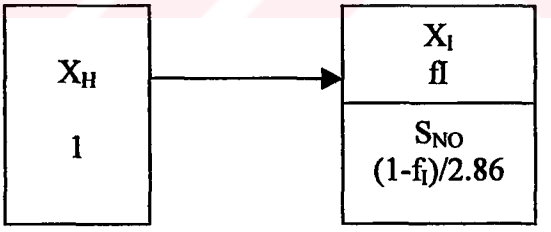

Figure 2.8 COD transformation in anoxic endogenous respiration

f_I: 0.20

x_7: -0.28: $-(1-f_I)/2.86$

y_7: 0.066: $(i_{NBM}-f_I.i_{NXI})$

z_7: 0.025: $(-x_7+y_7)/14$

8. Aerobic Respiration of X_{STO}: Respiration process occurring on stored polymers is illustrated in Figure 2.9.

x_8: -1

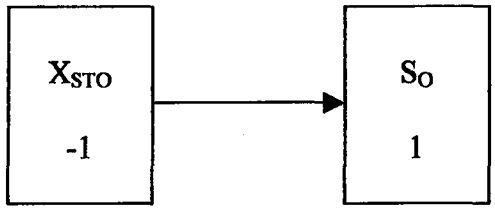

Figure 2.9 COD transformation in aerobic X_{STO} respiration

9. Anoxic Respiration of X_{STO}: Figure 2.10 represents the anoxic X_{STO} respiration.

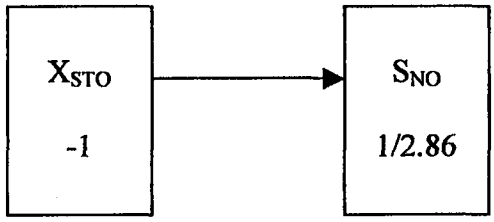

Figure 2.10 COD transformation in anoxic X_{STO} respiration

x_9: -0.35: -1/2.86

z_9: 0.025: $-x_9/14$

10. Aerobic Growth of Autotrophs: Stoichiometry of aerobic autotrophic growth is given in Figure 2.11 as below:

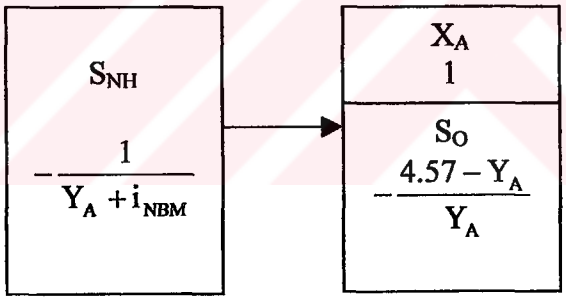

Figure 2.11 COD transformation in autotrophic aerobic growth

Y_A: 0.24 g X_A/g S_{NO}

x_{10}: -18.04: $-(4.57-Y_A)/Y_A$

y_{10}: -4.24: $-(1/Y_A+i_{NBM})$

z_{10}: -0.600: $(y_{10}-1/Y_A)/14$

11. Aerobic Endogenous Respiration of Autotrophs: Figure 2.12 shows the aerobic endogenous respiration of autotrophs.

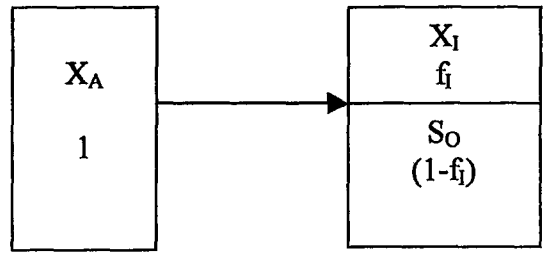

Figure 2.12 COD transformation in aerobic endogenous respiration of autotrophs

f_I: 0.20

x_{11}: -0.80: $-(1-f_I)$

y_{11}: 0.066: $(i_{NBM}-f_I.i_{NXI})$

z_{11}: 0.005: $y_{11}/14$: $(i_{NBM}-f_I.i_{NXI})/14$

12. Anoxic Endogenous Respiration of Autotrophs: Summarized in Figure 2.13.

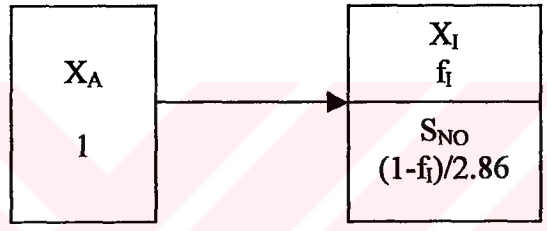

Figure 2.13 COD transformation in anoxic endogenous respiration of autotrophs

f_I: 0.20

x_{12}: -0.28: $-(1-f_I)/2.86$

y_{12}: 0.066: $(i_{NBM}-f_I.i_{NXI})$

z_{12}: 0.025: $(-x_{12}+y_{12})/14$

Process Kinetics: The kinetic expressions of ASM3 are based on switching functions (hyperbolic or saturation terms, Monod equations, S/(K+S)) as in ASM1 for all soluble compounds consumed. These switching functions relate to the ratio of X_{STO}/X_H and X_S/X_H for particulate products too. The summary of all kinetic expressions are given in Table 2.6 and typical kinetic parameters of ASM3 are given in Table 2.7. It is recommended to interpolate kinetic parameters k to different temperatures T with a correction factor as below:

$$k(T) = k(20°C) \cdot \exp(\theta_T \cdot (T - 20°C)) \quad (2.32)$$

$$\theta_T = \frac{\ln(k(T_1)/k(T_2))}{T_1 - T_2} \quad (2.33)$$

Table 2.6 Process kinetics for ASM3 (Gujer *et al.*, 2000)

j	Process	Process rate equation ρ_j, all $\rho_j \geq 0$
1	Hydrolysis	$k_H \cdot \frac{X_S/X_H}{K_X + X_S/X_H} \cdot X_H$
Heterotrophic organisms, aerobic and denitrifying activity		
2	Aerobic storage of S_S	$k_{STO} \cdot \frac{S_{O_2}}{K_{O_2} + S_{O_2}} \cdot \frac{S_S}{K_S + S_S} \cdot X_H$
3	Anoxic storage of S_S	$k_{STO} \cdot \eta_{NOX} \cdot \frac{K_{O_2}}{K_{O_2} + S_{O_2}} \cdot \frac{S_{NOX}}{K_{NOX} + S_{NOX}} \cdot \frac{S_S}{K_S + S_S} \cdot X_H$
4	Aerobic growth	$\mu_H \cdot \frac{S_{O_2}}{K_{O_2} + S_{O_2}} \cdot \frac{S_{NH_4}}{K_{NH_4} + S_{NH_4}} \cdot \frac{S_{ALK}}{K_{ALK} + S_{ALK}} \cdot \frac{X_{STO}/X_H}{K_{STO} + X_{STO}/X_H} \cdot X_H$
5	Anoxic growth (denitrification)	$\mu_H \cdot \eta_{NOX} \cdot \frac{K_{O_2}}{K_{O_2} + S_{O_2}} \cdot \frac{S_{NOX}}{K_{NOX} + S_{NOX}} \cdot \frac{S_{NH_4}}{K_{NH_4} + S_{NH_4}} \cdot \frac{S_{ALK}}{K_{ALK} + S_{ALK}} \cdot \frac{X_{STO}/X_H}{K_{STO} + X_{STO}/X_H} \cdot X_H$
6	Aerobic endogenous respiration	$b_{H,O_2} \cdot \frac{S_{O_2}}{K_{O_2} + S_{O_2}} \cdot X_H$
7	Anoxic endogenous respiration	$b_{H,NOX} \cdot \frac{K_{O_2}}{K_{O_2} + S_{O_2}} \cdot \frac{S_{NOX}}{K_{NOX} + S_{NOX}} \cdot X_H$
8	Aerobic respiration of X_{STO}	$b_{STO,O_2} \cdot \frac{S_{O_2}}{K_{O_2} + S_{O_2}} \cdot X_{STO}$
9	Anoxic respiration of X_{STO}	$b_{STO,NOX} \cdot \frac{K_{O_2}}{K_{O_2} + S_{O_2}} \cdot \frac{S_{NOX}}{K_{NOX} + S_{NOX}} \cdot X_{STO}$
Autotrophic organisms, nitrifying activity		
10	Aerobic growth of X_A, nitrification	$\mu_A \cdot \frac{S_{O_2}}{K_{A,O_2} + S_{O_2}} \cdot \frac{S_{NH_4}}{K_{A,NH_4} + S_{NH_4}} \cdot \frac{S_{ALK}}{K_{A,ALK} + S_{ALK}} \cdot X_A$
11	Aerobic endogenous respiration	$b_{A,O_2} \cdot \frac{S_{O_2}}{K_{A,O_2} + S_{O_2}} \cdot X_A$
12	Anoxic endogenous respiration	$b_{A,NOX} \cdot \frac{K_{A,O_2}}{K_{A,O_2} + S_{O_2}} \cdot \frac{S_{NOX}}{K_{A,NOX} + S_{NOX}} \cdot X_A$

Table 2.7 Typical values of kinetic parameters for ASM3 (Gujer *et al.*, 2000)

Symbol	Characterization	Temperature 10 °C	Temperature 20 °C	Units
k_H	Hydrolysis rate constant	2	3	g COD_{X_S} (g COD_{X_H})$^{-1}$ d^{-1}
K_X	Hydrolysis saturation constant	1	1	g COD_{X_S} (g COD_{X_H})$^{-1}$
Heterotrophic organisms X_H, aerobic and denitrifying activity				
k_{STO}	Storage rate constant	2.5	5	g COD_{S_S} (g COD_{X_H})$^{-1}$ d^{-1}
η_{NOX}	Anoxic reduction factor	0.6	0.6	—
K_{O_2}	Saturation constant for S_{NO_2}	0.2	0.2	g O_2 m^{-3}
K_{NOX}	Saturation constant for S_{NOX}	0.5	0.5	g NO_3^--N m^{-3}
K_S	Saturation constant for substrate S_S	2	2	g COD_{S_S} m^{-3}
K_{STO}	Saturation constant for X_{STO}	1	1	g $COD_{X_{STO}}$ (g COD_{X_H})$^{-1}$
μ_H	Heterotrophic max. growth rate of X_H	1	2	d^{-1}
K_{NH_4}	Saturation constant for ammonium, S_{NH_4}	0.01	0.01	g N m^{-3}
K_{ALK}	Saturation constant for alkalinity for X_H	0.1	0.1	mole HCO_3^- m^{-3}
b_{H,O_2}	Aerobic endogenous respiration rate of X_H	0.1	0.2	d^{-1}
$b_{H,NOX}$	Anoxic endogenous respiration rate of X_H	0.05	0.1	d^{-1}
b_{STO,O_2}	Aerobic respiration rate for X_{STO}	0.1	0.2	d^{-1}
$b_{STO,NOX}$	Anoxic respiration rate for X_{STO}	0.05	0.1	d^{-1}
Autotrophic organisms X_A, nitrifying activity				
μ_A	Autotrophic max. growth rate of X_A	0.35	1.0	d^{-1}
K_{A,NH_4}	Ammonium substrate saturation for X_A	1	1	g N m^{-3}
K_{A,O_2}	Oxygen saturation for nitrifiers	0.5	0.5	g O_2 m^{-3}
$K_{A,ALK}$	Bicarbonate saturation for nitrifiers	0.5	0.5	mole HCO_3^- m^{-3}
b_{A,O_2}	Aerobic endogenous respiration rate of X_A	0.05	0.15	d^{-1}
$b_{A,NOX}$	Anoxic endogenous respiration rate of X_A	0.02	0.05	d^{-1}

ASM3 has also provided suggestions for typical stoichiometric and composition parameters of the model as given Table 2.8.

Table 2.8 Typical values of stoichiometric and composition parameters for ASM3 (Gujer *et al.*, 2000)

Symbol	Characterization	Value	Units	
f_{S_I}	Production of S_I in hydrolysis	0	g COD_{S_I} (g COD_{X_I})$^{-1}$	
Y_{STO,O_2}	Aerobic yield of stored product per S_S	0.65	g $COD_{X_{STO}}$ (g COD_{S_S})$^{-1}$	
$Y_{STO,NOX}$	Anoxic yield of stored product per S_S	0.60	g $COD_{X_{STO}}$ (g COD_{S_S})$^{-1}$	Equation 5.3
Y_{H,O_2}	Aerobic yield of heterotrophic biomass	0.63	g COD_{X_H} (g $COD_{X_{STO}}$)$^{-1}$	
$Y_{H,NOX}$	Anoxic yield of heterotrophic biomass	0.54	g COD_{X_H} (g $COD_{X_{STO}}$)$^{-1}$	Equation 5.3
Y_A	Yield of autotrophic biomass per NO_3-N	0.24	g COD_{X_A} (g $N_{S_{NOX}}$)$^{-1}$	
f_{X_I}	Production of X_I in endog. respiration	0.20	g COD_{X_I} (g $COD_{X_{BM}}$)$^{-1}$	
i_{N,S_I}	N content of S_I	0.01	g N (g COD_{S_I})$^{-1}$	
i_{N,S_S}	N content of S_S	0.03	g N (g COD_{S_S})$^{-1}$	
i_{N,X_I}	N content of X_I	0.02	g N (g COD_{X_I})$^{-1}$	The values below are
i_{N,X_S}	N content of X_S	0.04	g N (g COD_{X_S})$^{-1}$	suggested if X_{SS} is used to
$i_{N,BM}$	N content of biomass, X_H, X_A	0.07	g N (g $COD_{X_{BM}}$)$^{-1}$	model VSS rather than SS:
i_{SS,X_I}	SS to COD ratio for X_I	0.75	g SS (g COD_{X_I})$^{-1}$	0.75 g VSS (g COD_{X_I})$^{-1}$
i_{SS,X_S}	SS to COD ratio for X_S	0.75	g SS (g COD_{X_S})$^{-1}$	0.75 g VSS (g COD_{X_S})$^{-1}$
$i_{SS,BM}$	SS to COD ratio for biomass, X_H, X_A	0.90	g SS (g $COD_{X_{BM}}$)$^{-1}$	0.75 g VSS (g $COD_{X_H \text{ or } X_A}$)$^{-1}$

SECTION 3 SUBSTRATE STORAGE PHENOMENA

3.1 Recognition of Storage Phenomena

Microorganisms are subjected to feast (presence of substrate) and famine (absence of substrate) periods in a variety of wastewater treatment processes. Reviewing the literature and the experimental researches conducted, it is proposed that the response of microorganisms, exposed to such conditions is to accumulate storage polymers when substrate is available. In the absence of substrate these storage polymers are used for growth and thus the organisms are able to balance their growth (van Loosdrecht *et al.*, 1997).

Generally, only growth and respiration processes are accepted to occur on soluble or particulate substrates (Gujer and Henze, 1991) but the accumulation of internal storage polymers has also been reported (Chudoba et.al., 1973; Zevenhuisen and Ebbnik 1974; Van den Eynde et.al., 1984).

In activated sludge modeling, storage polymers have been neglected, without considering that they might have a significant role. However, activated sludge systems are highly dynamic with respect to the feed period. Bacteria will have external substrate supply only for relatively short periods of time and will rapidly grow. The microorganisms would undergo long starvation periods without internally stored substrate. Bacteria that are able to store and consume this stored substrate will have a strong competitive advantage over the other organisms without the capacity of substrate storage. The significance of the storage polymers have been reported, especially for SBR processes more than continuously operated treatment plants (van Loosdrecht *et al.*, 1997)

In literature, various types of organic storage polymers have been reported as PHB, glycogen and lipids (Zevenhuizen and Ebbnik, 1974). A kind of microorganism called pseudomonas was isolated from activated sludge on the basis of its floc forming capacity in 0.1% casitone, 0.035% yeast extract and 0.2% glycerol medium. Morphological changes and flocculation took place accompanied by a significant

deposition of reserve matter is reported to the cell, in the late exponential phase of growth. Storage product composition depends on the carbon source used. Glycerol-grown cells contained mainly glycogen but no ether soluble lipid and no PHB. Glucose was largely converted into gluconic acid and excreted into medium before being deposited in the form of PHB as the primary product of assimilation. Subsequently PHB was metabolized being partly transformed into glycogen and ether-soluble lipid. Growth yields and storage products for different carbon sources at 25°C for 2 days are given in Table 3.1.

Table 3.1 Type of Storage Products for Various Carbon Sources (Zevenhuisen and Ebbnik, 1974)

Carbon source	Dry weight	Carbohydrate[1]	PHB[2]	Lipid[2]
D-Glucose	150	20.0	60.0	18.0
D-Galactose	128	30.6	11.3	39.4
D-Mannose	62	3.5	0.4	5.4
D-Fructose	141	32.6	–	54.5
L-Arabinose	115	31.4	–	25.6
Ca-D-gluconate	118	13.3	38.2	11.8
Na-DL-β-hydroxybutyrate	128	12.1	42.8	30.8
Ca-succinate	102	9.5	38.6	11.3
Ca-DL-malate	84	7.4	10.7	7.2
Glycerol	100	29.8	2.9	14.3
Ca-DL-lactate	125	14.9	24.0	13.0
Na-acetate	78	2.9	2.9	15.9

[1] Expressed as glucose;
[2] Calculated from the U.V.-spectrum in sulfuric acid at 235 nm (PHB), and at 295 nm (ether-soluble lipid) respectively.

Among the endogenous substrates of bacteria, glycogen and lipids including PHB are considered as carbon and energy stores. Most reports on bacterial reserves deal with only one type of product namely either glycogen or PHB. In some organisms only one type was believed to be present; in other organisms in which two or more types have been recognized they have been studied separately.

Lipids are present in small, constant amounts in all bacteria. They usually do not function as carbon and energy reserves and have to be considered as structural components of membranes (phospholipids) and of cell walls (lipopolysaccharides). Only in Mycobacterium, lipid was found to function as an endogenous substrate although glycogen, which was present at the same time, appeared to be preferred substrate.

PHB is the most significant polymer with respect to other organic polymers because it is formed out of the metabolite Acetyl-CoA. Formation of glycogen depends on the

presence of sugars in the influent. There are nearly no reports about the presence of lipids so the role of them is not clear. Studies on the growth of bacteria over storage products are very rare in literature. Furthermore, these few studies were done under conditions where growth limitation is effective due to nitrogen shortage. In reality, storage occurs independent of growth limitation.

The formation of storage polymers is a newly introduced phenomenon to standard aerobic or anoxic COD removal processes. Recent studies with respirometry and pure substrates give obvious results showing formation of storage polymers. Amount of oxygen utilized per amount of substrate removed is lower than found in pure culture studies, which indicates the presence of storage process.

3.1.1 Biological Processes Using Storage Polymers

Storage polymers have gained much attention with the recognition of specific biological processes, i.e. biological P-removal and bulking sludge control making use of storage phenomena.

Biological Phosphorus Removal: Fatty acids, accumulating in the cell during the anaerobic phase of the biological process are the dominant substrates for bio-P bacteria. Organic matter is fermented to fatty acids in the anaerobic step, which are then converted to PHB by bio-P bacteria at the expense of the energy released in the hydrolysis of glycogen and polyphosphate (Smolders *et al.,* 1995). Generated PHB is oxidized in the presence of electron acceptors in order to yield energy for growth and restoring the glycogen and polyphosphate levels (Smolders *et al.,* 1995). G-bacteria are also capable of storing polymers in the absence of electron acceptors (Cech *et al.,* 1994; Liu *et al.,* 1994) that are latterly used for growth in the presence of oxygen or nitrate. This storage is realized by the energy released in the conversion of sugars (glycogen or external substrates) to PHA.

Bulking Sludge Control: When the substrate concentration is low in activated sludge systems, filamentous bacteria successfully compete for substrate with floc forming bacteria due to their lower K_S value. On the other hand, floc forming bacteria have an advantage as higher maximal substrate uptake rate but filamentous bacteria can still become dominant in processes with a completely mixed reactor. Chudoba *et al.,* (1973) studied bulking sludge in plug-flow reactors with mixing return sludge and influent. Selectors have been designed based on the removal of easily biodegradable

COD from the liquid phase and having short residence time (15 minutes) when compared to the total residence time. It is observed that soluble COD is taken up by the sludge and stored in the biomass. Energy for this process is obtained from oxidation or from the hydrolysis of polyphosphate in case of an anaerobic selector.

According to van den Eynde *et al.* (1984) the floc forming bacterium, *A. globiformis* showed a larger overcapacity for substrate uptake, a larger accumulation of reserves (polysaccharides and PHB) and a more efficient mobilization of these polymers than the filamentous species *S. natans*. Continuously fed activated sludge systems had a high SVI and low storage capacity, whereas intermittently fed systems had a low SVI and high capacity for the accumulation of storage polymers. Consequently, intermittent feeding of activated sludge could prevent the excessive growth of filamentous bacteria. Whenever an amount of substrate is suddenly added to the steady state cultures, there is an immediate increase in substrate uptake rate; the growth rate not being able to switch to higher values (van den Eynde *et al.*, 1983). To study the phenomena in bacteria relieved from any growth limitation in more detail, two IC-chemostats were inoculated. Samples were analyzed for glucose and COD in the medium and for PS (polysaccharides), PHB and protein in the biomass. The relatively high substrate uptake rates recorded for both species again prove the overcapacity under a regime of intermittent feeding (Table 3.2). Initially the decrease in COD was equivalent to the glucose uptake. Towards the end of the COD curve diverted from the glucose uptake curve; this indicates the excretion of over-flow metabolites. Immediately after the addition of glucose both cultures started to accumulate reserves. *A. globiformis* produced exclusively PS, whereas *S. natans* accumulated both PS and PHB with a higher accumulation rate of PS. Growth continued in these batch experiments, a steady increase in protein concentration was found for both species. There was no tight coupling between glucose uptake and protein synthesis. When exogenous glucose was exhausted the cells adopted to this new situation; metabolism could rely on the reserves for growth and maintenance. After a lag phase the breakdown of PS started and with it as a source of carbon and energy protein synthesis could proceed.

Table 3.2 Comparison of Parameters for *A. globiformis* and *S. natans* (van den Eynde *et al.*, 1984)

	Growth rate $\mu = D$ (h^{-1})	Biomass D.W.[a] ($g \cdot l^{-1}$)	Balanced uptake rate[b]	q_{max}	PHB accumulated rate	PS accumulated rate[c]	Total response accumulated rate[c]	Total amount of response ($mg \cdot l^{-1}$)
A. globiformis	0.042	2.66	1.63	7.4	–	5.25	5.25	580
S. natans	0.05	2.59	1.94	3.3	0.35	0.51	0.86	231

[a] D.W. = dry weight
[b] The balanced uptake rate is necessary to allow growth with the same rate as in the chemostat; it is calculated according to the yield-values (Y) were taken from our previous paper (Van den Eynde et al. 1983)
[c] The total reserve accumulation rate is the sum of PHB and PS

From these results, it is evident that pulse feeding has a profound influence on the metabolism of the bacteria. Where the Monod equation would suggest an immediate increase of μ with higher concentrations of S, a completely different behaviour was found. Very small or no immediate increase in growth rate can be explained in numbers of ribosomes engaged in protein synthesis. The μ_{max} can only be attained after a lag phase during which RNA and more ribosomes must be synthesized. According to this mechanism the initial substrate uptake rate is too high and the excess of substrate is accumulated as reserves or excreted as overflow metabolites. The main features of *A. globiformis* and *S. natans* during a shift-up are the high substrate uptake rate compared to the previous growth rate (overcapacity), the lag phase in protein synthesis and the metabolism of reserve materials.

3.1.2 Hypothesis for Storage Polymer Formation

COD conversion: In plug-flow and completely mixed reactors, the conversion of glucose was studied (Chudoba *et.al.*, 1985). The yield of biomass on glucose for pure cultures was found to be 0.64 g COD/g COD, calculated from the amount of oxygen consumed till all glucose is converted whereas the theoretical yield for the formation of the glycogen is 0.96 g COD/g COD. The discrepancy between these yields significantly points out the formation of storage polymers. Based on a large literature review and thermodynamic reasoning that growth process requires a standard amount of energy utilization, the yield for aerobic growth can be evaluated as 0.5 g COD/g COD for a wide range of aerobic bacteria and substrates (Heijnen, 1994). This

difference between mixed cultures and pure cultures can be explained by the conversion of a fraction of substrate into storage polymers.

General aspects of storage polymer formation have been improved as a result of recent research carried out by Pot *et al.* (1996a; 1996b). This research is summarized in Figures 3.1 and 3.2. The effect of transition from continuous to batch culturing on a pure culture is shown in Figure 3.1. All substrate was converted to biomass at a constant rate and no biopolymers were formed in steady-state continuous culture. This steady state continuous culture was disturbed by a pulse of substrate (acetate) added, so the organism has taken up the substrate at a high rate. A direct increase in growth rate was not observed due to the change in substrate uptake rate. Polymer formation was occurred as the conversion of acetate surplus to PHB. When the external substrate was fully consumed the organism started to grow on the stored PHB. The growth rate on the stored polymer is definitely lower than it is on the original influent substrate. The organism can keep its balanced metabolism by forming PHB when there is a sudden change in substrate addition. The uptake rate is limited by the substrate concentration therefore when organisms are growing under limited substrate conditions; they need comparatively large quantity of substrate uptake enzymes. A rapid uptake of the substrate can be observed when the substrate concentration increases unexpectedly. However, in the cell this amount of substrate cannot be directly converted by the growth process and if the conversion of substrate to PHB does not occur the cell metabolism could not keep its balance. The organisms can regulate their growth rate if the substrate concentration stays high. However only during a limited period, in pulse-wise SBR systems or in plug-flow reactors, high substrate concentrations are experienced by the bacteria and storage process can play a dominant role.

The effect of pulsed or continuous substrate addition to an anoxic-aerobic SBR with a mixed, open sludge culture has been investigated by feeding the substrate to anoxic phase. As seen from Figure 3.2, PHB accumulation occurs in both modes of substrate feeding but it is larger in the pulse fed SBR than in the continuous fed SBR. Feast-famine periods enrich the mixed microbial community, which use storage polymers to balance their growth. Also the difference between the substrate need for growth and substrate uptake rate is balanced by the formation of storage polymers.

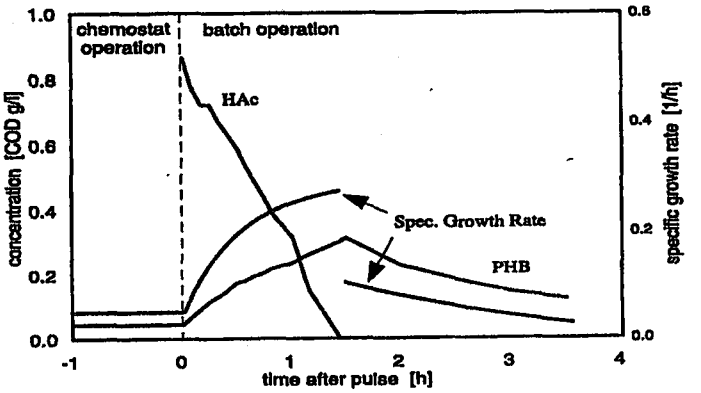

Figure 3.1 Concentrations of acetic acid and PHB after a pulse of acetate is added (van Loosdrecht *et al.*, 1997)

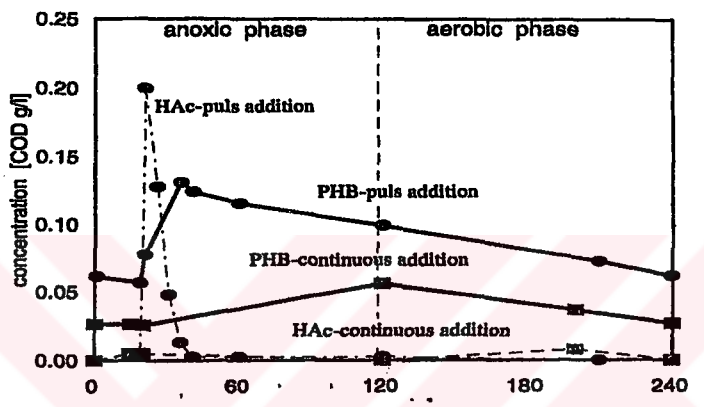

Figure 3.2 Profiles of acetic acid and PHB in an SBR (van Loosdrecht *et al.*, 1997)

The hypothesis proposed by van Loosdrecht *et al.* (1997), for the occurrence of storage polymer formation when there is no limiting condition for growth says that, microorganisms, regularly exposed to feast-famine periods, will be enriched and able to balance their growth independently from external substrate supply. Bacteria that cannot store substrate must find extra energy for rapid growth in feast periods, and deteriorate in famine periods. In case there is no available substrate left, they will be faced with maintenance problems to keep their proper shape of cell structure with the addition of a new substrate to the system. Bacteria that can store substrate as polymers e.g. PHB or similar compounds will be dominant because they can maintain more or less constant relatively low growth rate and can keep their viability in the case of external substrate depletion. Many substrates are degraded in the cell with Acetyl-CoA as intermediate so PHB is specifically interesting as a storage polymer and it is also the precursor for the formation of PHB.

3.2 Concise Review of Storage in Activated Sludge Processes

Biomass is subjected to concentration gradient of the carbon sources in activated sludge systems. This means biomass grows under dynamic conditions and storage is the main process for the removal of the substrate. Although the conditions show dynamic behavior, overall process is considered as steady-state. Sludge recycle is one of the reasons of dynamic conditions. Growth contributes to storage process and utilization of organic matter occurs (Majone *et al.*, 1999).

Microorganism adapts its cell composition (RNA, protein etc.) to the environment and reaches to a balanced growth, which shows that growth of cell is in optimum level and no further adaptation occurs (Roels, 1983; Grady *et al.*, 1996). If the culture is adopted to grow under a substrate-limited condition, available protein synthesis of the culture will not be enough to increase the growth rate when the limitation is removed. Therefore the protein synthesis and the specific growth rate will increase only gradually. However, if the adaptation of the culture to the old environment is not complete, there will be an extra protein synthesis available so the culture will increase its specific growth rate.

Storage process is very significant in activated sludge systems of dynamic conditions. In storage response, substrate uptake rate increases quickly and new solids are formed which are in different composition: all components during growth, but mainly storage polymers (generally polysaccharides and lipids) during storage. This leads to different kinetic and stoichiometric coefficients because synthesis of storage polymers is simpler than that of the whole cell: less physiological adaptation is required and also storage is faster than growth (Daigger and Grady, 1982a). Accumulation can also be considered as a substrate removal process (Grau *et al.*, 1982). Substrate is transported into cell and maintained in unchanged form or transformed to low molecular weight metabolic intermediates. Storage can be explained as a mechanism for preventing the accumulation of internal metabolites at toxic levels during the growth lags. Also the release of soluble metabolites or extracellular polymers has been observed as removal processes. Sorption is a simple physical-chemical interaction, which contributes to the fast removal of the soluble substrate in a similar way to the physical entrapment of the particulate one.

Biomass response mainly depends on its microbial composition and on the physiological state of the different microorganisms. Growth is a generally-known process, whereas storage, accumulation and release are alternative mechanisms when growth is too slow with respect to the dynamic conditions (Daigger and Grady, 1982a).

3.2.1 Experimental Approaches

Storage phenomena have been studied in pure and/or mixed cultures by many scientists. Typically, substrate uptake rate (SUR) and oxygen uptake rate (OUR) measurements are achieved to determine the dynamic response of the culture. In some cases of pure cultures (van den Eynde *et al.,* 1983), SUR and observed yields are higher than maximum values allowed under steady-state conditions, indicating that storage is a significant process in the removal of the substrate as a fast and high-yield response. The observed amount of polymer formed per unit of substrate removed ranges from 0.32 to 0.79 gCOD/gCOD. The yield has been observed as 0.73 gCOD/gCOD for PHB storage from acetate (van Aalst-van Leeuwen *et al.,* 1997) and 0.96 gCOD/gCOD for glycogen storage from glucose (van Loosdrecht et al., 1997). The stored products are firstly produced at a constant rate and then at a decreasing rate when the saturation of the maximum storage capacity is approached. This causes the overall and observed storage yields to vary over time on the F/M ratio of the experiment.

Intermittently fed sludges exhibit faster substrate uptake rates and higher observed yields then continuously fed ones. Capacity of accumulation is lower than the storage response, so Cech and Chudoba (1983) observed that substrate uptake rate is first quickly decreasing and then constant. Based on these approach, when sludge is intermittently fed both mechanisms are acting whereas only storage is possible for continuously fed sludge. The importance of storage response for mixed cultures has been confirmed by the determination of glycogen storage from glucose (van den Eynde et al., 1984; Matsuzawa and Mino, 1991) or PHB storage from acetate (Majone *et al.,* 1996).

Respirometric measurements give the most reliable results in the observation of microbial responses (Figure 3.3a). However Dircks *et al.* (1999) observed a tailing of the OUR curve and the respirogram has been divided into two phases (Figure 3.3b).

The yield in phase 1 is typically 0.71 gCOD/gCOD if acetate is added as substrate, similar with the experimental results of experiments carried out with excess acetate. These similarities are evidences for storage phenomena. This is confirmed that the observed yield obtained by considering both phases 1 and 2, is more in the range of what would be expected from the literature. The yield of acetate has a typical value of 0.5 gCOD/gCOD (Dircks *et al.*, 1999) as it is expected from aerobic bacteria growing without storage (van Loosdrecht *et al.*, 1997). If glucose is used as substrate supply, yields are higher with a range of 0.76-0.90 gCOD/gCOD. By considering that the theoretical yield for formation of glycogen from glucose is reported to be 0.96 gCOD/gCOD (van Loosdrecht *et al.*, 1997), these high values seem to confirm that storage is the main mechanism for the substrate removal. In the case of real wastewaters (containing a large fraction of slowly biodegradable substrate) the tailing in phase 2 is much more difficultly observed than the results with using only readily biodegradable substrates like acetate and glucose.

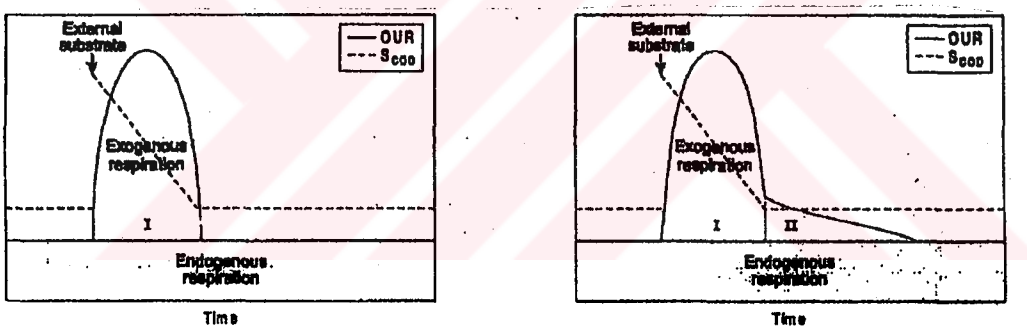

(a) (b)

Figure 3.3 (a) Typical respirogram from literature
(b) Respirogram exhibiting a tail (Dircks *et al.*, 1999)

Biosorption capacity of a sludge is defined as the specific amount of organic material which can be taken up in a real time. The term biosorption includes all the different mechanisms of substrate removal in the sludge (sorption, accumulation, storage, growth and oxidation). Therefore it is quite difficult to distinguish among them from simple bisorption experiments, where storage polymers are usually not measured. The yield that can be calculated from these experiments are also very high: 0.85 gCOD/gCOD (Gabb *et al.*, 1991).

3.2.2 Modeling Approaches

There are many approaches for the modeling of storage phenomena. These approaches can be summarized as unstructured and structured models (Majone *et al.*, 1999).

Unstructured Models: Changes in the internal composition of the biomass are ignored. The activities of the biomass are specified only by the amount of biomass itself. If there are no changes in the environment or these changes are very slow or very fast compared to changes in the biomass composition, these models provide a realistic approach (Harder and Roels, 1982; Roels, 1983). In this case the biomass can be assumed to be in a pseudo-steady-state as in the model of Monod for substrate limited growth of microorganisms. The active biomass and the storage products are considered as a whole in these models. As a matter of fact, soluble COD and oxygen are consumed and biological solids are formed in both storage and growth. Yields of these two processes are different but an overall yield will result that will lump them together. Then the utilization of internally stored products will contribute to the endogenous metabolism, which will be carried out at a higher rate. For that reason, the storage yield is higher and also the decay coefficient is bigger. Kinetic expressions for growth and storage on soluble substrate are different (growth is autocatalytic, storage is not), as well as for growth on stored products and endogenous metabolism (the amount of stored products will change by time, so endogenous metabolism will not be constant too). ASM1 (Henze *et al.*, 1987) can be considered as an unstructured model.

Structured models: If the adaptational mechanisms inside the biomass cannot be ignored any more, unstructured models become unreliable. Structured models are needed when a specific component of the biomass must be modeled as in the case of storage. The simplest approach can be proposed as the division of the biomass into an active cell fraction and a stored substrate fraction. Several storage models have been proposed for aerobic storage (Table 3.3). Very little or no energy requirement is taken into account for storage process, indicating that enmeshment, sorption and accumulation can be considered as dominating mechanisms. In fact, experimental studies show that there is a significant energy requirement for storage process due to soluble substrate removal. As seen from the Table 3.3, some models allow only storage firstly then growth on stored substrates whereas growth and storage occur

Table 3.3 Summary of kinetic models of storage and growth on stored products (Majone *et al.*, 1999)

Substrate	"Storage" related phenomena	STORAGE PHASE: Specific rate of storage as function of the concentration of: substrate	STORAGE PHASE: Specific rate of storage as function of the concentration of: stored product	Simultaneous growth on the substrate	Energy need (COD/ /COD)	CONSUMPTION PHASE: Specific rate of consumption of the stored product as function of:	CONSUMPTION PHASE: Maintenance or decay on the stored product	REFERENCE
soluble and particulate	adsorption storage	$f_{max}\frac{S}{K+S}$	$-\frac{X_{sto}}{X_{total}}$	no	no	$\frac{X_{sto}}{K_{sto}+X_{sto}}$	no	Andrews and Busby, 1973
particulate biodegradable	adsorption storage	S	$f_{max}-\frac{X_{sto}}{X_{total}}$	no	0.08	$\frac{X_{sto}/X_H}{K_{sto}+X_{sto}/X_H}$	yes	Ekama and Marais, 1979
unspecified	sorption internal storage external storage	S	$1-\frac{X_{sto}/X_H}{f_{max}}$	no	no	X_{sto}/X_H	yes	Padukone and Andrews, 1989
soluble readily biodegradable soluble rapidly hydrolysable	biosorption	S	$f_{max}-\frac{X_{sto}}{X_H}$	no yes	no no	$\frac{X_{sto}}{K_{sto}+X_{sto}}$	no	Novàk et al., 1995
soluble	accumulation storage	$\frac{S}{K+S}$	$\frac{K_I}{K_I+X_{sto}/X_H}$	no	0.10	$\frac{X_{sto}/X_H}{K_{sto}+X_{sto}/X_H}$	no	Hatziconstantinou and Andreadakis, 1994
acetate	storage	none	$1-\frac{X_{sto}/X_H}{f_{max}}$	yes	0.27	$(X_{sto}/X_H)-f_{min}$	yes	Van Aalst- van Leeuwen et al., 1997

Symbols: S substrate, X_{sto} stored product, X_{total} total biomass, X_H active biomass, f_{max} maximum storage capacity (maximum content of stored product per unit of biomass), f_{min} minimum content of storage products (per unit of biomass).

simultaneously in some of them. Simultaneous growth and storage means that the active biomass has the ability of immediately increasing its growth rate when substrate is added to the system. Storage before growth considers that the growth process can be regarded as negligible, growth rate starts to increase after storage is completed. The storage rate is always decreased by an increasing amount of the stored products in all of the approaches. This is an experimentally observed phenomenon; nevertheless reported storage capacities are often quite high. Thus this dependence could be of minor practical importance under sludge loading in the activated sludge systems. Storage rate has been proposed to be zero, first or shifting order, while for the growth on stored product it is first or shifting order. In the case of simultaneous growth and storage, there should be three different yield factors: for the growth of the biomass on the substrate, for the storage on the substrate and for the growth on the stored substrate. If there is no simultaneous growth and storage it is not necessary to define the yield for growth on external substrate.

The history of biomass (e.g. sludge age) can only be accounted for by adjusting kinetic parameters to the process conditions in the above models. As a matter of fact, structured modeling should include at least two components. Generally, synthetic and structural components are considered (Roels, 1983), even though much complicated approaches are discussed (Daigger and Grady, 1982a).

More knowledge should be improved on substrates different from acetate and glucose, in order to understand the behavior of high molecular weight soluble or colloidal substrates. It is precisely known that storage is more likely to occur on acetate and glucose than high molecular weight substrates but may be their storage can occur under very short-term conditions because of their fast hydrolysis. Also pure culture studies should be improved due to the cultivation of microorganisms at lower dilution rates and under cyclical dynamic conditions. In unstructured models, the storage is modeled in a potential way by the adjustment of growth and decay parameters. These types of models give good results where storage is not so important (e.g. for wastewaters with little concentration of soluble COD). Structured models, presenting a wide range of different expressions for stoichiometry and kinetics, are necessary if the population dynamics has to be taken into account.

3.3 Structured Metabolic Models

A metabolic model is based on the principle that the metabolism of organisms is composed of a limited number of metabolic pathways which results in more or less constant energy requirement and ultimately constant stoichiometry (Roels, 1983). Internal reactions are used for the description of metabolic pathways. These internal reactions are combined with reaction stoichiometry and degree of reduction balances to derive the linear equations describing the involved metabolism.

3.3.1 Metabolic Model for Aerobic Storage of Acetate for *Paracoccus Pantotrophus*

van Aalst-van Leeuwen *et al.* (1997) has proposed a metabolic model in which acetate is aerobically stored as PHB under dynamic conditions. In this metabolic approach the number of unknown parameters is reduced. A metabolically structured model based on the interpretation of experimental results has been proposed in order to describe the observed kinetics of PHB production and consumption by the selected microorganism. This model adequately describes the observed kinetics of PHB formation and consumption.

Biological wastewater treatment processes usually occur under dynamic conditions, volatile fatty acids (VFA) form the major soluble substrate in these processes. The microorganisms have the ability of fitting to rapidly changing conditions called as feast and famine periods, under these conditions the response of the activated sludge organisms is the production of storage polymers i.e., glycogen and poly-β-hydroxyalkonates (PHA). Under the conditions of excess carbon source, polyhydroxybutyrate (PHB) seems to be the more common storage polymer. Standard microbiological experiments use continuous cultures, which is in contrast with the study of van Aalst-van Leeuwen *et al.* (1997). Under conditions of a periodic carbon substrate surplus (feast/famine), the substrate uptake rate will be larger than required for growth. The uptake of substrate results in the formation of $NADH_2$ which is consumed by oxidative phosphorylation and leading to ATP formation. If the energy needed for growth is limited, then ATP will accumulate so $NADH_2$ will accumulate too. This explains why the production of a more reduced storage polymer-PHB (requires $NADH_2$) is more likely to be occurred when compared with the production of glycogen (leads $NADH_2$ formation).

van Aalst-van Leeuwen *et al.* (1997) used an acetic-acid limited continuous culture of *Paracoccus Pantotrophus* in order to observe the production and consumption of PHB. PHB production is observed when acetate is present and PHB consumption is followed when acetate is depleted. Biomass is assumed to contain two different parts as an active biomass compartment ($1-f_{PHB}$=capable of reproduction and growth) and a PHB fraction (f_{PHB}=used as storage for carbon and energy).

3.3.1.1 Metabolic Model for the Formation and Consumption of PHB

The aerobic metabolism of a microorganism capable of producing and consuming PHB can be described by seven internal reactions (Figure 3.4).

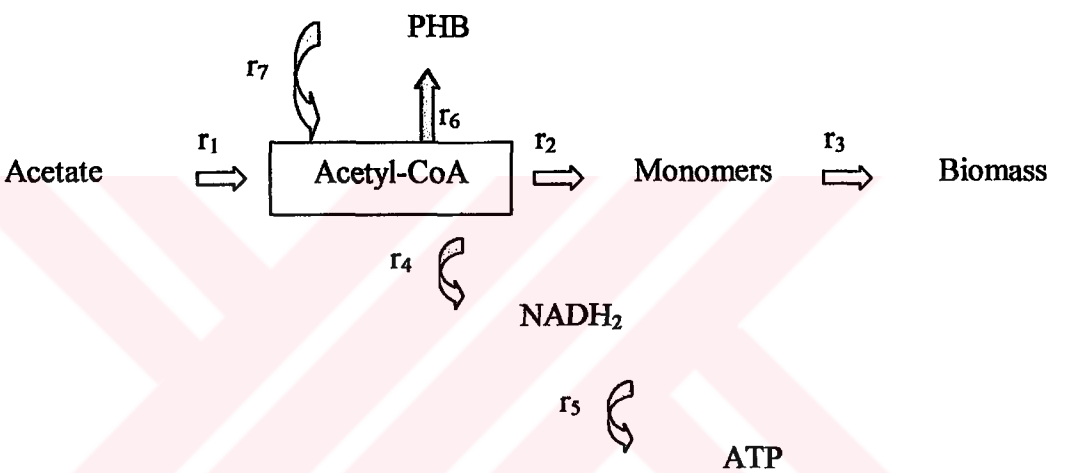

Figure 3.4 Schematic representation of the metabolism of an organism capable of forming and consuming PHB (van Aalst-van Leeuwen *et al.*, 1997)

Synthesis of Acetyl-CoA from Acetate, (r_1): Acetate is taken into cell by active transport, Acetyl-P is formed and at last conversion to Acetyl-CoA is completed.

Synthesis of biomass monomers from Acetyl-CoA, (r_2): This is the first part of the synthesis of active biomass.

Polymerization of biomass precursors and maintenance, (r_3): By this reaction, biomass formation is completed.

Carbon source catabolism, (r_4): Substrate uptake results in the formation of $NADH_2$.

Oxidative phosphorylation, (r_5): ATP is produced from $NADH_2$.

Synthesis of the storage product PHB from Acetyl-CoA, (r_6): The substrate is both used for the synthesis of biomass and PHB.

Synthesis of Acetyl-CoA from PHB, (r_7): In the absence of acetate, the microorganisms utilize the intracellulary accumulated PHB as carbon and energy source. The storage polymer is hydrolyzed and converted into Acetyl-CoA.

The metabolic model results in two equations describing the conversion processes for feast and famine phases. For the feast period, the linear equation describing acetate uptake, biomass growth, PHB production and maintenance is defined as below:

$$(-r_S) = \frac{1}{Y_{SX}^{max}} r_X + \frac{1}{Y_{SP}^{max}} r_P + m_S C_X \tag{3.1}$$

As similar, for the famine period describing PHB consumption, biomass growth, and maintenance is expressed with the following equation:

$$(-r_P) = \frac{1}{Y_{PX}^{max}} r_X + m_P C_X \tag{3.2}$$

where,

$$Y_{SX}^{max} = \frac{4\delta - 2}{4.13\delta + 4.32} \tag{3.3}$$

$$Y_{SP}^{max} = \frac{4\delta - 2}{4.5\delta} \tag{3.4}$$

$$Y_{PX}^{max} = \frac{4.5\delta - 0.5}{4.13\delta + 4.32} \tag{3.5}$$

$$m_S = \frac{m_{ATP}}{2\delta - 1} \tag{3.6}$$

$$m_P = \frac{m_{ATP}}{4.5\delta - 0.5} \tag{3.7}$$

The linear equations contain two unknown parameters namely, the ratio between ATP produced and electrons transferred from $NADH_2$ to an electron acceptor (δ) and the ATP consumption due to maintenance processes (m_{ATP}). Substituting of $r_X=\mu C_X$, $r_S=q_S C_X$, $r_P=q_P C_X$ followed by division by biomass concentration, C_X gives the following equation:

$$(-q_S) = \frac{1}{Y_{SX}^{max}}\mu + \frac{1}{Y_{SP}^{max}}q_P + m_S \qquad (3.8)$$

From earlier experiments (Pot, 1995), it was observed that maximum yield of biomass on acetate, Y_{SX}^{max} = 0.45 [C-mol/C-mol] and maintenance coefficient for growth on acetate, m_S = 0.038 [C-mol/C-mol.h]. The P/O ratio, δ = 1.84 [mol ATP/mol $NADH_2$] and the ATP maintenance coefficient, m_{ATP} = 0.102 [mol ATP/C-mol.h] were calculated by using the related equations and above values, also these parameters are considered to be constant within the experimental range. Maximum yield of PHB on acetate, Y_{SP}^{max} = 0.648 [C-mol/C-mol] was found by using the equation 3.4. Substituting these yield coefficients in eqn. 3.8 gives:

$$-q_S = 2.22\mu + 1.544q_P + 0.038 \qquad (3.9)$$

From the carbon balance and the degree of reduction balance relations for the specific carbon dioxide production rate (q_C) and for the specific oxygen consumption rate (q_O) can be derived as a function of μ and q_P:

$$q_C = (-q_S) - \mu - q_P = 1.22\mu + 0.544q_P + 0.038 \qquad (3.10)$$

$$(-q_O) = 1.188\mu + 0.419q_P + 0.038 \qquad (3.11)$$

Stoichiometry of the kinetic model for the PHB production can be based upon equations 3.9 – 3.11.

Maximum yield of biomass on PHB, Y_{PX}^{max} = 0.653 [C-mol/C-mol] and maintenance coefficient for growth on PHB, m_P = 0.0131 [C-mol/C-mol.h] were calculated for the famine phase. Below equations were derived by using these values:

$$(-q_P) = \frac{1}{Y_{PX}^{max}}\mu + m_P \qquad (3.12)$$

$$-q_P = 1.532\mu + 0.0131 \qquad (3.13)$$

$$q_C = 0.532\mu + 0.0131 \qquad (3.14)$$

$$(-q_O) = 0.693\mu + 0.0147 \qquad (3.15)$$

Stoichiometry of the kinetic model for the PHB consumption can be based upon equations 3.13 – 3.15.

It was observed from experimental and modelling results that, immediately after the pulse addition the substrate uptake rate reaches its maximum value. However the growth rate only slightly relates to the maximal growth rate (van Aalst-van Leeuwen *et al.,* 1997). The excess of substrate taken up is stored in the cell as PHB between the feast and famine periods. Stored substrate is used for growth process after all external substrate is consumed. The growth rate slowly decreases during the growth of PHB presumably related to the reduction in PHB amount. According to the standart theory, the substrate uptake rate in a chemostat is found by the multiplication of the maximal uptake rate and Monod factor for the substrate relationship. This is an evidence for that the organisms will induce a maximal level of substrate uptake enzymes, while the enzyme system for cell growth will presumably not be completely induced. So, even though the cells are cultivated close to growth rate of zero, the maximal substrate uptake activity will be maintained. The conditions are firmly different from a chemostat in wastewater treatment processes under dynamic conditions. It can be discussed that under such conditions microorganisms that have a fully induced substrate uptake system, accumulate more substrate and outcompete organisms that do have lower substrate uptake rates.

The maximal substrate uptake rate of an organism is generally independent of the real growth rate of that organism (Roels, 1983). In the model of van Aalst-van Leeuwen *et al.* (1997), it was proposed that PHB is generally used as a buffer for the substrate taken up but not directly needed for growth. The storage polymers can play a significant role in microbial growth under unbalanced conditions (van den Eynde *et al.,* 1984; van Loosdrecht *et al.,* 1997). PHB accumulation has been reported in many laboratary scale studies and also in activated sludge systems (van Loosdrecht *et al.,* 1997). PHB utilization by cells subjected to large concentration gradient in substrate amount is done for the effective balance of the differences between substrate uptake rate and substrate need for growth. So the cell can balance internal metabolism, and also can have advantage of competition among other microorganisms which are not capable of producing storage compounds.

In reality, the substrate is available mostly in a dynamic case. Substrate storage and so balanced growth has many advantages when compared with the periods of quick

growth and then periods of starvation. It is not sufficient to use only the conventional Monod type kinetics in order to predict the competition for the description of what is happening in wastewater treatment plants. The proposed model (van Aalst-van Leeuwen *et al.*, 1997) can be used with the aim of evaluating the growth on internally accumulated PHB in activated sludge systems.

3.3.2 Metabolic Model for Aerobic Storage of Acetate for Mixed Culture

PHB metabolism in aerobic, slow growing, activated sludge cultures based on a metabolic model has been observed by Beun *et al.* (2000). A mixed microbial population was subjected to external substrate under dynamic conditions. Formation of intracellular storage and PHB consumption was observed. A synthetic wastewater and sludge from a conventional activated sludge wastewater treatment plant were used in the experiments.

The metabolic model is the same as described in van Aalst-van Leeuwen *et al.* (1997), with the exception of biomass composition. van Aalst-van Leeuwen *et al.* (1997) formulated a metabolic model describing the stoichiometry of PHB metabolism by a pure culture of *Paracoccus Pantotrophus* under dynamic substrate supply as mentioned in the previous section. Linear equations for feast and famine phases, yield factors and maintenance coefficients; r_S, r_P, Y_{SX}, Y_{SP}, Y_{PX}, m_S, m_P are as the same with the model of van Aalst-van Leeuwen *et al.* (1997). For the yield coefficients regarding growth on PHB (Y_{PX}^{max}), there is a scarce information in literature. This value is reported for a mixed culture of bio-P bacteria by Smolders *et al.* (1994) and for a pure culture by van Aalst-van Leeuwen *et al.* (1997).

Storage of PHB in relation to activated sludge models is also defined particularly in Beun *et al.* (2000). In ASM1, the biomass is considered as one compound with a yield of total biomass (including PHB if present) on substrate. Stored substrate is accounted for as active biomass. Consumption of stored substrate is accounted for in the biomass decay process and characterized as slowly degradable substrate. In ASM3 and in metabolic models, the biomass is divided into two as an active biomass fraction with a yield of active biomass on substrate and a PHB fraction with a yield of PHB on substrate (Figure 3.5).

Beun *et al.* (2000) found that the bacteria can balance their growth rate under dynamic substrate supply, using the PHB metabolism and adjusting the substrate

uptake rate. So bacteria can compete effectively for substrate. In the feast period acetate is taken up with a maximal specific acetate uptake rate. Meanwhile PHB is produced with a constant rate. Biomass growth on PHB leads to only 4-10% lower biomass yield compared to direct utilization of acetate for growth. 66% - 100% of the acetate consumed is used for PHB synthesis process (in steady-state systems) and the rest of the acetate consumed is utilized for growth and maintenance. In activated sludge processes, it is relevant to determine whether the percentage of the acetate consumed which is utilized for PHB synthesis process is a constant value or depend on the conditions of the system.

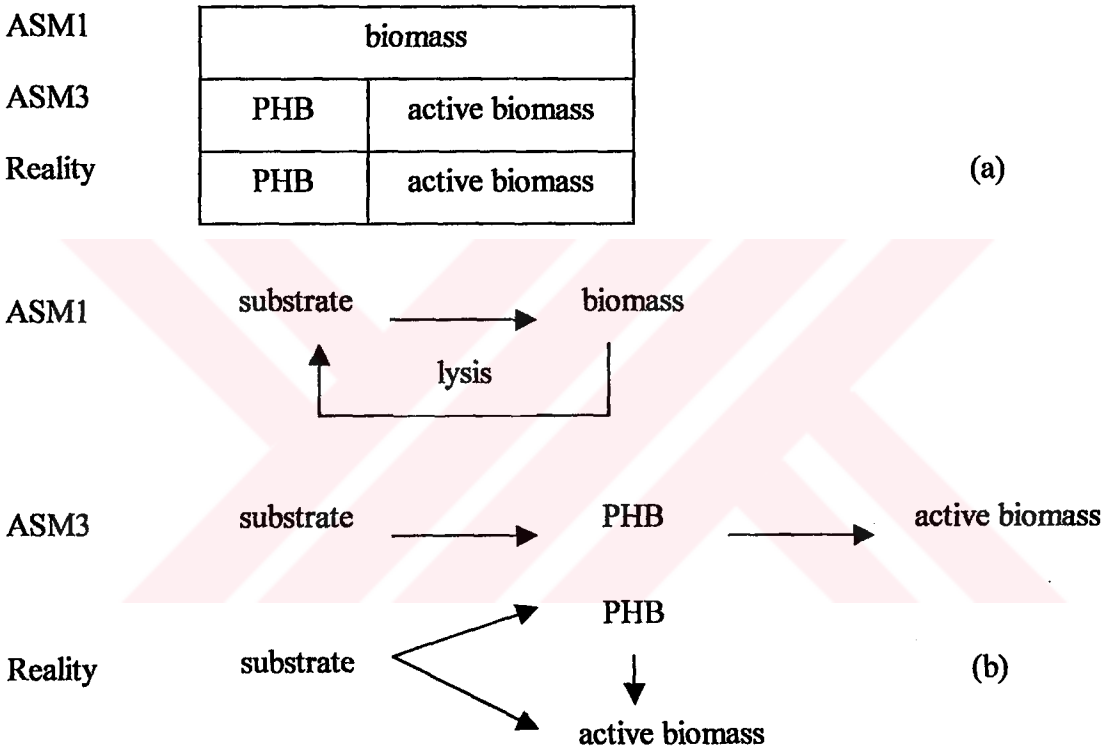

Figure 3.5. (a) Composition of the biomass in ASM1, ASM3 and reality.
(b) Comparison of major carbon flows in ASM1, ASM3 and reality.
(Beun *et al.*, 2000)

3.3.3 Metabolic Model with Structured Biomass

Growth can occur both on the external substrate and internal substrate under dynamic conditions. It must be evaluated whether bacteria utilize external substrate rather for cell growth or for storage process. In case of growth takes place on internal substrate, the situation can be evaluated defining only one rate and one stoichiometric yield coefficient. Experimentally it is observed that the growth rate in the presence of external substrate (acetate or glucose) is significantly faster than the growth rate on

the storage polymer (PHA or glycogen) with the same sludge (Beun *et al.*, 2000). Even though the yield coefficients of biomass and the specific substrate uptake rates are different with varying electron acceptors, the rate of consumption of PHA is the same under aerobic conditions (Beun *et al.*, 2000). In the feast phase the degradation rate of these substrates is only dependent on the character of storage polymer in the cells and independent of growth rate or the sludge age (Beun *et al.*, 2001). According to this, the growth on internal substrates is primarily determined by the substrate consumption rate, while growth rate and the respiration rate are coupled by stoichiometry. The conversion rate of PHA with respect to the PHA content of the biomass as a first order rate based on experimental observations although other rate order coefficients can give good description as well. Also in the definition of ASM3 it is suggested by a high value for the similarity coefficient for PHA (Gujer *et al.*, 2000).

The organisms have the chance to use the substrate for growth or storage processes if external substrate is available. Conventionally it is assumed that competing microorganisms maximize their growth rate and storage only occurs if some growth related compound (e.g. ammonium) is limited. In reality, the actual growth rate is the most important parameter in the competition for traditional batch&continous culture conditions. This approach may be too simple for most of the natural systems. Under dynamic conditions, a large quantity of organisms maximize their substrate uptake rate while growing at a approximately balanced rate (van Loosdrecht, 1997). The difference between actual substrate uptake rate and growth rate results in the storage of substrate. In other words, the bacteria compete on substrate uptake rate rather than growth rate. Therefore, in kinetic models a kinetic rate for substrate uptake rate can be chosen and the growth rate can be calculated from the stoichiometry. If substrate is used simultaneously for growth and storage by the organism then, two rates must be defined to calculate the conyersion rates for other compounds. In the study of Beun *et al.* (2001), the substrate uptake rate seems to be only a little dependent of the sludge age of the culture. This can be explained by the accumulation of the inert material. Microorganisms appear to maximize the substrate uptake rate. In case of non-occurence of storage, the maximal substarte uptake will correspond to the maximal growth rate by the maximal yield coefficient. It was experimentally observed that the organisms grow with a certain rate whereas the substrate which is

not used is converted into storage materials. Less substrate is converted into storage polymers at the higher growth rate. For pure cultures, with the sudden addition of substrate, the growth only slowly changes to a new higher value whereas the substrate uptake rate immediately reaches its maximal value (van Aalst-van Leeuwen *et al.*, 1997). PHA formation balances the difference between substrate uptake rate and consumption for growth.

In ASM3 it was suggested that growth always occur on stored polymers, which is not valid. Real process models are necessary for a detailed description and understanding of microbial processes. This implies that the variable growth rate on external substrate as a function of the sludge age requires description. Krishna *et al.* (1999b) proposed a hypothesis to predict the growth rates during the periods of substrate availability. The growth rate will depend on the level of the protein synthesising system (RNA's and anabolic enzymes) in the cell of the organism. This system can be a large mass fraction of the cellular composition (van Loosdrecht and Heijnen, 2002). The amount of enzymes needed to take up substrate and to convert it into storage polymers is quite limited, whereas the amount of RNA and enzymes required for growth at a maximum rate has a large metabolic burden. It seems more adventageous for an organism that grow under dynamic conditions to take up substrate if it is available immediately and utilize the accumulated substrate to grow over a longer period. Substrate storage and subsequent growth on it results into a slightly lessened net growth yield (Beun *et al.*, 2000). It could be that two types of organisms exist: the ones that maximize the growth rate and the ones that optimize the growth rate. Both of them will have a reduced yield under dynamic conditions but the differences can be so small that mutual existence is possible. In order to describe the storage process it is necessary to define model with a structured biomass not only with different fractions of storage polymers but also with a variable amount of anabolic enzymes (Harder and Roels, 1982).

3.3.3.1 Metabolic Model Based on Enzyme-Structured Biomass

Microbial cells try to balance the level of their protein synthesis system (RNA and enzymes). Generally, most RNA and enzymes will be induced when the substrate is available (under conditions when they are required). These cellular components are subject to a constant decay processes at the same time. This indicates that when

external substrate is available the anabolic enzymes are induced and the enzyme fraction in the cell will increase. Formation of this system will be repressed during conversion of storage polymers because there is an excess of protein synthesis capacity. Due to the enzyme decay and dilution of the newly generated cell material, the level of RNA and enzymes in the cells will reduce. The balance between enzyme synthesis and decay leads to the level of induction of protein synthesis system and consequently to the actual growth rate in the availability of external substrate.

A model is formulated by van Loosdrecht and Heijnen (2002) based on the model presented by Kompala *et al.* (1984) and extended by Turner and Ramkrishna (1988) to describe enzyme-structured biomass. The main difference is the absence of an precisely expressed maximum enzyme amount. It is assumed that the balance between production and decay will give a maximum enzyme level as occurring in real cells. Proposed model is based on the metabolic model of Beun *et al.* (2000) developed for PHB formation and consumption by mixed cultures. Conversion of acetate to PHB and new biomass in feast phase is described in equations 3.16 and 3.17 while equation 3.18 shows the growth on PHB in famine phase as below:

$$r_S = \frac{1}{Y_{SP}} r_{STO} + \frac{1}{Y_{SX}} r_X + m_S X_H \qquad (3.16)$$

$$r_{STO} = Y_{SP} r_S - \frac{Y_{SP}}{Y_{SX}} r_X - m_S Y_{SP} X_H \qquad (3.17)$$

$$r_X = Y_{PX} r_{STO} - m_P Y_{PX} X_H \qquad (3.18)$$

The model is presented in Table 3.4. The actual growth rate on a substrate is related to the level of enzyme induction for growth on that substrate (Kompala *et al.*, 1984; Turner and Ramkrishna, 1988). This general approach is also used in this model but there is a critical difference: the above authors assume the organisms try to grow as quick as possible, while in this model it was assumed that the protein synthesis system is only induced when there is an external substrate available while the organisms compete effectively only on substrate uptake rate. There is no stoichiometry for the enzyme conversion process since there is not sufficient information on yield coefficients or concentrations of enzymes. Reactor conditions

Table 3.4 Matrix representation of the proposed model structure (van Loosdrecht and Heijnen, 2002)

	Acetate S_{Hac}	Ammonium S_N	Oxygen S_O	Biomass X_H	PHB X_{PHA}	Anab. Enz. X_e	Rate
Feast Phase – aerobic							
Acetate Uptake	-1		$-(1-Y_{SP})$		Y_{SP}		$q_{HAc}^{max} \cdot M_{HAc} \cdot M_O \cdot X_H$
Growth		$-i_N$	$-\left(\frac{Y_{SP}}{Y_{SX}}-1\right)$	1	$-\frac{Y_{SP}}{Y_{SX}}$		$\mu^{max} * \frac{\mu^{max}+\beta}{\alpha+\alpha^*} * f_e \cdot M_{HAc} \cdot M_O \cdot M_N \cdot X_H$
Endogenous Rate			$-Y_{SP}$		$-Y_{SP}$		$m_S \cdot M_{HAc} \cdot M_O \cdot X_H$
Famine Phase – aerobic							
PHB consumption		$-i_N \cdot Y_{PX}$	$-(1-Y_{PX})$	Y_{PX}	-1		$k_{PHB} \cdot f_{PHB} \cdot I_{HAc} \cdot M_O \cdot M_N \cdot X_H$
Endogenous Rate		$i_N \cdot Y_{PX}$	$-Y_{PX}$	$-Y_{PX}$			$m_{PHB} \cdot I_{HAc} \cdot M_O \cdot X_H$
Feast Phase – anoxic			Nitrate S_{NO}				
Acetate Uptake	-1		$-(1-Y_{SP})/2.86$		Y_{SP}		$q_{HAc}^{max} \cdot M_{HAc} \cdot M_O \cdot X_H$
Growth		$-i_N$	$-\left(\frac{Y_{SP}}{Y_{SX}}-1\right)/2.86$	1	$-\frac{Y_{SP}}{Y_{SX}}$		$\mu^{max} * \frac{\mu^{max}+\beta}{\alpha+\alpha^*} * f_e \cdot M_{HAc} \cdot M_O \cdot M_N \cdot X_H$
Endogenous Rate			$-Y_{SP}/2.86$		$-Y_{SP}$		$m_S \cdot M_{HAc} \cdot M_O \cdot X_H$
Famine Phase – anoxic							
PHB consumption		$-i_N \cdot Y_{PX}$	$-(1-Y_{PX})/2.86$	Y_{PX}	-1		$k_{PHB} \cdot f_{PHB} \cdot I_{HAc} \cdot M_O \cdot M_N \cdot X_H$
Endogenous Rate		$i_N \cdot Y_{PX}$	$-Y_{PX}/2.86$	$-Y_{PX}$			$m_{PHB} \cdot I_{HAc} \cdot M_O \cdot X_H$
Protein synthesis system							
Rate						1	$(\alpha^* M_{HAc} * M_O * M_N - \beta * f_e + \alpha^*) * X_H$

$$f_{PHB} = \frac{X_{PHB}}{X_H} \qquad f_e = \frac{X_e}{X_H} \qquad M_i = \frac{S_i}{S_i + K_i} \qquad I_i = \frac{K_i}{K_i + S_i} \qquad \mu^{max} = Y_{SX} * q_{HAc}^{max}$$

$$Y_{SX} = \frac{4 \cdot \delta - 2}{4.2 \cdot \delta + 4.32} * \frac{4.2}{4}; \quad Y_{SP} = \frac{4 \cdot \delta - 2}{4.5 \cdot \delta} * \frac{4.5}{4}; \quad Y_{PX} = \frac{4.5 \cdot \delta - 0.5}{4.2 \cdot \delta + 4.32} * \frac{4.2}{4.5};$$

Aerobic growth: $\delta = 2.0$ molATP/2e$^-$; Anoxic growth : $\delta = 1.2$ molATP/2e$^-$

$$m_S = \frac{m_{ATP}}{2 \cdot \delta - 1} * \frac{4}{4.2}; \quad m_p = \frac{m_{ATP}}{2.25 \cdot \delta - 0.25} * \frac{4.5}{4.2};$$

m_{ATP}=0.02 molATP/C-mol.h

and kinetic values reported by Beun *et al.* (2001) were used for the model for aerobic, pulse fed, sequencing batch reactors.

The formation and decay rates of the protein synthesis system almost has not been studied and certainly not under conditions related to activated sludge systems (van Loosdrecht and Heijnen, 2002). It is possible that the formation and decay rates of enzymes are similar for all bacteria since the cell internal processes are generally similar for various microorganisms. In that case, there is a potential to improve the activated sludge models, because e.g. the growth rate on external substrate can be a predictable variable instead of a parameter, which has to be estimated from experiments. Growth on storage polymers is defined by the polymer consumption rate rather than the growth rate potential of the cells. This means that consumption rate of storage polymers should be used instead of growth rate in mathematical models like ASM3. The consumption rate of storage polymers should be described by a first order rate instead of saturation kinetic.

Proposed model includes RNA and anabolic enzymes and separate biomass compartments for storage polymers. This model is capable to simulate the behavior of organisms under dynamic conditions. The main objective of the proposed model is a general microbial ecology principle that bacteria compete on substrate uptake rate rather than on growth rate.

3.4 Storage Phenomena in ASM3 and Modifications

In ASM3 the aerobic storage process describes the storage of readily biodegradable substrate (S_S) in the form of cell internal storage products (X_{STO}). This process requires energy in the form of ATP, which is obtained from aerobic respiration. In ASM3, it is assumed that all the readily biodegradable organic matter is first taken up by the heterotrophic organisms through storage process and so converted to the stored material, which is then assimilated to biomass. It is known that this is probably not the reality but it was considered that there is no reason to complicate the model by introducing an extra coefficient for the division of substrate between storage and growth.

Simultaneous storage and growth is observed in many experiments, also stored polymers are utilized only after the depletion of the primary substrate. So

modifications in ASM3 were made for a more consistent description including growth on primary substrate. There are two mechanisms for storage under aerobic conditions: PHB storage when fed with acetate and glycogen storage when fed with glucose.

3.4.1 Modified ASM3 for Acetate

This model is the first attempt to evaluate the deficiencies of ASM3. Conversion of acetate, ammonium, oxygen, biomass and PHB were measured at different temperatures in a laboratory SBR system. These measurements are compared to a simplified version of ASM3 including only those processes and components relevant for the aerobic conversion of acetate. An adopted model structure is proposed based on the deviation between model and experiments.

ASM3 is simplified for the case of only aerobic heterotrophic conversions and acetate as the only substrate. The matrix form of simplified version of ASM3 is given in Table 3.5 and kinetic parameters are shown in Table 3.6. The processes included in the simplified version of ASM3 are the aerobic storage of readily biodegradable substrate, aerobic growth of heterotrophs, aerobic endogenous respiration and aerobic respiration of storage products. All expressions and parameters were chosen according to the description of Gujer *et al.*, (2000), except the conversion of particulate COD components to TSS and fraction of nitrogen in the biomass. Experimentally observed values were used for those parameters.

Simulation results were not so successful in predicting the observed experimental results. Simplified ASM3 simulations gave too low acetate uptake rate, very high PHB turn-over, low MLSS concentrations and low OUR and growth rate for feast phase. To evaluate whether the choice of stoichiometric parameters was the cause of bad model predictions, the stoichiometric coefficients of simplified ASM3 were changed with that of obtained in earlier experiments of van Aalst-van Leeuwen et al. (1997). According to this study, the maximum yield of PHB on acetate was Y_{SP}^{max} = 0.648 [C-mol/C-mol] and the yield of biomass on PHB was Y_{PX}^{max} = 0.653 [C-mol/C-mol]. Those yield coefficients were used in the matrix with new stoichiometric coefficients for the SBR process using acetate as a sole substrate supply whereas the kinetic parameters remain the same. New simulation results showed not much

Table 3.5. Matrix representation of simplified ASM3 (Krishna and van Loosdrecht, 1999)

Component → / Process ↓	1 S_O	2 S_S	3 S_{NH}	4 X_I	5 X_H	6 X_{STO}	7 X_{TS}	8 Process Rate
1. Aerobic storage of COD (PHB storage)	$-(1-Y_{STO})$	-1				Y_{STO}		$k_{STO}\frac{S_O}{K_O+S_O}\frac{S_S}{K_S+S_S}X_H$
2. Aerobic growth on PHB	$-\frac{1-Y_{H2}}{Y_{H2}}$				1	$-\frac{1}{Y_{H2}}$		$\mu_{H2}\frac{S_O}{K_O+S_O}\frac{K_S}{S_S+K_S}\frac{S_{NH}}{K_{NH}+S_{NH}}\frac{X_{STO}/X_H}{K_{STO}+X_{STO}/X_H}X_H$
3. Aerobic endogenous respiration	$-(1-f_I)$			f_I	-1			$b_{H,O2}\frac{S_O}{K_O+S_O}X_H$
4. Aerobic respiration of PHB	-1					-1		$b_{STO,O2}\frac{S_O}{K_O+S_O}X_H$
5. Aerobic growth on acetate	$-\frac{1-Y_{H1}}{Y_{H1}}$	$-\frac{1}{Y_{H1}}$			1			$\mu_{H1}\frac{S_O}{K_O+S_O}\frac{S_S}{K_S+S_S}\frac{S_{NH}}{K_{NH}+S_{NH}}X_H$

improvement that the HAc uptake rate was too slow, the PHB turnover was still too high and growth rate in feast phase was low.

Table 3.6. Kinetic parameters of simplified ASM3
(Krishna and van Loosdrecht, 1999)

Parameter	Characterization	Model A	Simplified ASM3
$b_{H,O2}$, d^{-1}	Aerobic endogenous respiration rate of X_H	0.2	0.2
$b_{STO,O2}$, d^{-1}	Aerobic respiration rate of X_{STO}	0.2	0.2
K_I, g COD m^{-3}	Acetate inhibition of growth on PHB	0.1	
K_{NH}, g N m^{-3}	Ammonium saturation as nutrient	0.01	0.01
K_O, g O_2 m^{-3}	Saturation constant for S_O	0.2	0.2
K_S, g COD m^{-3}	Saturation constant for substrate S_S, (HAC)	0.1	0.1
k_{STO}, g SS g^{-1} $X_H d^{-1}$	Storage rate constant	10	5
K_{STO}, g X_{STO} g^{-1} X_H	Saturation constant for X_{STO}	1	1
μ_{H1}, d^{-1}	Heterotrophic maximum growth rate on HAC	4	2
μ_{H2}, d^{-1}	Heterotrophic maximum growth rate on PHB	2	

It was decided to calibrate the model on kinetic coefficients for storage and heterotrophic growth (k_{STO} and μ) because of the deviation between the model predictions and experimental results. The simulation results with adjusted stoichiometric and kinetic coefficients were generally in agreement with experimental results (Table 3.7). Predicted OUR, was in good accordance as illustrated in Figure 3.6, however the growth rate shows great difference (Figure 3.7). When the acetate uptake stopped, a discontinuity is observed in experiments for growth rate like observed before by van Aalst-van Leeuwen *et al.* (1997). This discontinuity cannot be adequately subject to simulation when growth occurs on a single substrate.

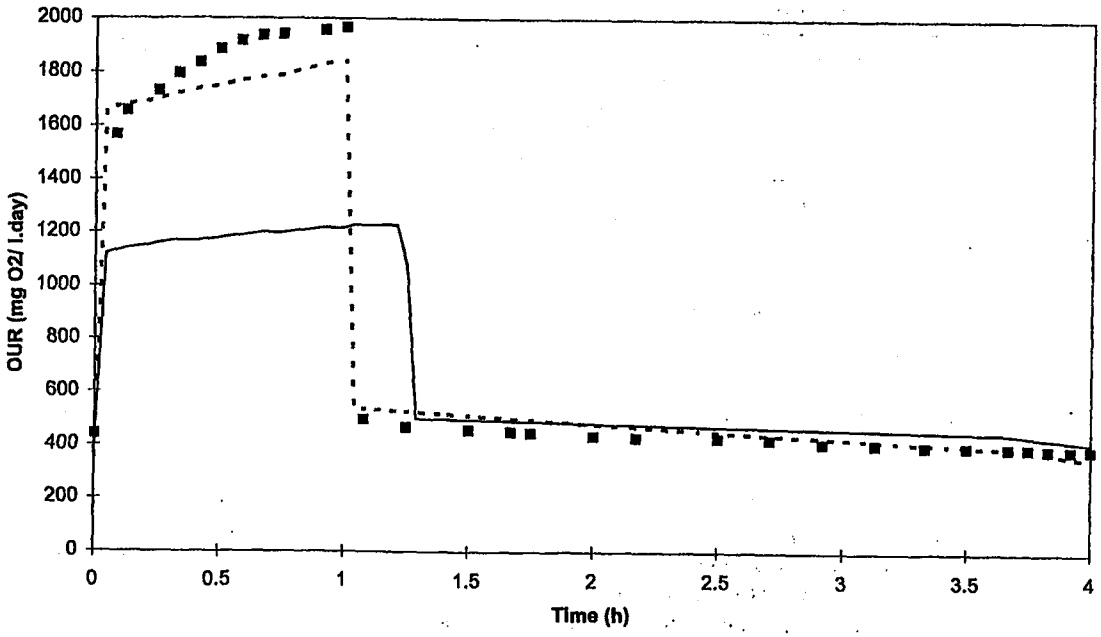

Figure 3.6 Comparison of OUR with ASM3 and Simplified ASM3 (Krishna and van Loosdrecht, 1999)

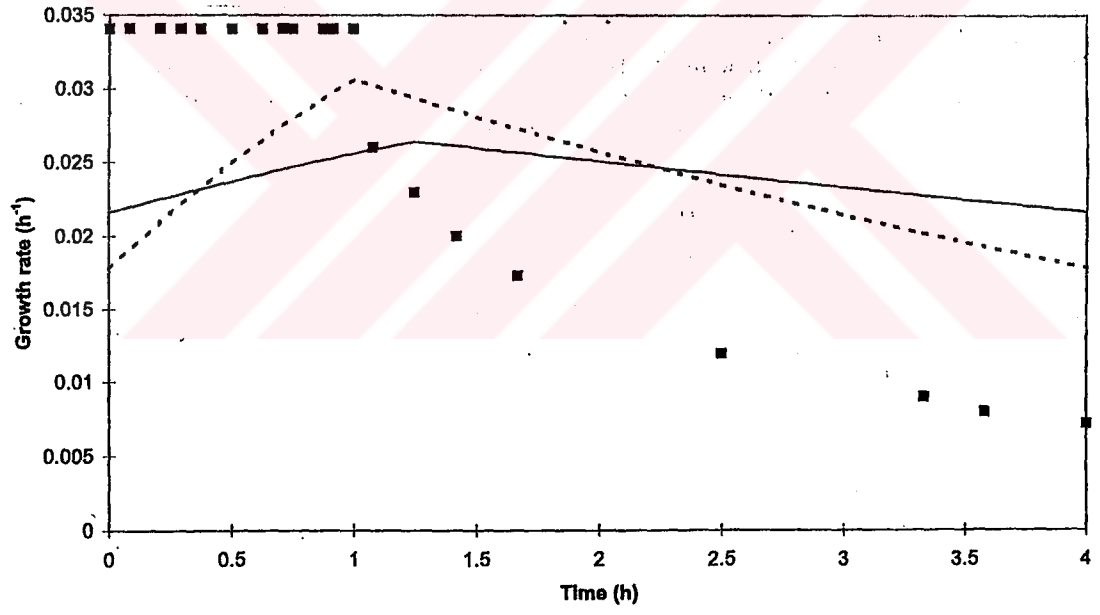

Figure 3.7 Comparison of Growth Rate with ASM3 and Simplified ASM3 (Krishna and van Loosdrecht, 1999)

Alternative model structure for heterotrophic growth and substrate storage in activated sludge processes proposed by Krishna and van Loosdrecht (1999) is called as Model A. Differences between ASM3 and Model A is illustrated in Figure 3.8. The components of new model and simplified ASM3 are the same. The original model structure of ASM3 as presented in Table 3.5, (processes 1 and 4) was expanded by adding the growth process on soluble substrate (acetate for this case;

process 5 in the concerned table). It is also assumed that HAc is inhibiting the growth of heterotrophs on PHB (process 2).

A simulation with kinetic data as obtained in the previous simulations gave already reasonable results. Only the growth in famine phase was too high and acetate uptake rate was slower. So the kinetic coefficient for growth on PHB was decreased and the aerobic respiration of PHB was increased. The aerobic endogenous respiration was left unchanged because it is believed that a large part of the endogenous respiration is due to predation (van Loosdrecht and Henze, 1999). The respiration rate on storage products then accounts for this predation plus the maintenance substrate requirements of the cells. Aerobic endogenous respiration rate of heterotrophs is then only associated to this predation process. Calibrated rate coefficients used in new simulations were given in Table 3.6. Table 3.8 gives a comparison between simulation results with model A and experimental results, indicating a satisfactory fit. With the defined model structure, the differences in growth rate between feast and famine phases could easily be described (Figure 3.9).

Table 3.7. Comparison of experimental results and simulations with the simplified ASM3, ASM3 with experimentally obtained yield coefficients on HAc and with calibrated kinetic coefficients at 20°C (Krishna and van Loosdrecht, 1999)

Process components	**Measured Value**	**Standard**	**Simplified ASM3**	
			HAc yield coefficients	**HAc yield and calibrated kinetic coefficients**
PHB conversion (mg COD/l)	120	110	100	115
NH_4 consumption (mg N/l)	5.7	5.2	4.9	6.0
TSS (mg/l)	830	815	765	855
		feast phase		
ΔN(mg N/l)	2.6	2.0	1.8	2.4
f_{PHB} (end of feast phase)	0.23	0.43	0.41	0.23
HAc (end of feast phase) (mg COD/l)	0	36	44	0.1
		famine phase		
ΔN(mg N/l)	3.1	3.2	3.0	3.6
f_{PHB} (end of feast phase)	0.10	0.33	0.32	0.11

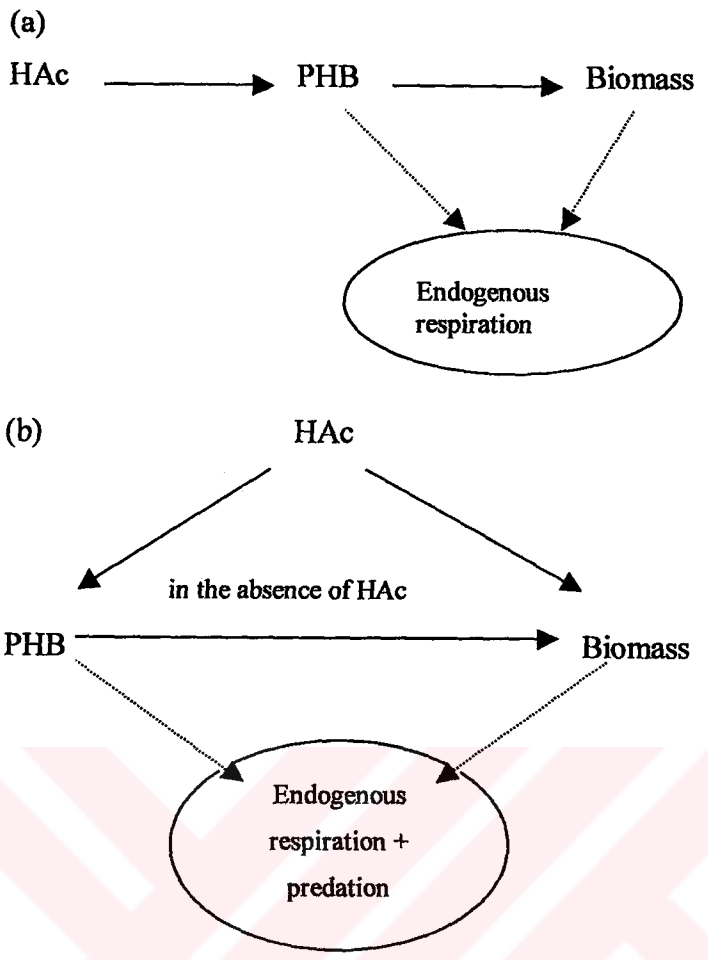

Figure 3.8. (a) Schematic representation of the substrate flux in ASM3.
(b) Schematic representation of the substrate flux in the new model (model A)
(Krishna and van Loosdrecht, 1999)

Table 3.8. Comparison of experimental results and simulations with modelA
(Krishna and van Loosdrecht, 1999)

Process components	Measured value	Simulated value with model A
PHB conversion (mg COD/l)	120	105
NH_4 consumption (mg N/l)	5.7	5.8
TSS (mg/l)	830	840
	feast phase	
ΔN(mg N/l)	2.6	2.6
f_{PHB} (end of feast phase)	0.23	0.23
HAc (end of feast phase) (mg COD/l)	0	0
	famine phase	
ΔN(mg N/l)	3.1	3.2
f_{PHB} (end of feast phase)	0.10	0.11

As a result, simplified ASM3 gives a reasonable description of the studied SBR processes, but the discontinuity in growth rate between feast and famine phases cannot be described. Therefore a new model structure is proposed based on experimental observations (Krishna and van Loosdrecht, 1999).

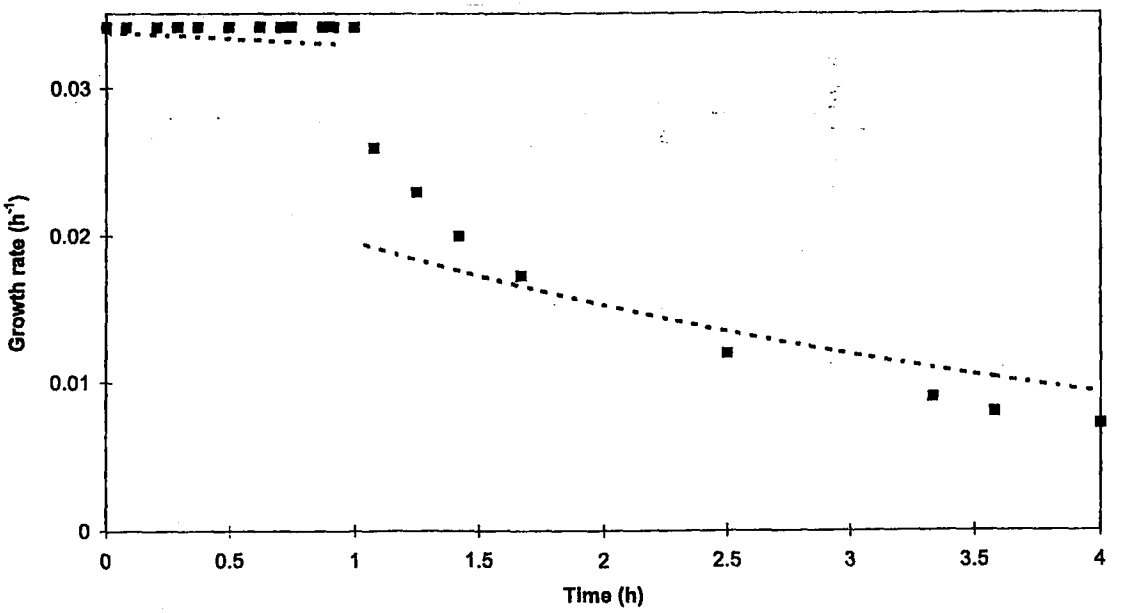

Figure 3.9 Comparison of the Growth Rate with Model A
(Krishna and van Loosdrecht, 1999)

3.4.2 Modified ASM3 for Both Acetate and Glucose

In Karahan-Gül *et al.* (2002b) ASM3 is modified due to the assumption of simultaneous growth and storage on the primary external substrate. According to the proposed modified version, direct heterotrophic growth on primary external substrate is included as a new process. Storage of external substrate as internal storage products and growth on these storage polymers after the depletion of external substrate are also included in the model.

Depending on previous studies (van Aalst-van Leeuwen *et al.*, 1997; Krishna and van Loosdrecht, 1999; Beun *et al.*, 2000), Karahan-Gül *et al.* (2002b) stated that they are different from ASM3, because ASM3 says growth is only occured on stored polymers. ASM3 also fails to simulate high rate of oxygen utilization in feast phase and lower rate in famine phase due to above single growth process definition.

There are two different mechanisms explaining the storage of S_S as said before. PHB metabolism has been described by van Aalst-van Leeuwen *et al.* (1997) and the stoichiometry and kinetics have been studied by Beun *et al.*, (2000). Glycogen metabolism and relevant stoichiometric and kinetic coefficients have been studied by Dircks *et al.*, (2000). Yield values found for acetate and glucose are summarized in Table 3.9.

Table 3.9 Yields of acetate and glucose (Karahan-Gül *et al.*, 2002b)

Substrate →	**Acetate**		**Glucose**
Yield value ↓	**van Aalst-van Leeuwen *et al.* (1997)**	**Beun *et al.* (2000)**	**Dircks *et al.* (2001)**
Growth yield under feast conditions (g cell COD/g COD)	0.47	0.41	0.57
Storage yield (g COD/g COD)	0.73	0.69	0.91
Growth yield under famine conditions (g cell COD/g COD)	0.60	0.57	0.60

Based on the scientific background suggested by metabolic models, the addition of growth process on the primary (external) carbon source to ASM3 was proposed. The modeling studies were conducted by Krishna and van Loosdrecht (1999a). The modified version for the carbon removal processes of ASM3 has been prepared by Karahan-Gül *et al.* (2002b) and presented in Table 3.10. The proposed model consists of hydrolysis, endogenous respiration of biomass and respiration of storage products processes as described in ASM3. Storage of readily biodegradable substrate and primary growth processes were described as simultaneous processes competing for substrate and electron acceptor. Both processes have reaction rates according to Monod kinetics where growth process has ammonia nitrogen and bicarbonate limitations. Secondary growth process is inhibited when primary substrate is present in the system, uses products as substrate and process kinetics was defined as surface reaction kinetics similar to ASM3.

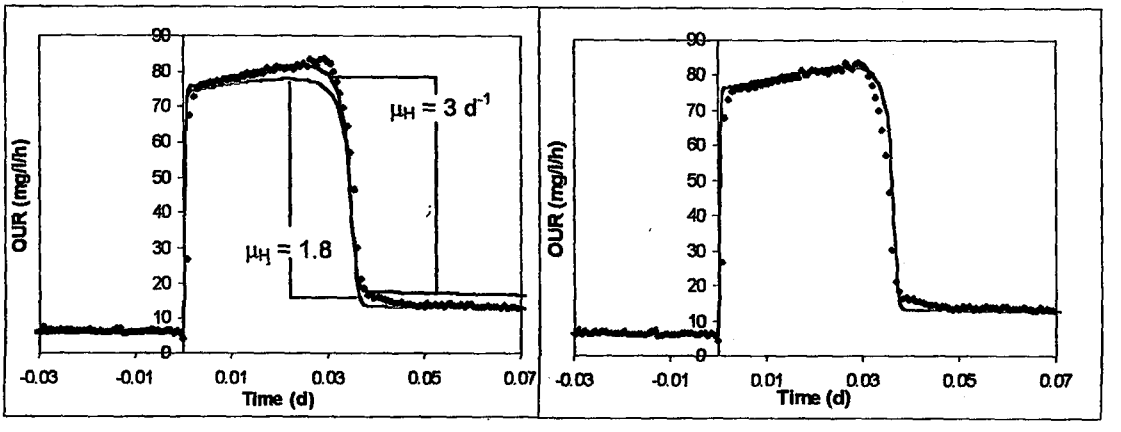

Figure 3.10 OUR simulations for (a) ASM3 with two different growth rates (b) modified ASM3 (Karahan-Gül *et al.*, 2002b)

Table 3.10 Matrix representation of the proposed model structure (Karahan-Gül *et al.*, 2002)

Component / *Process*	S_O O_2	S_I COD	S_S COD	X_I CO	X_S CO	X_H CO	X_{STO} COD	*Rate*
Hydrolysis		f_{SI}	$1-f_{SI}$		-1			$k_H \frac{X_S/X_H}{K_X + X_S/X_H} X_H$
Aerobic Storage of COD	$-\frac{1-Y_{STO}}{Y_{STO}}$		$-1/Y_{STO}$				1	$k_{STO} \frac{S_O}{K_O + S_O} \frac{S_S}{K_S + S_S} X_H$
Growth on S_S	$-\frac{1-Y_{H1}}{Y_{H1}}$		$-1/Y_{H1}$			1		$\mu_{H1} \frac{S_O}{K_O + S_O} \frac{S_{NH}}{K_{NH} + S_{NH}} \frac{S_{HCO}}{K_{HCO} + S_{HCO}} \frac{S_S}{K_S + S_S} X_H$
Growth on X_{STO}	$-\frac{1-Y_{H2}}{Y_{H2}}$					1	$-1/Y_{H2}$	$\mu_{H2} \frac{S_O}{K_O + S_O} \frac{K_S}{K_S + S_S} \frac{S_{NH}}{K_{NH} + S_{NH}} \frac{S_{HCO}}{K_{HCO} + S_{HCO}} \frac{X_{STO}/X_H}{K_{STO} + X_{STO}/X_H} X_H$
Endogenous Respiration	$-(1-f_I)$			f_I		-1		$b_{H,O2} \frac{S_O}{K_O + S_O} X_H$
Respiration of X_{STO}	-1						-1	$b_{STO,O2} \frac{S_O}{K_O + S_O} X_{STO}$

OUR experiments were carried out for acetate and results were compared with the OUR curve of the model proposed simulation. The results have provided strong indication that there was a need for considering direct growth on primary substrate as a significant biological mechanism (Figure 3.10, Table 3.11) (Karahan-Gül *et al.*, 2002b). Same experiments were also carried out for glucose. The proposed model was simulated for the experimental conditions of the SBR system using AQUASIM (Reichert *et al.*, 1998) and results are given in Figure 3.11 with the experimental data (Table 3.12) (Karahan-Gül *et al.*, 2002b).

Table 3.11 Kinetic and Stoichiometric coefficients for acetate (Karahan-Gül *et al.*, 2002b)

Model Coefficient	ASM3	Modified ASM3
$k_{STO}(d^{-1})$	16	14
K_S (mgl^{-1} COD)	4	3
Y_{STO} (gCOD/gCOD)	0.80	0.80
μ_{H1}, (direct growth)(d^{-1})	-	4
μ_{H2}, (growth on PHB)(d^{-1})	3 & 1.8	3
K_{STO}	1	0.4
Y_{H1} (direct growth)(g cellCOD/gCOD)	-	0.65
Y_{H2} (growth on PHB)(g cellCOD/gCOD)	0.63	0.75
b_{STO} (d^{-1})	0.24	0.24
b_H (d^{-1})	0.24	0.24
f_l (gCOD/gCOD)	0.20	0.20

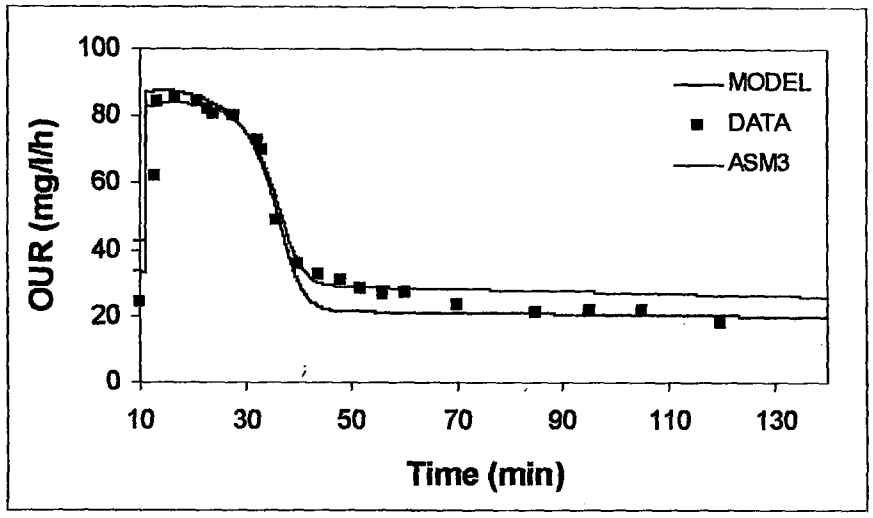

Figure 3.11 OUR simulations for ASM3 and modified ASM3 (Karahan-Gül *et al.*, 2002b)

Table 3.12 Kinetic and stoichiometric coefficients for glucose (Karahan-Gül *et al.*, 2002b)

Model Coefficient	ASM3	Modified ASM3
$k_{STO}(d^{-1})$	12	8
K_S (mgl^{-1} COD)	18	18
Y_{STO} (gCOD/gCOD)	0.88	0.90
μ_{H1}, (direct growth)(d^{-1})	-	2
μ_{H2}, (growth on glycogen)(d^{-1})	2.5	2.5
K_{STO}	1	1
Y_{H1} (direct growth)(g cellCOD/gCOD)	-	0.67
Y_{H2} (growth on glycogen)(g cellCOD/gCOD)	0.60	0.70
b_{STO} (d^{-1})	0.10	0.10
b_H (d^{-1})	0.20	0.20
f_i (gCOD/gCOD)	0.20	0.20

The experimental results correlated well with the performed simulations of the proposed model. The substrate utilization and the OUR response of the system under feast conditions were equally well simulated with both models, however ASM3 could not cope with the decrease of the OUR level in the famine phase (Karahan-Gül *et al.*, 2002b). Two different growth rates are necessary to simulate the system response which can also be observed from the OUR data. The two different growth rates observed in the system are due to two different growth process occurring; growth on primary substrate and growth on storage products (Karahan-Gül *et al.*, 2002b).

ASM3 cannot simulate lower electron acceptor utilization rate in the famine phase. Proposed model by Karahan-Gül *et al.* (2002b) resulted in two different specific growth rates where the specific growth rate in famine phase was 33% of that of the feast phase as shown in Figure 3.12. ASM3 generates a lower growth rate throughout the experiment, which gives a lower biomass yield. The modeling results for tests carried out with acetate provided a good description of the OUR response. However, the yields of the two growth processes have been found to be higher than those presented in literature. The modeling results for tests conducted with glucose yielded a maximum secondary growth rate higher than primary growth rate due to the definition of secondary growth process in terms of Monod kinetics (Karahan-Gül *et al.*, 2002b).

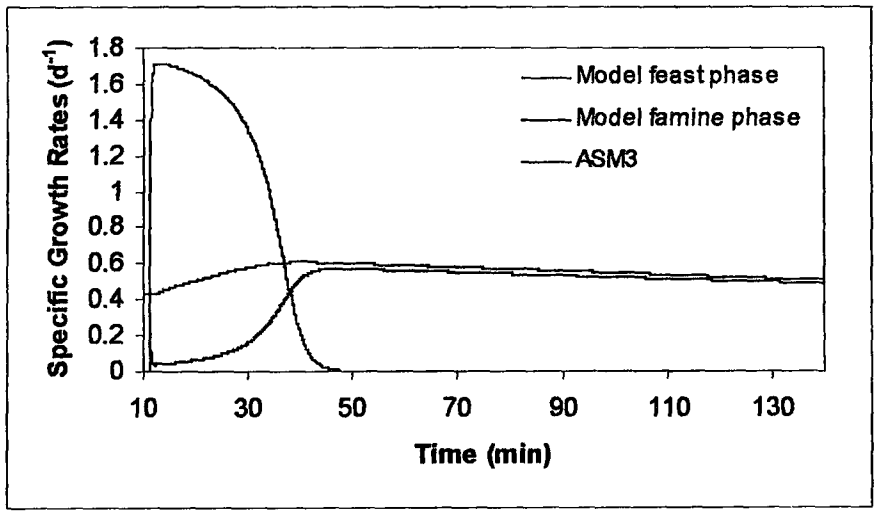

Figure 3.12 Specific growth rates obtained for proposed model and for ASM3 (Karahan-Gül *et al.*, 2002b)

The proposed model by Karahan-Gül *et al.* (2002b) gave better description of the results obtained for batch tests in terms of oxygen utilization, glycogen generation and biomass production compared to ASM3 for a selected range of kinetic coefficients.

SECTION 4 LEATHER TANNING INDUSTRY WASTEWATERS

4.1 Tannery Wastewater Characteristics and Treatment Processes for Turkey

Wastewater management in the tannery industry involves subcategorization because of the variability of wastewaters. Six subcategories are defined for tannery effluent so far (Tünay *et al.,* 1995) on the basis of differences in wastewater quality, treatment technology and applicable effluent limitations. Organized industrial districts give reliable information on wastewater character as they homogenize quality variations from individual plants. Istanbul Organized Leather Tanning Industrial District presently has 107 tanneries processing both cattle hide and sheepskin, with a resulting wastewater flow of 12 000 to 15 000 m^3/d. Leather processing industry involves all foundations converting raw or semi-processed animal hides and skins to leather, displaying physical properties like softness, plasticity, elasticity, resistance towards tear, abrasion and pressure. Processed leather also should be unaffected by heat when wet. These conversion processes can be named as:

1. Beamhouse operations
2. Tanyard processes
3. Retanning and wet finishing processes

Flow chart of the industry is illustrated in Figure 4.1. Detailed flow scheme is also given as shown in Figure 4.2. Tannery wastewaters show very complex and strong characteristics since above stages involve the use of raw materials like salts (Chromic, sodium chlorides and sulfides, ammonium sulfides), lime, dyes and acids. Significant amount of water is used in leather processing industry. Raw hides and skins are washed, chemical materials are added by water in all stages like dying, oiling, etc., undesirable remnants after processes are disposed and also all of the cleanliness is proposed by water. Wastewaters are collected with three different pipes called as general wastewater line (16.5 km), line for wastewaters containing sulfur

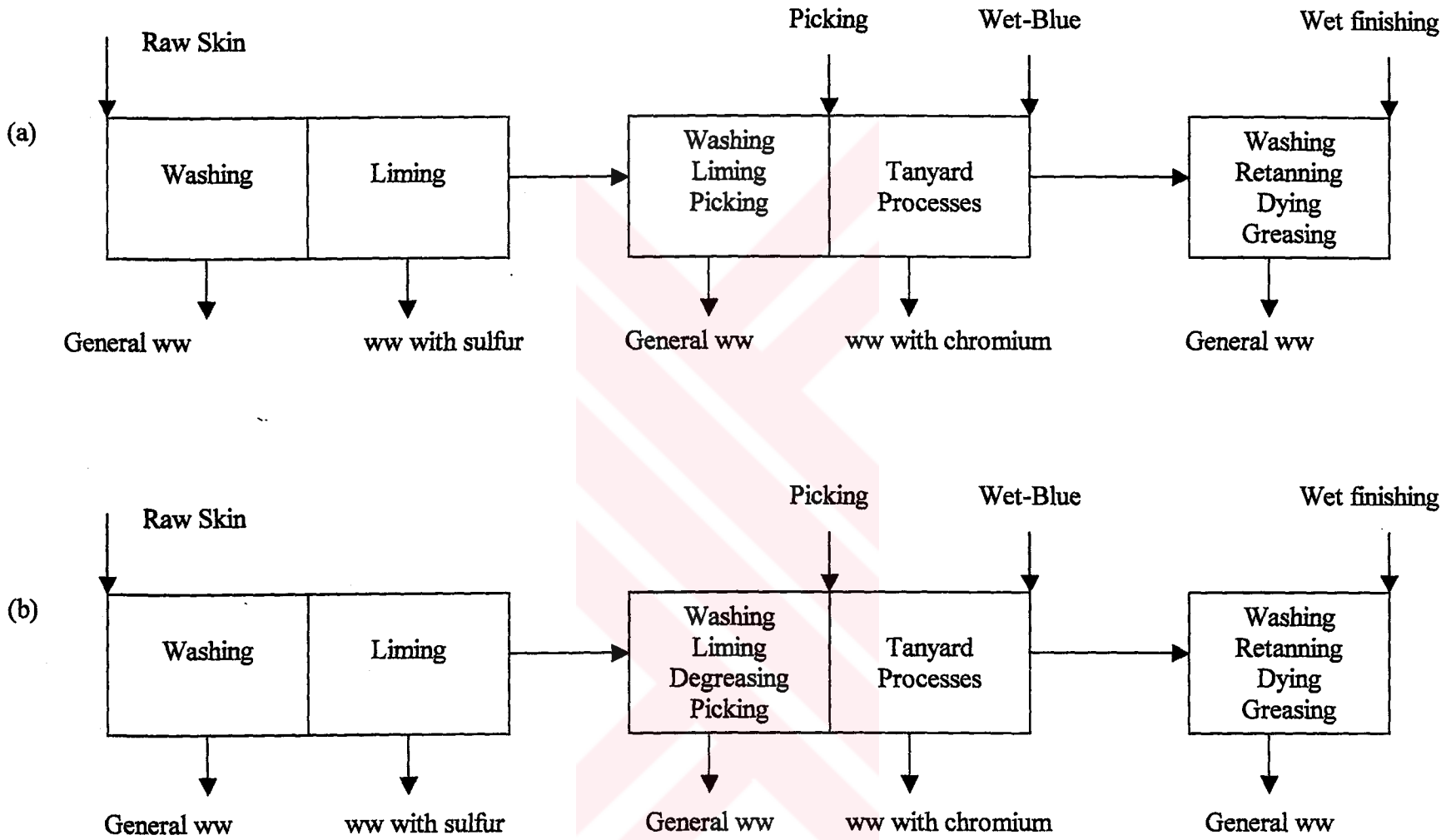

Figure 4.1. Flow Scheme of Leather Processing Industry (Ateş Genceli, 1997)
(a) Leather Processing of Cow etc.
(b) Leather Processing of Sheep etc.

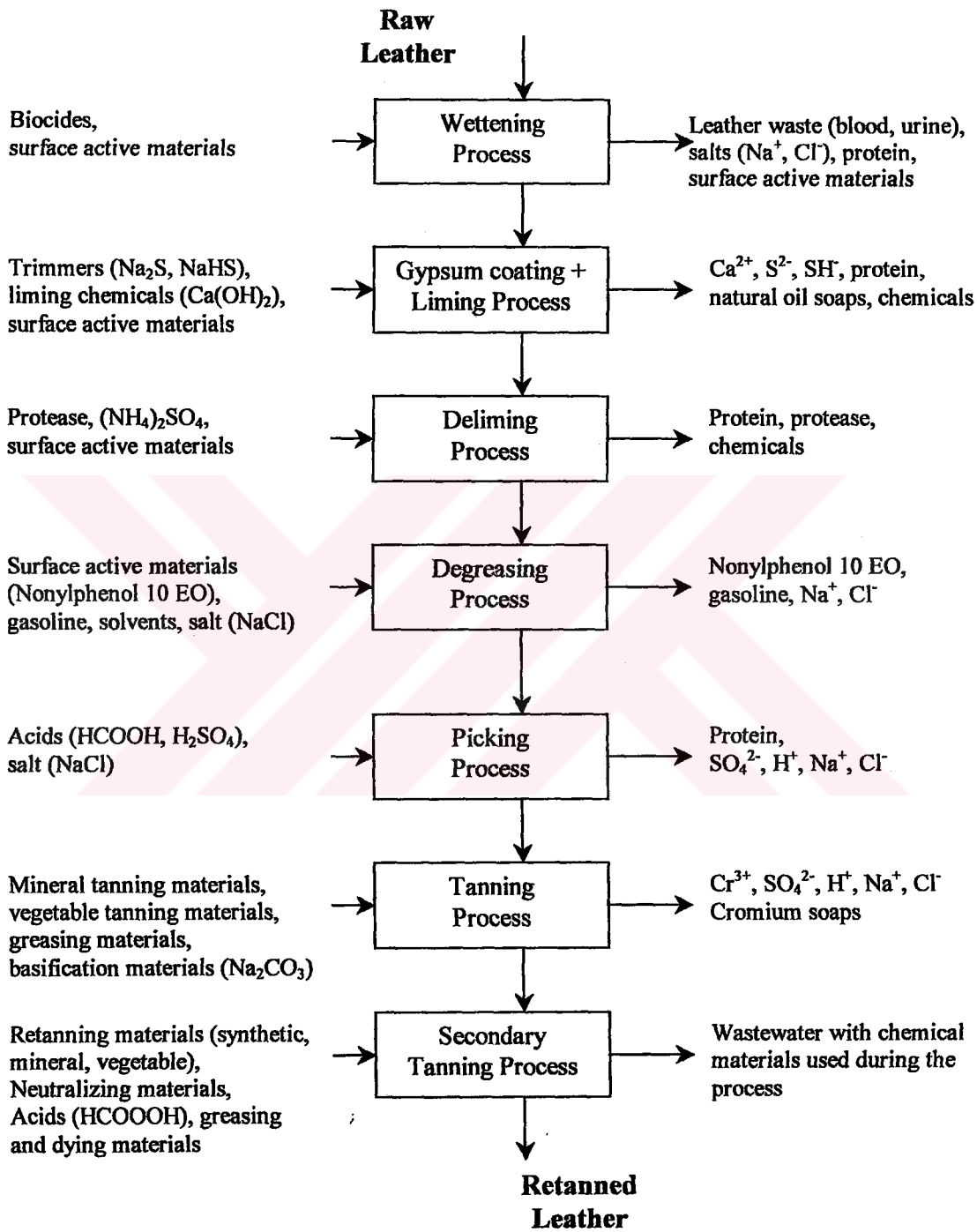

Figure 4.2 Detailed flow scheme of tannery industry (Turkey)

Table 4.1 General Characterization for Tannery Wastewaters (Ateş Genceli, 1997)

COD (mg/l)	BOD_5 (mg/l)	TKN (mg/l)	NH_3-N (mg/l)	TSS (mg/l)	S^{-2} (mg/l)	Total Cr (mg/l)	References
26500	4648	78.6	12	13639	-	-	Parker, 1970
2950	650-950	192	145	10430	-	300	Thackston, 1973
-	1000	250	-	2500	280	140	Huber and Jones, 1974
-	1323	180-445	-	1530	-	0.17	Nemerow *et al.*, 1978
1320	440	-	-	710	-	47	Bishop, 1978
-	3734	-	-	4806	300	82	Huber and Doane, 1980
1500-4500	600-1600	-	-	1000-3000	100-300	20-80	Kalender, 1981
536	460	-	-	1630	224	-	Cheda *et al.*, 1984
3600	3100	-	-	1500	-	-	Cheda *et al.*, 1984
3087	930	-	-	952	200	-	Cheda *et al.*, 1984
609	380	-	-	640	95	104	Cheda *et al.*, 1984
5000	100	-	-	360	300	23.5	Kaul *et al.*, 1993
4775-6400	-	993-1280	560-568	1232-2993	59-158	367-1329	Kabdaşlı *et al.*, 1993
4230	1500	-	-	3270	134	61	Şenol and Gürel, 1993
10380-26100	-	-	-	-	20	192	Kabdaşlı *et al.*, 1993
3250	1844	-	-	6840	49.8	209	Şenol and Gürel, 1993
3500-11200	2100-5400	24-106	-	780-2030	150	5-168	Talınlı, 1994
7450-9635	-	1068-1180	900-906	-	10	10-110	Tünay *et al.*, 1994
11145	-	-	-	-	278	76	Tünay *et al.*, 1994

(15 km) and line for wastewaters involving chromium (13.1 km). General characterization of tannery wastewater referring many studies is given in Table 4.1, as seen from the table, tannery-processing effluents show a very wide range characteristics. Characterization of raw wastewater generating from Organized Leather Tanning District is shown in Table 4.2.

Table 4.2 Raw wastewater characterization of Tuzla (Ateş Genceli, 1997)

Parameter	TUZLA	
	Average (mg/l)	Range (mg/l)
Total COD	5094	3235-7420
Soluble COD	2336	1040-3810
BOD_5	1760	600-2600
TSS	2229	1470-3474
VSS	-	-
TKN	358	112-640
Organic-N	223	102-347
NH_3-N	135	48-245
TP	-	-
Total Cr	115.6	58-213
S^{2-}	51	17-110
Alkalinity	1350	797-1818
Cl^-	10300	6370-12800
pH	8.1	6.4-9.98

4.1.1 Treatment Processes

Pretreatment is necessary in leather tanning industry because of inhibiting compounds as Cr^{+3}, S^{-2} and many toxic organisms. There are two basic alternatives for pretreatment:

1. Wastewater streams containing chromium and sulfide can be segregated and treated by special methods, then combined with general wastewaters and undergo plain settling with little chemical polishing before biological treatment. This alternative is not so useful because segregation of wastewaters is hardly achieved.
2. Chemical settling for all the effluent can be selected as a more useful pretreatment alternative.

There are four treatment processes in the treatment plant:

1. Treatment of general wastewaters (domestic wastewater etc.)

2. Treatment of wastewaters involving sulfur generating from beamhouse operations
3. Treatment of wastewaters involving chromium generating from tanyard and retanning - wet finishing processes and recycling of chromium.
4. Recycling of solvents.

Wastewaters are firstly treated physically (screening, filtering, oil-sand trapper), then chemical treatment is applied for sulfur and chromium removal. After primary and chemical treatment units, there is an equalization tank and primary settlers in order to prepare the wastewater for biological treatment. Secondary settling tanks follow the biological processes and treated wastewater is discharged to the Marmara Sea. Sludge from settlers are finally taken to sludge filter presses and disposed as sludge cakes.

4.1.2 Wastewater Characterization and Modeling

Conventional characterization experiments were carried out on both the effluents after plain settling and chemical settling. The results were significantly different as summarized in Table 4.3. Total COD concentration reduced approximately by one half and 20% lower than the soluble (filtered) COD level of plain settled effluent after chemical settling. Also the SS concentration gave a result less than 200 mg/l while it was 768 mg/l after plain settling. These concentrations are presumably due to the effective coagulation of finer particles escaping from leather processing. Chemical treatment was also effective in almost the complete treatment of chromium within the pH range maintained between 7.5-8.5 and settling of particulate nitrogen, inducing a total TKN reduction of nearly 35%. The phosphorus content of tannery wastewaters is very low in contrast to their high nitrogen content. It can be seen from the primary effluent average that the high value of 2.06 mg COD/mgVSS, as the COD equivalent of VSS, indicated that a significant portion of the organic particulate matter can be accounted as soluble COD.

Process kinetics and stoichiometry for tannery wastewaters can be evaluated by using a multicomponent model based on the concept of endogenous decay, including initial soluble inert matter and residual microbial products as separate model components (Orhon and Artan, 1994).

Table 4.3 Effect of Chemical Settling on Wastewater Characterization (Orhon *et. al.*, 1998)

Parameter	Primary effluent Average (mg/l)	Chemical settling effluent Average (mg/l)
Total COD	2255	1091
Soluble COD	1290	1035
Suspended Solids, SS	768	157
Volatile Suspended Solids, VSS	467	56
Total Kjeldahl Nitrogen, TKN	214	197
Soluble Kjeldahl Nitrogen, TKN	180	175
NH_3-N	164	164
Total P	5.9	1.8
Alkalinity	1417	1140
$S^=$	37	10
Total Cr	40	0.03
pH	7.9	8.4

The organic content of tannery wastewater after pretreatment by plain settling could be characterized by average concentrations of 435 mg/l readily biodegradable COD, 270 mg/l particulate inert COD, 215 mg/l soluble inert COD and a residual metabolic products potential expressed as 6.3% of the total biodegradable COD in the wastewater. Chemically treated effluents gave a totally different composition in terms of COD fractionation as 16% of soluble inert, 35% of readily biodegradable and 49% of rapidly hydrolyzable and almost no particulate fractions as summarized in Table 4.4

Table 4.4 Typical data for the modeling of tannery wastewaters (Orhon *et al.*, 1999)

Parameters	Unit	Plain settling effluent	Chemical settling effluent
Influent COD			
Total COD, C_{TI}	(mg/l)	2300	1100
Total soluble COD, S_{TI}	(mg/l)	1300	1100
Total particulate COD, X_{TI}	(mg/l)	1000	-
COD components			
Readily biodegradable COD, S_{SI}	(mg/l)	435	385
S_{SI}/C_{TI}	(%)	19	35
Rapidly hydrolyzable COD, S_{HI}	(mg/l)	650	540
S_{HI}/C_{TI}	(%)	28.5	49
Soluble inert COD, S_{II}	(mg/l)	215	175
S_{II}/C_{TI}	(%)	9.5	16
Slowly hydrolyzable COD, X_{SI}	(mg/l)	730	-
X_{SI}/C_{TI}	(%)	31.5	
Particulate inert COD, X_{II}	(mg/l)	270	-
X_{II}/C_{TI}	(%)	11.5	
Stoichiometric and kinetic constants			
Yield coefficient Y_H	(mg cell COD/mg COD)	0.64	0.64
Maximum specific growth rate, $\hat{\mu}_H$	(day^{-1})	2.2	4.3
Half-saturation constant, K_S	(mg/l)	28	23
Endogenous decay rate, b_H	(day^{-1})	0.12	0.12
Maximum specific hydrolysis rate, k_h	(mg COD/mg cell COD.day)	0.9	2.0
Half-saturation constant for hydrolysis, K_X	(mg COD/mg cell COD)	0.3	0.08
Particulate inert fraction, f_{EX}	(mg COD/mg COD)	0.2	0.2
Soluble residual product ratio, Y_{SP}	(mg COD/mg COD)	0.063	0.063
Soluble residual fraction, f_{ES}	(mg COD/mg COD)	0.10	0.10

Kinetic and stoichiometric constants related to tannery wastewaters can be summarized as f_{EX}, f_{ES}, Y_H, μ_H, b_H, K_S, k_h and K_X. Those coefficients evaluated on both plain settled and chemically settled samples are also summarized in Table 4.4.

A double hydrolysis mechanism containing both soluble and particulate slowly biodegradable COD as separate model components provide better results than single-hydrolysis mechanism in the interpretation of model outputs for tannery wastewater, where chemical treatment was shown to greatly increase the rate of hydrolysis by removing the more slowly biodegradable particulate COD.

4.2 Tannery Wastewater Characteristics and Treatment Processes for The Netherlands

Wastewater characterization of a tannery industry using the leather for shoe-production and located in Dongen, Noord Brabant was evaluated for optimizing the treatment process and modeling the activated sludge system (Rojas, 2001). In leather tanning industry there are basically three stages applied, namely preservation or preparation, tanning and finishing. Since these stages involve the use of many chemicals and large amounts of water tannery wastewaters show high pollutant characteristics. Generally, there are pollutants from hides, products from their decomposition and leaching and many chemical solutions used for the preservation of the hides and during the tanning processes. Figure 4.3 shows the flow scheme of tannery operations.

4.2.1 Treatment Processes

A general scheme of treatment plant for tannery wastewaters is illustrated in Figure 4.4. As seen from the figure, treatment involves mainly two parts: primary treatment or pretreatment and secondary treatment (biological processes). Firstly, wastewater containing chromium is segregated in order to be treated by chemical precipitation, then the supernatant is sent to the equalization tank and mixed with general wastewaters. In the equalization tank all wastewaters are combined and chemically treated, so S^{2-} compounds are removed from the wastewater. There are primary settlers after equalization tank, removing a significant part of the particulate solids. Primary treatment is ended with the neutralization of wastewaters. Secondary treatment contains a conventional plug-flow activated sludge system, denitrification

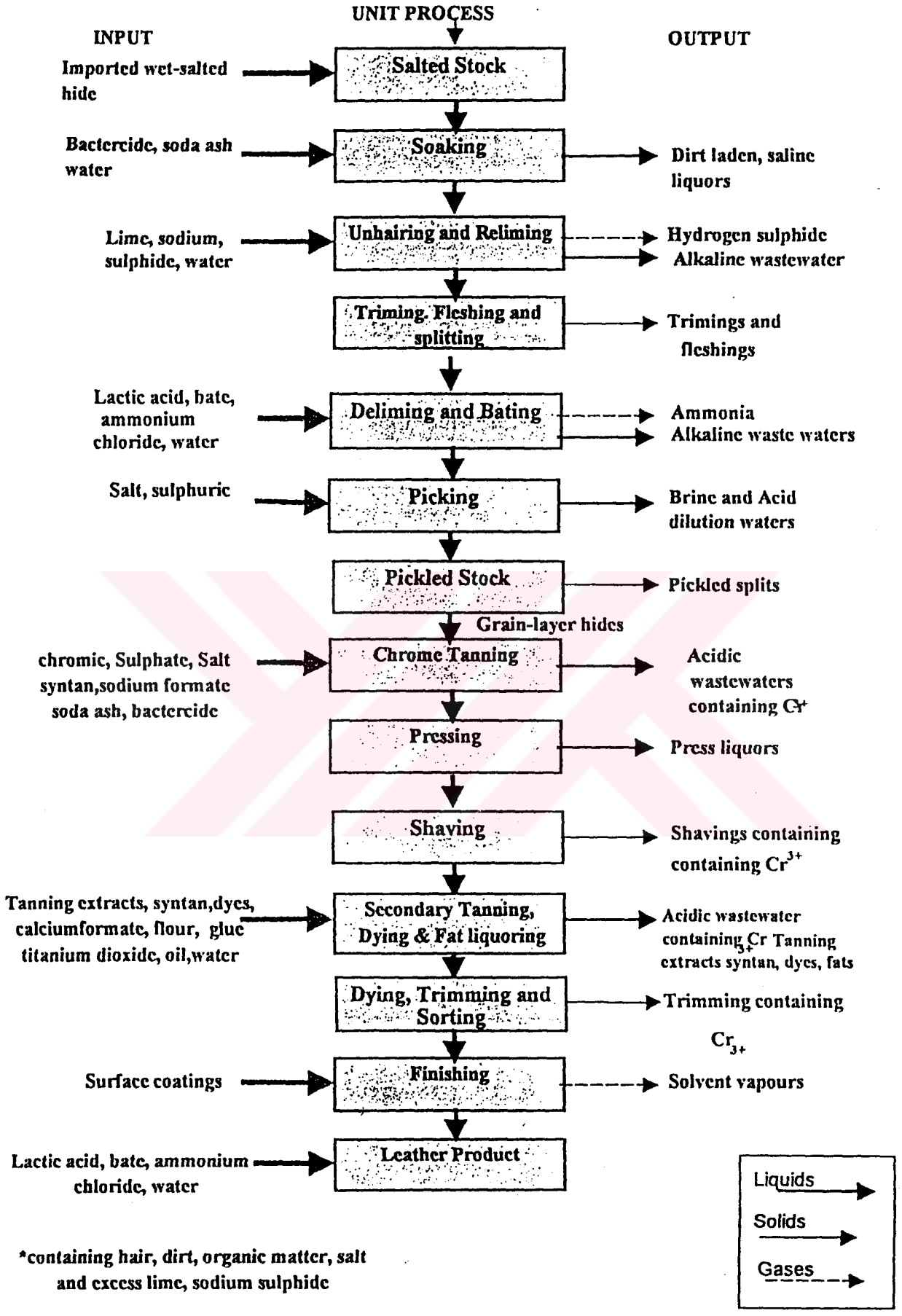

Figure 4.3 Detailed flow scheme of tannery industry (The Netherlands)(Rojas, 2001)

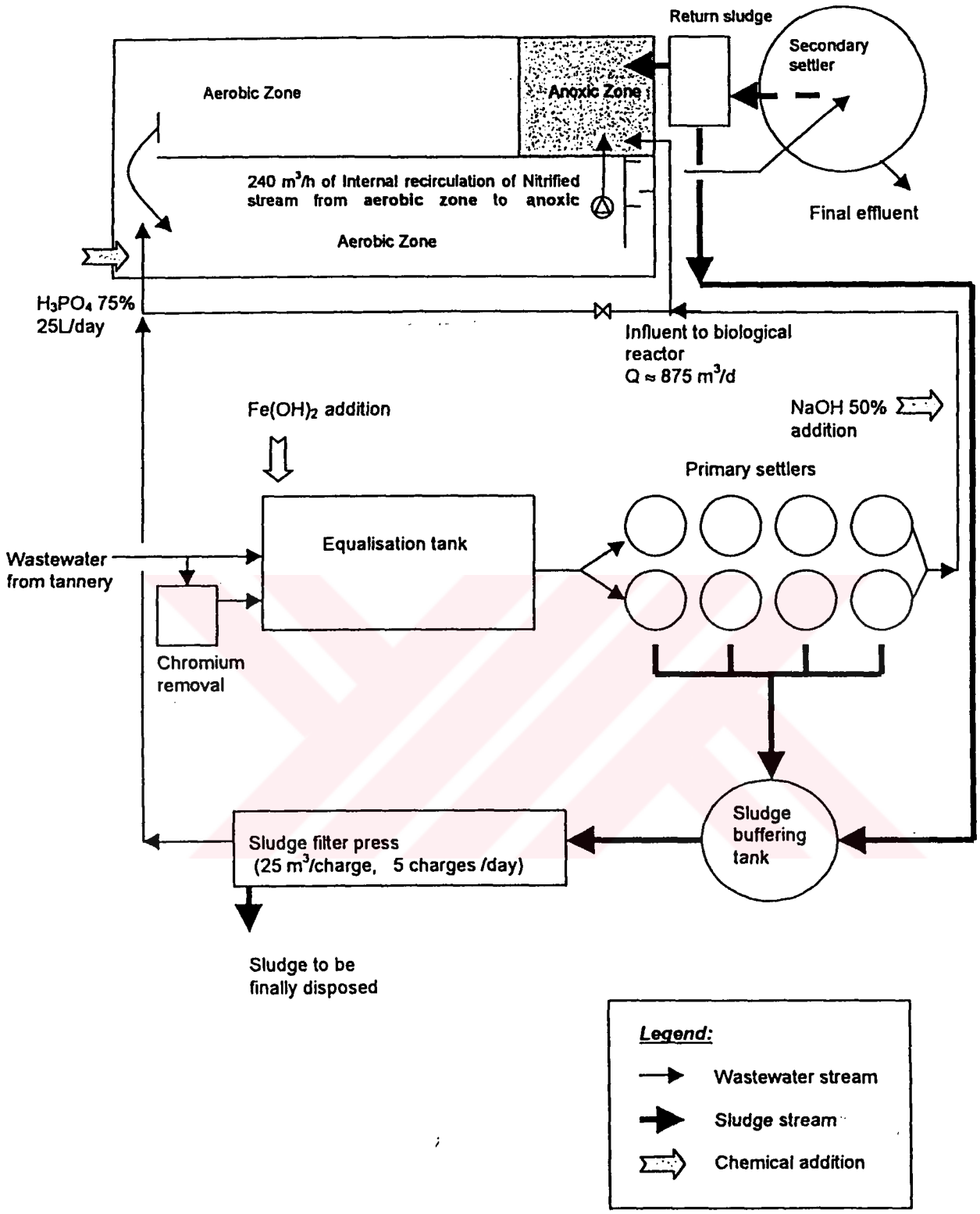

Figure 4.4 Schematic illustration of the wastewater treatment system (Rojas, 2001)

is also achieved in biological treatment. Then there is a secondary settler from where the supernatant is sent to another tretment plant in order to be combined with

domestic wastewater and after combined treatment effluent is discharged to sea. Sludges from settlers are conditioned in a buffering tank, then sent to a filter press and disposed as sludge cakes. Influent wastewater flow Q to reactor during the week is 1000 m^3/day, including the stream coming from sludge filter press and the hydraulic retention time is 8 days (Table 4.5).

Table 4.5 Main Operational Characteristics of the WWTP (Rojas, 2001)

Parameter, description	Unit	Value
Influent wastewater flow Q to reactor, [including stream coming from sludge filter press during the week]	m^3/day	1000
Sludge recirculation flow	m^3/hour	80
Recycle ratio, [(80 m^3/h)/(1000.025 m^3/24 h)]	-	1.9
Excess sludge purged	m^3/day	80
Volume of entire reactor	m^3	8000
Volume of anoxic zone in the reactor	m^3	1000
Volume of secondary settler, [Φ=20 m]	m^3	775
Hydraulic retention time, [(8000 m^3)/(1000.025 m^3/day)]	Days	8
Flow addition of H_3PO_4 75% to reactor, [only during the week]	l/day	25

4.2.2 Wastewater Characterization and Modeling of Tannery Wastewater in The Netherlands

The kinetic and stoichiometric coefficients used for the modeling purposes of tannery wastewater treatment plant is given in Table 4.6. The influent and effluent characteristics of the wastewater treatment plant is given in Table 4.7. Also the influent composition required for the model is involved in this table.

Table 4.6 Kinetic and Stoichiometric Coefficients (Rojas, 2001)

Parameter	Units	Value
Yield coefficient, Y_H	mg cell COD/mg COD	0.64
Endogenous decay rate, b_H	day^{-1}	0.12
Half saturation coefficient, $K_{O,H}$	mg O_2/l	0.2
Maximum specific hydrolysis rate for S_H, k_{hS}	day^{-1}	1.1
Maximum specific hydrolysis rate for X_S, k_{hX}	day^{-1}	0.3
Half saturation coefficient for the hydrolysis of S_H, K_{XS}	mg COD/mg cell COD	0.2
Half saturation coefficient for the hydrolysis of X_S, K_{XX}	mg COD/mg cell COD	0.2

Table 4.7 Influent and effluent characteristics of the wastewater required for modeling (Moussa *et al.*, 2001)

Measurements				Model Influent Composition				
	Value					Value		
Description	*Influent*	*Effluent*	units	*Description*	Symbol	Dynamic	Steady -state	units
Total COD, COD_{Total}	2525 *(2920)*	167 *(190)*	$gCOD/m^3$	***Soluble compounds***				
Soluble COD, COD_S	1785	143	$gCOD/m^3$	Dissolved oxygen	S_{O2}	0.3	0.3	$gCOD/m^3$
Total N-Kj	488 (515)	7 *(11)*	gN/m^3	Readily biodegradable COD	S_S	840	972	$gCOD/m^3$
Soluble N-Kj	454	6	gN/m^3	Soluble Inert COD	S_I	177	205	$gCOD/m^3$
Ammonium, NH_4^+	438	10	gN/m^3	Ammonium	S_{NH4}	438	448	gN/m^3
Nitrite, NO_2^-	0	0 *(0.1)*	gN/m^3	Nitrite	S_{NO2}	0	0	gN/m^3
Nitrate NO_3^-	0	99 *(50)*	gN/m^3	Nitrate	S_{NO3}	0	0	gN/m^3
Total phosphorus, P_{Total}	0.4	3.3	gP/m^3	Alkalinity	S_{Alk}	50	50	mole HCO_3/l
Ortho phosphate, PO_4^{2-}	0.1	2.8	gP/m^3					
Total Chromium, Cr^{3+}	0.23	0.2 *(0.1)*	gCr/m^3					
Calcium, Ca^{2+}	200	320 *(400)*	gCa/m^3	***Particulate compounds***				
Chloride, Cl^-	8066	7960 *(7380)*	gCL/m^3	Inert particulate COD	X_I	454	525	$gCOD/m^3$
Sulfate, SO_4^{2-}	3700	3900 *(3100)*	gSO_4/m^3	Slowly biodegradable COD	X_S	1060	1226	$gCOD/m^3$
Total Suspended Solids, TSS	1593	500	g/m^3	Heterotrophics	X_H	0	0	$gCOD/m^3$
Volatile Suspended Solids, VSS	255	127	g/m^3	Ammonia oxidisers	X_A	0	0	$gCOD/m^3$
Alkalinity	2030	570	$gCaCO_3/m^3$	Nitrite oxidisers	X_N	0	0	$gCOD/m^3$
Temperature	22	22	°C					
pH	9 *(9.4)*	7.5 *(7.1)*						
Dissolved Oxygen, DO	0.3	6.7	gO_2/m^3					

Table 4.8 Stoichiometry matrix of the activated sludge model (modified ASM1) proposed by Moussa et al. (2001)

Component i j Process expressed as	1 X_I COD	2 X_H COD	3 X_A COD	4 X_N COD	5 X_S COD	6 S_I COD	7 S_S COD	8 S_{NH4} N	9 S_{NO2} N	10 S_{NO3} N	11 S_{O2} -COD	13 S_{Alk} Mole
Heterotrophic organisms, Degradation of organic material, Denitrification												
1. Aerobic growth		+1					$\frac{-1}{Y_H}$	$-i_{BX}$			$\frac{-1+Y_H}{Y_H}$	$-\frac{i_{XB}}{14}$
2. Anoxic growth Denitrification (NO_2)		+1					$\frac{-1}{Y_H}$	$-i_{XB}$	$\frac{-1+Y_H}{1.71Y_H}$			$\frac{1-Y_H}{24Y_H}-\frac{i_{XB}}{14}$
3. Anoxic growth Denitrification (NO_3)		+1					$\frac{-1}{Y_H}$	$-i_{XB}$		$\frac{-1+Y_H}{2.86Y_H}$		$\frac{1-Y_H}{40Y_H}-\frac{i_{XB}}{14}$
4. Decay, lysis	f_{XI}	-1			1-f_{XI}			$i_{XB}-f_{XI}(i_{XI})-(1-f_{XI})(i_{XS})$				$[i_{XB}-f_{XI}(i_{XI})-(1-f_{XI})(i_{XS})]/14$
Autotrophic organisms, Nitrification												
5. Aerobic growth of ammonia oxidisers			+1					$-i_{XB}-1/Y_A$	$1/Y_A$		$\frac{-3.43+Y_A}{Y_A}$	$\frac{-1}{7\cdot Y_A}-\frac{i_{XB}}{14}$
6. Aerobic growth of nitrite oxidisers				+1				$-i_{XB}$	$-1/Y_N$	$1/Y_N$	$\frac{-1.14+Y_N}{Y_N}$	$-\frac{i_{XB}}{14}$
7. Decay, lysis of ammonia oxidisers	f_{XI}		-1		1-f_{XI}			$i_{XB}-f_{XI}(i_{XI})-(1-f_{XI})(i_{XS})$				$[i_{XB}-f_{XI}(i_{XI})-(1-f_{XI})(i_{XS})]/14$
8. Decay, lysis of nitrite oxidisers	f_{XI}			-1	1-f_{XI}			$i_{XB}-f_{XI}(i_{XI})-(1-f_{XI})(i_{XS})$				$[i_{XB}-f_{XI}(i_{XI})-(1-f_{XI})(i_{XS})]/14$
Hydrolysis of colloidal, particulate												
9. Aerobic hydrolysis of organic matter					-1		+1	i_{XS}				$\frac{i_{XS}}{14}$
10. Anoxic hydrolysis of organic matter					-1		+1	i_{XS}				$\frac{i_{XS}}{14}$

Stoichiometric Parameters:

Y_H = Yield Coefficient for Heterotrophs [M M^{-1}]
YA = Yield Coefficient for ammonia oxidisers [M M^{-1}]
Y_N = Yield Coefficient for nitrite oxidisers [M M^{-1}]

i_{XB} Nitrogen content of biomass X_H, X_A, X_N
i_{XI} Nitrogen content of inert particulate COD X_I
i_{XS} Nitrogen content of particulate substrate X_S
f_{XI} Fraction of inert COD generated in biomass lysis

Some modifications were made in ASM1 while modeling the tannery wastewaters for plant optimization. Most important modification is that the nitrification was considered as a two-step process because ammonia oxidizers grow faster than nitrite oxidizers at temperatures above 15-20°C (Hellinga et al., 1999; Ekama et al., 1986). Describing the nitrification in two steps enables the identification of any inhibition by compounds present in industrial wastewater and the detection of partial nitrification (NO_2 accumulation). The stoichiometry and kinetics of the model are given in Tables 4.8 and 4.9.

Table 4.9 Process kinetics of modified ASM1 for a tannery industry (Moussa *et al.*, 2001)

J. Process	Process rate law ρ_J [$M L^{-3} T^{-1}$]
Heterotrophic organisms, Degradation of organic material, Denitrification	
1. Aerobic growth	$\mu_{m,H} \cdot \frac{S_S}{K_S + S_S} \cdot \frac{S_{O2}}{K_{O2H} + S_{O2}} \cdot X_H$
2. Anoxic growth, Denitrification (NO_2)*	$\mu_{m,H} \cdot n_g \cdot \frac{K_{O2H}}{K_{O2H} + S_{O2}} \cdot \frac{S_S}{K_S + S_{S1}} \cdot \frac{S_{NO2}}{K_{NO2} + S_{NO2}} \cdot X_H$
3. Anoxic growth, Denitrification (NO_3)*	$\mu_{m,H} \cdot n_g \cdot \frac{K_{O2H}}{K_{O2H} + S_{O2}} \cdot \frac{S_S}{K_S + S_{S1}} \cdot \frac{S_{NO3}}{K_{NO3} + S_{NO3}} \cdot X_H$
4. Decay, Lysis	$b_H \cdot X_H$
Autotrophic organisms, Nitrification	
5. Aerobic growth of Ammonia oxidizers	$\mu_{m,A} \cdot \frac{S_{NH4}}{K_{NH4} + S_{NH4}} \cdot \frac{S_{O2}}{K_{O2A} + S_{O2}} \cdot X_A$
6. Aerobic growth of Nitrite oxidizers	$\mu_{m,N} \cdot \frac{S_{NO2}}{K_{NO2} + S_{NO2}} \cdot \frac{S_{O2}}{K_{O2N} + S_{O2}} \cdot X_N$
7. Decay of Ammonia oxidizers	$b_A \cdot X_A$
8. Decay of Nitrite oxidizers	$b_N \cdot X_N$
Hydrolysis of colloidal, particulate	
9. Aerobic Hydrolysis of organic matter	$k_h \cdot \frac{X_S / X_H}{K_{XS} + X_S / X_H} \cdot \frac{S_{O2}}{K_{O2H} + S_{O2}} \cdot X_H$
10. Anoxic Hydrolysis of organic matter	$k_h n_h \cdot \frac{K_{O2H}}{S_{O2}} \cdot \frac{X_S / X_H}{K_{XS} + X_S / X_H} \cdot \frac{S_{NO3}}{K_{NO3} + S_{NO3}} \cdot X_H$

Kinetic parameters:
$\mu_{m,i}$ = max. growth rate [T^{-1}]
K_{ji} = saturation coefficient [$M_l L^{-3}$]
b_i = Decay rate constant [T^{-1}]
k_h = Hydrolysis rate constant for hydrolysable]
COD [$M_S M_3^{-1} T^{-1}$
n_g, n_h = Correction factor for anoxic growth and hydrolysis

Indices i :
H for Heterotrophic biomass.
A, N for Ammonia oxidizers and N for Nitrite oxidizers.
S,NH4,NO2,NO3,O2 for component 7,8,9,10 and 11.

*The sum of the anoxic growth on NO_2 and NO_3 (process 2+3) never exceeds $\mu_{m,H} \cdot n_g$

For the use of the proposed model a detailed wastewater characterization was made. The sludge age is markedly important in the simulation of wastewater treatment plants (Meijer *et al.*, 2001; Brdjanovic et al., 2000). If COD load or sludge production, are assumed incorrectly, simulated oxygen utilization of the process can compensate them. The modified ASM1 proposed for COD and N removal described

the performance of the treatment plant well with the adjustment of only two parameters (K_{O2A} and K_{O2H}). This application of the model is very useful for the industrial wastewater treatment plants, especially for tannery wastewaters. Activated sludge models usually applied for domestic sewage treatment plants could be used for industrial wastewaters by changing and/or adding some steps. An accurate description of the whole system configurations and the balance of the operational data with the measurements should be made for the definite calculation of flow rates and sludge age. Selection of the proper model processes and components is also a very important step. Wastewater and sludge characterization must be made in each case. Finally calibration should be made under steady-state conditions and model validation under dynamic conditions (Moussa *et al.*, 2001).

4.3 Comparison of Tannery Wastewater Characteristics in Turkey and in The Netherlands

Comparison of tannery wastewaters originating from Istanbul, Turkey and Noord Brabant, The Netherlands after primary chemical treatment is given in Table 4.10.

Table 4.10 Comparison of Tannery Wastewaters from Turkey and The Netherlands (Orhon *et al.*, 1998; Moussa *et al.*, 2001)

Parameter	Average value (mg/l)	
	Turkey	The Netherlands
Total COD	1091	2525
Soluble COD	1035	1785
TSS	157	1593
VSS	56	255
TKN	197	488
NH_3-N	164	-
Sol-N	175	454
NH_4^+	-	438
TP	1.8	0.4
PO_4^{2-}	-	0.1
Total Cr	0.03	0.23
S_2^-	10	-
SO_4^{2-}	-	3700
Cl^-	-	8066
Alkalinity	1140	2030
pH	8.4	9

As seen from Table 4.10, COD, suspended solid and nitrogen concentrations are significantly lower in Turkey when compared with The Netherlands. Alkalinity and pH are also higher in The Netherlands. Total chromium concentration is nearly the same, whereas only the amount of phosphorus is a little bit higher in Turkey.

SECTION 5 CONCEPTUAL APPROACH

5.1 Kinetics of Homogenous Reactions

5.1.1 Kinetic View of Equilibrium for Elementary Reactions

Rate of disappearance of a compound A, is given by the following equation for a single reaction of A plus B giving R:

$$-r_A = kC_AC_B \tag{5.1}$$

where, C_A and C_B are the concentrations of compounds A and B (Levenspiel, 1972).

Considering the reversible reactions:

$$A + B \xrightarrow{k1} R + S \tag{5.2}$$

$$A + B \xleftarrow[k2]{} R + S \tag{5.3}$$

the rate of formation of R is written as in equation (5.4) and the disappearance by the reverse reaction is as in equation (5.5):

$$r_{R\,forward} = k_1C_AC_B \tag{5.4}$$

$$-r_{R\,reverse} = k_2C_RC_S \tag{5.5}$$

where k_1 and k_2 are the rate coefficients of formation and disappearance reactions (Levenspiel, 1972).

There is no net formation of R at equilibrium, therefore:

$$r_{R\,forward} + r_{R\,reverse} = 0 \tag{5.6}$$

$$K_C = \frac{C_RC_S}{C_AC_B} = \frac{k_1}{k_2} \tag{5.7}$$

where, K_C is the equilibrium constant (Levenspiel, 1972).

For that reason, distinguishing one equation, which represents the elementary reaction and the many possible representations of the stoichiometry needs great consideration. For example, from the following reaction many rate equations may be written referring to different compounds (Levenspiel, 1972):

$$B + 2D \xrightarrow{ki} 3T \tag{5.8}$$

If the rate is measured in terms of B, the rate equation is:

$$-r_B = k_i' C_B C_D^2 \tag{5.9}$$

If it refers to D, the rate equation is:

$$-r_D = k_i'' C_B C_D^2 \tag{5.10}$$

or if it refers to the product T, then it can be written as below:

$$r_T = k_i''' C_B C_D^2 \tag{5.11}$$

But from the stoichiometry below equations are obtained:

$$-r_B = -\frac{1}{2} r_D = \frac{1}{3} r_T \tag{5.12}$$

$$k_i' = \frac{1}{2} k_i'' = \frac{1}{3} k_i''' \tag{5.13}$$

5.1.2 Kinetic Models for Non-elementary Reactions

In non-elementary reactions it is assumed that, a sequence of elementary reactions is actually occurring but the intermediates formed cannot be measured or observed because they are only present in very minute quantities and only the initial reactants and final products can be observed (Levenspiel, 1972). For example, if the kinetics of the reaction is:

$$A_2 + B_2 \longrightarrow 2AB \tag{5.14}$$

A series of elementary steps can be derivated to explain the kinetics, such as:

$$A_2 \leftrightarrow 2A^* \tag{5.15}$$

$$A^* + B_2 \leftrightarrow AB + B^* \tag{5.16}$$

$$A^* + B^* \leftrightarrow AB \tag{5.17}$$

In non-chain reactions, the intermediate is formed in the first reaction and then disappears as it reacts further to give the product (Levenspiel, 1972).

Reactants → *(Intermediates)**

*(Intermediates)** → Products

In chain reactions, the intermediate is formed in a first reaction called the chain initiation step. It then combines with reactant to form product and more intermediates are formed in the chain propagation step. The intermediate disappears in the chain termination step (Levenspiel, 1972).

Reactants → *(Intermediates)** (Initiation)

*(Intermediates)** + Reactants → *(Intermediates)** + Products (Propagation)

*(Intermediates)** → Products (Termination)

For example, the general class of enzyme-catalyzed fermentation reactions, A to R (with enzymes) proceed as follows:

$$A + \text{enzyme} \leftrightarrow (A.\text{enzyme})^*$$

$$(A.\text{enzyme})^* \rightarrow R + \text{enzyme}$$

5.1.3 Enzyme – Substrate Reactions

A reactant, namely the substrate is converted into product by the action of an enzyme, which can be described as a high molecular weight (MW>10000) protein like substance. An enzyme is a highly specific substance catalyzing only one particular reaction or one group of reactions. Many of these reactions exhibit the following rate characteristics (Levenspiel, 1972):

1. The rate is proportional to the concentration of enzyme induced into the mixture, $[E_O]$.

2. At low reactant concentrations, the rate is proportional to the reactant concentration.
3. At high reactant concentrations, the rate levels off to become independent of reactant concentration.

Michaelis and Menten (1913) was the first to explain this general behavior with the following mechanism:

$$\begin{aligned} A + E &\xrightarrow{k1} (A.E)^* \\ A + E &\xleftarrow[k2]{} (A.E)^* \end{aligned} \qquad (5.18)$$

$$(A.E)^* \xrightarrow{k3} R + E \qquad (5.19)$$

The model is based on the assumption that the concentration of intermediate can be appreciable, in which case the total enzyme is distributed as follows:

$$[E_o] = [E] + [(A.E)^*] \qquad (5.20)$$

Since the enzyme concentration cannot be followed, a rate equation for this reaction can be developed in terms of $[E_O]$ and [A] and using the steady-state approximation.

An example for enzyme kinetics:

An enzyme substrate complex is formed and consumed as shown below:

$$\begin{aligned} E + S &\xrightarrow{k1} ES \xrightarrow{k3} E + P \\ E + S &\xleftarrow[k2]{} ES \xrightarrow{k3} E + P \end{aligned} \qquad (5.21)$$

The rate of disappearance of enzyme and substrate is defined as:

$$R_1 = k_1 [E][S] \qquad (5.22)$$

The formation of enzyme-substrate complex is given by equation (5.23) and the disappearance of the complex is described by equation (5.24):

$$R_2 = k_2 [ES] \qquad (5.23)$$

$$R_3 = k_3 [ES] \qquad (5.24)$$

The steady state rate definition of the enzyme-substrate complex is then described by expression (5.25):

$$\frac{dES}{dt} = r_1 - r_2 - r_3 = k_1[E][S] - (k_2 + k_3)[ES] \quad (5.25)$$

The enzyme concentration can be calculated as follows, when the initial enzyme concentration is expressed as in equation (5.27):

$$[E] = \frac{k_2 + k_3}{k_1}\frac{[ES]}{[S]} \quad (5.26)$$

$$E = E_O - ES \quad (5.27)$$

The famous Michaelis-Menten relation can be achieved by combining the above equations:

$$ES = E_O \frac{S}{k + S} \quad (5.28)$$

5.2 General Equations for Activated Sludge Systems under Dynamic Conditions

The overall COD mass balance equation in an activated sludge system under dynamic conditions is given by the equation (5.29) where four components of COD are substrate, storage material, biomass and oxygen in the system.

$$R_S + R_{STO} + R_X + R_{O2} = 0 \quad (5.29)$$

The metabolic modeling approaches have investigated such activated sludge systems in two phases, i.e. feast phase (when exogenous substrate is present) and famine phase (when no external substrate is present).

The conversion rates of organic matter in the feast phase is expressed by the following mass balance equations under steady-state:

$$R_S + R_{STO,P} + R_{X,PI} = 0 \quad (5.30)$$

$$-R_S = R_{STO,P} + R_{X,PI} \quad (5.31)$$

A similar mass balance for organic matter holds for famine phase as described by below equations:

$$R_{STO,C} + R_{X,P2} = 0 \quad (5.32)$$

$$-R_{STO,C} = R_{X,P2} \quad (5.33)$$

The conversion rates are combinations of process stoichiometry and kinetics as shown in the general expression (5.34):

$$R=Y.r \quad (5.34)$$

where,

Y = Stoichiometric coefficient

r = Process rate

5.3 ASM3 and Modifications Adapted for Tannery Wastewater

There are three relevant rates with the assumption of simultaneous direct growth and storage. If two of these rates are known, third one can be calculated. The sum of growth rate (r_X) and storage rate (r_{STO}) gives the substrate uptake rate (r_S) as shown in Figure 5.1.

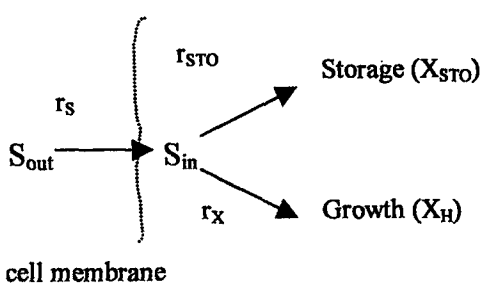

Figure 5.1 Schematic illustration of growth and storage rates

If feast and famine phases are taken into account, it can be seen that there are two different growth rates as illustrated in Figure 5.2.

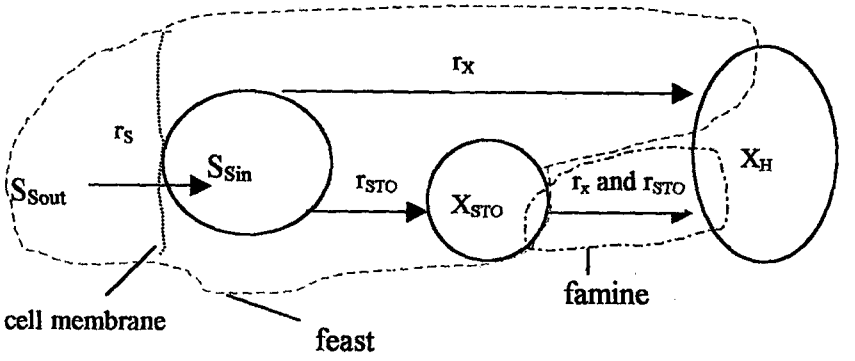

Figure 5.2 Schematic illustration of rates in feast and famine phases

For feast phase;

r_S = rate of consumption of S_S

r_{STO} = rate of production of X_{STO}

r_X = rate of production of X_H over substrate

For famine phase;

r_{STO} = rate of consumption of X_{STO}

r_X = rate of production of X_H over stored polymer

As a result, storage rates and growth rates are symbolized as the same for both phases but their meanings are different. For that reason, symbols are rewritten in this study in order to prevent the misunderstandings:

For feast phase;

$r_{S,C}$ = rate of consumption of S_S

$r_{STO,P}$ = rate of production of X_{STO}

$r_{X,P1}$ = rate of production of X_H over substrate

For famine phase;

$r_{STO,C}$ = rate of consumption of X_{STO}

$r_{X,P2}$ = rate of production of X_H over stored polymer

For both phases;

$r_{O,C}$ = rate of consumption of oxygen = OUR

Modified illustration is shown in Figure 5.3

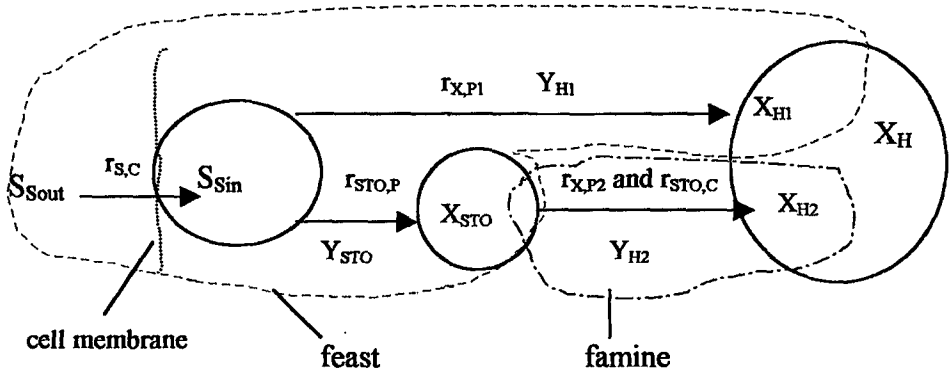

Figure 5.3 Modified schematic illustration of rates in feast and famine phases

5.3.1 ASM3 Adapted for Tannery Wastewater

Orhon *et al.* (1999) developed a matrix according to ASM1 involving endogenous decay (Table 5.1) and Gujer *et al.* (2000) proposed ASM3 and a matrix according to that model (Table 5.2). With reference to these matrices, a new model is proposed and illustrated in matrix form in Table 5.3 for tannery wastewaters. Although the subject matrix has been developed according to ASM3 the soluble inert, S_I and soluble microbial product, S_P fractions have been indicated separately, whereas in the version of Gujer *et al.,* (2000) S_P was included in S_I and X_P was included in X_I. Some modifications were made in order to develop this matrix according to ASM3 making use of some ASM1 concepts. Hydrolysis concept has been accepted as in ASM1 instead of ASM3 and endogenous respiration of X_H has also been accepted as in ASM1.

Carbon removal is defined with eight components and three processes according to Table 5.1 (Orhon *et al.,* 1999). Components (S_I, S_S, X_I and X_S) define the organic nature of the wastewater. An additional parameter defining the soluble portion of the slowly biodegradable COD, or the rapidly hydrolyzable COD, S_H, is considered to be a useful process component for tannery effluent. Other components reflected the viable heterotrophic biomass X_H, with a soluble residual microbial product S_P and particulate residual microbial product X_P. The authors have stated that there was a general agreement to consider X_P as a separate component but, S_P was often considered together with S_I in terms of fictitious influent COD fraction. This approximation is considered acceptable for domestic wastewater but it would bring

Table 5.1 Process Kinetics and Stoichiometry for Carbon Removal Involving Endogenous Decay (Orhon *et al.*, 1999)

Component→	1	2	3	4	5	6	7	8	Process Rate
Process↓	S_S	X_H	X_P	S_P	S_I	X_I	X_S	S_O	$ML^{-3}T^{-1}$
Growth	$-\frac{1}{Y_H}$	1		α_D				$-\frac{1-Y_H}{Y_H}$	$\hat{\mu}_H \frac{S_S}{(K_S+S_S)} X_H$
Decay		-1	f_{EX}	f_{ES}				$-(1-f_{EX}-f_{ES})$	$b_H X_H$
Hydrolysis	1						-1		$k_h \frac{X_S/X_H}{(K_X+X_S/X_H)} X_H$
Parameters, ML^{-3}	COD	Cell COD	COD	COD	COD	COD	COD	O_2	

Table 5.2 *MATRIX REPRESENTATION OF ACTIVATED SLUDGE MODEL NO.3 (ASM3)*

COMPONENT PROCESS	S_O O_2	S_I COD	S_S COD	S_{NH} N	S_{N2} N	S_{NO} N	S_{HCO} mole	X_I COD	X_S COD	X_H COD	X_{STO} COD	X_A COD	X_{TS} TSS	RATE
Hydrolysis		f_{SI}	$1-f_{SI}$	i_{NSI}			$\frac{i_{NSI}}{14}$		-1				$-i_{TSXS}$	$k_H \frac{X_S/X_H}{K_X+X_S/X_H} X_H$
Heterotrophic Organisms, Denitrification														
Aerobic Storage of COD	$-(1-Y_{STO,O2})$		-1	i_{NSS}			$\frac{i_{NSS}}{14}$				$Y_{STO,O2}$		$i_{TSSTO} Y_{STO,O2}$	$k_{STO} \frac{S_O}{K_O+S_O} \frac{S_S}{K_S+S_S} X_H$
Anoxic Storage of COD			-1	i_{NSS}	$\frac{(1-Y_{STO,NO})}{2.86}$	$-\frac{(1-Y_{STO,NO})}{2.86}$	$\frac{(1-Y_{STO,NO})}{14\cdot 2.86}-\frac{i_{NSS}}{14}$				$Y_{STO,NO}$		$i_{TSSTO} Y_{STO,NO}$	$k_{STO} \eta_{NO} \frac{K_O}{K_O+S_O} \frac{S_{NO}}{K_{NO}+S_{NO}} \frac{S_S}{K_S+S_S} X_H$
Aerobic Growth	$-\frac{(1-Y_{H,O2})}{Y_{H,O2}}$			$-i_{NBM}$			$-\frac{i_{NBM}}{14}$			1	$-1/Y_{H,O2}$		$i_{TSBM}-\frac{i_{TSSTO}}{Y_{H,O2}}$	$\mu_H \frac{S_O}{K_O+S_O} \frac{S_{NH}}{K_{NH}+S_{NH}} \frac{S_{HCO}}{K_{HCO}+S_{HCO}} \frac{X_{STO}/X_H}{K_{STO}+X_{STO}/X_H} X_H$
Anoxic Growth (Denitrification)				$-i_{NBM}$	$\frac{(1-Y_{H,NO})}{2.86\cdot Y_{H,NO}}$	$-\frac{(1-Y_{H,NO})}{2.86\cdot Y_{H,NO}}$	$\frac{(1-Y_{H,NO})}{14\cdot 2.86\cdot Y_{H,NO}}-\frac{i_{NBM}}{14}$			1	$-1/Y_{H,NO}$		$i_{TSBM}-\frac{i_{TSSTO}}{Y_{H,NO}}$	$\mu_H \eta_{NO} \frac{K_O}{K_O+S_O} \frac{S_{NO}}{K_{NO}+S_{NO}} \frac{S_{NH}}{K_{NH}+S_{NH}} \frac{S_{HCO}}{K_{HCO}+S_{HCO}} \frac{X_{STO}/X_H}{K_{STO}+X_{STO}/X_H} X_H$
Aerobic Endogenous Respiration	$-(1-f_I)$			$i_{NBM}-f_I i_{NXI}$			$\frac{i_{NBM}-f_I i_{NXI}}{14}$	f_I		-1			$-i_{TSBM}+f_I i_{TSXI}$	$b_{H,O2} \frac{S_O}{K_O+S_O} X_H$
Anoxic Endogenous Respiration				$i_{NBM}-f_I i_{NXI}$	$\frac{(1-f_I)}{2.86}$	$-\frac{(1-f_I)}{2.86}$	$\frac{(1-f_I)}{14\cdot 2.86}+\frac{i_{NBM}-f_I i_{NXI}}{14}$	f_I		-1			$-i_{TSBM}+f_I i_{TSXI}$	$b_{H,NO} \frac{K_O}{K_O+S_O} \frac{S_{NO}}{K_{NO}+S_{NO}} X_H$
Aerobic Respiration of X_{STO}	-1										-1		$-i_{TSSTO}$	$b_{STO,O2} \frac{S_O}{K_O+S_O} X_{STO}$
Anoxic Respiration of X_{STO}					1/2.86	-1/2.86	1/(14·2.86)				-1		$-i_{TSSTO}$	$b_{STO,NO} \frac{K_O}{K_O+S_O} \frac{S_{NO}}{K_{NO}+S_{NO}} X_{STO}$
Autotrophic Organisms, Nitrification														
Nitrification	$-\frac{(4.57-Y_A)}{Y_A}$			$-(1/Y_A+i_{NBM})$		$1/Y_A$	$-\frac{2/Y_A-i_{NBM}}{14}$					1	i_{TSBM}	$\mu_A \frac{S_O}{K_{A,O}+S_O} \frac{S_{NH}}{K_{A,NH}+S_{NH}} \frac{S_{HCO}}{K_{A,HCO}+S_{HCO}} X_A$
Aerobic Endogenous Respiration	$-(1-f_I)$			$i_{NBM}-f_I i_{NXI}$			$\frac{i_{NBM}-f_I i_{NXI}}{14}$	f_I				-1	$-i_{TSBM}+f_I i_{TSXI}$	$b_{A,O2} \frac{S_O}{K_O+S_O} X_A$
Anoxic Endogenous Respiration				$i_{NBM}-f_I i_{NXI}$	$\frac{(1-f_I)}{2.86}$	$-\frac{(1-f_I)}{2.86}$	$\frac{(1-f_I)}{14\cdot 2.86}+\frac{i_{NBM}-f_I i_{NXI}}{14}$	f_I				-1	$-i_{TSBM}+f_I i_{TSXI}$	$b_{A,NO} \frac{K_O}{K_O+S_O} \frac{S_{NO}}{K_{NO}+S_{NO}} X_A$
Composition Matrix														
Conservatives														
COD g COD	-1	1	1		-1.71	-4.57		1	1	1	1	1		
Nitrogen g N		i_{NSI}	i_{NSS}	1	1	1		i_{NXI}	i_{NXS}	i_{NBM}		i_{NBM}		
Ionic Charge Mole +				1/14		-1/14	-1							
Observables														
TSS g TSS								i_{TSXI}	i_{TSXS}	i_{TSBM}	i_{TSSTO}	i_{TSBM}		

operational difficulties in the correct assessment of other process compounds, especially X_I. Orhon *et al.* (1999) suggested that the component S_P should deserve a separate consideration in the biological treatability of industrial wastewater. For tannery wastewater, generation of soluble residual microbial product has been defined by means of a decay associated mechanism assuming that a fraction f_{ES} of the endogenous biomass is not oxidized but converted to inert products (Orhon and Artan, 1994).

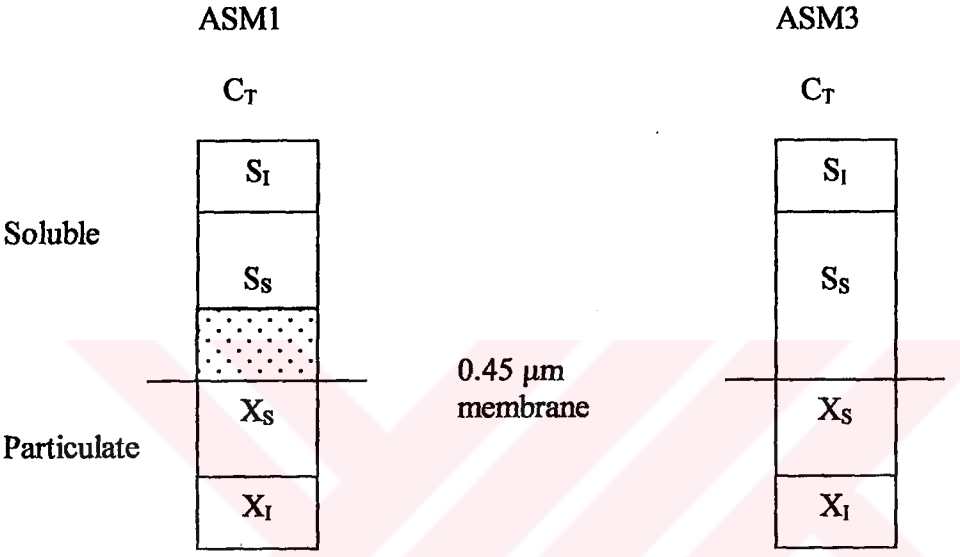

Figure 5.4. Wastewater components according to activated sludge models

One of the main differences encountered in ASM1 and ASM3 is the definitions of COD fractions in wastewater. As shown above in Figure 5.4, definition of readily biodegradable COD, S_S and slowly biodegradable COD, X_S are different according to the models. In ASM1, X_S has both soluble and particulate portions whereas; it is defined to be only particulate in ASM3. Hydrolysis is much more important in ASM1 because X_S has higher concentration due to the rapidly hydrolyzable soluble part (S_H). Equation (5.35) accounts for both of the models, while total soluble COD is different in ASM1 as in equation (5.36) and in ASM3 as in equation (5.37).

$$X_S=C_T-S_I-S_S-X_I \quad (5.35)$$

$$S_T=S_I+S_S+S_H \quad (5.36)$$

$$S_T=S_I+S_S \quad (5.37)$$

Table 5.3 Matrix representation of the proposed model structure-ASM3 adapted for tannery WW by Dizdaroglu-Risvanoglu

Component → / ↓Process	S_O O_2	S_S COD	S_P COD	S_I COD	X_S COD	X_H COD	X_{STO} COD	X_P COD	X_I COD	*Process Rate*
Hydrolysis		*1*			*-1*					$k_H \frac{X_S/X_H}{K_X + X_S/X_H} X_H$
Aerobic Storage of S_S	$-(1-Y_{STO})$	*-1*					Y_{STO}			$k_{STO} \frac{S_O}{K_O + S_O} \frac{S_S}{K_S + S_S} X_H$
Growth	$-\frac{1-Y_H}{Y_H}$					*1*	$-1/Y_H$			$\mu_H \frac{S_O}{K_O + S_O} \frac{X_{STO}/X_H}{K_{STO} + X_{STO}/X_H} X_H$
Endogenous Respiration of X_H	$-(1-f_{ES}-f_{EV})$		f_{ES}			*-1*		f_{EX}		$b_H \frac{S_O}{K_O + S_O} X_H$
Respiration of X_{STO}	*-1*						*-1*			$b_{STO} \frac{S_O}{K_O + S_O} X_{STO}$

ASM3 differentiates soluble and particulate components by 0.45 μm membrane filtration whereas a significant fraction of X_S defined in ASM1 would be contained in the filtrate (Figure 5.4). Readily biodegradable organic substrate (S_S) has special importance in ASM3 because it is first converted to storage products (X_{STO}), and then becomes available for the usage of biomass. Required energy for this conversion is compensated by respiration. According to ASM3, slowly biodegradable substrate (X_S) must undergo hydrolysis before it is used by the biomass because this COD fraction is composed of high molecular weight, colloidal and particulate organic compounds that cannot be directly used. The products of the hydrolysis are assumed to be readily biodegradable or soluble inert organics. It must be reminded that all X_S contained in the influent is not involved in the filtrate of 0.45 μm membrane filter in ASM3. Cell external hydrolysis in ASM3 does not consume any electron acceptor. Active biomass is responsible for the hydrolysis of X_S and storage process. Cell internal storage products (X_{STO}) consists of PHA, glycogen etc., which are only defined as a functional component required for modeling but not directly identifiable chemically.

The rate equations of the components of the proposed model, namely ASM3 adapted for tannery wastewater can be deduced as follows:

$$\frac{dS_S}{dt} = -k_{STO}\frac{S_O}{K_O+S_O}\frac{S_S}{K_S+S_S}X_H + k_H\frac{X_S/X_H}{K_X+X_S/X_H}X_H \qquad (5.38)$$

$$\frac{dX_S}{dt} = -k_H\frac{X_S/X_H}{K_X+X_S/X_H}X_H \qquad (5.39)$$

$$\frac{dX_H}{dt} = \mu_H\frac{S_O}{K_O+S_O}\frac{X_{STO}/X_H}{K_{STO}+X_{STO}/X_H}X_H - b_H\frac{S_O}{K_O+S_O}X_H \qquad (5.40)$$

$$\frac{dX_P}{dt} = f_{EX}\,b_H\frac{S_O}{K_O+S_O}X_H \qquad (5.41)$$

$$\frac{dS_P}{dt} = f_{ES}\,b_H\frac{S_O}{K_O+S_O}X_H \qquad (5.42)$$

$$\frac{dX_{STO}}{dt} = Y_{STO}\, k_{STO} \frac{S_O}{K_O + S_O} \frac{S_S}{K_S + S_S} X_H - \frac{1}{Y_H} \mu_H \frac{S_O}{K_O + S_O} \frac{X_{STO}/X_H}{K_{STO} + X_{STO}/X_H} X_H$$

$$- b_{STO} \frac{S_O}{K_O + S_O} X_{STO} \qquad (5.43)$$

$$\frac{dS_O}{dt} = -(1 - Y_{STO})\, k_{STO} \frac{S_O}{K_O + S_O} \frac{S_S}{K_S + S_S} X_H - (1 - f_{EX} - f_{ES})\, b_H \frac{S_O}{K_O + S_O} X_H$$

$$- \frac{1 - Y_H}{Y_H} \mu_H \frac{S_O}{K_O + S_O} \frac{X_{STO}/X_H}{K_{STO} + X_{STO}/X_H} X_H - b_{STO} \frac{S_O}{K_O + S_O} X_{STO} \qquad (5.44)$$

The stoichiometric COD transformations and the relevant rates of formation and disappearance of the COD components for each process defined in the model are reviewed in the following section.

1. Hydrolysis: Hydrolysis of slowly biodegradable substrate, X_S, is illustrated in Figure 5.5.

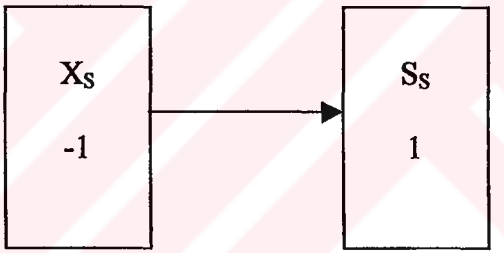

Figure 5.5 COD transformation in hydrolysis referring to Table 5.3

The rate of production of readily biodegradable COD, S_S, through hydrolysis is given in equation (5.45):

$$r_{S,P} = k_H \frac{X_S / X_H}{K_X + X_S / X_H} X_H \qquad (5.45)$$

2. Aerobic Storage of S_S: Stoichiometry of storage of readily biodegradable substrate, S_S, as storage polymer, X_{STO}, and of the consumption of dissolved oxygen during this process is given in Figure 5.6. The rates for the consumption of substrate through storage process, production of the storage polymer and consumption of the oxygen are given in equations (5.46), (5.47) and (5.48) respectively.

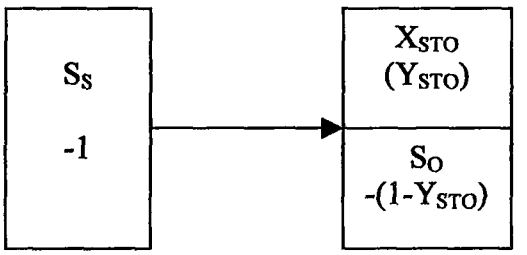

Figure 5.6 COD transformation in storage referring to Table 5.3

$$-r_{S,C} = k_{STO} \frac{S_O}{K_O + S_O} \frac{S_S}{K_S + S_S} X_H \tag{5.46}$$

$$r_{STO,P} = Y_{STO} k_{STO} \frac{S_O}{S_O + K_O} \frac{S_S}{K_S + S_S} X_H \tag{5.47}$$

$$-r_{O,C} = (1 - Y_{STO}) k_{STO} \frac{S_O}{K_O + S_O} \frac{S_S}{K_S + S_S} X_H \tag{5.48}$$

3. Aerobic Growth of Heterotrophs: Heterotrophic biomass grows on the stored polymers, X_{STO}, and utilizes oxygen during this process (Figure 5.7).

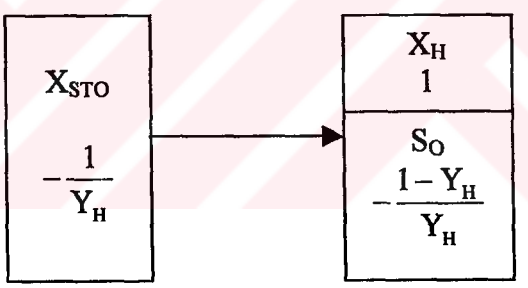

Figure 5.7 COD transformation in growth referring to Table 5.3

The rate of production of X_H and the rate of consumption of X_{STO} are given in equations (5.49) and (5.50). The rate of consumed oxygen is expressed by (5.51).

$$r_{X,P} = \mu_H \frac{S_O}{K_O + S_O} \frac{X_{STO}/X_H}{K_{STO} + X_{STO}/X_H} X_H \tag{5.49}$$

$$-r_{STO,C} = \frac{\mu_H}{Y_H} \frac{S_O}{K_O + S_O} \frac{X_{STO}/X_H}{K_{STO} + X_{STO}/X_H} X_H \tag{5.50}$$

$$-r_{O,C} = \frac{1 - Y_H}{Y_H} \mu_H \frac{S_O}{K_O + S_O} \frac{X_{STO}/X_H}{K_{STO} + X_{STO}/X_H} X_H \tag{5.51}$$

4. Endogenous Respiration of X_H: Active biomass is converted to soluble and particulate microbial products (S_P and X_P) by endogenous respiration. Stoichiometry of COD transformation is illustrated in Figure 5.8 as below:

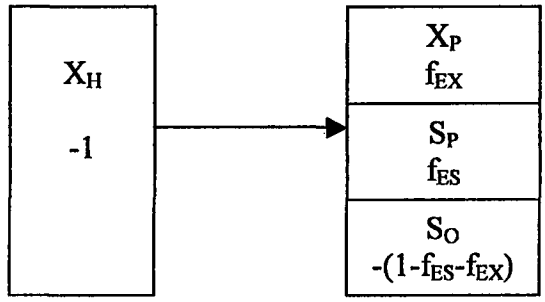

Figure 5.8 COD transformation in endogenous respiration referring to Table 5.3

The rates of consumption of active biomass ($-r_{X,C}$) and oxygen utilization are given in equations (5.52) and (5.53).

$$-r_{X,C} = b_H \frac{S_O}{K_O + S_O} X_H \tag{5.52}$$

$$-r_{O,C} = (1 - f_{ES} - f_{EX})\, b_H \frac{S_O}{K_O + S_O} X_H \tag{5.53}$$

5. X_{STO} Respiration: Respiration process occurring on stored polymers is illustrated in Figure 5.9 and the rates of consumption of X_{STO} ($-r_{XSTO,C}$) and oxygen are given by the expressions (5.54) and (5.55).

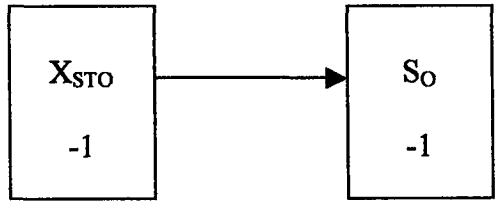

Figure 5.9 COD transformation in X_{STO} respiration referring to Table 5.3

$$-r_{XSTO,C} = b_{STO} \frac{S_O}{K_O + S_O} X_{STO} \tag{5.54}$$

$$-r_{O,C} = b_{STO} \frac{S_O}{K_O + S_O} X_{STO} \tag{5.55}$$

5.3.2 ASM3 Adapted for Tannery Wastewater (Model A)

Krishna and van Loosdrecht (1999) fixed r_S and r_{STO} in their model and calculated r_X with the following equation considering metabolic modeling concepts:

$$r_X = Y_{SX} r_S - \frac{Y_{SX}}{Y_{SP}} r_P \tag{5.56}$$

where, Y_{SX} is the yield of biomass on acetate and Y_{SP} is the yield of storage of polyhydroxybutyrate (PHB) on acetate. Modified version of this model for tannery wastewater involves some differences in symbols; also there are some neglections such as nitrogenous and bicarbonate fractions. The hydrolysis process has also been added to the model defined for acetate (Table 5.4).

The biomass production in the feast phase is defined as:

$$r_{X,P1} = Y_{H1} r_{S,C} - \frac{Y_{H1}}{Y_{STO}} r_{STO,P} \tag{5.57}$$

where,

$$Y_{H1} = \frac{\Delta X_{H1}}{\Delta S_S} \text{ (yield of biomass on substrate)} \tag{5.58}$$

$$Y_{STO} = \frac{\Delta X_{STO}}{\Delta S_S} \text{ (yield of stored polymer on substrate)} \tag{5.59}$$

$$Y_{H2} = \frac{\Delta X_{H2}}{\Delta X_{STO}} \text{ (yield of biomass on stored polymer)} \tag{5.60}$$

1. Hydrolysis: Hydrolysis of X_S is involved in this adapted model (Figure 5.10).

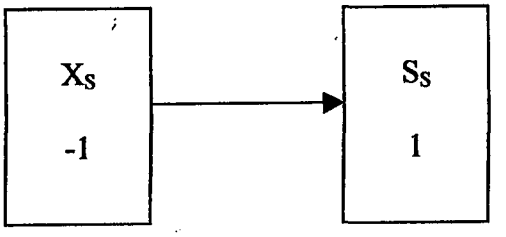

Figure 5.10 COD transformation in hydrolysis referring to Table 5.4

Table 5.4 Matrix representation of the Model A proposed by Krishna and van Loosdrecht (1999) adapted for tannery WW by Dizdaroglu-Risvanoglu

Component → / ↓ Process	S_O O_2	S_S COD	S_P COD	S_I COD	X_S COD	X_H COD	X_{STO} COD	X_P COD	X_I COD	Process Rate
Hydrolysis		1			-1					$k_H \frac{X_S/X_H}{K_X + X_S/X_H} X_H$
Feast Phase										
Aerobic Storage of S_S	$-(1-Y_{STO})$	-1					Y_{STO}			$k_{STO} \frac{S_O}{K_O + S_O} \frac{S_S}{K_S + S_S} X_H$
Direct Growth	$-\frac{1-Y_{H1}}{Y_{H1}}$	$-1/Y_{H1}$				1				$\mu_{H1} \frac{S_O}{K_O + S_O} \frac{S_S}{K_S + S_S} X_H$
Famine Phase										
Growth on X_{STO}	$-\frac{1-Y_{H2}}{Y_{H2}}$					1	$-1/Y_{H2}$			$\mu_{H2} \frac{S_O}{K_O + S_O} \frac{K_S}{K_S + S_S} \frac{X_{STO}/X_H}{K_{STO} + X_{STO}/X_H} X_H$
All Phases										
Endogenous Respiration of X_H	$-(1-f_{ES}-f_{EV})$		f_{ES}			-1		f_{EX}		$b_H \frac{S_O}{K_O + S_O} X_H$
Respiration of X_{STO}	-1						-1			$b_{STO} \frac{S_O}{K_O + S_O} X_{STO}$

The rate of production of readily biodegradable COD by hydrolysis is given in expression (5.61):

$$r_{S,P} = k_H \frac{X_S / X_H}{K_X + X_S / X_H} X_H \qquad (5.61)$$

2. Aerobic Storage of S_S (feast): Illustration of aerobic storage of readily biodegradable COD as X_{STO} on stoichiometric basis is given in Figure 5.11.

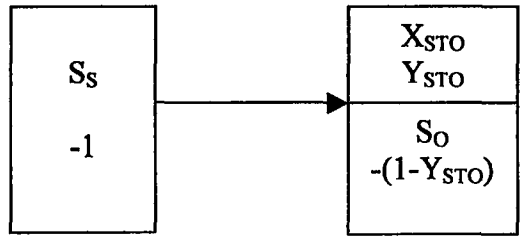

Figure 5.11 COD transformation in storage referring to Table 5.4

Rate of readily biodegradable substrate consumption, rate of storage polymer formation and rate of oxygen utilization during these processes are given as below:

$$-r_{S,C} = \left[k_{STO} + \frac{\mu_{H1}}{Y_{H1}} \right] \frac{S_O}{K_O + S_O} \frac{S_S}{K_S + S_S} X_H \qquad (5.62)$$

$$r_{STO,P} = Y_{STO} k_{STO} \frac{S_O}{K_O + S_O} \frac{S_S}{K_S + S_S} X_H \qquad (5.63)$$

$$-r_{O,C} = (1 - Y_{STO})\, k_{STO} \frac{S_O}{K_O + S_O} \frac{S_S}{K_S + S_S} X_H \qquad (5.64)$$

3. Direct Growth on S_S (feast): Growth of biomass on exogenous readily biodegradable substrate is illustrated in Figure 5.12.

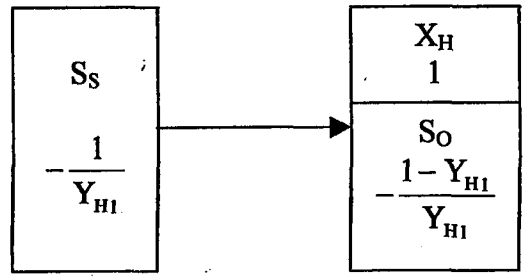

Figure 5.12 COD transformation in direct growth referring to Table 5.4

The rate of production of XH in feast phase is given by the expression (5.65). The oxygen utilization rate is also given in equation (5.66):

$$r_{X,P1} = \mu_{H1} \frac{S_O}{S_O + K_O} \frac{S_S}{K_S + S_S} X_H \tag{5.65}$$

$$-r_{O,C} = \frac{1 - Y_{H1}}{Y_{H1}} \mu_{H1} \frac{S_O}{S_O + K_O} \frac{S_S}{K_S + S_S} X_H \tag{5.66}$$

4. Growth on X_{STO} (famine): In famine phase growth of the active biomass occurs on stored polymers (Figure 5.13). The rates for the production of X_H and consumption of X_{STO} and O_2 are given in equations (5.67), (5.68) and (5.69) respectively.

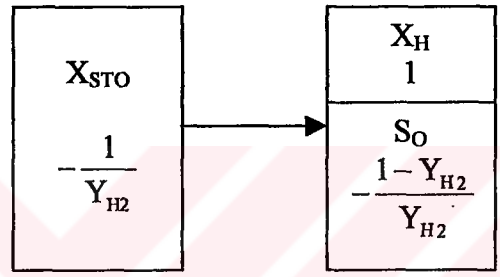

Figure 5.13 COD transformation in growth over X_{STO} referring to Table 5.4

$$-r_{STO,C} = \frac{\mu_{H2}}{Y_{H2}} \frac{S_O}{K_O + S_O} \frac{K_S}{K_S + S_S} \frac{X_{STO}/X_H}{K_{STO} + X_{STO}/X_H} X_H \tag{5.67}$$

$$r_{X,P2} = \mu_{H2} \frac{S_O}{K_O + S_O} \frac{K_S}{K_S + S_S} \frac{X_{STO}/X_H}{K_{STO} + X_{STO}/X_H} X_H \tag{5.68}$$

$$-r_{O,C} = \frac{1 - Y_{H2}}{Y_{H2}} \mu_{H2} \frac{S_O}{K_O + S_O} \frac{K_S}{K_S + S_S} \frac{X_{STO}/X_H}{K_{STO} + X_{STO}/X_H} X_H \tag{5.69}$$

5. Endogenous Respiration of X_H: COD transformation during the endogenous respiration of X_H is given in Figure 5.14.

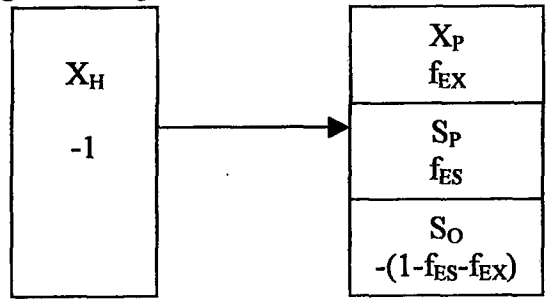

Figure 5.14 COD transformation in endogenous respiration referring to Table 5.4

The rates of consumption of active biomass and oxygen are expressed as below:

$$-r_{X,C} = b_H \frac{S_O}{K_O + S_O} X_H \tag{5.70}$$

$$-r_{O,C} = (1 - f_{ES} - f_{EX})\, b_H \frac{S_O}{K_O + S_O} X_H \tag{5.71}$$

6. Respiration of X_{STO}: Figure 5.15 shows the X_{STO} respiration and expressions (5.72) and (5.73) gives the rates for the utilization of X_{STO} and oxygen.

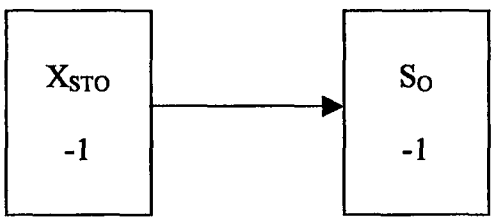

Figure 5.15 COD transformation in X_{STO} respiration referring to Table 5.4

$$-r_{XSTO,C} = b_{STO} \frac{S_O}{K_O + S_O} X_{STO} \tag{5.72}$$

$$-r_{O,C} = b_{STO} \frac{S_O}{K_O + S_O} X_{STO} \tag{5.73}$$

5.3.3 ASM3 Adapted for Tannery Wastewater (Model B)

Karahan-Gül *et al.* (2002) assumed that r_X and r_{STO} are defined so r_S can be found by the addition of the reactions in terms of metabolic modeling:

$$-r_S = \frac{1}{Y_{SX}} r_X + \frac{1}{Y_{SP}} r_P + m_S C_X \tag{5.74}$$

$m_S C_X$ term in this equation is neglected because in this model (Table 5.5), endogenous decay is defined over oxygen utilization whereas it is defined by substrate consumption in Beun *et al.* (2001). Modified version of above equation is shown below:

$$-r_{S,C} = \frac{1}{Y_{H1}} r_{X,P1} + \frac{1}{Y_{STO}} r_{STO,P} \tag{5.75}$$

Table 5.5 Matrix representation of the Model B proposed by Karahan-Gül *et al.* (2002b) adapted for tannery WW by Dizdaroglu-Risvanoglu

Component → / ↓ Process	S_O O_2	S_S COD	S_P COD	S_I COD	X_S COD	X_H COD	X_{STO} COD	X_P COD	X_I COD	Process Rate
Hydrolysis		1			-1					$k_H \frac{X_S/X_H}{K_X + X_S/X_H} X_H$
Feast Phase										
Aerobic Storage of S_S	$-\frac{1-Y_{STO}}{Y_{STO}}$	$-1/Y_{STO}$					1			$k_{STO} \frac{S_O}{K_O + S_O} \frac{S_S}{K_S + S_S} X_H$
Direct Growth	$-\frac{1-Y_{H1}}{Y_{H1}}$	$-1/Y_{H1}$				1				$\mu_{H1} \frac{S_O}{K_O + S_O} \frac{S_S}{K_S + S_S} X_H$
Famine Phase										
Growth on X_{STO}	$-\frac{1-Y_{H2}}{Y_{H2}}$					1	$-1/Y_{H2}$			$\mu_{H2} \frac{S_O}{K_O + S_O} \frac{K_S}{K_S + S_S} \frac{X_{STO}/X_H}{K_{STO} + X_{STO}/X_H} X_H$
All Phases										
Endogenous Respiration of X_H	$-(1-f_{ES}-f_{EV})$		f_{ES}			-1		f_{EX}		$b_H \frac{S_O}{K_O + S_O} X_H$
Respiration of X_{STO}	-1						-1			$b_{STO} \frac{S_O}{K_O + S_O} X_{STO}$

1. Hydrolysis: Production of S_S through the hydrolysis of X_S is also involved in this model (Figure 5.16).

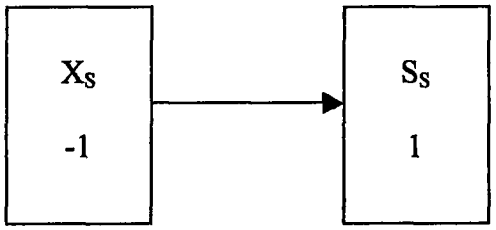

Figure 5.16 COD transformation in hydrolysis referring to Table 5.5

The rate of readily biodegradable COD formation from the hydrolysis of slowly biodegradable COD is given in equation (5.76) as similar to previous models:

$$r_{S,P} = k_H \frac{X_S / X_H}{K_X + X_S / X_H} X_H \tag{5.76}$$

2. Aerobic Storage of S_S (feast): Storage of readily biodegradable substrate as X_{STO} in feast phase is given in Figure 5.17. Rate expressions for the S_S consumption, X_{STO} production and oxygen utilization are given in equations (5.77), (5.78) and (5.79) respectively.

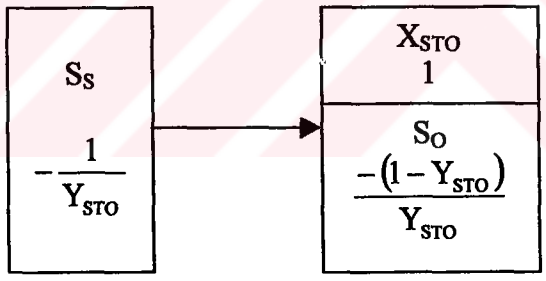

Figure 5.17 COD transformation in storage referring to Table 5.5

$$-r_{S,C} = \left[\frac{k_{STO}}{Y_{STO}} + \frac{\mu_{H1}}{Y_{H1}} \right] \frac{S_O}{K_O + S_O} \frac{S_S}{K_S + S_S} X_H \tag{5.77}$$

$$r_{STO,P} = k_{STO} \frac{S_O}{K_O + S_O} \frac{S_S}{K_S + S_S} X_H \tag{5.78}$$

$$-r_{O,C} = \frac{1 - Y_{STO}}{Y_{STO}} k_{STO} \frac{S_O}{K_O + S_O} \frac{S_S}{K_S + S_S} X_H \tag{5.79}$$

3. Direct Growth on S_S (feast): Growth of biomass in feast phase means the depletion of readily biodegradable substrate (S_S). Stoichiometry of direct growth is given in Figure 5.18.

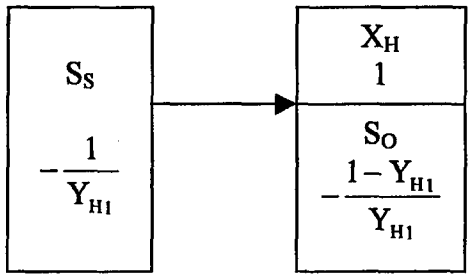

Figure 5.18 COD transformation in direct growth referring to Table 5.5

Production of X_H and consumption of oxygen rates in feast phase are given by equations (5.80) and (5.81) as similar to the adapted model of Krishna and van Loosdrecht (1999).

$$r_{X,P1} = \mu_{H1} \frac{S_O}{S_O + K_O} \frac{S_S}{K_S + S_S} X_H \tag{5.80}$$

$$-r_{O,C} = \frac{1-Y_{H1}}{Y_{H1}} \mu_{H1} \frac{S_O}{S_O + K_O} \frac{S_S}{K_S + S_S} X_H \tag{5.81}$$

4. Growth on X_{STO} (famine): Active biomass is also produced in famine phase over stored polymers as in Figure 5.19:

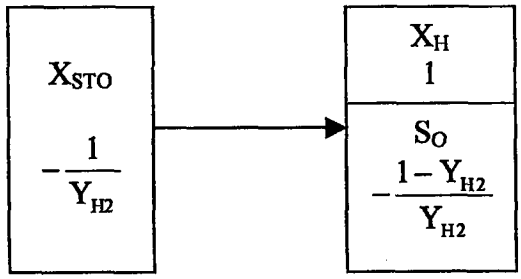

Figure 5.19 COD transformation in growth over X_{STO} referring to Table 5.5

$$-r_{STO,C} = \frac{\mu_{H2}}{Y_{H2}} \frac{S_O}{K_O + S_O} \frac{K_S}{K_S + S_S} \frac{X_{STO}/X_H}{K_{STO} + X_{STO}/X_H} X_H \tag{5.82}$$

$$r_{X,P2} = \mu_{H2} \frac{S_O}{K_O + S_O} \frac{K_S}{K_S + S_S} \frac{X_{STO}/X_H}{K_{STO} + X_{STO}/X_H} X_H \tag{5.83}$$

$$-r_{O,C} = \frac{1-Y_{H2}}{Y_{H2}} \mu_{H2} \frac{S_O}{K_O + S_O} \frac{K_S}{K_S + S_S} \frac{X_{STO}/X_H}{K_{STO} + X_{STO}/X_H} X_H \quad (5.84)$$

5. Endogenous Respiration of X_H: Endogenous respiration of active biomass is similar in all models as illustrated in Figure 5.20. The rates for the related processes are also similar as given in equations (5.85) and (5.86).

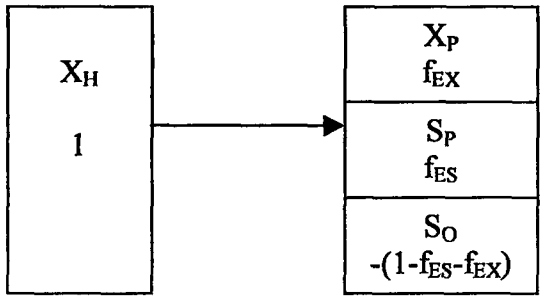

Figure 5.20 COD transformation in endogenous respiration referring to Table 5.5

$$-r_{X,C} = b_H \frac{S_O}{K_O + S_O} X_H \quad (5.85)$$

$$-r_{O,C} = (1 - f_{ES} - f_{EX})\, b_H \frac{S_O}{K_O + S_O} X_H \quad (5.86)$$

6. Respiration of X_{STO}: Respiration of stored polymers is given in Figure 5.21.

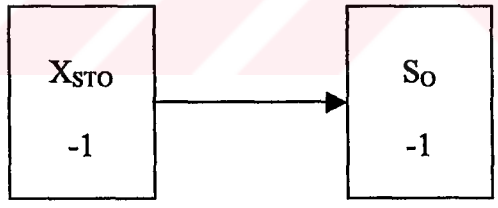

Figure 5.21 COD transformation in X_{STO} respiration referring to Table 5.5

The rates for the consumption of X_{STO} and oxygen are also given as below:

$$-r_{XSTO,C} = b_{STO} \frac{S_O}{K_O + S_O} X_{STO} \quad (5.87)$$

$$-r_{O,C} = b_{STO} \frac{S_O}{K_O + S_O} X_{STO} \quad (5.88)$$

5.3.4 Model Adapted for Tannery Wastewater in ASM3 Terms (Model C)

Models proposed by Krishna and van Loosdrecht (1999) and Karahan-Gül *et al.* (2002b) have defined storage process similar to ASM3, whereas van Loosdrecht and Heijnen (2002) have described substrate uptake. In other words, van Loosdrecht and Heijnen (2002) have chosen substrate uptake rate and growth rate on primary substrate as fixed processes in the feast phase and used storage as a pool for S_S surplus when growth fails to utilize all the substrate taken up. Therefore "q_S" (substrate uptake rate) term is used instead of k_{STO} parameter.

Another different concept in the model of van Loosdrecht and Heijnen (2002) is that, consumption of storage products are utilized with a linear process rate with respect to X_{STO} concentration, instead of Monod type of saturation function as in ASM3. Matrix representation of the adapted model structure is given in Table 5.6. Below expressions are used in the model:

$$-r_{HAC} = \frac{1}{Y_{SP}} r_{PHB} + \frac{1}{Y_{SX}} r_X + m_S X_H \qquad \text{(feast phase, for } H_{AC}\text{)} \qquad (5.89)$$

$$r_{PHB} = Y_{SP} r_{HAC} - \frac{Y_{SP}}{Y_{SX}} r_X - m_S Y_{SP} X_H \qquad \text{(feast phase)} \qquad (5.90)$$

$$r_X = Y_{PX} r_{PHB} - m_P Y_{PX} X_H \qquad \text{(famine phase)} \qquad (5.91)$$

These equations are also changed to obtain the following equations:

$$r_{STO,P} = Y_{STO} r_{S,C} - \frac{Y_{STO}}{Y_{H1}} r_{X,P1} \qquad \text{(feast phase)} \qquad (5.92)$$

$$r_{X,P2} = Y_{H2} r_{STO,C} \qquad \text{(famine phase)} \qquad (5.93)$$

Table 5.6 Matrix representation of the Model C proposed by van Loosdrecht and Heijnen (2002) adapted for tannery WW in ASM3 terms by Dizdaroglu-Risvanoglu

Component → / ↓ Process	S_O O_2	S_S COD	S_P COD	S_I COD	X_S COD	X_H COD	X_{STO} COD	X_P COD	X_I COD	Process Rate
Hydrolysis		1			-1					$k_H \frac{X_S/X_H}{K_X + X_S/X_H} X_H$
Feast Phase										
S_S Uptake	$-(1-Y_{STO})$	-1					Y_{STO}			$q_S \frac{S_O}{K_O + S_O} \frac{S_S}{K_S + S_S} X_H$
Direct Growth	$-\frac{Y_{STO} - Y_{H1}}{Y_{H1}}$					1	$-\frac{Y_{STO}}{Y_{H1}}$			$\mu_H \frac{S_O}{K_O + S_O} \frac{S_S}{K_S + S_S} X_H$
Famine Phase										
Growth on X_{STO}	$-(1-Y_{H2})$					Y_{H2}	-1			$k_{X_{STO}} \frac{S_O}{K_O + S_O} \frac{K_S}{K_S + S_S} \frac{X_{STO}}{X_H} X_H$
All Phases										
Endogenous Respiration of X_H	$-(1-f_{ES} - f_{EV})$		f_{ES}			-1		f_{EX}		$b_H \frac{S_O}{K_O + S_O} X_H$
Respiration of X_{STO}	-1						-1			$b_{STO} \frac{S_O}{K_O + S_O} X_{STO}$

1. Hydrolysis: Production of S_S through hydrolysis is illustrated in Figure 5.22.

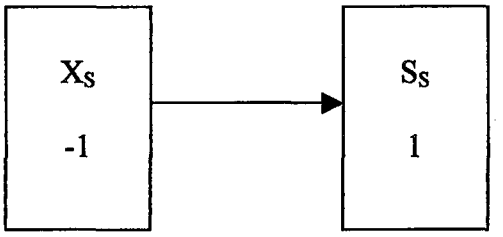

Figure 5.22 COD transformation in hydrolysis referring to Table 5.6

Rate equation for the production of readily biodegradable substrate is given by the following expression:

$$r_{S,P} = k_H \frac{X_S / X_H}{K_X + X_S / X_H} X_H \tag{5.94}$$

2. S_S (acetate) Uptake (feast): Uptake of the readily biodegradable substrate (acetate) is given in Figure 5.23 and the related rate equations are given by expressions (5.95), (5.96) and (5.97).

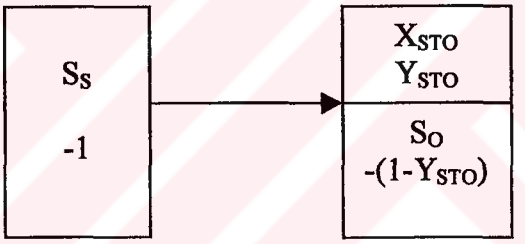

Figure 5.23 COD transformation in S_S uptake referring to Table 5.6

$$-r_{S,C} = q_S \frac{S_O}{K_O + S_O} \frac{S_S}{K_S + S_S} X_H \tag{5.95}$$

$$r_{STO,P} = Y_{STO} q_S \frac{S_O}{K_O + S_O} \frac{S_S}{K_S + S_S} X_H - \frac{Y_{STO}}{Y_{HI}} \mu_H \frac{S_O}{K_O + S_O} \frac{S_S}{K_S + S_S} X_H \tag{5.96}$$

$$-r_{O,C} = (1 - Y_{STO})\, q_S \frac{S_O}{K_O + S_O} \frac{S_S}{K_S + S_S} X_H \tag{5.97}$$

3. Direct Growth (feast): Growth of biomass on X_{STO} in feast phase is concerned as direct growth in this model (Figure 5.24). The rate of production of active biomass, X_H by using stored polymer, X_{STO} is given by equation (5.98) and the rate of consumption of oxygen is given in equation (5.99).

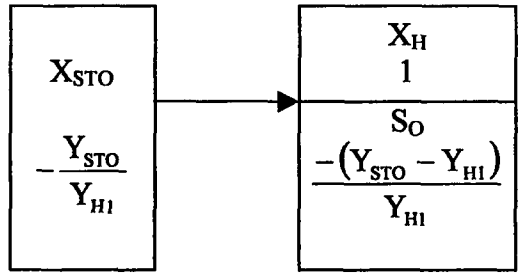

Figure 5.24 COD transformation in direct growth over X_{STO} referring to Table 5.6

$$r_{X,P1} = \mu_H \frac{S_O}{S_O + K_O} \frac{S_S}{K_S + S_S} X_H \tag{5.98}$$

$$-r_{O,C} = \frac{Y_{STO} - Y_{H1}}{Y_{H1}} \mu_H \frac{S_O}{S_O + K_O} \frac{S_S}{K_S + S_S} X_H \tag{5.99}$$

4. Growth on X_{STO} (famine): In famine phase, stored polymer is used as substrate and active biomass is produced by growth process as shown in Figure 5.25:

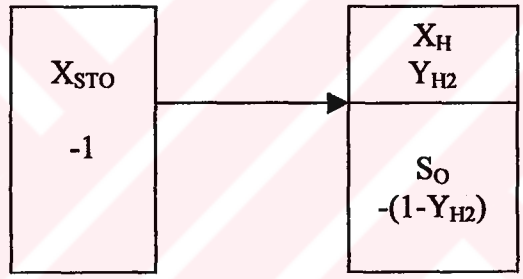

Figure 5.25 COD transformation in growth over X_{STO} referring to Table 5.6

$$-r_{STO,C} = k_{X_{STO}} \frac{S_O}{K_O + S_O} \frac{K_S}{K_S + S_S} \frac{X_{STO}}{X_H} X_H \tag{5.100}$$

$$r_{X,P2} = Y_{H2} k_{X_{STO}} \frac{S_O}{K_O + S_O} \frac{K_S}{K_S + S_S} \frac{X_{STO}}{X_H} X_H \tag{5.101}$$

$$-r_{O,C} = (1 - Y_{H2})\ k_{X_{STO}} \frac{S_O}{K_O + S_O} \frac{K_S}{K_S + S_S} \frac{X_{STO}}{X_H} X_H \tag{5.102}$$

5. Endogenous Respiration of X_H: Stoichiometric representation of endogenous respiration of X_H is given in Figure 5.26 and the related rate equations are given in expressions (5.103) and (5.104).

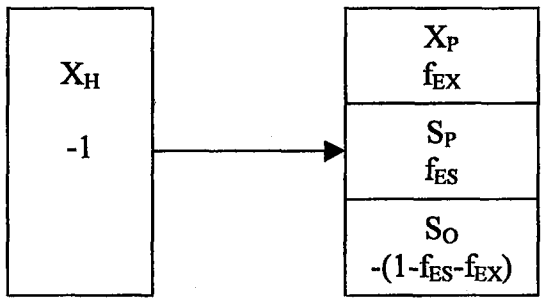

Figure 5.26 COD transformation in endogenous respiration referring to Table 5.6

$$-r_{X,C} = b_H \frac{S_O}{K_O + S_O} X_H \tag{5.103}$$

$$-r_{O,C} = (1 - f_{ES} - f_{EX})\, b_H \frac{S_O}{K_O + S_O} X_H \tag{5.104}$$

6. Respiration of X_{STO}: Respiration of stored polymers is given in Figure 5.27.

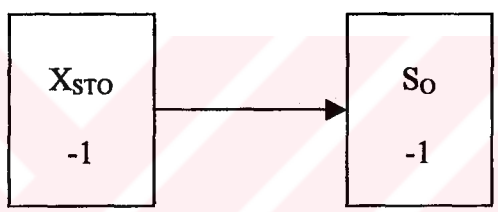

Figure 5.27 COD transformation in X_{STO} respiration referring to Table 5.6

The rates for the consumption of X_{STO} and oxygen are also given in the below equations:

$$-r_{XSTO,C} = b_{STO} \frac{S_O}{K_O + S_O} X_{STO} \tag{5.105}$$

$$-r_{O,C} = b_{STO} \frac{S_O}{K_O + S_O} X_{STO} \tag{5.106}$$

Summary of these modified models is shown in Table 5.7. Most important modification made for tannery wastewater in the models of Krishna and Van Loosdrecht (1999), Karahan-Gül *et al.* (2002b) and van Loosdrecht and Heijnen, (2002) was the addition of the hydrolysis process in order to compare these models with the ASM3 model adapted for tannery wastewater.

Table 5.7 Feast phase rate equations of three modified models

Model	Modified Rate Equations	Explanations
Model A	$r_{X,PI} = Y_{HI} r_{S,C} - \frac{Y_{HI}}{Y_{STO}} r_{STO,P}$	r_S and r_{STO} are fixed r_X is calculated
Model B	$-r_{S,C} = \frac{1}{Y_{HI}} r_{X,PI} + \frac{1}{Y_{STO}} r_{STO,P}$	r_X and r_{STO} are fixed r_S is calculated
Model C	$r_{STO,P} = Y_{STO} r_{S,C} - \frac{Y_{STO}}{Y_{HI}} r_{X,PI}$	r_S and r_X are fixed r_{STO} is calculated

In this study, S_{NH}, X_{TS} and f_I parameters were removed from the original matrix of Krishna and Van Loosdrecht (1999) and S_P, S_I, X_S, f_{ES} and f_{EX} parameters were accessed. In the model of Karahan-Gül *et al.* (2002b), f_{SI} and f_I parameters were changed as f_{ES} and f_{EX}, also S_P and X_P parameters were added. van Loosdrecht and Heijnen, (2002) explained a protein synthesizing system in their models with biochemical transformations via enzymes, however the adapted version presented in this study does not include the enzymatic expressions. Also S_N and X_e parameters were neglected and S_P, S_I, X_S, X_P and X_I parameters were added together with hydrolysis process.

The same symbols in the kinetics can have different values in the above-mentioned four different models adapted for tannery wastewater. k_{STO} in ASM3 version adapted for tannery wastewater is not the same as k_{STO} in other modified models but they are correlated to each other because they should eventually give the same uptake rate (Table 5.8). Similar aspects must be taken into account for other conversions as well as given in Table 5.9 and 5.10. Derivations of the rate equations for four modified models are given in Appendix A.

Table 5.8 Correlation of k_{STO} parameter in four modified models

Model	Explanations
ASM3 adapted for tannery WW	k_{STO}
Model A	$k_{STO}+(\mu_{HI}/Y_{HI})$
Model B	$(k_{STO}/Y_{STO})+(\mu_{HI}/Y_{HI})$
Model C	q_S

Table 5.9 Process rates in four modified models

	ASM3 adapted for tannery ww	Model A	Model B	Model C
Rate of consumption of S_S, $r_{S,C}$	$k_{STO}\frac{S_O}{K_O+S_O}\frac{S_S}{K_S+S_S}X_H$	$\left[k_{STO}+\frac{\mu_{H1}}{Y_{H1}}\right]\frac{S_O}{K_O+S_O}\frac{S_S}{K_S+S_S}X_H$	$\left[\frac{k_{STO}}{Y_{STO}}+\frac{\mu_{H1}}{Y_{H1}}\right]\frac{S_O}{K_O+S_O}\frac{S_S}{K_S+S_S}X_H$	$q_S\frac{S_O}{K_O+S_O}\frac{S_S}{K_S+S_S}X_H$
Rate of production of X_{STO}, $r_{STO,P}$	$Y_{STO}.\,k_{STO}\frac{S_O}{K_O+S_O}\frac{S_S}{K_S+S_S}X_H$	$Y_{STO}.\,k_{STO}\frac{S_O}{K_O+S_O}\frac{S_S}{K_S+S_S}X_H$	$k_{STO}\frac{S_O}{K_O+S_O}\frac{S_S}{K_S+S_S}X_H$	$\left[Y_{STO}q_S-\frac{Y_{STO}}{Y_{H1}}\mu_H\right]\frac{S_O}{K_O+S_O}\frac{S_S}{K_S+S_S}X_H$
Rate of production of X_H (feast), $r_{X,P1}$	$\mu_H\frac{S_O}{K_O+S_O}\frac{X_{STO}/X_H}{K_{STO}+X_{STO}/X_H}X_H$	$\mu_{H1}\frac{S_O}{K_O+S_O}\frac{S_S}{K_S+S_S}X_H$	$\mu_{H1}\frac{S_O}{K_O+S_O}\frac{S_S}{K_S+S_S}X_H$	$\mu_H\frac{S_O}{K_O+S_O}\frac{S_S}{K_S+S_S}X_H$
Rate of consumption of X_{STO}, $r_{STO,C}$	$\frac{\mu_H}{Y_H}\frac{S_O}{K_O+S_O}\frac{X_{STO}/X_H}{K_{STO}+X_{STO}/X_H}X_H$	$\frac{\mu_{H2}}{Y_{H2}}\frac{S_O}{K_O+S_O}\frac{K_S}{K_S+S_S}\frac{X_{STO}/X_H}{K_{STO}+X_{STO}/X_H}X_H$	$\frac{\mu_{H2}}{Y_{H2}}\frac{S_O}{K_O+S_O}\frac{K_S}{K_S+S_S}\frac{X_{STO}/X_H}{K_{STO}+X_{STO}/X_H}X_H$	$k_{X_{STO}}\frac{S_O}{K_O+S_O}\frac{K_S}{K_S+S_S}\frac{X_{STO}}{X_H}X_H$
Rate of production of X_H (famine), $r_{X,P2}$	$\mu_H\frac{S_O}{K_O+S_O}\frac{X_{STO}/X_H}{K_{STO}+X_{STO}/X_H}X_H$	$\mu_{H2}\frac{S_O}{K_O+S_O}\frac{K_S}{K_S+S_S}\frac{X_{STO}/X_H}{K_{STO}+X_{STO}/X_H}X_H$	$\mu_{H2}\frac{S_O}{K_O+S_O}\frac{K_S}{K_S+S_S}\frac{X_{STO}/X_H}{K_{STO}+X_{STO}/X_H}X_H$	$Y_{H2}.\,k_{X_{STO}}\frac{S_O}{K_O+S_O}\frac{K_S}{K_S+S_S}\frac{X_{STO}}{X_H}X_H$

Table 5.10 Maximum rate coefficients in four modified models

	ASM3 adapted for tannery ww	**Model A**	**Model B**	**Model C**
Maximum Rate coefficient of consumption of S_S, max $r_{S,C}$	k_{STO}	$k_{STO} + \frac{\mu_{H1}}{Y_{H1}}$	$\frac{k_{STO}}{Y_{STO}} + \frac{\mu_{H1}}{Y_{H1}}$	q_S
Maximum Rate coefficient of production of X_{STO}, max $r_{STO,P}$	$Y_{STO} \cdot k_{STO}$	$Y_{STO} \cdot k_{STO}$	k_{STO}	$Y_{STO} q_S - \frac{Y_{STO}}{Y_{H1}} \mu_H$
Maximum Rate coefficient of production of X_H (feast), max $r_{X,P1}$	$\mu_H \frac{X_{STO}/X_H}{K_{STO} + X_{STO}/X_H}$	$\mu_{H1} \frac{S_S}{K_S + S_S}$	$\mu_{H1} \frac{S_S}{K_S + S_S}$	$\mu_H \frac{S_S}{K_S + S_S}$
Maximum Rate coefficient of consumption of X_{STO}, max $r_{STO,C}$	$\frac{\mu_H}{Y_H} \frac{X_{STO}/X_H}{K_{STO} + X_{STO}/X_H}$	$\frac{\mu_{H2}}{Y_{H2}} \frac{X_{STO}/X_H}{K_{STO} + X_{STO}/X_H}$	$\frac{\mu_{H2}}{Y_{H2}} \frac{X_{STO}/X_H}{K_{STO} + X_{STO}/X_H}$	$k_{X_{STO}} \frac{X_{STO}}{X_H}$
Maximum Rate coefficient of production of X_H (famine), max $r_{X,P2}$	$\mu_H \frac{X_{STO}/X_H}{K_{STO} + X_{STO}/X_H}$	$\mu_{H2} \frac{X_{STO}/X_H}{K_{STO} + X_{STO}/X_H}$	$\mu_{H2} \frac{X_{STO}/X_H}{K_{STO} + X_{STO}/X_H}$	$Y_{H2} \cdot k_{X_{STO}} \frac{X_{STO}}{X_H}$

SECTION 6 MATERIALS AND METHODS

Detailed wastewater characterization, biomass in activated sludge and wastewater and also kinetic and stoichiometric coefficients defining the biological processes must be experimentally determined for the modeling of activated sludge systems. There are many models for the design of treatment systems but as mentioned in previous sections; ASM1 and ASM3 are the basic and most applicable ones. Assessment of ASM1 and ASM3 parameters will be defined according to the recent researches in experimental procedures.

6.1. Assessment of ASM1 Parameters

6.1.1 Assessment of COD Fractions

Determination of organic matter content is important since activated sludge systems are used for the removal of organic matter. As told in Section 2, COD is the superior parameter for the characterization of organic compounds. Experimental methods evaluated for the assessment of readily biodegradable and inert COD are given in this section.

6.1.1.1 Determination of Readily Biodegradable COD, S_S

Readily biodegradable COD includes soluble compounds like volatile fatty acids, simple carbohydrates, alcohols and amino acids that can be directly absorbed for biomass synthesis. This component can be expressed as a fraction of total influent COD (C_{T0}), by the following reaction. f_{SS} is the readily biodegradable fraction of total influent COD.

$$S_{S0} = f_{SS}C_{T0} \qquad (6.1)$$

All the methods proposed for the estimation of readily biodegradable organic matter depend on respirometric measurements conducted with continuous or batch reactor systems under aerobic or anoxic conditions. Aerobic batch tests aim to measure the oxygen utilization rate (OUR) that symbolizes the amount of oxygen utilized as a

result of microbial activities in unit time for a unit of reactor volume. If food-microorganism ratio (F/M), is chosen appropriately, OUR value is nearly constant for a period of 1-3 hours (Ekama *et al.*, 1986). After the consumption of readily biodegradable organic matter, electron acceptor (O_2) utilization rate will be lower according to the hydrolysis rate of slowly biodegradable organic matter.

Electron acceptor quantity can be simply expressed as below; first term shows the growth while the second expression concerns endogenous decay.

$$\frac{e^- acceptor}{\Delta t} = -(1-Y_H)\frac{(C_{S0}-C_S)}{\Delta t} - (1-f_E).b_H.X_H \qquad (6.2)$$

The total difference in oxygen concentration in a certain time interval in an aerobic environment can be written as below:

$$\frac{\Delta S_0}{\Delta t} = -(1-Y_H)\frac{C_{S0}-C_S}{\Delta t} - (1-f_E)b_H X_H \qquad (6.3)$$

A respirometric method has been presented by Ekama *et al.*, (1986) for the measurement of oxygen utilization rate (OUR) versus time under aerobic and anoxic conditions in batch reactors. The researchers stated that heterotrophic microorganisms grow on readily biodegradable substrate so below expressions can be written:

$$\frac{dX_H}{dt} = \mu_H X_H \qquad (6.4)$$

$$\frac{dX_H}{dt} = Y_H \frac{dS_S}{dt} \qquad (6.5)$$

Combining equations (6.4) and (6.5), equation (6.6) is formed:

$$\frac{dS_S}{dt} = \frac{1}{Y_H}\mu_H X_H \qquad (6.6)$$

$$\frac{dS_S}{dt} = \frac{C_{S0}-C_S}{\Delta t} \qquad (6.7)$$

Rearranging (6.6) and (6.7), expression (6.8) can be written:

$$\frac{C_{S0} - C_S}{\Delta t} = \frac{1}{Y_H} \mu_H X_H \qquad (6.8)$$

Consequently, equations (6.4) and (6.8) are used together and equation (6.9) can be obtained:

$$\frac{\Delta S_O}{\Delta t} = \frac{(1 - Y_H)}{Y_H} \mu_H X_H - (1 - f_E).b_H.X_H \qquad (6.9)$$

In this approach OUR profile is constant during the growth on S_S, it starts to decrease as readily biodegradable COD is used up and makes a second plateau on hydrolysis stage of slowly biodegradable organic matter (Figure 6.1).

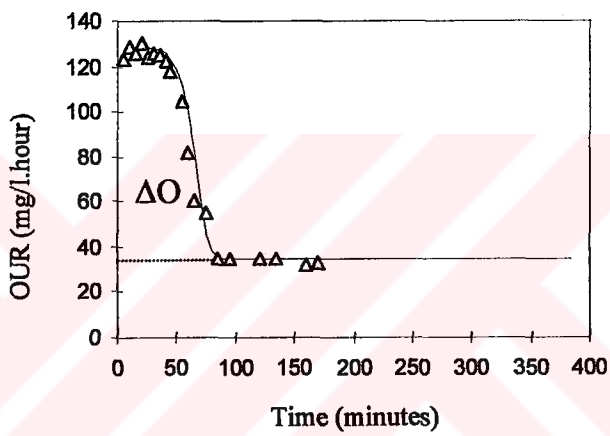

Figure 6.1 OUR Profile

In the beginning of the experiment, it is accepted that readily biodegradable COD is completely used during Δt and following expressions are written:

$$\frac{\Delta S_O}{\Delta t} \cong \frac{(1 - Y_H)}{Y_H} \mu_H X_H \qquad (6.10)$$

$$OUR = -\frac{\Delta S_0}{dt} \qquad (6.11)$$

Expressions (6.10) and (6.11) are combined and (6.12) is formed:

$$OUR \cong (1 - Y_H) \frac{C_{S0} - C_S}{\Delta t} \qquad (6.12)$$

$$OUR = \frac{OR}{\Delta t} \tag{6.13}$$

Expression (6.14) is obtained by the help of (6.7), (6.12) and (6.13):

$$\frac{OR}{\Delta t} = (1 - Y_H)\frac{dS_S}{dt} \tag{6.14}$$

The integration of expression (6.14) results the following equations:

$$OR = (1 - Y_H)\int_0^t \frac{dS_S}{dt}\Delta t \tag{6.15}$$

$$\frac{OR}{1 - Y_H} = \int_0^t \frac{dS_S}{dt}\Delta t \tag{6.16}$$

The amount of readily biodegradable COD according to ASM1 is obtained as shown in equation (6.17):

$$S_{S0} = \frac{\Delta O}{1 - Y_H} \tag{6.17}$$

ΔO value in equation (6.17) can be calculated graphically by the help of OUR profile shown in Figure 6.1.

6.1.1.2 Determination of Inert Fractions, S_I and X_I

Determination of inert fractions is very important because inert COD indirectly indicates the biodegradable COD, which is available for microbial growth and electron acceptor utilization. There are two inert COD fractions, namely particulate inert COD (X_I) and soluble inert COD (S_I). Orhon *et al.,* (1999) proposed a new experimental procedure for the assessment of inert particulate COD, by providing the necessary data for the calculation of S_I, f_{ES} and f_{EX} from simultaneous but independent tests carried out. The procedure consists of running three aerated batch reactors: one fed with raw wastewater sample, one with soluble (filtered) wastewater sample and the last one with glucose solution having the same COD concentration as the soluble wastewater reactor. Proposed procedure also explains the effect of

residual microbial products on the experimental assessment of the particulate inert COD in wastewaters.

Assessment of S_{II}: The proposed approach adopts the procedure proposed by Germirli *et al.* (1991), which consists of running two parallel aerated batch reactors, one with the soluble (filtered) wastewater sample and the other with glucose. The procedure relies on the assumption that both reactors may be characterized with the same f_{ES} value. In other words, glucose is the central compound of almost all metabolic cycles of heterotrophic microorganisms, where residual metabolic products are generated in following steps. In this experiment, when all biodegradable substrate in the two reactors are depleted, the soluble COD concentration in the filtered wastewater reactor will be observed to drop from S_{T1} (initial soluble COD of wastewater) to $(S_T)_2$, where $(S_T)_2$ defines the sum of the initial soluble inert COD, S_{I1} and the COD reflecting soluble residual metabolic products, $(S_P)_2$ generated in the reactor. Similarly, the soluble COD concentration in the glucose reactor will decrease from S_{G1} (initial COD of glucose) to $(S_G)_1$, where $(S_G)_1$ is equal to the soluble residual COD, $(S_P)_G$. f_{ES} value must be known for the calculations.

Since,

$$(S_P)_2 = (S_T)_2 - S_{I1} = f_{ES} \cdot Y_H (S_{T1} - S_{I1}) \tag{6.18}$$

S_{I1} may be calculated from the following expression:

$$S_{I1} = \frac{(S_T)_2 - f_{ES} Y_H S_{T1}}{(1 - f_{ES} Y_H)} \tag{6.19}$$

Assessment of X_{II} : Results of the first reactor fed with the raw wastewater sample and f_{EX} value are required at this stage. The stoichiometric expressions that may be derived on the basis of experimental observations are listed below:

$$(X_T)_1 = (C_T)_1 - (S_T)_1 = X_{I1} + (X_P)_1 \tag{6.20}$$

$$C_{S1} = C_{T1} - X_{I1} - S_{I1} \tag{6.21}$$

$$(X_P)_1 = f_{EX} \cdot Y_H \cdot (C_{T1} - X_{I1} - S_{I1}) \tag{6.22}$$

$$X_{II} = \frac{(X_T)_I - f_{EX} Y_H (C_{TI} - S_{II})}{(1 - f_{EX} Y_H)} \qquad (6.23)$$

The proposed procedure only requires the experimentally calculated (by respirometric measurements) value of the heterotrophic yield coefficient, Y_H defined for the investigated wastewater. Each run (three aerated batch reactors with raw and filtered wastewaters and glucose solution) should be continued for several weeks with periodic COD measurements, until all biological activity is completed and no meaningful changes are observed in the COD levels.

6.1.2 Assessment of Kinetic and Stoichiometric Coefficients

Respirometric measurements have a significant place in the determination of many kinetic and stoichiometric coefficients as well as the wastewater characterization. Some of the kinetic coefficients like K_{OH}, K_{NO}, K_{OA} are not too sensitive to wastewater characteristics so they do not have to be estimated for each case. But most of them (b_H, Y_H, μ_H, f_{ES}, f_{EX}) must be assessed for every investigated wastewater.

6.1.2.1 Determination of endogenous decay rate, b_H

The traditional approaches measures the endogenous decay rate, k_d, by volatile suspended solids, VSS term and this causes many confusions because VSS parameter can not differentiate between active biomass, particulate inert matter and inert particulate microbial products generated by the decay of biomass. Multi-component approaches evaluated a parameter called aerobic endogenous decay rate, b_H.

The current practice for the determination of b_H is based on the observation of the decrease in oxygen utilization rates for a sludge having endogenous decay phase. So OUR values are measured as $b_H X_H$ and because these measured values are very low, they are not so sensitive. The data obtained have a wide-spread range, results are not consistent. Also the VSS contains particulate slowly biodegradable substrate aside from active biomass that is related by the sludge age. This X_S causes interference in the experiment and different b_H values can be found from one study (Avcıoğlu *et al.*, 1998).

Proposed method developed by Avcıoğlu *et al* (1998), relies on the observation of the decrease in OUR rates during the growth phase, so $\mu_H X_H$ term is used

dominantly. By that method low OUR values and interference of X_S is no more problem. OUR measured during growth phase can be expressed as follows if there is adequate amount of readily biodegradable substrate in the environment:

$$OUR = \frac{1-Y_H}{Y_H}\hat{\mu}_H X_H + (1-f_E)b_H X_H \qquad (6.24)$$

Proposed method aims to assure the constant unlimited growth and constant μ_H level as to reflect the variation of X_H. There are two parallel, aerated reactors; one the main endogenous decay reactor, other the feed reactor operated at daily intervals. Biomass seed from endogenous decay reactor and readily biodegradable substrate, S_S, are added to that feed reactor to ensure the maximum growth conditions. The initial OUR value in the feed reactor at time zero can be expressed as below:

$$OUR_{1(t0)} = \frac{1-Y_H}{Y_H}\hat{\mu}_H X_{H0} + (1-f_E)b_H X_{H0} \qquad (6.25)$$

As similar, the initial OUR value after a time t can be written as:

$$OUR_{1(t)} = \frac{1-Y_H}{Y_H}\hat{\mu}_H X_{H(t)} + (1-f_E)b_H X_{H(t)} \qquad (6.26)$$

OUR values observed after a time t are lower than the values at time zero because the activity of biomass in the main reactor decreases by time. The concentration of the heterotrophic active biomass can be written as a function of initial active biomass concentration:

$$X_{H(t)} = X_{H0}\, e^{-b_H t} \qquad (6.27)$$

So, the initial OUR expression at any time can be written as a function of initial active biomass concentration:

$$OUR_{1(t)} = \left[\frac{1-Y_H}{Y_H}\hat{\mu}_H + (1-f_E)b_H\right] X_{H0}\, e^{-b_H t} \qquad (6.28)$$

When above equation is linearized, aerobic endogenous respiration rate b_H, can be calculated from the slope of the linearized equation:

$$\ln OUR_{I(0)} = \ln\left[\frac{1-Y_H}{Y_H}\hat{\mu}_H + (1-f_E)b_H\right]X_{H0} - b_H t \qquad (6.29)$$

6.1.2.2 Determination of heterotrophic growth rate, μ_H and activity coefficient, f_a

The method defined by Ekama *et. al.* (1986) for the determination of S_S may also be used in the assessment of $\hat{\mu}_H$ with the understanding that the initial OUR values reflect maximum growth conditions, neglecting the interferences induced by hydrolysis and endogenous respiration. Experimental procedure consists of running an aerobic reactor at suitably low initial F/M value based on the assumption that the initial rate of electron acceptor utilization would stay proportional to the maximum specific growth rate if the readily biodegradable COD concentration in the tested wastewater is not rate limiting ($S_{SI} >> K_S$). The $\hat{\mu}_H X_H$ value is a ratio of initially observed OUR as given in the expression below:

$$OUR_I = \frac{dS_O}{dt} = \frac{1-f_X Y_H}{Y_H}\hat{\mu}_H X_H \qquad (6.30)$$

The maximum heterotrophic growth rate can also be determined on the basis of initial OUR value at the F/M ratio recommended. The method developed by Kappeler and Gujer (1992) involves a batch test with a small amount of biomass corresponding to a high initial F/M ratio of nearly 4. A linear expression with a slope of $\hat{\mu}_H - b_H$ is derived from the observed OUR profile:

$$\ln\frac{OUR}{OUR_I} = (\hat{\mu}_H - b_H)t \qquad (6.31)$$

Activity coefficient f_a, is a value used in the determination of active biomass X_H, as a ratio of total biomass X_T:

$$X_H = f_a X_T \qquad (6.32)$$

For calculating the active biomass fraction, two aerobic reactors of one with low F/M ratio (Ekama *et al.,* 1986) and the other with high F/M ratio (Kappeler and Gujer, 1992) can be used. Correlation of $\hat{\mu}_H$ obtained by the method suggested by Kappeler and Gujer (1992) yields the following equation:

$$f_a = \frac{Y_H}{1 - f_X Y_H} \frac{OUR_i}{\hat{\mu}_H X_T} \qquad (6.33)$$

6.1.2.3 Determination of Heterotrophic Yield Coefficient, Y_H

For oxygen uptake rate measurements, samples are taken from the prepared reactors in very short intervals. Results obtained from these samples are used in curve fitting. Soluble COD analyses can also be made on samples in order to obtain soluble COD profiles besides OUR profiles as shown in Figure 6.2. Endogenous respiration is negligible compared to respiration during growth. Also soluble residual microbial products are not significant enough within the limited duration of the experiment.

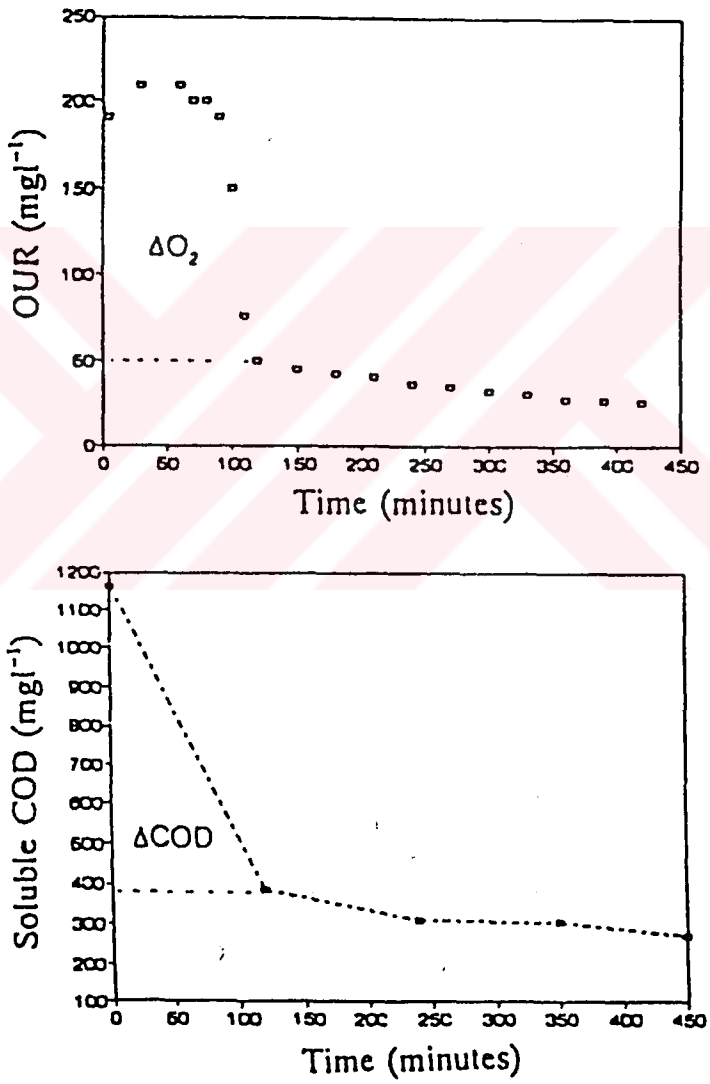

Figure 6.2 Determination of Y_H from OUR and Soluble COD Profiles

For the determination of the yield coefficient Y_H, the procedure developed by Ubay Çokgör *et. al.* (1997) can be followed. Simultaneously obtained OUR and COD data should be used on the basis of the following equation for yield determination:

$$Y_H = 1 - \frac{\Delta O_2}{\Delta COD_{soluble}} \quad (6.34)$$

6.1.2.4 Determination of f_{ES} and f_{EX}

f_{EX} should not be assumed as a constant value due to the difference in the magnitude of particulate residual products generation for various organic carbon sources.

Assessment of f_{ES}: For the determination of f_{ES} parameter, same procedure as defined in the assessment of S_I is applied. At the end of the experiment the fraction of biodegradable COD converted into soluble inert metabolic products, Y_{SP} may be defined as

$$Y_{SP} = f_{ES} . Y_H = \frac{(S_P)_G}{S_{G1}} \quad (6.35)$$

So, f_{ES} can be calculated as follows:

$$f_{ES} = \frac{1}{Y_H} \frac{(S_P)_G}{S_{G1}} \quad (6.36)$$

Assessment of f_{EX} : The experimental determination of f_{EX} is based on the concept that in an aerated batch reactor operated long enough for the depletion of all biological activity, the level of the particulate metabolic products generated will be proportional to the amount of biodegradable substrate utilized, as defined by the below equation:

$$(X_P)_1 = f_{EX} . Y_H . C_{S1} \quad (6.37)$$

The reactor fed by the soluble wastewater sample is very convenient for this purpose, as $(X_P)_2$ may be expressed as follows, being the only particulate COD component at the end of the experiment:

$$(X_P)_2 = (C_T)_2 - (S_T)_2 = Y_{XP} (S_{T1} - S_{I1}) \quad (6.38)$$

where, Y_{XP} is the fraction of biodegradable COD converted into particulate inert metabolic products:

$$Y_{XP} = f_{EX} Y_H \quad (6.39)$$

f_{EX} may be calculated as follows, using the last two expressions:

$$f_{EX} = \frac{1}{Y_H} \frac{[(C_T)_2 - (S_T)_2]}{(S_{T1} - S_{I1})} \tag{6.40}$$

6.1.2.5 Hydrolysis Concept

The aerobic batch experiments show that the OUR values give high results at the beginning because of the rapid growth on readily biodegradable COD, S_S, then drop to a lower plateau correlated with the growth on slowly biodegradable COD, X_S (Ekama *et.al.*, 1986). The evaluation of S_S from the OUR curve is illustrated in Figure 6.3. Theoretical OUR profiles are given separately as OUR1, OUR2 and OUR3. OUR1 reflects the S_S, OUR2 reflects the X_S and OUR3 reflects the total profile as the combination of S_S and X_S.

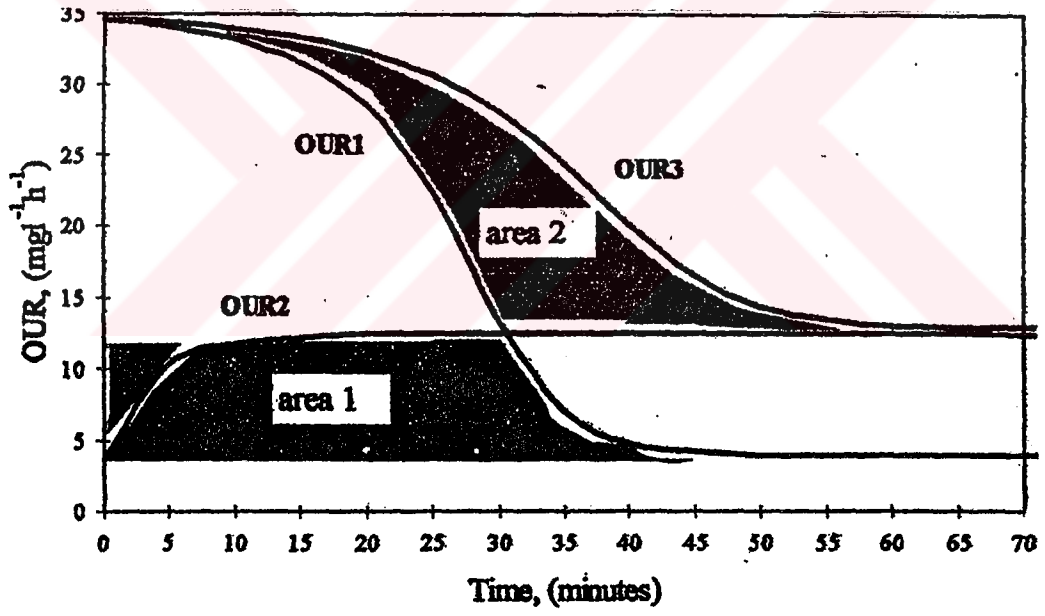

Figure 6.3 Effect of S_S and X_S on the OUR profile (Ubay Çokgör *et al.*, 1998)

As seen from the figure, the experiment only yields the total OUR curve and defines S_S in proportion to the area between OUR2 and OUR3 curves. Comparison of OUR1 and OUR3 profiles shows that the presence of X_S or in other words hydrolysis does not effect the initial portion of the total OUR curve caused as a result of readily biodegradable substrate removal by maximum growth rate. Hydrolysis of X_S only causes a slight OUR increase in the following stages of the experiment. S_S generated through hydrolysis is reduced in the later stages of the experiment where the

substrate utilization potential exceeds the hydrolysis rate and the equilibrium is established at the X_S plateau after the depletion of all remaining S_S.

The F/M ratio largely affects the shape of the OUR curve, so the observation of the lower plateau. If high F/M ratios are chosen for the respirometric measurements, it is difficult to identify the hydrolysis zone from the transition area. Proper evaluations due to respirometric measurements are possible with the choice of appropriate F/M ratio.

In single hydrolysis model, only the hydrolysis of slowly biodegradable substrate (X_S) is taken into account whereas the hydrolysis of soluble slowly biodegradable substrate (S_H) is involved in dual hydrolysis model:

$$\frac{dS_H}{dt} = -k_{hs} \frac{S_H / X_H}{K_{XS} + S_H / X_H} X_H \qquad (6.41)$$

$$\frac{dX_S}{dt} = -k_{hx} \frac{X_S / X_H}{K_{XX} + X_S / X_H} X_H \qquad (6.42)$$

Experiments made on different wastewaters including the tannery wastewater showed that the dual hydrolysis approach is needed in many cases for proper curve fitting and so correct kinetic expressions. Hydrolysis kinetics (k_{hs} and K_{XS}) for the soluble slowly biodegradable substrate is obtained by repeating the same batch OUR experiment on both soluble and total portions of the wastewater, then the kinetic coefficients for the hydrolysis of slowly biodegradable substrate (k_{hx} and K_{XX}) can be estimated by reevaluating the total OUR profile with simultaneous dual hydrolysis approach. Kinetic coefficients for tannery wastewater due to the single and dual hydrolysis approaches are summarized in Table 6.1. It can be seen that the hydrolysis of rapidly hydrolyzable COD, S_H, is significantly higher than the hydrolysis of slowly hydrolyzable COD, X_S. Also, the kinetic data derived for S_H are nearly the same with the ones found by single hydrolysis model indicating that the procedure tends to define S_H rather than the total slowly biodegradable COD. Consequently, the single hydrolysis model was observed to involve a significant overestimation for the biodegradation of particulate COD. Furthermore, the hydrolysis rates for the particulate-slowly hydrolyzable COD appear to be at the same level as the endogenous decay constant of the biomass. This observation challenges the validity

of this value and underlines the possibility of interference of the slowly hydrolyzable COD in the aerobic digestion tests used for the measurement of endogenous decay constant (Avcıoğlu *et. al.*, 1998).

Table 6.1 Dual Hydrolysis Kinetics for Tannery wastewaters (Orhon et al., 1998)

Dual Hydrolysis Model				*Single Hydrolysis Model*			
Rapidly Hydrolyzable COD, S_H		*Slowly Hydrolyzable COD, X_S*		*Plain Settling Effluent*		*Chemical Settling Effluent*	
K_{hs}	K_{xs}	K_{hx}	K_{xx}	K_h	K_x	K_h	K_x
0.7	0.1	0.3	0.1	0.6	0.15	1.0	0.15
1.4	0.1	0.1	0.1	0.5	0.15	0.6	0.1
1.6	0.4	0.2	0.1	1.3	0.4	1.6	0.5
0.6	0.1	0.2	0.1	0.7	0.1	0.8	0.1
1.2	0.2	0.6	0.5	1.0	0.2	1.3	0.2
1.1	0.1	0.25	0.2	0.8	0.2	1.2	0.1
1.1	0.2	0.3	0.2	0.8	0.2	1.1	0.2

6.1.3 Interpretation of OUR Response According to ASM1

A typical OUR curve for tannery wastewater simulated according to ASM1 is illustrated in Figure 6.4 as below:

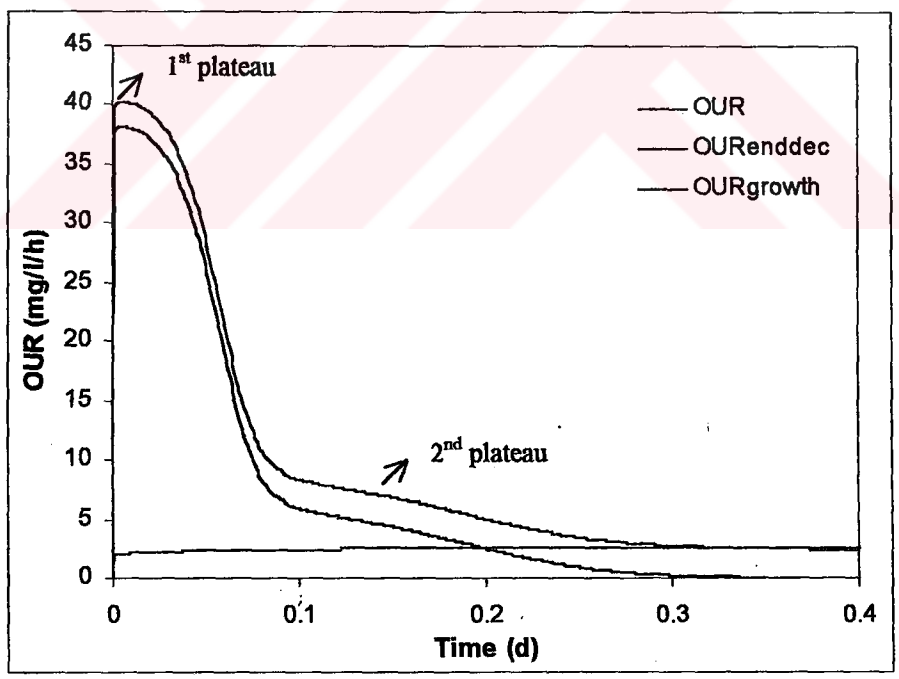

Figure 6.4 OUR components according to ASM1

OUR curve (Total OUR): This curve shows a very rapid increase at the beginning, then there is a slightly increasing phase (first plateau) and after a maximum value the curve drops to the second plateau. The slope of the first plateau is determined by μ_H

and K_S. This phase can be named as growth process. Maximum OUR value and the slope of the drop are also estimated by using the K_S parameter.

OUR growth curve: The initial OUR value after the addition of the substrate is given by $\mu_H X_H$. So, if the active biomass concentration is known the maximum growth rate can be calculated from the initial OUR value. Increasing and decreasing tendencies are similar to the total OUR curve.

OUR endogenous decay curve: The slope of the endogenous decay curve gives the b_H value and the active biomass concentration in the reactor can be estimated by using this b_H value, since the endogenous decay level is given by $b_H X_H$. The slope of the second plateau is also given by b_H. The difference in OUR values between the initial endogenous decay level and the beginning of the second plateau is due to the new biomass produced.

6.2 Assessment of ASM3 Parameters

6.2.1 Assessment of Yield Coefficient

There are two phases that causes oxygen consumption in activated sludge systems. First phase is the growth of biomass on added substrate, then second phase continues on the stored polymers (PHA, glycogen). Stored polymers within the bioflocs are utilized when there is no ready substrate in the wastewater. This indicates that both growth and storage reactions occur after substrate is added to the system.

By measuring both the oxygen and substrate consumptions, the conversion factor known as yield coefficient can be calculated. If yield coefficient is not correct there will be great errors in the calculation of consumed substrate. Biomass makes exogenous respiration on the substrate, also endogenous respiration for the maintenance of itself. According to Dircks *et al.* (1999), yield coefficient can be found by subtracting the endogenous respiration from measured respiration. In this approach, endogenous respiration is measured for the sludge just before the substrate is added. Then exogenous respiration is calculated by the help of endogenous respiration. Direct growth on added substrate causes a high peak in the respiration rate (first phase), and then it levels off and continues in a constantly decreasing manner (second phase) till it reaches the original endogenous respiration rate. Second phase is probably caused by the stored polymers as said before (Figure 6.5).

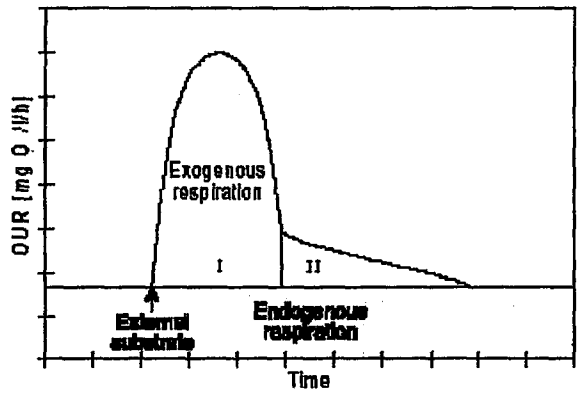

Figure 6.5 An example for OUR response (Dircks *et al.* 1999)

Two different sludges having sludge ages of 7 and 16 days are used as biomass and pure substrates like acetate, glucose and ethanol are used as wastewater. Every substrate gave different yield coefficients, also when glucose is used sludge age changes the results too. This means that the determination of readily biodegradable COD concentration should not be based on a constant yield coefficient because it differs for every sludge and substrate, also organic matter concentrations do not effect the results (Dircks *et al.* 1999).

6.2.2 Calibration of ASM3 for Domestic Sewage

Respiration tests assembling the oxygen utilization rate gives a curve as in Figure 6.6. This phenomenon can be modeled with the storage products X_{STO} introduced in ASM3. Many stoichiometric and kinetic parameters for the aerobic storage and growth of heterotrophic biomass could be estimated on the basis of aerobic batch experiments with acetate as the substrate. According to Koch *et al.* (2000), $Y_{STO,O2}$ and k_{STO} are the most sensitive parameters after substrate addition during substrate respiration and could be determined from Figure 6.6. $Y_{H,O2}$, k_{STO} and μ_H are sensitive both before and after substrate respiration. The half saturation constant K_S could be determined during the sudden decrease of the oxygen consumption rate. The net yield of heterotrophic biomass produced per unit of substrate removed results in $Y_{NET,O2} = Y_{STO,O2} * Y_{H,O2} = 0.72 * 0.80 = 0.58$ g X_H $g^{-1}S_S$ according to Koch *et al.* (2000), which is about 8 % higher than the value suggested by Gujer *et. al.* (2000).

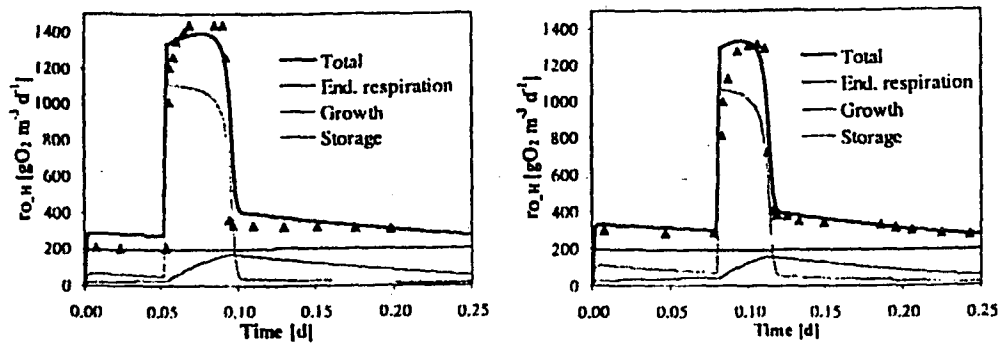

Figure 6.6 OUR simulations carried out in various times (Koch *et al.* 2000)

The characteristic of the oxygen utilization curve depends on the available substrate. In the study, soluble COD from primary sludge acidification was used for aerobic batch experiments. The net yield from readily biodegradable fraction of the total soluble COD is $Y_{NET,O2} = 0.8*0.8 = 0.64$ g X_H $g^{-1}S_S$ (Koch *et al.*, 2000). This value is considerably higher than that observed from acetate batch tests and that suggested by Gujer *et. al.* (2000). The aerobic storage rate constant k_{STO} has to be increased by 100 % in order to obtain a good fit with measured data. The maximum oxygen consumption rate based on dissolved fermentation products is higher than that based on simple substrate acetate. This can be explained by the wide variety of substrates in the fermentation products and their individual uptake rates. It is assumed that fermentation products tend to induce oxygen consumption curves which are more similar to wastewater than acetate as a single substrate (Koch *et al.*, 2000).

Readily biodegradable COD can also be estimated from respirometric measurements by curve fitting in contrast to ASM3 suggestion that S_S may be approximated by the total soluble inlet COD as determined by 0.45 μm membrane filtration (Koch *et al.*, 2000). Otherwise, different aerobic yields for wastewater components and different fermentation products as the substrate are required. The level of the basic respiration (respiration after consumption of readily biodegradable substrate) could only be modeled by a considerable increase of the hydrolysis rate constant, k_H.

6.2.3 Experimental Assessment of Storage Yield

ASM3 has differences when compared with ASM1 since it includes the storage phenomena. Especially, the determination of the yield factor for bacterial storage (Y_{STO}) needs careful consideration of the OUR response.

Karahan-Gül *et al.* (2002a), proposed an experimental procedure for the respirometric assessment of bacterial storage yield, Y_{STO}. Y_{STO} is a significant parameter because it represents the stoichiometric amount of substrate converted into storage products, which are then utilized for growth. Experimental procedure of Karahan-Gül *et al.* (2002a) is based on respirometry and doesn't involve the measurement of storage products, since it is not always possible to determine the amount of all the storage products when a complex substrate like tannery wastewater in this study is concerned.

The basic stoichiometry of the storage process can be expressed with the following equation according to ASM3:

$$\Delta O_{STO} = (1 - Y_{STO})\Delta S_S \qquad (6.43)$$

At the depletion of external substrate, Y_{STO} can be derivated from the above expression:

$$Y_{STO} = (1 - \frac{\Delta O_{STO}}{S_{SI}}) \qquad (6.44)$$

Respirometric measurements provide the oxygen utilization rate (OUR) of the overall system and not the OUR specific for the desired process alone, therefore it is necessary to understand and interpret the components of an overall OUR associated with the biodegradation of a soluble substrate. Figure 6.7 illustrates a typical OUR curve obtained through model simulation using Aquasim (Reichert *et al.*, 1998), for the default kinetic and stoichiometric coefficients as suggested in ASM3. Proposed procedure involves drawing a line connecting the initial OUR level due to endogenous decay, up to the inflection point of the overall OUR curve. This reflects that the external substrate is finished, so storage process is completed. The area above the drawn line directly yields the oxygen used for storage.

The proposed procedure calculates the Y_{STO} in accordance with ASM3, which says storage and growth, does not occur simultaneously. In contrast, there are many experimental evidences showing that both storage and growth can occur on external substrate, and then growth continues on internal storage products after the depletion of external substrate (Majone *et al.*, 1996; Beun *et al.*, 2000; Dircks *et al.*, 2001).

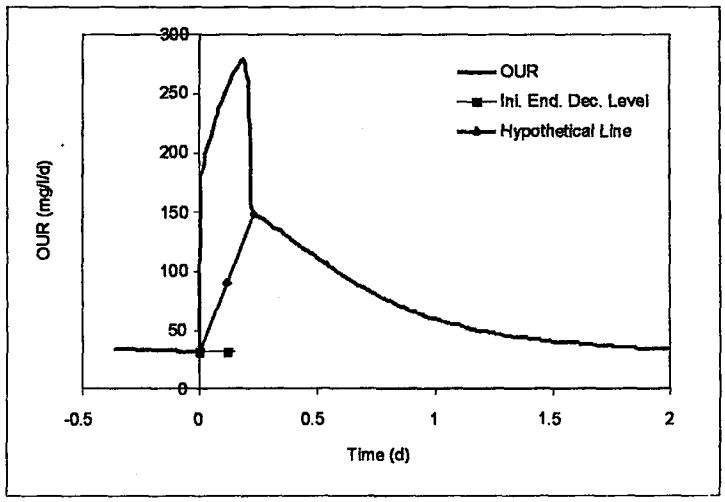

Figure 6.7 Proposed graphical procedure for the determination of ΔO_{STO} (Karahan-Gül *et al.*, 2002a)

This means, limiting external substrate at low F/M ratios would allow simultaneous microbial growth as in conventionally operated activated sludge systems, whereas a sudden increase of external substrate at high F/M ratios after a famine period would cause internal storage to be the dominant mechanism. So the average yield value reflected by overall OUR measurements would exhibit a changing pattern parallel to the changing F/M values. Also the calculations were made with the assumption that the entire soluble biodegradable COD could be regarded as readily biodegradable substrate, which is not true in real cases as it is in tannery wastewater with complex substrate compositions. In these cases, the corresponding oxygen consumption can be interpreted with a superficially higher Y_{STO}. The proposed experimental procedure may also be used to calculate the readily biodegradable COD for a generally adopted Y_{STO} value, as it defines a stoichiometric procedure between the storage yield and the readily biodegradable substrate.

6.2.4 Calibration of ASM3 for Aerobic and Anoxic Conditions

ASM3 introduced a number of kinetic and stoichiometric coefficients with the new processes defined in the model, also suggested some default values. Recent studies showed that parameter determination limits the applicability of ASM3 to special cases. Respirometric procedures should be involved for the calibration of ASM3 parameters, also stoichiometric and kinetic coefficients under both aerobic and anoxic conditions (Avcıoğlu *et al.*, 2002).

A simplified matrix has been proposed by Avcıoğlu *et al.* (2002) for aerobic and anoxic conditions (Table 6.2). Respirometric batch tests have been used to evaluate different activated sludge models and thus respirometric responses obtained from batch tests can be evaluated to estimate ASM3 parameters as shown in Figure 6.8 (Avcıoğlu *et al.*, 2002). Tests were carried out in completely mixed batch reactors seeded with active biomass acclimated to acetate. Results of the OUR experiments are shown in Table 6.3. Amount of active heterotrophic biomass was calculated from endogenous phase OUR data. The storage yield was estimated from the storage (second) phase as defined before (Karahan-Gül *et al.*, 2002a). The rate of storage was determined for different substrate concentrations and F/M ratios, consequently obtained results were much higher than the default value of ASM3, but in agreement with that of Krishna and van Loosdrecht (1999), where k_{STO} for acetate was reported as 10 d^{-1} (Avcıoğlu *et al.*, 2002).

Table 6.2 Modified ASM3 matrix for aerobic and anoxic processes (Avcıoğlu *et al.*, 2002)

Component Process	1 S_S COD	2 S_O COD	3 S_{NO} N	4 X_P COD	5 X_H COD	6 X_{STO} COD	Process rate equation, ρ_j,all $\rho_j \geq 0$
Aerobic storage of COD	-1	$-(1-Y_{STO})$				Y_{STO}	$k_{STO}\frac{S_S}{K_S+S_S}X_H\frac{S_O}{K_O+S_O}$
Anoxic storage of COD	-1		$-\frac{1-Y_{STOD}}{2.86}$			Y_{STOD}	$k_{STO}\eta_D\frac{S_S}{K_S+S_S}X_H\frac{S_{NO}}{K_{NO}+S_{NO}}$
Aerobic growth		$-\frac{1-Y_H}{Y_H}$			1	$-\frac{1}{Y_H}$	$\mu_H\frac{X_{STO}/X_H}{K_{STO}+X_{STO}/X_H}X_H\frac{S_O}{K_O+S_O}$
Anoxic growth			$-\frac{1-Y_{HD}}{2.86Y_{HD}}$		1	$-\frac{1}{Y_{HD}}$	$\mu_H\eta_D\frac{X_{STO}/X_H}{K_{STO}+X_{STO}/X_H}X_H\frac{S_{NO}}{K_{NO}+S_{NO}}$
Aerobic endogenous respiration		$-(1-f_{EX})$		f_{EX}	-1		$b_H X_H\frac{S_O}{K_O+S_O}$
Anoxic endogenous respiration			$-\frac{1-f_{EX}}{2.86}$	f_{EX}	-1		$b_{HD}X_H\frac{S_{NO}}{K_{NO}+S_{NO}}$
Aerobic respiration of X_{STO}		-1				-1	$b_{STO}X_{STO}\frac{S_O}{K_O+S_O}$
Anoxic respiration of X_{STO}			$-\frac{1}{2.86}$			-1	$b_{STOD}X_{STO}\frac{S_{NO}}{K_{NO}+S_{NO}}$

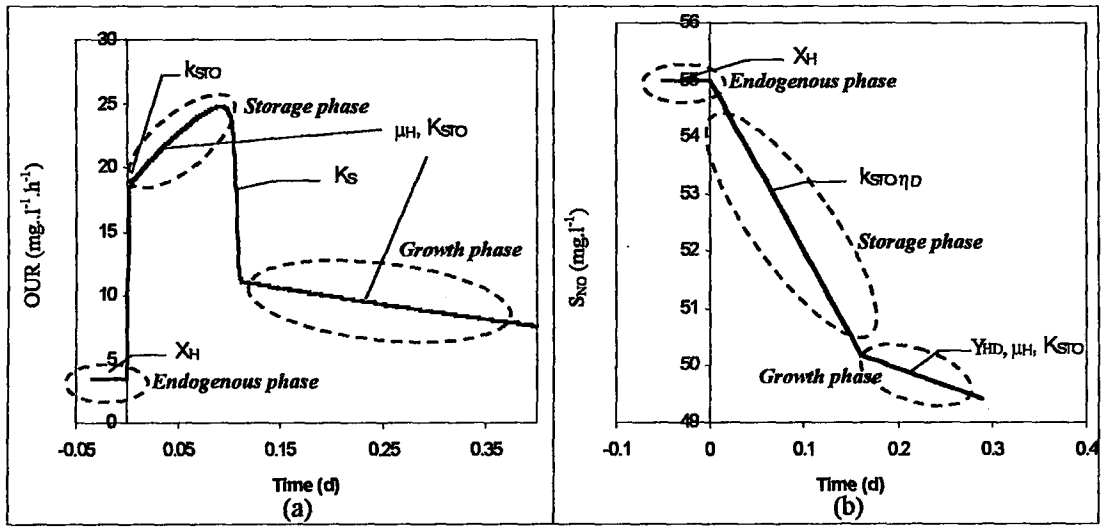

Figure 6.8 Estimated parameters of ASM3 using (a) aerobic curves (b) anoxic curves (Avcıoğlu *et al.*, 2002).

μ_H, K_{STO}, K_S and Y_H are estimated from the model simulations while b_H, b_{STO} and f_{EX} were assumed as the default values in the proposed model of Avcıoğlu *et al.* (2002). The simulation results of aerobic respirometric data indicated that it was not possible to obtain ASM3 calibration by using a single value of μ_H. Higher μ_H fit the first plateau and lower μ_H fit the second plateau. As a result, two different growth rates were required for simulating the OUR data (Figure 6.9) (Avcıoğlu *et al.*, 2002).

Table 6.3 Aerobic kinetic and stoichiometric coefficients of ASM3 obtained for acetate (Avcıoğlu *et al.*, 2002).

		Set 1	Set 2	Set 3	Set 4
S_{SI}	mgCOD.l^{-1}	164	187	274	548
F/M	gCOD.g^{-1}VSS	0.22	0.25	0.29	0.64
b_H	d^{-1}	0.20	0.20	0.20	0.20
b_{STO}	d^{-1}	0.20	0.20	0.20	0.20
f_{EX}		0.20	0.20	0.20	0.20
K_S	mgCOD.l^{-1}	3	2	3	2
K_{STO}		1	1	1	1
k_{STO}	d^{-1}	16	12	10	14
μ_H (2nd phase)	d^{-1}	5	6	3	4
μ_H (3rd phase)	d^{-1}	2	2.5	1.6	2
Y_H	gCOD.g^{-1}COD	0.63	0.63	0.63	0.63
Y_{STO}	gCOD.g^{-1}COD	0.77	0.75	0.80	0.80

6.2.5 Interpretation of OUR Response According to ASM3

OUR components for tannery wastewater simulated according to ASM3 can be interpreted as in Figure 6.10.

OUR curve (Total OUR): This curve firstly shows a rapid, then slower increase. The slope of the slow-increasing phase (first plateau) gives the growth rate since it is

dependent on μ_H and K_{STO} parameters. After a maximum value it starts to decrease, then reaches to the second plateau. Maximum OUR and the transient area is determined by using K_S and K_{STO} parameters.

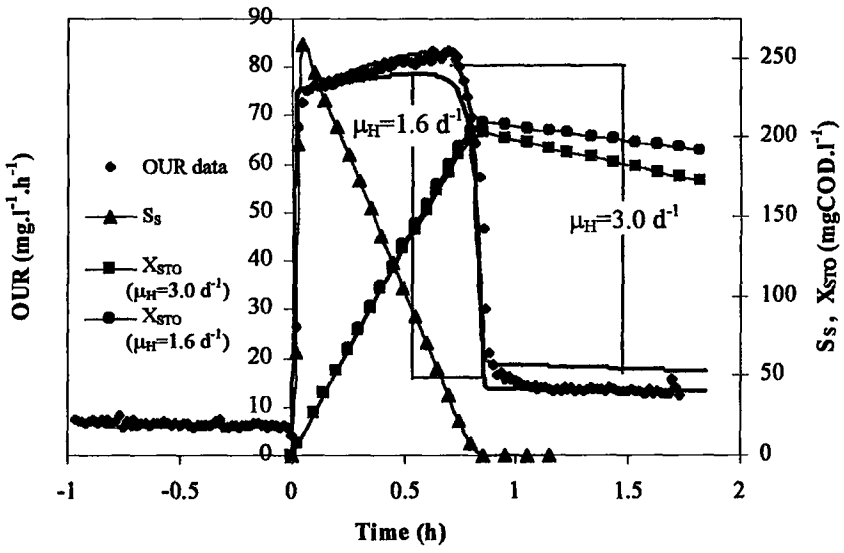

Figure 6.9 ASM3 simulation results for acetate aerobic run no 3 (Avcıoğlu *et al.*, 2002)

OUR storage curve: Initial value of this curve is given by $k_{STO}X_H$ after the addition of substrate. It firstly increases then decreases. If the active biomass (X_H) concentration in the reactor is known, storage rate can be estimated from the initial OUR value. Minimum point of OUR storage gives the maximum value of stored polymer concentration (S_S is depleted); K_S is effective for this zone.

OUR growth curve: Slope of this curve gives μ_H and K_{STO} values. Increasing and decreasing trends are similar to the first and second plateaus of OUR curve. It increases till the maximum X_{STO} value and then starts to decrease.

OUR endogenous decay curve: The slope of endogenous decay curve gives the endogenous decay coefficient, b_H since the initial decay level is given by b_HX_H. Active biomass concentration can be calculated if the endogenous decay coefficient is known.

OUR endogenous decay curve for stored polymers (PHA): The slope of this curve gives the endogenous decay coefficient for stored polymers, b_{STO}.

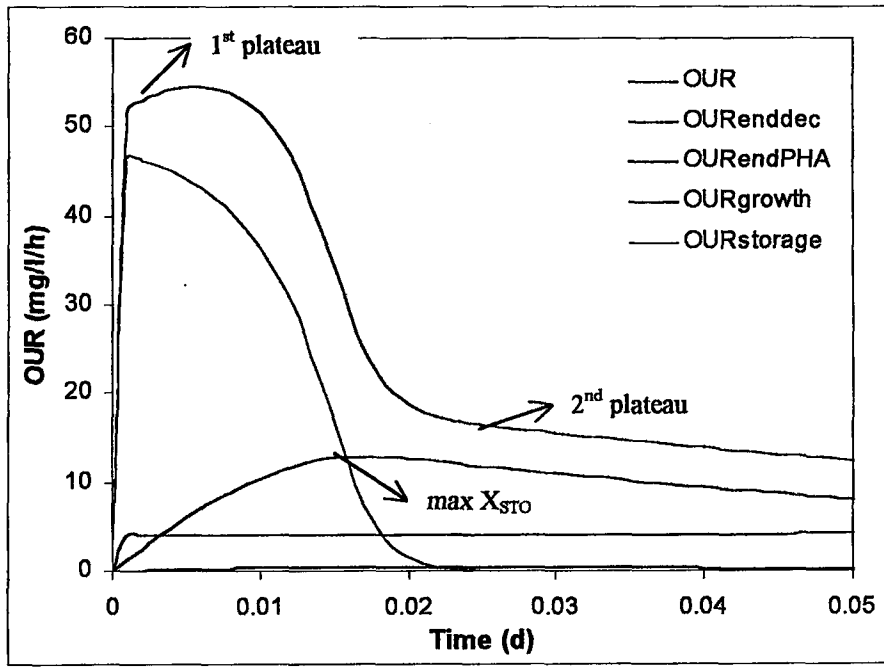

Figure 6.10 OUR components according to ASM3

6.3 Experimental Setup

Respirometric measurements were conducted for the calibration of different activated sludge models for tannery wastewaters. Detailed characterization of tannery wastewater was determined under aerobic conditions. For that purpose, oxygen utilization rate (OUR) was measured and inert COD experiments were carried out. Experimental studies involve acclimation and also the estimation of kinetic and stoichiometric parameters from obtained OUR and inert COD data.

For the acclimation of microorganisms to tannery wastewater from Tuzla organized district, fill and draw reactors of 4 liter volume and having a sludge age of 20 days were used. During acclimation studies, dissolved oxygen concentration in the reactors was supplied by using aerators. Magnetic stirrers were used for the proper mixing of biomass and wastewater. After the acclimation was achieved, acclimated biomass from these reactors were used in OUR and inert COD experiments.

Parallel tests were performed to visualize the effect of the initial F/M ratio and hydrolysis process. The tests were carried out in completely mixed, aerated 2-3 l batch reactors, seeded with active biomass taken from fill and draw acclimation reactors operated at steady state.

OUR experiments were carried out with both raw and filtered wastewater in parallel reactors. These batch reactors were prepared according to the selected F/M values. Dissolved oxygen concentration under aerobic circumstances was adjusted to 6-7 mg/l. Nitrification inhibitor (Formula 2533™, Hach Company) was also added in small amounts in order to prevent the growth of autotrophs. Nutritional requirement of biomass was supported by special solutions as shown in Table 6.4. The amount of the solutions that should be added is given as 10 ml for 1000 mg/l COD (O'Connor, 1972).

Table 6.4 Buffer and Mineral Solutions (O'Connor, 1972)

Solution A	K_2HPO_4	320 g/l
	KH_2PO_4	160 g/l
Solution B	$MgSO_4.7H_2O$	15 g/l
	$FeSO_4.7H_2O$	0.5 g/l
	$ZnSO_4.7H_2O$	0.5 g/l
	$MnSO_4.3H_2O$	0.5 g/l
	$CaCl_2$	2.0 g/l

The initial active biomass concentration was estimated by model simulation on the basis of an endogenous decay rate, b_H of 0.2 d^{-1}, the suggested value in Orhon *et al.*, 1999. OUR measurements were conducted with a Manotherm RA-1000 continuous respirometer with PC connection. In the experiments, pH was kept in the range of 7.0-8.0, suitable for biological activity. COD measurements were performed as described in the method ISO6060 (1986). Filtration was performed through 0.45 μm cellulose acetate filters.

6.4 Modeling studies

Measured data must be interpreted in a proper way, which is a common problem for all scientific studies. In the case of environmental studies, measured data are used indirectly based on the implications of the hypotheses about the mechanisms involved within a given system. Mathematical models are proposed to state the hypotheses about functional relationships in environmental systems. This mathematical formulation makes quantitative derivation of model behavior possible. As a result, computer programs become necessary for calculating the consequences of model assumptions.

Model hypothesis should be tested as directly as possible e.g., by limiting the investigation to the isolated subsystem that is most sensitive to the hypothesis to be tested. More direct tests mean the formulation of a model for the complete system performing such a test is less important. Both laboratory and field studies should be done for understanding the behavior of environmental systems. Isolated processes under controlled conditions can be characterized by laboratory studies while the behavior of the system as a whole is characterized by field investigations. Laboratory experiments make easier to quantify the contributions of different processes to the true transformation rates observed in the field. There are many external influences and internal interactions in environmental systems, leading to a multi-output and multi-input conditions in which inputs can only be measured but not controlled. Also results from laboratory studies must be taken into account for the evaluation of field data. The use of advanced mathematical models and parameter identification techniques for hypothesis testing is therefore so much important in environmental sciences.

Computer programs should be as simple as possible, but also adequately complex allowing model comparisons needed for the process of system identification and describing the features shown by measured data. Models for environmental systems are variable that system identification programs are not flexible enough for them. Simultaneous use of general-purpose simulation software and identification programs is difficult. Consequently, a more universal, user-friendly and flexible simulation and identification tool for environmental systems is designed. This simulation and identification program can be used for most of the aquatic systems in the environment, in technical plants and in the laboratory by the aim of providing an instrument for scientific researches.

The investigated models for tannery wastewater have been simulated using Aquasim (Reichert *et al.,* 1998). An example of prepared models in Aquasim is presented in Appendix B.

SECTION 7 EXPERIMENTAL DATA

7.1 Wastewater Characterization

For the characterization of tannery wastewater, three set of experiments were conducted with different F/M ratios in Istanbul Technical University Environmental Engineering Department by Environmental Biotechnology Group in February, 2002. One set was for raw wastewater and experiment was carried out at an F/M ratio of 0.05 mg COD/mg VSS. Other two sets were for filtered wastewater of different F/M ratios of 0.07 mg COD/mg VSS and 0.2 mg COD/mg VSS. Table 7.1 summarizes the relevant COD fractions of experimental sets.

Table 7.1 Characterization of Tannery Wastewater

Parameter	Value (mg COD.l^{-1})
C_{T1}	2550
S_{T1}	1500
C_{S1}	1475
S_{I1}	190
X_{S1}	165
X_{I1}	685
X_{H1}	200
VFA content	820

7.2 Modeling Studies

Modeling studies were carried out with the calculation of initial conditions with respect to different definitions of COD fractions for ASM1 and ASM3 and model simulations were conducted for the estimation of kinetic and stoichiometric model parameters.

7.2.1 Calculation of Model Initial Conditions

Experimental data were evaluated in order to be used in modeling studies. Evaluations were made on the basis of both ASM1 and ASM3 because calculation procedure is different in these two models.

7.2.1.1 Initial Conditions for ASM1

Set 1-Filtered Wastewater (F/M=0.07 mg COD/mg VSS): Basic data used in the calculations are given in Table 7.2 and COD fractions calculated according to ASM1 are also given in details as below.

Table 7.2 Volume and COD fractions of Set 1
(Filtered Wastewater F/M=0.07 mg COD/mg VSS)

Volume Fractions (l)			COD Fractions (mg/l)		
Initial Volume	Volume of Wastewater added	Total Volume	Soluble COD	Soluble Inert COD	VFA Content
V_{ini}	V_{WW}	V_T	S_{T1}	S_{I1}	S_{VFA}
2.00	0.14	2.14	1500	190	820

S_{S1}=820 mg/l (Assumed to be equal to VFA content)

$X_S=S_H=S_{T1}-S_{S1}-S_{I1}$=1500-820-190=490 mg/l

$S_{S1,ini}$=820*0.14/2.14=54 mg/l

$X_{S,ini}=S_{H,ini}$=490*0.14/2.14=32 mg/l

Set 2-Filtered Wastewater (F/M=0.2 mg COD/mg VSS): Same procedure is applied to filtered wastewater of F/M=0.2 mg COD/mg VSS. Data are shown in Table 7.3 and calculations are also given.

Table 7.3 Volume and COD fractions of Set 2
(Filtered Wastewater F/M=0.2 mg COD/mg VSS)

Volume Fractions (l)			COD Fractions (mg/l)		
Initial Volume	Volume of Wastewater added	Total Volume	Soluble COD	Soluble Inert COD	VFA Content
V_{ini}	V_{WW}	V_T	S_{T1}	S_{I1}	S_{VFA}
2.0	0.4	2.4	1500	190	820

S_{S1}=820 mg/l (Assumed to be equal to VFA content)

$X_S=S_H=S_{T1}-S_{S1}-S_{I1}$=1500-820-190=490 mg/l

$S_{S1,ini}$=820*0.4/2.4=137 mg/l

$X_{S,ini}=S_{H,ini}$=490*0.4/2.4=82 mg/l

Set 3-Raw Wastewater (F/M=0.05 mg COD/mg VSS): Raw wastewater consists of more components due to the particulate parts (Table 7.4).

Table 7.4 Volume and COD fractions of Set 3
(Raw Wastewater F/M=0.05 mg COD/mg VSS)

Volume Fractions (l)			COD Fractions (mg/l)					
Initial Volume V_{ini}	Volume of WW added V_{WW}	Total Volume V_T	Total COD C_{T1}	Soluble COD S_{T1}	Soluble Inert COD S_{I1}	Particulate Inert COD X_{I1}	Biomass Content X_{H1}	VFA Content S_{VFA}
2.0	0.1	2.1	2550	1500	190	685	200	820

COD fractions in the reactor according to ASM1 are calculated as below:

S_{S1}=820 mg/l (Assumed to be equal to VFA content)

$X_S=C_{T1}-S_{S1}-S_{I1}-X_{I1}-X_{H1}$=2550-820-190-685-200=655 mg/l

$S_{S1,ini}$=820*0.1/2.1=39 mg/l

$X_{S,ini}$=655*0.1/2.1=31 mg/l

$S_{I1,ini}$=190*0.1=19/2.1=9 mg/l

$X_{I1,ini}$=685*0.1=69/2.1=33 mg/l

7.2.1.2 Initial Conditions for ASM3 and Modifications

Same data (from Tables 7.2, 7.3 and 7.4) are used for the calculations of ASM3 components. Calculations are given in details for each set of experiment as below.

Set 1-Filtered Wastewater (F/M=0.07 mg COD/mg VSS):

$S_{S1}=S_{T1}-S_{I1}$=1500-190=1310 mg/l

$S_{S1,ini}$=1310*0.14/2.14=86 mg/l

$S_{I,ini}$=190*0.14/2.14=12 mg/l

Set 2-Filtered Wastewater (F/M=0.2 mg COD/mg VSS):

$S_{S1}=S_{T1}-S_{I1}$=1500-190=1310 mg/l

$S_{S1,ini}$=1310*0.4/2.4=218 mg/l

$S_{I,ini}$=190*0.4/2.4=32 mg/l

Set 3-Raw Wastewater (F/M=0.05 mg COD/mg VSS):

$S_{S1}=S_{T1}-S_{I1}$=1500-190=1310 mg/l

$X_T=C_{T1}-S_{T1}$=2550-1500=1050 mg/l

$X_{S1}=X_T-X_{I1}-X_{H1}$=1050-685-200=165 mg/l

$X_{S1,ini}$=165*0.1=17/2.1=8 mg/l

$S_{S1,ini}$=1310*0.1=131/2.1=62 mg/l

$S_{I1,ini}$=190*0.1=19/2.1=9 mg/l

$X_{I1,ini}$=685*0.1=69/2.1=33 mg/l

The set of model parameters used for each simulation is summarized in Table 7.5.

Table 7.5 Model parameters used in the simulations

Parameter, unit	ASM1			ASM3 and modifications		
	Set 1	Set 2	Set 3	Set 1	Set 2	Set 3
Volume fractions, l						
V_{ini}	2.00	2.00	2.00	2.00	2.00	2.00
V_{WW}	0.14	0.4	0.1	0.14	0.4	0.1
V_T	2.14	2.4	2.1	2.14	2.4	2.1
COD fractions, mg/l						
C_{T1}	-	-	121	-	-	121
S_{T1}	98	250	-	98	250	-
$S_{I1,ini}$	12	32	9	12	32	9
$X_{I1,ini}$	-	-	33	-	-	33
X_{H1}	-	-	10	-	-	10
S_{VFA}	54	137	39	-	-	-
$S_{S1,ini}$	54	137	39	86	218	62
$S_{H,ini}$	32	82	-	-	-	-
$X_{S,ini}$	-	-	31	-	-	8

7.2.2 Respirometric Data

The respirometric data obtained in each set of experiment according to ASM1 are given in Figures 7.1, 7.2 and 7.3.

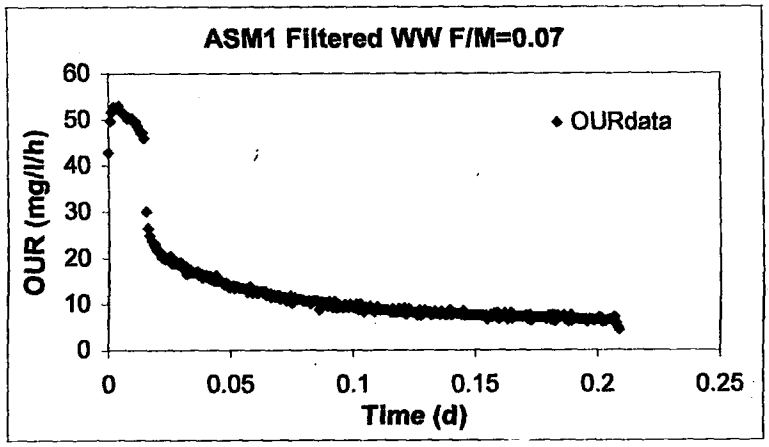

Figure 7.1 OUR data for Set 1 (filtered wastewater F/M=0.07 mg COD/mg VSS)

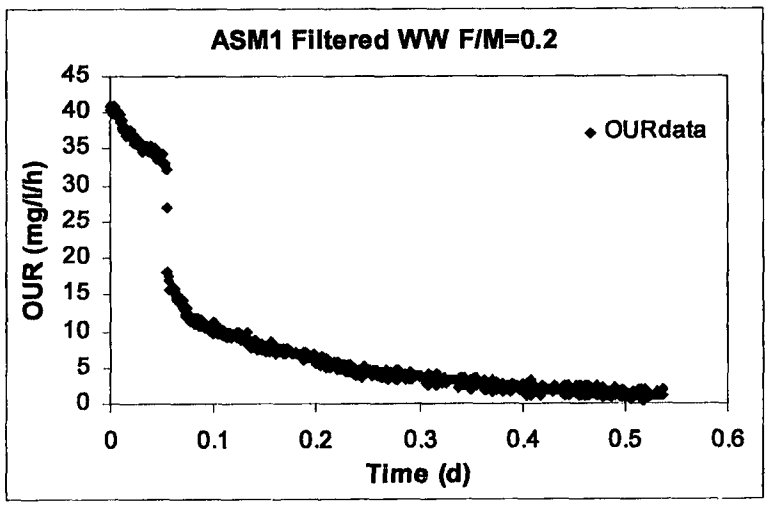

Figure 7.2 OUR data for Set 2 (filtered wastewater F/M=0.2 mg COD/mg VSS)

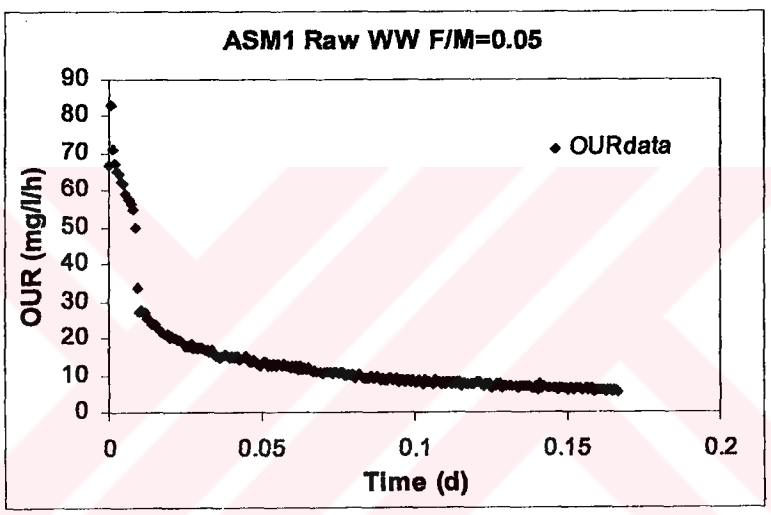

Figure 7.3 OUR data for Set 3 (raw wastewater F/M=0.05 mg COD/mg VSS)

SECTION 8 RESULTS AND DISCUSSION

8.1 Sensitivity of Model Coefficients

8.1.1 Sensitivity of ASM1 Coefficients

Heterotrophic growth rate, μ_H and heterotrophic yield coefficient, Y_H are the most significant parameters in ASM1 simulations. Sensitivity of endogenous decay rate, b_H and substrate half saturation constant, K_S are also illustrated as follows.

Sensitivity of heterotrophic growth rate: The OUR curve is shifted up as μ_H is increased, but the area under the curve remains the same. Also the steepness of the first plateau and the maximum OUR value would increase too (Figure 8.1).

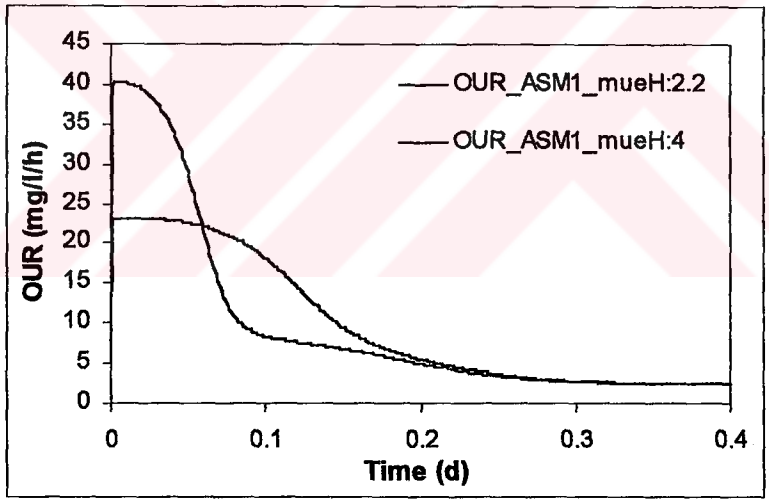

Figure 8.1 Sensitivity of heterotrophic growth rate, μ_H according toASM1

Sensitivity of heterotrophic yield coefficient: The area under the curve decreases as Y_H value increases as shown in Figure 8.2.

Sensitivity of endogenous decay rate: The total OUR curve is shifted up at nearly equal amounts if the value of b_H is increased (Figure 8.3).

Sensitivity of substrate half saturation constant: If K_S is smaller, the OUR curve will exhibit a steeper drop as shown in Figure 8.4.

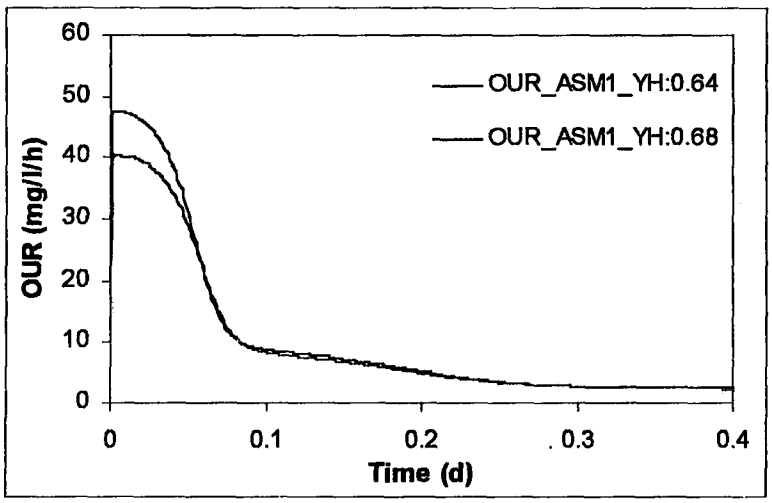

Figure 8.2 Sensitivity of heterotrophic yield coefficient, Y_H according to ASM1

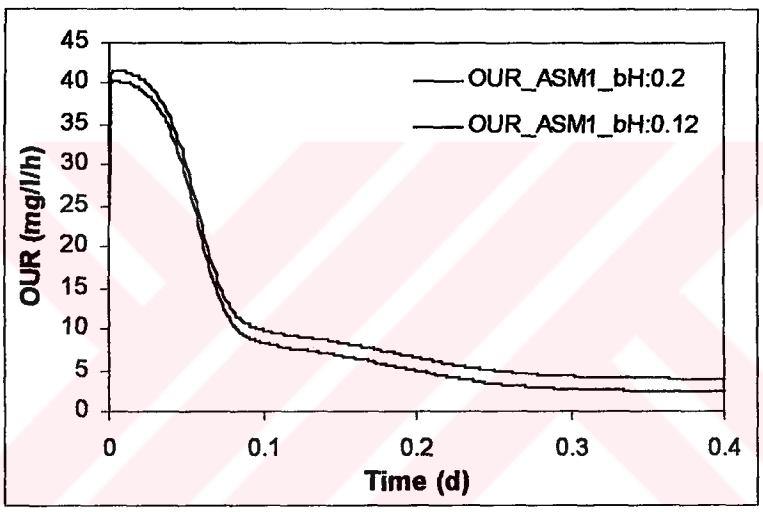

Figure 8.3 Sensitivity of endogenous decay rate, b_H according to ASM1

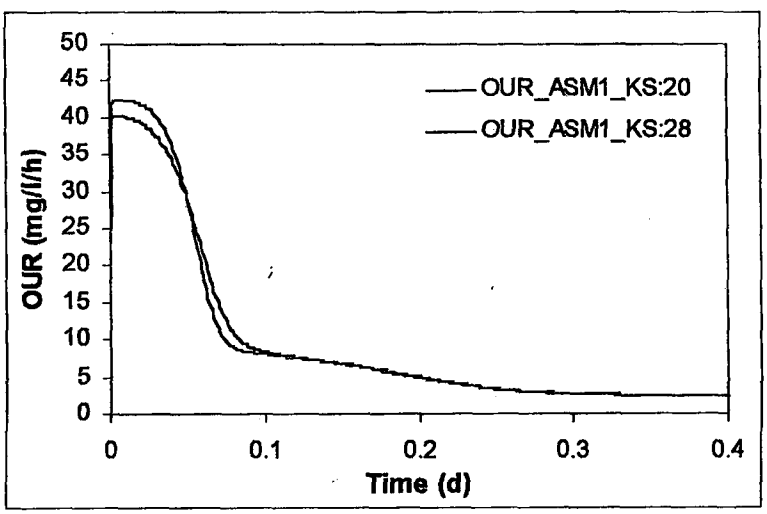

Figure 8.4 Sensitivity of substrate half saturation constant, K_S according to ASM1

8.1.2 Sensitivity of ASM3 Coefficients

Most sensitive parameter is storage yield coefficient, Y_{STO} in ASM3 simulations. Substrate storage rate, k_{STO} and substrate half saturation constant, K_S are also effective for storage process. Heterotrophic growth rate, μ_H and storage products' half saturation constant, K_{STO} couple is important in the modeling of growth process. Sensitivity of heterotrophic yield coefficient, Y_H, endogenous decay rate for heterotrophs, b_H and endogenous decay rate for stored polymers, b_{STO} were also investigated.

Sensitivity of storage yield coefficient: When Y_{STO} is increased, area under the curve is decreased as shown in Figure 8.5. Ever, it is increased by a value of 0.1 results are significantly changed.

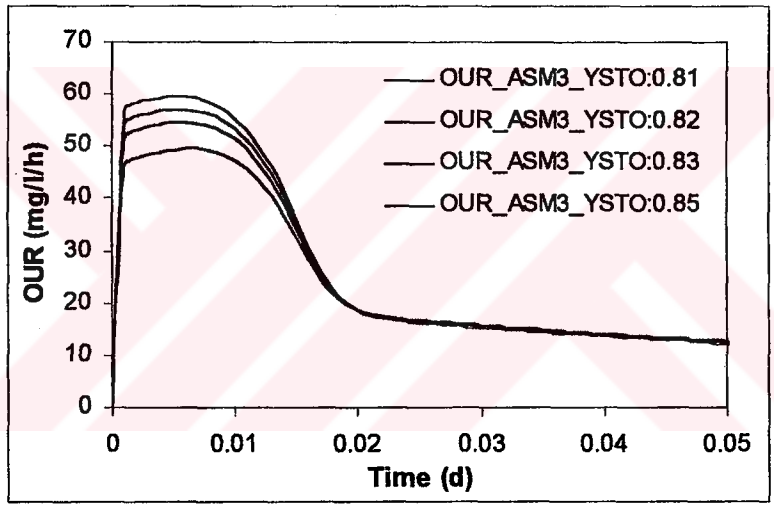

Figure 8.5 Sensitivity of storage yield coefficient, Y_{STO}

Sensitivity of substrate storage rate: If k_{STO} is increased, the OUR curve is shifted up, but the area under the curve gives the same value. Sensitivity of k_{STO} is illustrated in Figure 8.6.

Sensitivity of substrate half saturation constant: K_S seems to have not much influence on OUR curve, but it has impact on the maximum reachable value of OUR by decreasing the observed storage rate. If K_S is higher, decrease of OUR is smoother (Figure 8.7).

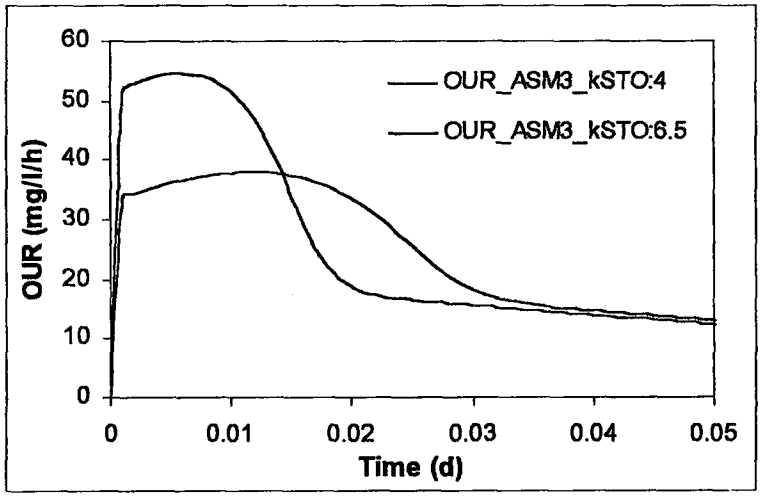

Figure 8.6 Sensitivity of substrate storage rate, k_{STO}

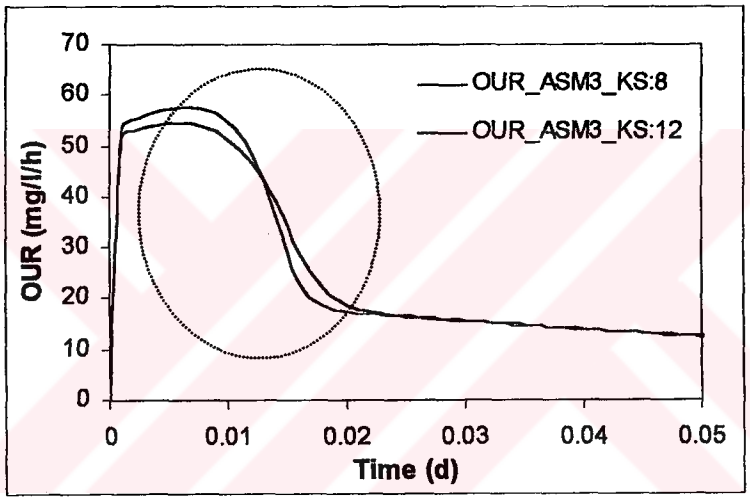

Figure 8.7 Sensitivity of substrate half saturation constant, K_S

Sensitivity of heterotrophic growth rate: Growth rate has effects on both the first and second plateaus of the OUR curve as shown in Figure 6.10 before. First plateau increases sharply and the maximum OUR value has a higher level if μ_H is increased. Also the slope of the second phase would increase too. μ_H is generally estimated from the slope of the second plateau. Sensitivity of μ_H is investigated and illustrated in Figure 8.8.

Sensitivity of storage products' half saturation constant: As similar to K_S, K_{STO} decreases the observed growth rate and therefore effects the OUR curve. If K_{STO} increases, the heterotrophic growth rate decreases so a more rounded curve is observed as in Figure 8.9.

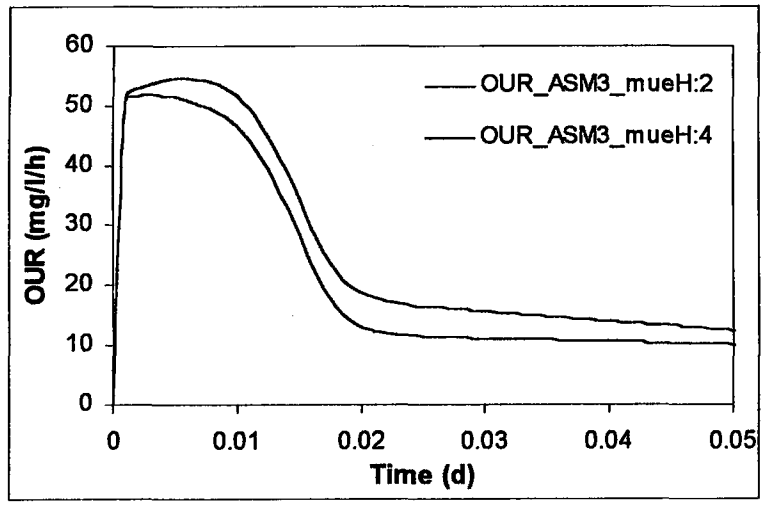

Figure 8.8 Sensitivity of heterotrophic growth rate, μ_H

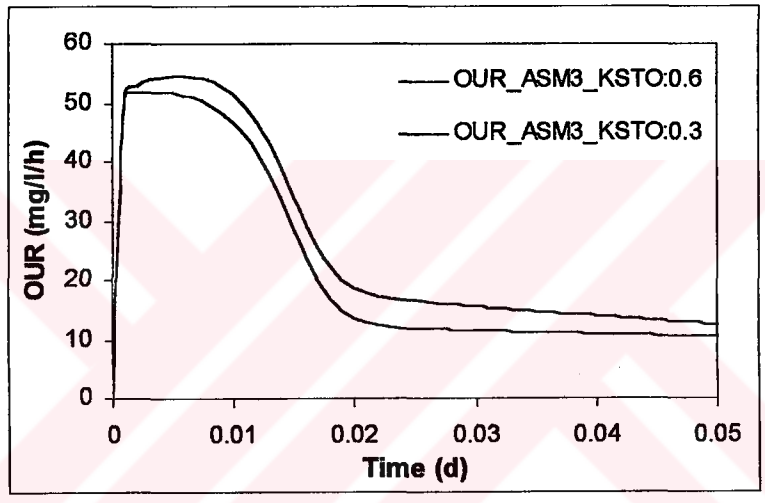

Figure 8.9 Sensitivity of storage products' half saturation constant, K_{STO}

Sensitivity of endogenous decay rate for heterotrophs: As b_H increases the OUR curve shifts up at nearly equal amounts (Figure 8.10).

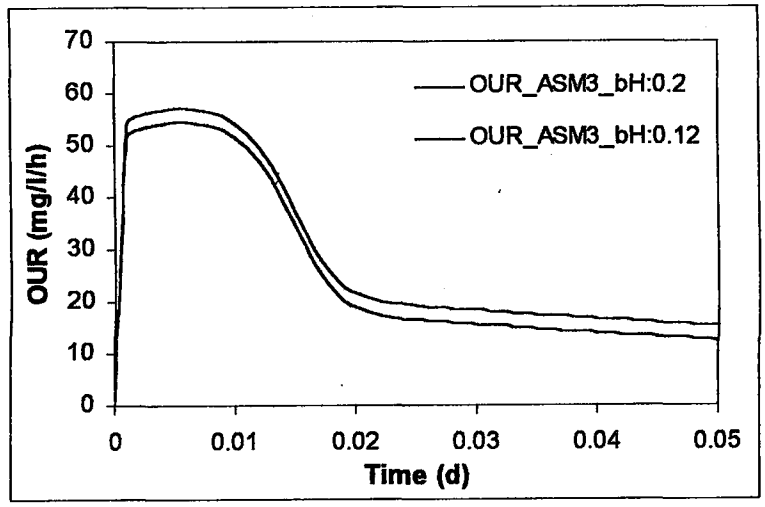

Figure 8.10 Sensitivity of endogenous decay rate for heterotrophs, b_H

Sensitivity of endogenous decay rate for stored polymers: There is no change in the OUR curve even the b_{STO} value is increased nearly by 70% (Figure 8.11).

Sensitivity of heterotrophic yield coefficient: As Y_H increases the area under the OUR curve decreases but the impact is not so important as illustrated in Figure 8.12.

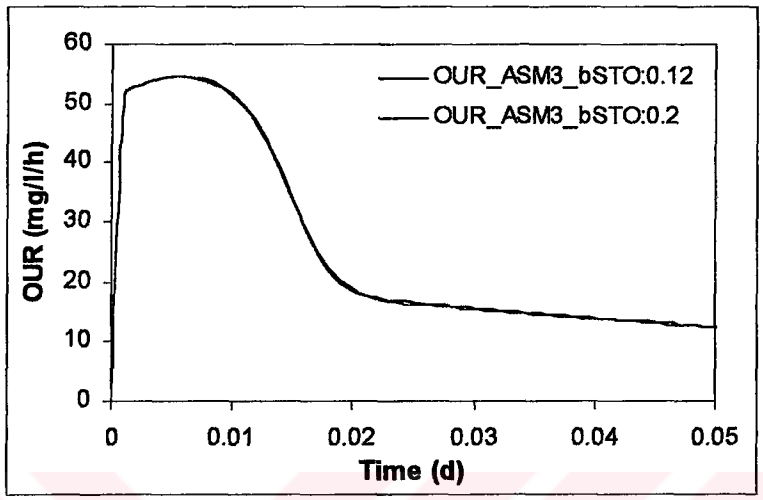

Figure 8.11 Sensitivity of endogenous decay rate for stored polymers, b_{STO}

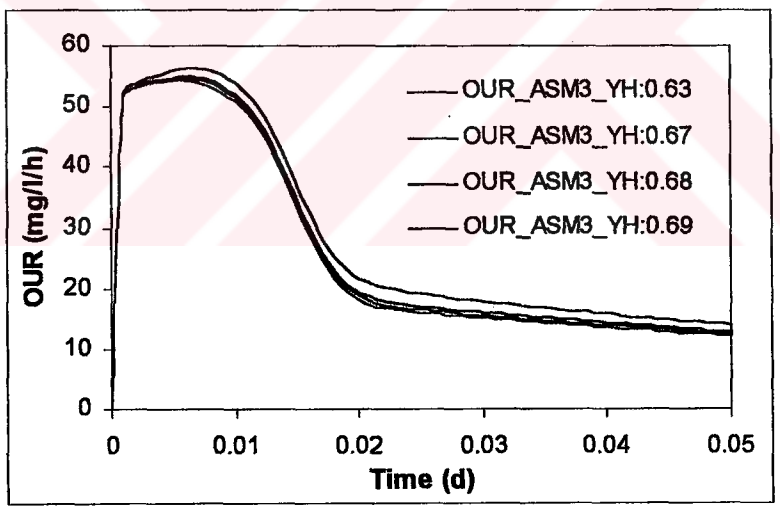

Figure 8.12 Sensitivity of heterotrophic yield coefficient, Y_H

8.2 Simulation Results

OUR simulations of the experimental data were conducted by using the volumes and COD fractions as calculated and summarized in Section 7. Default values for kinetic and stoichiometric coefficients of ASM1 determined by Orhon *et al.* (1999) for tannery wastewater and suggested in ASM3 by Gujer *et al.* (2000) for domestic wastewater are summarized in Table 8.1. Five models were used in the simulation of

all set of experiments; namely ASM1, ASM3 and ASM3 based models proposed by Krishna and van Loosdrecht (1999), Karahan-Gül *et al.* (2002b) and van Loosdrecht and Heijnen (2002), all adapted for tannery wastewater in ASM3 terms. Kinetic and stoichiometric coefficients estimated via model simulations are presented for experimental data obtained with filtered and raw wastewater. The OUR curves of each process is illustrated as separate components.

Table 8.1 Default values for kinetic and stoichiometric coefficients under normal conditions at 20 °C (Orhon *et al.*, 1999; Gujer *et al.*, 2000)

Parameter, unit	ASM1 (for tannery)	ASM3 (for domestic)
b_H, d^{-1}	0.12	0.2
b_{STO}, d^{-1}	-	0.2
f_{ES}, COD/COD	0.1	-
f_{EX}, COD/COD	0.2	-
k_H, d^{-1}	0.9	3
K_X, COD/COD	0.3	1
K_{O2}, mg O_2/l	0.2	0.2
K_S, mg COD/l	28	2
k_{STO}, d^{-1}	-	5
K_{STO}, COD/COD	-	1
μ_H, d^{-1}	2.2	2
Y_H, COD/COD	0.64	0.63
Y_{STO}, COD/COD	-	0.85

8.2.1 Simulation results for ASM1

Model simulations have been performed according to ASM1, based on the matrix given in Table 5.1 in Section 5 (Orhon *et al.* 1999).

Filtered Wastewater (F/M=0.07 mg COD/mg VSS): Table 8.2 shows the kinetic and stoichiometric coefficients chosen for the best fit and the resulting OUR curves are presented in Figure 8.13.

Table 8.2 Kinetic and stoichiometric coefficients used in the ASM1 simulation of Set 1 (Filtered wastewater F/M=0.07 mg COD/mg VSS)

Parameter	Unit	Value
b_H	d^{-1}	0.12
K_S	mg COD/l	28
μ_H	d^{-1}	4
Y_H	COD/COD	0.68
$X_{H,ini}$	mg COD/l	1200
k_{HS}	d^{-1}	0.9
K_{XS}	COD/COD	0.03

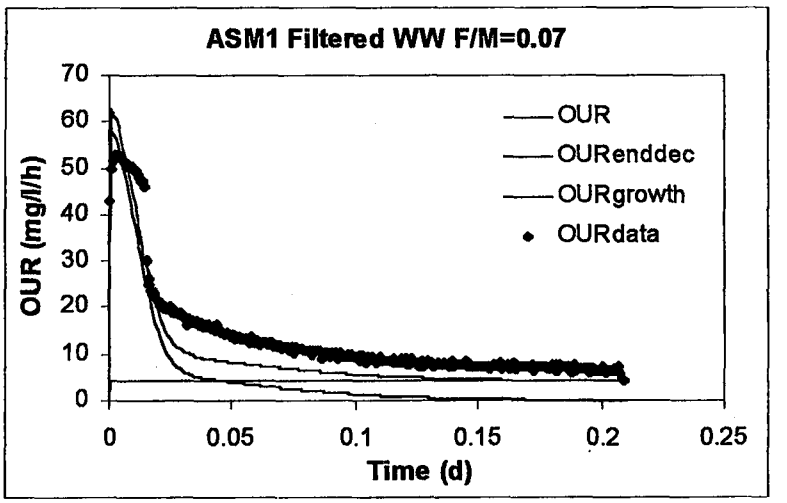

Figure 8.13 Resulting OUR components for filtered wastewater according to ASM1 (F/M=0.07 mg COD/mg VSS)

Filtered Wastewater (F/M=0.2 mg COD/mg VSS): Kinetic and stoichiometric coefficients used in the simulation of wastewater of F/M=0.2 mg COD/mg VSS is given in Table 8.3 and OUR curves are illustrated in Figure 8.14 as below:

Table 8.3 Kinetic and stoichiometric coefficients used in the ASM1 simulation of Set 2 (Filtered wastewater F/M=0.2 mg COD/mg VSS)

Parameter	Unit	Value
b_H	d^{-1}	0.12
K_S	mg COD/l	28
μ_H	d^{-1}	4
Y_H	COD/COD	0.68
$X_{H,ini}$	mg COD/l	600
k_{HS}	d^{-1}	0.9
K_{XS}	COD/COD	0.03

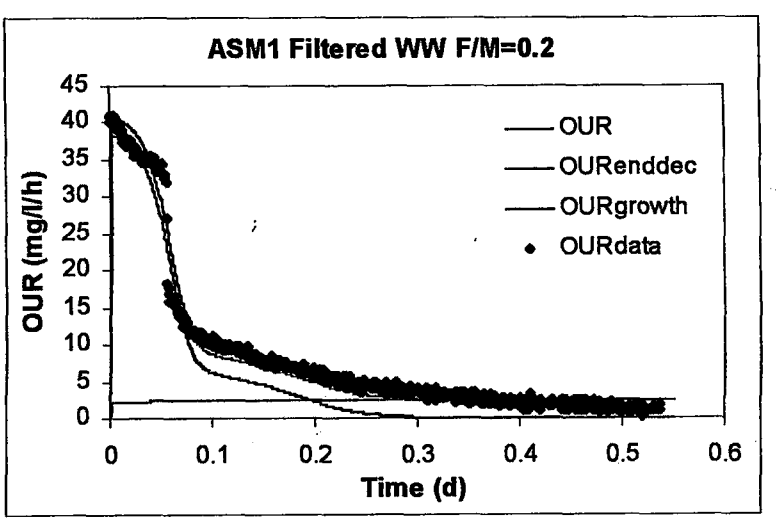

Figure 8.14 Resulting OUR components for filtered wastewater according to ASM1 (F/M=0.2 mg COD/mg VSS)

Raw Wastewater (F/M=0.05 mg COD/mg VSS): In the modeling of raw wastewater, dual hydrolysis model is considered as different from filtered wastewater simulations. For that reason, hydrolysis rate constant (k_H) and half saturation constant (K_X) for the hydrolysis of slowly biodegradable COD are involved in the kinetic and stoichiometric coefficients (Table 8.4). OUR curve obtained by the simulation of raw wastewater of F/M=0.05 mg COD/mg VSS is given in Figure 8.15.

Table 8.4 Kinetic and stoichiometric coefficients used in the ASM1 simulation of Set 3 (Raw wastewater F/M=0.05 mg COD/mg VSS)

Parameter	Unit	Value
b_H	d^{-1}	0.12
K_S	mg COD/l	28
μ_H	d^{-1}	4
Y_H	COD/COD	0.68
$X_{H,ini}$	mg COD/l	1900
k_{HS}	d^{-1}	0.9
k_H	d^{-1}	0.8
K_{XS}	COD/COD	0.03
K_X	COD/COD	0.01

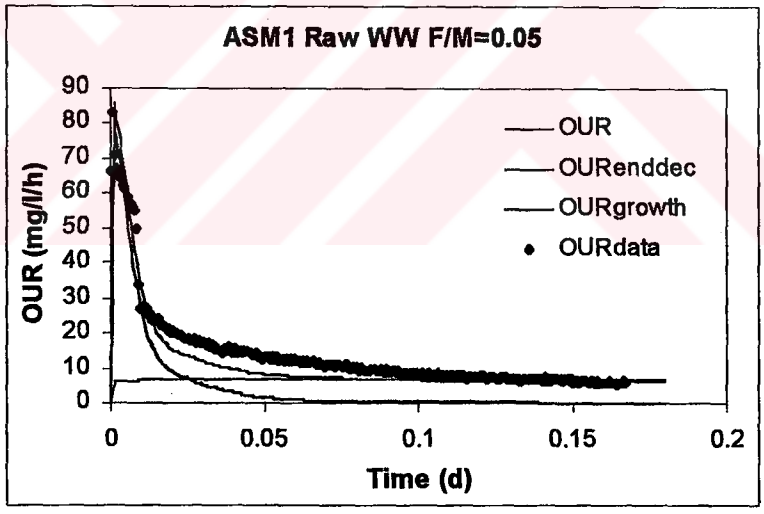

Figure 8.15 Resulting OUR components for raw wastewater according to ASM1 (F/M=0.05 mg COD/mg VSS)

8.2.2 Simulation Results for ASM3 Adapted for Tannery Wastewater

Simulations according to ASM3 adapted for tannery wastewater were done referring to the matrix given by Table 5.3.

Filtered Wastewater (F/M=0.07 mg COD/mg VSS): Kinetic and stoichiometric coefficients are given in Table 8.5 and OUR curves for the model are given by Figure 8.16.

Table 8.5 Kinetic and stoichiometric coefficients used in the ASM3 simulation of Set 1 (filtered wastewater F/M=0.07 mg COD/mg VSS)

Parameter	Unit	Value
b_H	d^{-1}	0.12
b_{STO}	d^{-1}	0.2
K_S	mg COD/l	12
K_{STO}	COD/COD	0.3
k_{STO}	d^{-1}	6.5
μ_H	d^{-1}	4
Y_H	COD/COD	0.68
Y_{STO}	COD/COD	0.83
$X_{H,ini}$	mg COD/l	1200

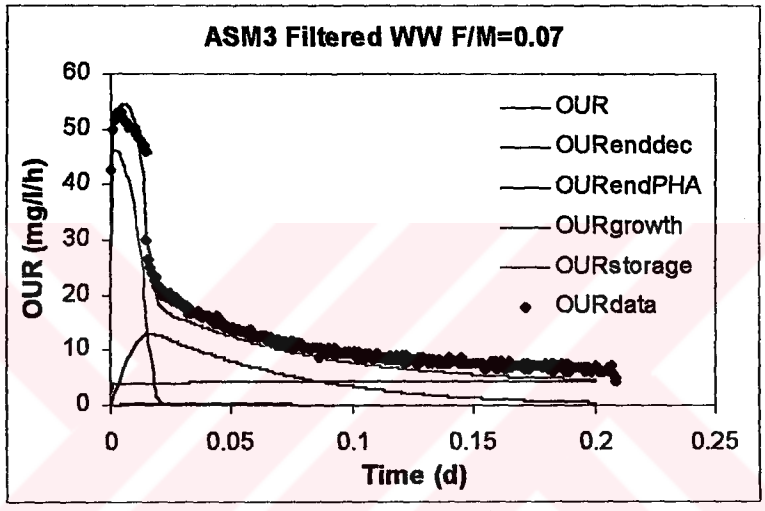

Figure 8.16 Resulting OUR components for filtered wastewater according to ASM3 (F/M=0.07 mg COD/mg VSS)

Filtered Wastewater (F/M=0.2 mg COD/mg VSS): Kinetic and stoichiometric coefficients used in the simulation of wastewater of F/M=0.2 mg COD/mg VSS according to ASM3 is given in Table 8.6 and OUR curves are illustrated by Figure 8.17 as below:

Table 8.6 Kinetic and stoichiometric coefficients used in the ASM3 simulation of Set 2 (filtered wastewater F/M=0.2 mg COD/mg VSS)

Parameter	Unit	Value
b_H	d^{-1}	0.12
b_{STO}	d^{-1}	0.2
K_S	mg COD/l	12
K_{STO}	COD/COD	0.4
k_{STO}	d^{-1}	7
μ_H	d^{-1}	3
Y_H	COD/COD	0.68
Y_{STO}	COD/COD	0.83
$X_{H,ini}$	mg COD/l	600

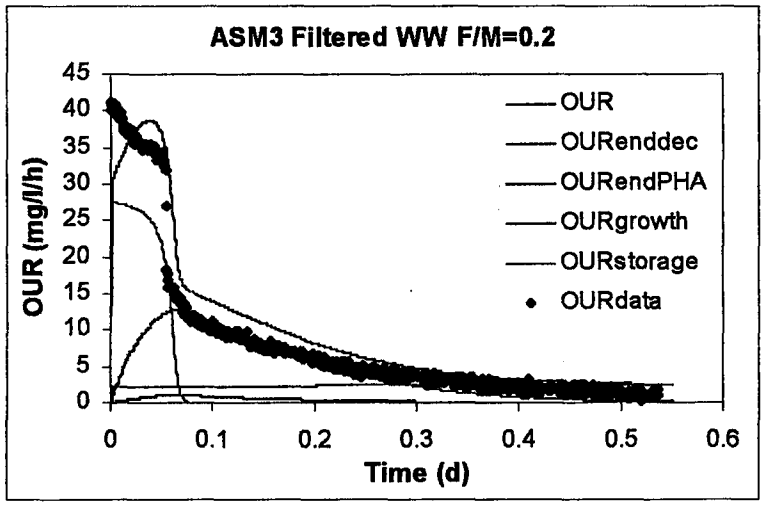

Figure 8.17 Resulting OUR components for filtered wastewater according to ASM3 (F/M=0.2 mg COD/mg VSS)

Raw Wastewater (F/M=0.05 mg COD/mg VSS): Kinetic and stoichiometric coefficients used for the best fit are summarized as below (Table 8.7). OUR curves obtained by the simulations for raw wastewater of F/M=0.05 mg COD/mg VSS are given in Figure 8.18.

Table 8.7 Kinetic and stoichiometric coefficients used in the ASM3 simulation of Set 3 (raw wastewater F/M=0.05 mg COD/mg VSS)

Parameter	Unit	Value
b_H	d^{-1}	0.12
b_{STO}	d^{-1}	0.2
k_H	d^{-1}	0.8
K_X	COD/COD	0.01
K_S	mg COD/l	12
K_{STO}	COD/COD	0.3
k_{STO}	d^{-1}	7
μ_H	d^{-1}	4
Y_H	COD/COD	0.68
Y_{STO}	COD/COD	0.83
$X_{H,ini}$	mg COD/l	1900

8.2.3 ASM3 Adapted for Tannery Wastewater (MODEL A)

Simulations according to ASM3 based model proposed by Krishna and van Loosdrecht (1999) adapted for tannery wastewater were done based on the expressions reported in Table 5.4.

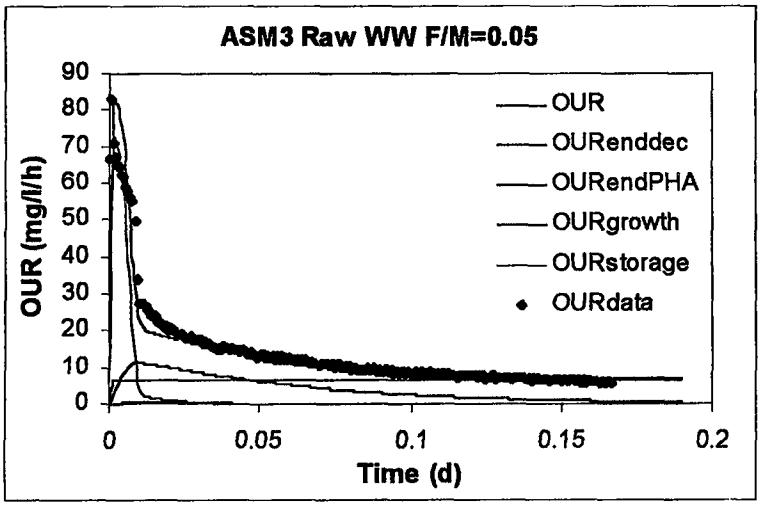

Figure 8.18 OUR components for raw wastewater according to ASM3 (F/M=0.05 mg COD/mg VSS)

Filtered Wastewater (F/M=0.07 mg COD/mg VSS): Kinetic and stoichiometric coefficients used in model simulations are given in Table 8.8 and OUR curves of the model are given by Figure 8.19.

Table 8.8 Kinetic and stoichiometric coefficients used in MODEL A simulation of Set 1 (filtered wastewater F/M=0.07 mg COD/mg VSS)

Parameter	Unit	Value
b_H	d^{-1}	0.12
b_{STO}	d^{-1}	0.2
K_S	mg COD/l	12
K_{STO}	COD/COD	0.04
k_{STO}	d^{-1}	5
μ_{H1}	d^{-1}	0.65
μ_{H2}	d^{-1}	1
Y_{H1}	COD/COD	0.67
Y_{H2}	COD/COD	0.68
Y_{STO}	COD/COD	0.83
$X_{H,ini}$	mg COD/l	1200

Filtered Wastewater (F/M=0.2 mg COD/mg VSS): Table 8.9 summarizes the coefficients used in the simulation. Figure 8.20 shows the OUR curves obtained for filtered wastewater for each component.

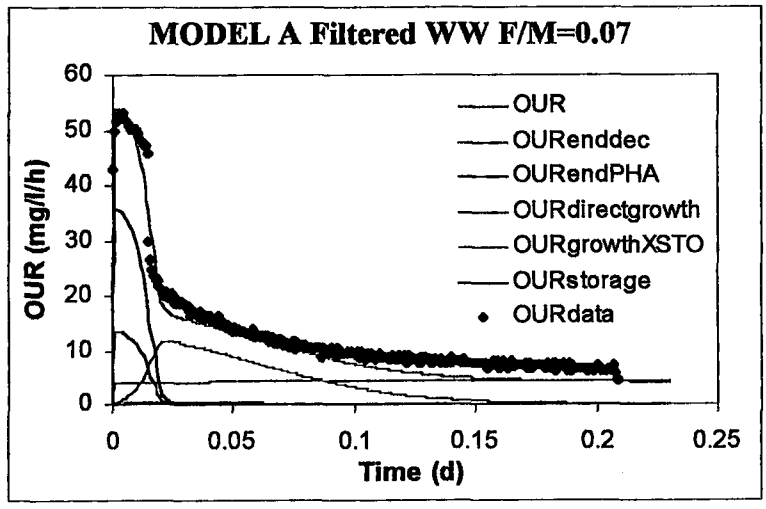

Figure 8.19 OUR components for filtered wastewater according to MODEL A (F/M=0.07 mg COD/mg VSS)

Table 8.9 Kinetic and stoichiometric coefficients used in MODEL A simulation of Set 2 (filtered wastewater F/M=0.2 mg COD/mg VSS)

Parameter	Unit	Value
b_H	d^{-1}	0.12
b_{STO}	d^{-1}	0.2
K_S	mg COD/l	12
K_{STO}	COD/COD	0.04
k_{STO}	d^{-1}	6
μ_{H1}	d^{-1}	0.9
μ_{H2}	d^{-1}	0.8
Y_{H1}	COD/COD	0.67
Y_{H2}	COD/COD	0.68
Y_{STO}	COD/COD	0.83
$X_{H,ini}$	mg COD/l	600

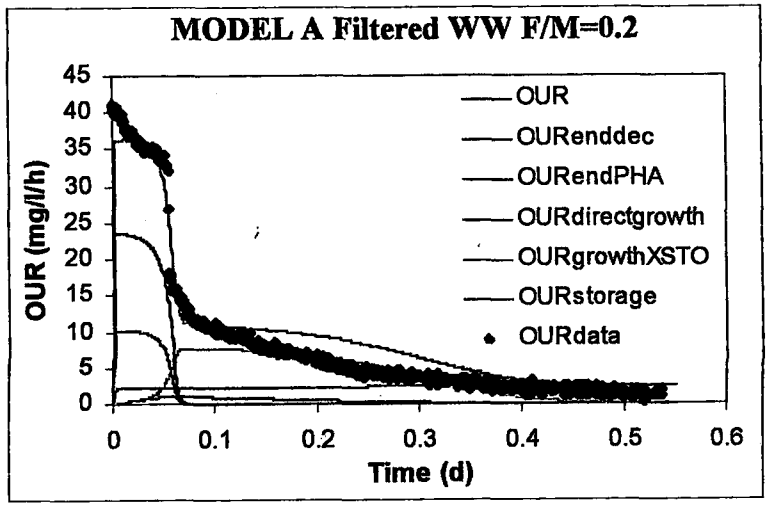

Figure 8.20 OUR components for filtered wastewater according to MODEL A (F/M=0.2 mg COD/mg VSS)

Raw Wastewater (F/M=0.05 mg COD/mg VSS): Table 8.10 summarizes the coefficients used in the simulation. Hydrolysis of slowly biodegradable COD is involved in this simulation as in all simulations done for raw wastewater because raw wastewater contains slowly biodegradable particulate components. Figure 8.21 shows the OUR curves obtained for raw wastewater of F/M=0.05 mg COD/mg VSS based on MODEL A.

Table 8.10 Kinetic and stoichiometric coefficients used in MODEL A simulation of Set 3 (raw wastewater F/M=0.05 mg COD/mg VSS)

Parameter	Unit	Value
b_H	d^{-1}	0.12
b_{STO}	d^{-1}	0.2
k_H	d^{-1}	0.8
K_X	COD/COD	0.01
K_S	mg COD/l	12
K_{STO}	COD/COD	0.04
k_{STO}	d^{-1}	5
μ_{H1}	d^{-1}	0.7
μ_{H2}	d^{-1}	1
Y_{H1}	COD/COD	0.67
Y_{H2}	COD/COD	0.68
Y_{STO}	COD/COD	0.83
$X_{H,ini}$	mg COD/l	1900

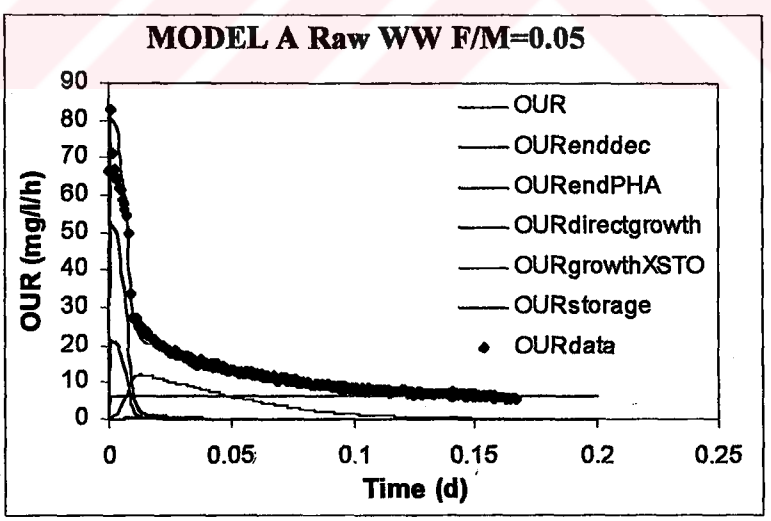

Figure 8.21 OUR components for raw wastewater according to MODEL A (F/M=0.05 mg COD/mg VSS)

8.2.4 ASM3 Adapted for Tannery Wastewater (MODEL B)

Simulations according to ASM3 based model proposed by Karahan-Gül *et al.* (2002b) adapted for tannery wastewater were done referring to the matrix given in Table 5.5.

Filtered Wastewater (F/M=0.07 mg COD/mg VSS): Kinetic and stoichiometric coefficients for the best fit are given in Table 8.11 and OUR curves of MODEL B are given in Figure 8.22.

Table 8.11 Kinetic and stoichiometric coefficients used in MODEL B simulation of Set 1 (filtered wastewater F/M=0.07 mg COD/mg VSS)

Parameter	Unit	Value
b_H	d^{-1}	0.12
b_{STO}	d^{-1}	0.2
K_S	mg COD/l	12
K_{STO}	COD/COD	0.04
k_{STO}	d^{-1}	4
μ_{H1}	d^{-1}	0.7
μ_{H2}	d^{-1}	1
Y_{H1}	COD/COD	0.67
Y_{H2}	COD/COD	0.68
Y_{STO}	COD/COD	0.83
$X_{H,ini}$	mg COD/l	1200

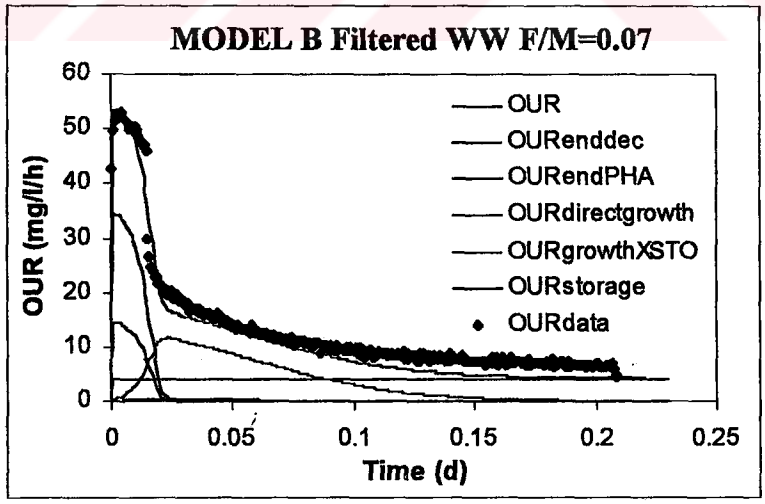

Figure 8.22 OUR components for filtered wastewater according to MODEL B (F/M=0.07 mg COD/mg VSS)

Filtered Wastewater (F/M=0.2 mg COD/mg VSS): Kinetic and stoichiometric coefficients used in the model are given in Table 8.12.

Table 8.12 Kinetic and stoichiometric coefficients used in MODEL B simulation of Set 2 (filtered wastewater F/M=0.2 mg COD/mg VSS)

Parameter	Unit	Value
b_H	d^{-1}	0.12
b_{STO}	d^{-1}	0.2
K_S	mg COD/l	12
K_{STO}	COD/COD	0.04
k_{STO}	d^{-1}	5
μ_{H1}	d^{-1}	0.9
μ_{H2}	d^{-1}	0.8
Y_{H1}	COD/COD	0.67
Y_{H2}	COD/COD	0.68
Y_{STO}	COD/COD	0.83
$X_{H,ini}$	mg COD/l	600

OUR curves for the simulation of filtered wastewater of F/M=0.2 mg COD/mg VSS are given by Figure 8.23.

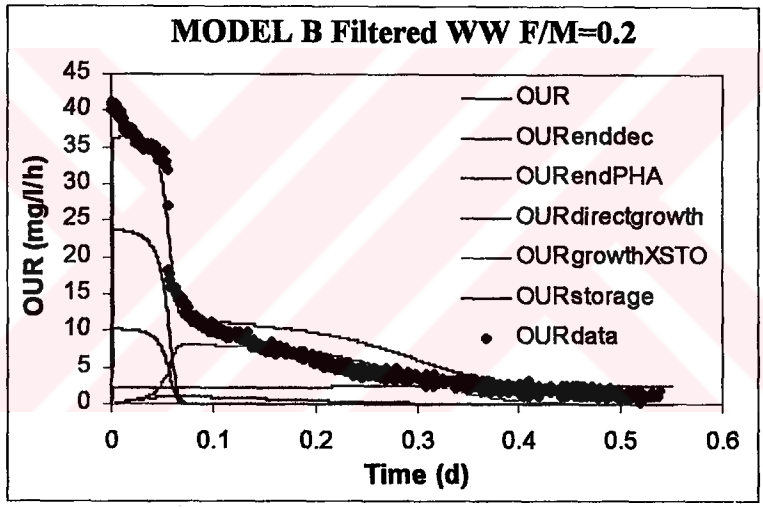

Figure 8.23 OUR components for filtered wastewater according to MODEL B (F/M=0.2 mg COD/mg VSS)

Raw Wastewater (F/M=0.05 mg COD/mg VSS): Table 8.13 shows the kinetic and stoichiometric coefficients used in the simulation. Figure 8.24 illustrates the OUR curves obtained for the raw wastewater of F/M=0.05 mg COD/mg VSS.

Table 8.13 Kinetic and stoichiometric coefficients used in MODEL B simulation of Set 3 (raw wastewater F/M=0.05 mg COD/mg VSS)

Parameter	Unit	Value
b_H	d^{-1}	0.12
b_{STO}	d^{-1}	0.2
k_H	d^{-1}	0.8
K_X	COD/COD	0.01
K_S	mg COD/l	12
K_{STO}	COD/COD	0.04
k_{STO}	d^{-1}	4.2
μ_{H1}	d^{-1}	0.7
μ_{H2}	d^{-1}	1
Y_{H1}	COD/COD	0.67
Y_{H2}	COD/COD	0.68
Y_{STO}	COD/COD	0.83
$X_{H,ini}$	mg COD/l	1900

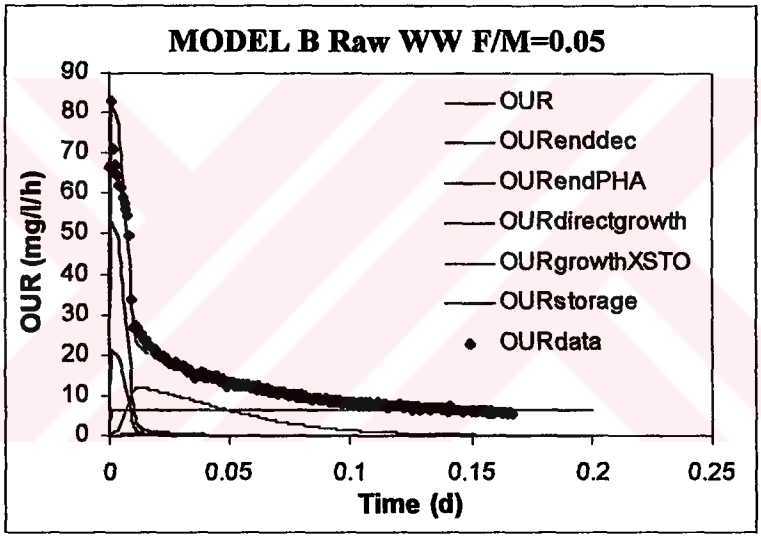

Figure 8.24 OUR components for raw wastewater according to MODEL B (F/M=0.05 mg COD/mg VSS)

8.2.5 Model Adapted for Tannery Wastewater in ASM3 Terms (MODEL C)

Simulations according to model proposed by van Loosdrecht and Heijnen (2002) adapted for tannery wastewater in ASM3 terms were done according to the matrix given in Table 5.6.

Filtered Wastewater (F/M=0.07 mg COD/mg VSS): Table 8.14 gives the kinetic and stoichiometric coefficients used in the simulation. Figure 8.25 illustrates the OUR curves obtained for filtered wastewater of F/M=0.07 mg COD/mg VSS.

Table 8.14 Kinetic and stoichiometric coefficients used in MODEL C simulation of Set 1 (filtered wastewater F/M=0.07 mg COD/mg VSS)

Parameter	Unit	Value
b_H	d^{-1}	0.12
b_{STO}	d^{-1}	0.2
K_S	mg COD/l	12
k_{XSTO}	d^{-1}	4.2
μ_H	d^{-1}	0.7
Y_{H1}	COD/COD	0.67
Y_{H2}	COD/COD	0.68
Y_{STO}	COD/COD	0.83
q_S	d^{-1}	5.8
$X_{H,ini}$	mg COD/l	1200

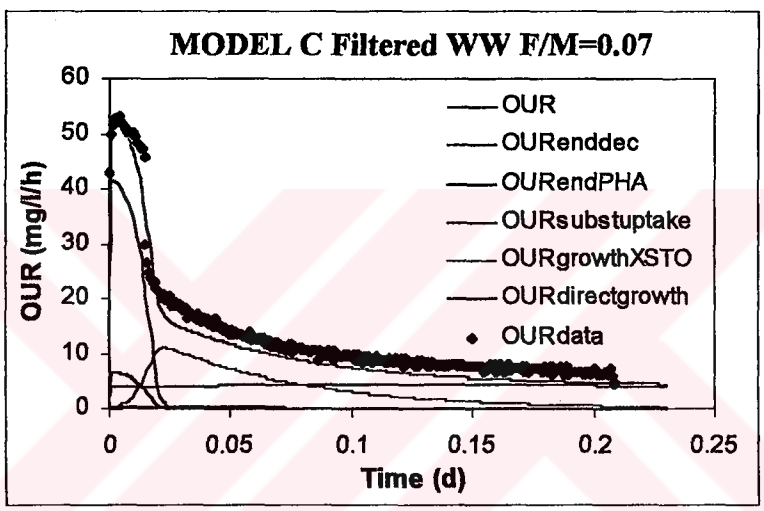

Figure 8.25 OUR components for filtered wastewater according to MODEL C (F/M=0.07 mg COD/mg VSS)

Filtered Wastewater (F/M=0.2 mg COD/mg VSS): Kinetic and stoichiometric coefficients used in the model simulation are given in Table 8.15. Figure 8.26 represents the OUR curves obtained.

Raw Wastewater (F/M=0.05 mg COD/mg VSS): Kinetic and stoichiometric coefficients used in the simulation for set 2 are given in Table 8.16. Figure 8.27 represents the OUR curves for Model C.

Table 8.15 Kinetic and stoichiometric coefficients used in MODEL C simulation of Set 2 (filtered wastewater F/M=0.2 mg COD/mg VSS)

Parameter	Unit	Value
b_H	d^{-1}	0.12
b_{STO}	d^{-1}	0.2
K_S	mg COD/l	12
k_{XSTO}	d^{-1}	9
μ_H	d^{-1}	0.7
Y_{H1}	COD/COD	0.67
Y_{H2}	COD/COD	0.68
Y_{STO}	COD/COD	0.83
q_S	d^{-1}	8.5
$X_{H,ini}$	mg COD/l	600

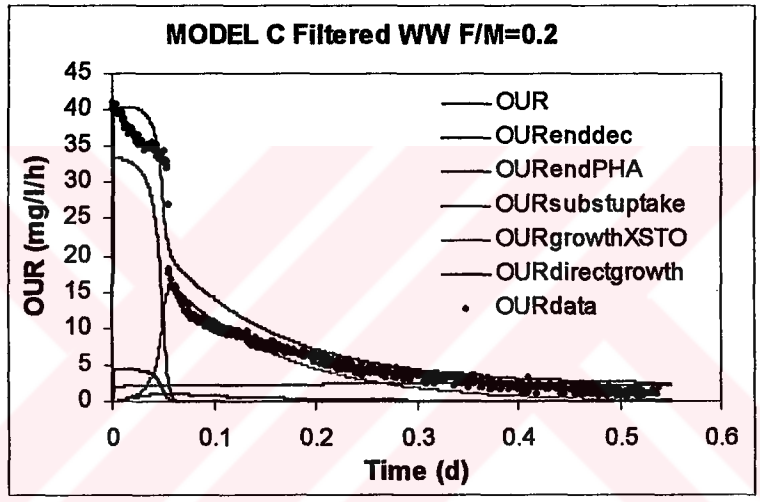

Figure 8.26 OUR components for filtered wastewater according to MODEL C (F/M=0.2 mg COD/mg VSS)

Table 8.16 Kinetic and stoichiometric coefficients used in MODEL C simulation of Set 3 (filtered wastewater F/M=0.2 mg COD/mg VSS)

Parameter	Unit	Value
b_H	d^{-1}	0.12
b_{STO}	d^{-1}	0.2
k_H	d^{-1}	0.8
K_X	COD/COD	0.01
K_S	mg COD/l	12
k_{XSTO}	d^{-1}	21
μ_H	d^{-1}	0.65
Y_{H1}	COD/COD	0.67
Y_{H2}	COD/COD	0.68
Y_{STO}	COD/COD	0.83
q_S	d^{-1}	6
$X_{H,ini}$	mg COD/l	1900

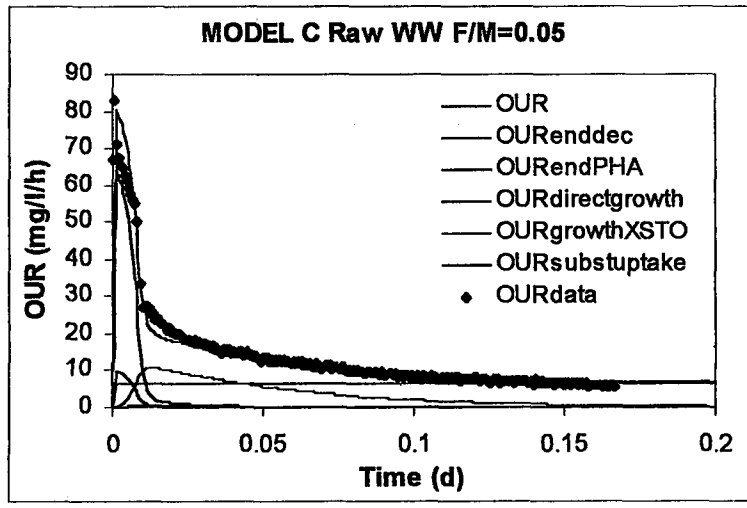

Figure 8.27 OUR components for raw wastewater according to MODEL C (F/M=0.05 mg COD/mg VSS)

Table 8.17 summarizes the kinetic and stoichiometric coefficients estimated for the best fit obtained in the simulation of five different models concerned.

8.3 Discussion of Modeling Results

Different activated sludge models including storage phenomena for tannery industry wastewater have been investigated and evaluated in this study. The activated sludge system treating both domestic and/or industrial wastewaters is the most widely used biological wastewater treatment process. Computer modeling is accepted as a useful tool for understanding the behavior of activated sludge wastewater treatment systems. ASM models developed by IAWQ task group introduced a common language for computer modeling. Computer models are mainly applied for domestic wastewater treatment plants; their application to industrial wastewater treatment plants requires different modeling approaches and accurate estimation of wastewater fractions and that of kinetic and stoichiometric model parameters that are different from the ones used for domestic wastewater.

IAWQ Task Group introduced ASM1 (Henze *et al.*, 1987) for the design and simulation of activated sludge systems. Later ASM1 was improved for biological phosphorus removal and presented as ASM2 and ASM2d by Henze *et al.* (1995; 1999). Recently, Task Group introduced ASM3 (Gujer *et al.*, 2000), which emphasizes the importance of storage concept.

Table 8.17 Summary of the kinetic and stoichiometric coefficients estimated for different models

Parameter	Unit	ASM1			ASM3			Model A			Model B			Model C		
		Set 1	Set 2	Set 3	Set 1	Set 2	Set 3	Set 1	Set 2	Set 3	Set 1	Set 2	Set 3	Set 1	Set 2	Set 3
b_H	d^{-1}	0.12	0.12	0.12	0.12	0.12	0.12	0.12	0.12	0.12	0.12	0.12	0.12	0.12	0.12	0.12
b_{STO}	d^{-1}	-	-	-	0.2	0.2	0.2	0.2	0.2	0.2	0.2	0.2	0.2	0.2	0.2	0.2
k_{HS}	d^{-1}	0.9	0.9	0.9	-	-	-	-	-	-	-	-	-	-	-	-
k_H	d^{-1}	-	-	0.8	-	-	0.8	-	-	0.8	-	-	0.8	-	-	0.8
K_{XS}	gCOD/gCOD	0.03	0.03	0.03	-	-	-	-	-	-	-	-	-	-	-	-
K_X	gCOD/gCOD	-	-	0.01	-	-	0.01	-	-	0.01	-	-	0.01	-	-	0.01
K_S	mg COD.l^{-1}	28	28	28	12	12	12	12	12	12	12	12	12	12	12	12
K_{STO}	mgl^{-1}	-	-	-	0.3	0.4	0.3	0.04	0.04	0.04	0.04	0.04	0.04	-	-	-
k_{STO}	d^{-1}	-	-	-	6.5	7	7	5	6	5	4	5	4.2	-	-	-
μ_{H1}	d^{-1}	4	4	4	4	3	4	0.65	0.9	0.7	0.7	0.9	0.7	0.65	0.65	0.65
μ_{H2}	d^{-1}	-	-	-	-	-	-	1	0.8	1	1	0.8	1	-	-	-
Y_{H1}	gCOD/gCOD	0.68	0.68	0.68	0.68	0.68	0.68	0.67	0.67	0.67	0.67	0.67	0.67	0.67	0.67	0.67
Y_{H2}	gCOD/gCOD	-	-	-	-	-	-	0.68	0.68	0.68	0.68	0.68	0.68	0.68	0.68	0.68
Y_{STO}	gCOD/gCOD	-	-	-	0.83	0.83	0.83	0.83	0.83	0.83	0.83	0.83	0.83	0.83	0.83	0.83
k_{XSTO}	d^{-1}	-	-	-	-	-	-	-	-	-	-	-	-	17	9	21
q_S	d^{-1}	-	-	-	-	-	-	-	-	-	-	-	-	5.8	8.5	6
$X_{H,ini}$	mgCOD.l^{-1}	1200	600	1900	1200	600	1900	1200	600	1900	1200	600	1900	1200	600	1900

Table 8.18 Summary of the kinetic and stoichiometric coefficients for different models in literature

Parameter	Unit	ASM1 (Henze *et al.*, 1987)	ASM1 (Orhon *et al.*, 1999)	ASM3 (Gujer *et al.*, 2000)	ASM3 (Koch *et al.*, 2000)	ASM3 (Krishna and van Loosdrecht, 1999)	ASM3 (Karahan-Gül *et al.*, 2002b)		ASM3 (Avcıoğlu *et al.*, 2002)	Modified ASM3 (Krishna and van Loosdrecht, 1999)	Modified ASM3 (Karahan-Gül *et al.*, 2002b)	
		default	**tannery**	**default**	**domestic**	**acetate**	**acetate**	**glucose**	**acetate**	**acetate**	**acetate**	**glucose**
b_H	d^{-1}	0.62	0.12	0.2	0.3	0.2	0.24	0.2	0.2	0.2	0.24	0.2
b_{STO}	d^{-1}	-	-	0.2	0.3	0.2	0.24	0.1	0.2	0.2	0.24	0.1
k_{HS}	d^{-1}	-	2	-	-	-	-	-	-	-	-	-
k_H	d^{-1}	3	0.9	3	9	-	-	-	-	-	-	-
K_{XS}	gCOD/gCOD	-	0.08	-	-	-	-	-	-	-	-	-
K_X	gCOD/gCOD	0.03	0.3	1	1	-	-	-	-	-	-	-
K_S	mg COD.l^{-1}	20	28	2	10	0.1	4	18	2.5	0.1	3	18
K_{STO}	mgl^{-1}	-	-	1	0.1	1	1	1	1	1	0.4	1
k_{STO}	d^{-1}	-	-	5	12	5	16	12	13	5	14	8
μ_{H1}	d^{-1}	6	2.2	2	3	2	1.8	2.5	4.5&2	4	4	2
μ_{H2}	d^{-1}	-	-	-	-	-	-	-	-	2	3	2.5
Y_{H1}	gCOD/gCOD	0.67	0.64	0.63	0.8	-	0.63	0.6	0.63	0.41*	0.65	0.67
Y_{H2}	gCOD/gCOD	-	-	-	-	-	-	-	-	0.57*	0.75	0.70
Y_{STO}	gCOD/gCOD	-	-	0.85	0.8	-	0.80	0.88	0.78	0.69*	0.80	0.90
k_{XSTO}	d^{-1}	-	-	-	-	-	-	-	-	-	-	-
q_S	d^{-1}	-	-	-	-	-	-	-	-	-	-	-

* Beun *et al.* (2000)

In the literature, only a few studies are present for the application of ASM3 whereas a number of ASM1 calibrations are reported for industrial wastewaters. In the proposed model of Gujer *et al.* (2000) stoichiometric and kinetic coefficients are suggested as default values for domestic wastewater. The other studies on ASM3 applications are those presented by Koch *et al.* (2000) for domestic wastewater, Krishna and van Loosdrecht (1999) for acetate, Karahan-Gül *et al.* (2002b) for glucose and acetate, Avcıoğlu *et al.* (2002) for acetate.

In this study, application and comparison of modeling studies for ASM1 and ASM3 for tannery wastewater were handled and it is the first attempt in this field. Additionally, ASM3 was extended and adapted for tannery wastewater according to the simultaneous growth and storage concept. In literature, simultaneous growth and storage models were applied for acetate by Krishna and van Loosdrecht (1999) and, for acetate and glucose by Karahan-Gül *et al.* (2002b). There is no available research for the application of above-mentioned structured models for tannery wastewater. Therefore, comparison and evaluation of the results obtained for tannery wastewater in this study presents a conceptual framework for the application of different structured models for industrial wastewaters.

Different experimental studies conducted for the calibration and validation of ASM models for carbon removal, namely ASM1 and ASM3 have resulted in a number of values for the kinetic and stoichiometric parameters applicable for systems fed with various substrates as shown in Table 8.18. The summary presented in Table 8.18, reflects the variations expected for the values clearly of model parameters when different models and different substrates are concerned. Therefore the results highlight the need for reliable estimation of model parameters with respect to each specific wastewater of concern.

Model simulations conducted in this study were based on previous literature data obtained for tannery effluents (Orhon *et al.*, 1999). The endogenous decay process rate, b_H, was assumed to be 0.12 d^{-1} as given by Orhon *et al.* (1999) and the corresponding active heterotrophic biomass concentrations were estimated as 1200, 600 and 1900 mg COD/l for experimental sets 1, 2 and 3 respectively.

Consequently the estimated F/M ratios on COD basis considering active heterotrophic biomass fraction were found as 0.08, 0.42 and 0.06, reflecting 60%, 34% and 55% of VSS used as seed could be considered as active.

In this context, all the model simulations were based on the same endogenous decay rate and active heterotrophic biomass concentrations as one of the initial experimental conditions. The initial wastewater COD fractions were calculated based on the definitions in ASM1 and ASM3 as given in Section 7.2. For ASM1 simulations, the readily biodegradable substrate concentration was assumed to be equal to the VFA content, whereas the biodegradable portion of soluble COD fraction was considered as S_S for ASM3 and modifications.

Model simulation results for ASM1 were quite consistent with those given in literature (Orhon et al., 1999) as given in Table 8.19.

Table 8.19 Comparison of ASM1 Modeling Results

Parameter	Unit	ASM1 (Henze *et al.*, 1987)	ASM1 (Orhon *et al.*, 1999)	ASM1 This Study
		default	tannery	tannery
b_H	d^{-1}	0.62	0.12	0.12
k_{HS}	d^{-1}	-	2	0.9
k_H	d^{-1}	3	0.9	0.8
K_{XS}	gCOD/gCOD	-	0.08	0.03
K_X	gCOD/gCOD	0.03	0.3	0.01
K_S	mg COD.l^{-1}	20	28	28
μ_H	d^{-1}	6	2.2	4
Y_H	gCOD/gCOD	0.67	0.64	0.68

The modeling results presented in this study yielded higher growth rates and heterotrophic yield coefficients when compared to the literature values for tannery wastewaters. This difference is due to the fact that in the previous study (Orhon *et al.*, 1999), the yield coefficient and growth rate were estimated with respirometric tests together with S_S, where this study assumes readily biodegradable COD fraction to be equal to the VFA content. As a consequence, the estimated hydrolysis rates in this study are slower than that of Orhon et al. (1999). Half saturation coefficient, K_S was found to be 28 mg.l^{-1} in this study for both raw and filtered wastewaters and these results are in accordance with the results given in literature. Heterotrophic growth rate, μ_H is 4 d^{-1} in this study. This value is less than that of ASM1 default (Henze *et al.*, 1987), which is expected when the complexity of tannery effluent with respect to domestic sewage is concerned.

If ASM3 is chosen as the valid model for tannery effluent applications the simulation results present a better description of the dynamic OUR response compared to ASM1. This result is obviously a consequence of the high amount of VFA content and prevailing transient conditions in batch experiments.

The simulation results of ASM3 are presented in Table 8.20 in comparison with ASM3 default values and various results reported in literature for different substrates.

Table 8.20 Comparison of ASM3 modeling results

Parameter	Unit	ASM3 (Gujer *et al.*, 2000)	ASM3 (Koch *et al.*, 2000)	ASM3 (Krishna and van Loosdrecht, 1999)	ASM3 (Karahan-Gül *et al.*, 2002b)		ASM3 (Avcıoğlu *et al.*, 2002)	ASM3 This Study
		default	**domestic**	**acetate**	**acetate**	**glucose**	**acetate**	**tannery**
b_H	d^{-1}	0.2	0.3	0.2	0.24	0.2	0.2	0.12
b_{STO}	d^{-1}	0.2	0.3	0.2	0.24	0.1	0.2	0.2
k_H	d^{-1}	3	9	-	-	-	-	0.8
K_X	gCOD/gCOD	1	1	-	-	-	-	0.01
K_S	mg COD.l^{-1}	2	10	0.1	4	18	2.5	12
K_{STO}	mgl^{-1}	1	0.1	1	1	1	1	0.33
k_{STO}	d^{-1}	5	12	5	16	12	13	6.8
μ_H	d^{-1}	2	3	2	1.8	2.5	4.5&2	3.7
Y_H	gCOD/gCOD	0.63	0.8	-	0.63	0.6	0.63	0.68
Y_{STO}	gCOD/gCOD	0.85	0.8	-	0.80	0.88	0.78	0.83

Value of b_H is found to be 0.12 d^{-1} in this study as in the study of Orhon *et al.* (1999) and also lower from the values given in six of the models as in Table 8.20. All of these simulation studies were achieved for different substrates, acetate, glucose and domestic sewage, which are more biodegradable than tannery effluent.

Endogenous decay rate for stored polymers, b_{STO} is accepted as 0.2 d^{-1} like in ASM3 (Gujer *et al.*, 2000) default, Krishna and van Loosdrecht (1999) and Avcıoğlu *et al.* (2002). Koch *et al.* (2000) found b_{STO} as 0.3 d^{-1} and Karahan-Gül *et al* (2002b) as 0.24 d^{-1} for acetate, but 0.1 d^{-1} for glucose. The modeling results for the endogenous degradation of stored polymers should be investigated further with specific tests.

For particulate substrate, k_H and K_X values are found to be 0.8 d^{-1} and 0.01 gCOD/gCOD respectively. Comparison of these values is only available with data given in ASM3 (Gujer *et al.*, 2000) default and Koch *et al.* (2000) and they both seem to be very higher than the values found in this study. These differences are due to the wastewater composition; tannery wastewaters exhibit more complex characteristics than domestic sewage. K_S is 12 mg COD.l^{-1} in ASM3 simulation of

tannery wastewater, which is higher than all of the values except Karahan-Gül *et al* (2002b) for glucose. Especially the result of 0.1 mg COD.l^{-1} found by Krishna and van Loosdrecht (1999) is very small.

Half saturation constant for stored polymers, K_{STO} is 0.3 gCOD/gCOD for filtered wastewater of F/M=0.07 and raw wastewater of F/M=0.05 while the value for filtered wastewater of F/M=0.2 is found to be 0.4 gCOD/gCOD. These values are bigger than the value of Koch *et al.* (2000) and smaller than the values of other ASM3 models. Substrate storage rate, k_{STO} is 6.5 d^{-1} for filtered wastewater of F/M=0.07, whereas 7 d^{-1} for filtered wastewater of F/M=0.2 and raw wastewater of F/M=0.05. These values are similar to ASM3 (Gujer *et al.,* 2000) default and Krishna and van Loosdrecht (1999), but smaller from the other simulation results.

Heterotrophic growth rate is 4 d^{-1} for filtered wastewater of F/M=0.07 and raw wastewater of F/M=0.05 while the value for filtered wastewater of F/M=0.2 is found to be 3 d^{-1}. μ_H for F/M=0.2 filtered wastewater is same as in the study of Koch *et al.* (2000). Other values range between 1.8 and 4.5 d^{-1}. Y_H is found to be 0.68 gCOD/gCOD for all wastewaters, which is higher than all of the values except in Koch *et al.* (2000). Storage yield coefficient, Y_{STO} is same for all wastewaters: 0.83 gCOD/gCOD. This value is between the range of 0.78 and 0.88 gCOD/gCOD, so calculated Y_{STO} is in good accordance with the literature.

There are three modified versions of ASM3 for simultaneous growth and storage models evaluated in this study; namely Model A, Model B and Model C. These models were simulated for tannery wastewater and compared with the models of Krishna and van Loosdrecht (1999) for acetate and Karahan-Gül *et al.* (2002b) for both acetate and glucose as presented in Table 8.21.

Endogenous decay rate, b_H was found to be 0.12 d^{-1} as in ASM1 and ASM3. This value is lower than the values of both of the models as it is in ASM3 because the value of 0.12 was adopted from the study of Orhon *et al.* (1999) and gave good results in the simulations. b_{STO} was found to be 0.2 d^{-1} for all of the models which is similar with the study of Krishna and van Loosdrecht (1999). But the values found by Karahan-Gül *et al.* (2002b) both for acetate (0.24 d^{-1}) and glucose (0.1 d^{-1}) differ from the value found in this study. k_H and K_X were found as 0.8 d^{-1} and 0.01 COD/COD respectively, which were not considered in the compared models.

Table 8.21 Comparison of simultaneous growth and storage modeling results

Parameter	Unit	Modified ASM3 (Krishna and van Loosdrecht, 1999)	Modified ASM3 (Karahan-Gül *et al.*, 2002b)		Model A	Model B	Model C
					This Study		
		acetate	acetate	glucose		tannery	
b_H	d^{-1}	0.2	0.24	0.2	0.12	0.12	0.12
b_{STO}	d^{-1}	0.2	0.24	0.1	0.2	0.2	0.2
k_H	d^{-1}	-	-	-	0.8	0.8	0.8
K_X	gCOD/gCOD	-	-	-	0.01	0.01	0.01
K_S	mg COD.l^{-1}	0.1	3	18	12	12	12
K_{STO}	mgl^{-1}	1	0.4	1	0.04	0.04	-
k_{STO}	d^{-1}	5	14	8	5.3	4.4	-
μ_{H1}	d^{-1}	4	4	2	0.75	0.77	0.70
μ_{H2}	d^{-1}	2	3	2.5	0.93	0.93	-
Y_{H1}	gCOD/gCOD	0.41*	0.65	0.67	0.67	0.67	0.67
Y_{H2}	gCOD/gCOD	0.57*	0.75	0.70	0.68	0.68	0.68
Y_{STO}	gCOD/gCOD	0.69*	0.80	0.90	0.83	0.83	0.83
k_{XSTO}	d^{-1}	-	-	-	-	-	15.6
q_S	d^{-1}	-	-	-	-	-	6.77

Substrate half saturation constant, K_S is determined as 12 mg COD.l^{-1}, which is very higher than the value (0.1 mg COD.l^{-1}) determined by Krishna and van Loosdrecht (1999). Karahan-Gül *et al* (2002b) calculated the values of 3 mg COD.l^{-1} for acetate and 18 mg/l for glucose, which are also not in accordance with this study. The rate of storage k_{STO} is estimated as 5.3 d^{-1} for Model A and 4.4 d^{-1} for Model B which are in perfect agreement with the rates reported by Krishna and van Loosdrecht (1999), however Karahan-Gül *et al* (2002b) found higher values as 14 d^{-1} and 8 d^{-1} for acetate and glucose respectively.

Two different heterotrophic growth rates were defined in Model A and Model B; for direct growth, μ_{H1} and for the growth on stored polymer, μ_{H2}, whereas there is only one μ_H in Model C for direct growth. Growth on storage polymers is defined with k_{XSTO} parameter, which is defined as PHB degradation rate coefficient in Model C. For Model A, μ_{H1} was found to be 0.65 d^{-1} and 0.9 d^{-1} for filtered wastewater of F/M=0.07 and 0.2 respectively; 0.7 d^{-1} for raw wastewater. In Model B, this value is 0.7 and 0.65 d^{-1} for filtered F/M=0.07 and raw, 0.9 d^{-1} for filtered F/M=0.2. In Model C, it is 0.65 d^{-1} for filtered F/M=0.07 and raw, 0.81 d^{-1} for filtered F/M=0.2. μ_{H2} is 1 d^{-1} for both of the models in the case of F/M=0.07 filtered and raw wastewater, whereas it is 0.8 d^{-1} for F/M=0.2. All of these values are smaller from the values found in the models of Krishna and van Loosdrecht (1999) and Karahan-Gül *et al* (2002b). This result is interpreted as a consequence of the possible differences in the composition of studied microbial communities.

As similar to heterotrophic growth rate, two different coefficients were defined for heterotrophic yield constants as Y_{H1} for direct growth and Y_{H2} for growth on X_{STO} in all of the models A, B and C. Y_{H1} is 0.67 gCOD/gCOD for three of the models which is same to the value of Karahan-Gül *et al.* (2002b) for glucose, acetate value is also similar. Krishna and van Loosdrecht (1999) adapted this Y_{H1} value from Beun *et al.* (2000) as 0.41 gCOD/gCOD which is very low. Y_{H2} value is found as 0.68 gCOD/gCOD, adapted value of Beun *et al.* (2000) is again lower, being 0.57 gCOD/gCOD, but the values of Karahan-Gül *et al.* (2002b) for both of the substrates are higher. Storage yield coefficient, Y_{STO} is estimated as 0.83 gCOD/gCOD. Beun *et al.* (2000) reported the same value as 0.69 gCOD/gCOD while Karahan-Gül *et al.* (2002b) calculated the values of 0.80 for acetate and 0.90 for glucose. The storage yield for tannery effluent is in agreement with the findings of Karahan-Gül *et al.* (2002b) when high VFA content of tannery wastewaters is concerned.

As previously explained, two new parameters were introduced in the modified Model C. These parameters are stored polymer consumption rate coefficient, k_{XSTO} and substrate uptake rate, q_S. k_{XSTO} is found to be 17 d^{-1} for filtered F/M=0.07, 9 d^{-1} for filtered F/M=0.2 and 21 d^{-1} for the experimental data of raw wastewater, whereas q_S values are estimated as 5.8 d^{-1} for filtered F/M=0.07, 8.5 d^{-1} for filtered F/M=0.2 and 6 d^{-1} for raw wastewater.

When the simulation results of five different models are compared, it can be concluded that the possibility of describing the real case increases as the model gets more detailed. A comparative representation of the modeling results obtained with five different models are presented in Figures 8.28, 8.29 and 8.30 for three sets of experiments with filtered F/M=0.07 and F/M=0.2 and raw wastewater (F/M=0.05), respectively. The modeling results of ASM3 show that the consumption of stored polymers has a considerable effect on the 2nd plateau (famine phase) observed in the OUR response in batch tests. When ASM1 is used to simulate OUR responses observed in batch tests at relatively low F/M ratios, in other words when the effect of hydrolysis is less dominant, the model cannot describe the higher OUR level of 2nd plateau. On the contrary, ASM3 results together with Models A and B, for the experiment with high F/M ratio clearly emphasizes the challenge in the definition of readily biodegradable COD, S_S.

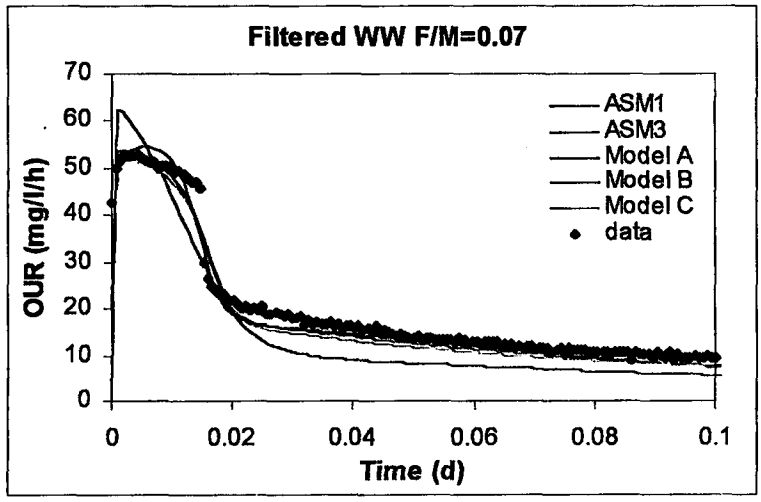

Figure 8.28 Comparison of the simulation results of five different models for Set 1

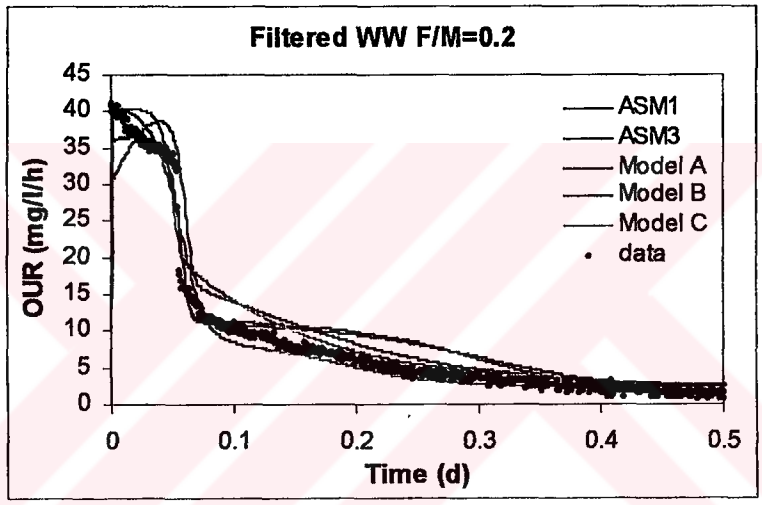

Figure 8.29 Comparison of the simulation results of five different models for Set 2

The results also point out that, the missing hydrolysis process in ASM3 and Models A, B and C, in other words the neglected soluble portion of slowly biodegradable COD, S_H, -as described in ASM1 adapted for tannery wastewaters (Orhon *et al.*, 1999)- can be compensated with the secondary growth process, when process kinetics are defined with first order rates with respect to X_{STO} concentration as seen in ASM3 and Model C. In other words, the low K_{STO} values estimated for Models A and B, 0.04 gCOD/gCOD cannot compensate with the neglected hydrolysis process in the 2nd plateau of OUR curves whereas ASM3 results, with higher K_{STO} coefficients, 0.33 gCOD/gCOD resemble first order kinetics as described in Model C.

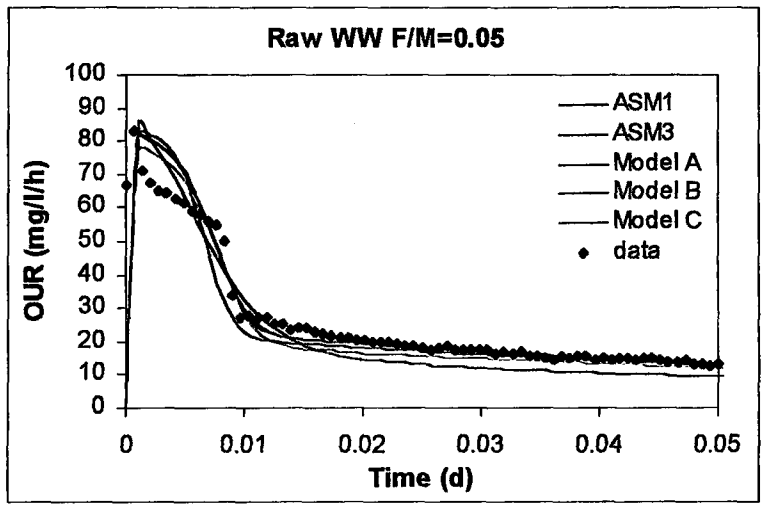

Figure 8.30 Comparison of the simulation results of five different models for Set 3

Although structured models can generally be regarded as the best interpretation to describe the dynamic behavior observed for tannery effluents, the insufficiency experienced in the experimental determination of all the storage products when complex substrate compositions are concerned, hinders the correct determination of model coefficients. Thus, when the case of experimental determination of model parameters are concerned Model C is favorable since storage polymers are considered as the excess substrate pool and therefore this model does not need the measurement of storage polymers.

It should be noted that although storage polymers (X_{STO}) for tannery wastewaters could not be measured experimentally, the modeling simulations for all of the four structured models involving substrate storage process were conducted to give approximately the same amounts of stored polymers (Figure 8.31).

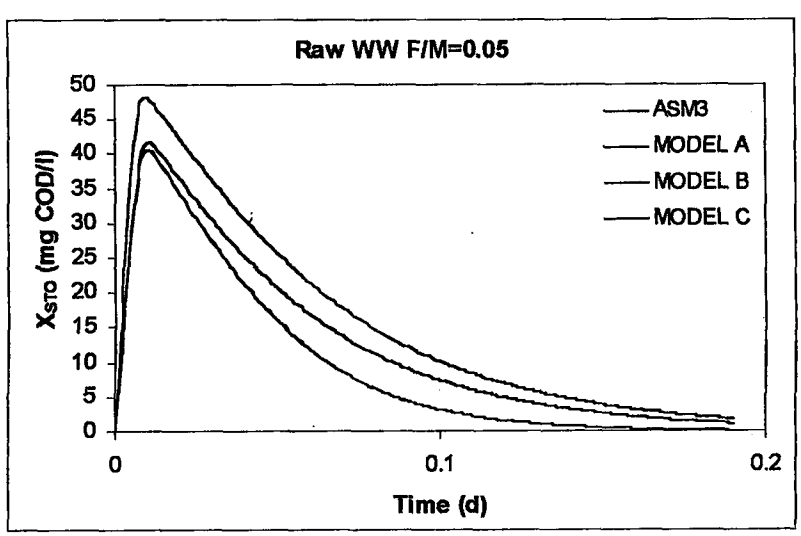

Figure 8.31 Comparison of the simulation results of stored polymer amounts

SECTION 9 CONCLUSIONS AND RECOMMENDATIONS

Activated sludge modeling has gained much importance with the urge for more specialized design for specific applications of biological treatment, such as nutrient removal, bulking sludge prevention and industrial wastewater treatment. The activated sludge models introduced by IAWQ Task Group have presented useful tools in the design and operation of activated sludge systems. ASM1 (Henze *et al.*, 1987) introduced a common language for computer modeling and with the improvement for bio-P removal, storage phenomena has been encountered in ASM2 and ASM2d (Henze *et al.*, 1995; 1999). Recently, Task Group introduced ASM3 (Gujer *et al.*, 2000), which emphasizes the importance of storage concept.

In activated sludge modeling, storage polymers have been neglected, without considering that they might have a significant role. However, activated sludge systems are highly dynamic with respect to their feeding patterns. Bacteria will have external substrate supply only for relatively short periods of time and will rapidly grow. The microorganisms would undergo long starvation periods without internally stored substrate. Bacteria that are able to store and consume this stored substrate will have a strong competitive advantage over the other organisms without the capacity of substrate storage. The significance of the storage polymers has been reported, especially for SBR processes more than continuously operated treatment plants.

In spite of a variety of model structures proposed for activated sludge systems, calibration of these models for industrial wastewaters still stands untouched. In this study, application and comparison of modeling using ASM1 and ASM3 for tannery wastewater has been handled. Additionally, ASM3 was extended and adapted for tannery effluent according to the simultaneous growth and storage concept. In literature, simultaneous growth and storage models were applied for acetate and glucose. There is no available research for the application of above-mentioned structured models for tannery wastewater. Therefore, comparison and evaluation of the results obtained for tannery wastewater in this study presents a conceptual

framework for the application of different structured models for industrial wastewaters.

The modeling results obtained in this study, in comparison with literature highlight the need for reliable estimation of model parameters with respect to each specific wastewater of concern. Model simulations conducted in this study were based on previous literature data obtained for tannery effluents. In this context, all the model simulations were based on the same endogenous decay rate and active heterotrophic biomass concentrations as one of the initial experimental conditions. The initial wastewater COD fractions were calculated based on the definitions in ASM1 and ASM3. Model simulation results for ASM1 were quite consistent with those given in literature.

ASM3 modeling results yielded a better description of the dynamic OUR response compared to ASM1. This result is obviously a consequence of the high amount of VFA content and prevailing transient conditions in batch experiments. When ASM3 simulation results are compared with the set of model coefficients reported in literature, it can be stated that lower process rates are estimated for tannery wastewaters, than those reported for different substrates, which are more biodegradable than tannery effluent. This result is interpreted as a consequence of the possible differences in the composition of studied microbial communities.

In addition to IAWQ Task Group Models ASM1 and ASM3 modified versions of ASM3 involving simultaneous growth and storage under dynamic conditions have also been investigated in the scope of this study.

When the simulation results of five different models are compared, it can be concluded that the possibility of describing the real case increases as the model gets more detailed. The results have shown that the hydrolysis process is less effective when batch tests with low F/M ratios are concerned but the calibration studies at high F/M ratios clearly emphasize the challenge in the definition of readily biodegradable COD. The results also point out that, the neglected OUR response due to the hydrolysis of soluble slowly biodegradable substrate can be compensated when first order kinetics is chosen to describe the growth response on storage polymers.

Although structured models can generally be regarded as the best interpretation to describe the dynamic behavior observed for tannery effluents, the insufficiency

experienced in the experimental determination of all the storage products when complex substrate compositions are concerned, hinders the correct determination of model coefficients. Thus, when the case of experimental determination of model parameters are concerned the adapted model considering substrate uptake could be used more effectively since this model does not need the measurement of storage polymers.

It should be noted that although storage polymers for tannery wastewaters could not be measured experimentally, the modeling simulations for all of the four structured models involving substrate storage process were conducted in this study. Approximately the same amounts of stored polymers were achieved. Thus, modeling results can be used as estimate values for the experimental determination of storage polymers.

It is recommended that the modeling studies conducted for structured models should be repeated with initial conditions applied for ASM1, in order to evaluate the effect of hydrolysis.

Further research should be conducted on the assessment of specific parameters of structured models for industrial wastewaters. The description of readily biodegradable substrate still needs additional experimental studies and the choice of definition on the readily biodegradable fraction of influent COD should be dealt with significant care and this choice should be made meticulously depending on the purpose of modeling application for industrial wastewaters.

REFERENCES

Andrews, J. F. and Busby, J. R., 1973. Dynamic modeling and control strategies for the activated sludge process. *Wat. Res.*, **8**, 261-289.

APHA, 1998. Standart methods for the enamination of water and wastewater. 20th edition, American Public Health Association, Washington, DC.

Ateş Genceli, E., 1997. Biological treatability and kinetic characterization of tannery industry wastewaters. *Ph.D. Thesis*, I.T.U. Institute of Science and Technology, Istanbul.

Avcıoğlu, E., Orhon, D. and Sözen, S., 1998. A new method for the assesment of heterotrophic endogenous respiration rate under aerobic and anoxic conditions. *Wat. Sci. Tech.*, **38**(8-9), 95-103.

Avcıoğlu, E., Karahan-Gül, Ö. and Orhon, D., 2002. Estimation of stoichiometric and kinetic coefficients of ASM3 under aerobic and anoxic conditions via respirometry. *Proceedings of Environmental Biotechnology Conference*, Palmerston, New Zealand, April 15-17.

Beun, J. J., Paletta, F., van Loosdrecht, M. C. M. and Heijnen, J. J., 2000. Stoichiometry and kinetics of poly-β-hydroxybutyrate metabolism in aerobic, slow growing, activated sludge cultures. *Biotechnol. Bioeng.* **67**(4), 379-389.

Beun, J. J., Dircks, K., van Loosdrecht, M. C. M. and Heijnen, J. J., 2001. Poly-β-hydroxybutyrate metabolism in dynamically fed mixed microbial cultures. *Wat. Res.*, **36**(5), 1167-1180.

Bishop, P. L., 1978. Physicochemical Pretreatment of Wastes from a secondary tannery. *Proceedings of the 33rd Industrial Waste Conference*, Purdue University, IN USA, May 9-11, pp. 64-72.

Brdjanovic, D., van Loosdrecht, M. C. M. Versteeg, P., Hooijmans, C. M., Alaerts G. J. and Heijnen, J. J., 2000. Modelling COD, N and P removal in a full-scale WWTP Haarlem Waarderpolder. *Wat. Res.*, **34**(3), 846-858.

Cech, J. S. and Chudoba, J., 1983. Influence of accumulation capacity of activated sludge microorganisms on kinetics of glucose removal, *Wat. Res.*, **17** (6), 659-666.

Cech, J. S., Hartman, P. and Macek, M., 1994. Bacteria and protozoa population dynamics in biological phosphate removal systems. *Wat. Sci. Tech.*, **29**(7), 109-117.

Cheda, P. V., Mandlekar, U. V., Handa, B. K., Khanna, P., 1984. Joint wastewater management for a cluster of Tanneries at Kanpur. *Proceedings of the 39th Industrial Waste Conference*, Purdue University, IN USA, pp. 151-162.

Chudoba, J., Grau, P. and Ottova, V., 1973. Control of activated sludge filamentous bulking-II Selection of microorganisms by means of a selector. *Wat. Res.* 7, 1389-1406.

Chudoba, J., Cech, J. S., Farkac, J. and Grau, P , 1985. Control of activated sludge filamentous bulking- experimental verification of a kinetic selection theory. *Wat. Res.* **19**, 191-196.

Daigger, G. T. and Grady, C. P. L. Jr., 1982a. The dynamics of microbial growth on soluble substrates, a unifying theory, *Wat. Res.*, **16**, 365-382.

Daigger, G. T. and Grady, C. P. L. Jr., 1982b. An assesment of the role of physiological adaptation in the transient response of bacterial cultures. *Biotechnol. Bioeng.*, **24**, 1427-1444.

Dircks, K., Pind, P. F., Mosbaek, H., and Henze, M., 1999. Yield determination by respirometry–The possible influence of storage under aerobic conditions in activated sludge. *Water SA.* **25**(1), 69-74.

Dircks, K., Beun, J. J., van Loosdrecht, M., Heijnen, J. J. and Henze, M. 2001. Glycogen metabolism in aerobic mixed cultures. *Biotech. Bioeng.*, **73**(2), 85-94.

Dold, P. L., Ekama, G. A. and Marais, G. v. R., 1980. A general model for the activated sludge process. *Prog. Wat. Tech.*, **12**, 47-77.

Dold, P. L., Ekama, G. A. and Marais, G. v. R., 1986. Evaluation of the activated sludge model proposed by the IAWPRC Task Group, *Wat. Sci. Tech.*, **18** (6), 63-90.

Ekama, G. A. and Marais, G, v. R., 1979. Dynamic behaviour of the activated sludge process. *Journal WPCF,* **51**(3), 534-556.

Ekama, G. A., Dold, P. L. and Marais, G. v. R., 1986. Procedures for determining influent COD fractions and maximum specific growth rate of heterotrophs in activated sludge systems. *Wat. Sci. Tech.*, **18**(6), 91-114.

Gabb, D. M. D., Still, D. A., Ekama, G. A., Jenkins, D. and Marais, G. v. R., 1991. the selector effect on filamentous age activated sludge systems. *Wat. Sci. Tech.*, **23**(4-6), 867-877.

Germirli, F., Orhon, D. and Artan, N., 1991. Assessment of the initial inert soluble COD in industrial wastewaters. *Wat. Sci. Tech.*, **23**(4-6), 1077-1086.

Grady, C. P. L. Jr., Smets, B. F. and Barbeu, D. S., 1996. Variability in Kinetic parameter estimates: a review of possible causes and proposed terminology. *Wat. Res.*, **30**(3), 742-748.

Grau, P., Chudoba, J. and Dohanyos, J., 1982. Theory and practice of accumulation-regeneration approach to control of activated sludge filamerntous bulking. In: *Bulking of activated sludge. Preventive and remedial methods,* Chambers, B. And Tomlinson J. (eds), Ellis Horward Publ., Chichester, 111-127.

Gujer, W. and Henze, M., 1991. Activated sludge modeling and simulation. *Wat. Sci. Tech.*, **23**(4-6), 1011-1023.

Gujer, W., Henze, M., Takashi, M. and van Loosdrecht, M. C. M., 2000. Activated Sludge Model No.3. In: *Activated Sludge Models ASM1, ASM2, ASM2D and ASM3*, Henze, M., Gujer, W., Mino, T., van Loosdrecht, M. (eds.) IWA Scientific and Technical Report No.9. IWA London. ISBN: 1 900222 24 8.

Harder, A. and Roels, J. A., 1982. Application of simple structured models in bioengineering. *Adv. Biochem. Eng.* **21**, 56-107.

Hatziconstantinou, G. J. and Andreadakis, A. D., 1996. Uptake and storage of soluble carbon under transient conditions in preDN activated sludge reactors. *IAWQ Conference on Sequencing Batch Technology (Preprint), Munich, Germany.* March 18-20, 123-131.

Heijnen, J. J., 1994. Thermodynamics of microbial growth and its implications for process design. *Tibtech*, **12**, 483-492.

Hellinga, C., van Loosdrecht, M. C. M. and Heijnen, J. J., 1999. Model based designed of a novel process for ammonia removal from concentrated flow. *Mathematical and Computer Modeling of Dynamic Systems*, **5**(4), 351-371.

Henze, M., Grady, C. P. L. jr., Gujer, W., Marais, G. v. R. and Matsuo, T., 1987. Activated Sludge Model No:1 IAWPRC Scientific and Technical report. No.1, IAWPRC, London.

Henze, M., Grady, C. P. L. jr., Gujer, W., Marais, G. v. R. and Matsuo, T., 1987. A general model for single-sludge wastewater treatment systems, *Wat. Res.*, **21** (5), 505-515.

Henze, M., 1992. Characterization of wastewater modelling of activated sludge processes. *Wat. Sci. Tech.*, **25** (6), 1-15.

Henze, M., Gujer, W., Mino, T., Matsuo, T., Wentzel, M. C. and Marais, G. v. R., 1995. Activated Sludge Model No.2. IAWPRC Scientific and Technical Report No.2, IAWQ, London.

Huber, C. V. and Jones, G. E., 1974. Combined treatment of leather tanning and municipal waste at Grand Haven, Michigan. *Proceedings of the 29th Industrial Waste Conference*, Purdue University, IN USA, May 7-9, pp. 608-616.

Huber, C. V. and Doane, 1980. A case study- Tannery meets EPA Pretreatment Standarts. *Proceedings of the 35th Industrial Waste Conference*, Purdue University, IN USA, pp. 95-104.

ISO, 1986. Water Quality – Determination of the chemical oxygen demand. Ref.No. ISO 6060-1986.

Kabdaşlı, I., Tünay, O. and Orhon, D., 1993. The treatability of chromium tannery wastewaters. *Wat. Sci. Tech.*, **28**(2), 97-105.

Kalender, A., 1981. Deri sanayi sıvı atıklarının aktif çamur metodu ile tasfiyesinin kinetiği üzerine bir araştırma. (*In Turkish*). Ph.D. Thesis, Istanbul Technical University, Turkey.

Kappeler, J. and Gujer , W., 1992. Estimation of kinetic parameters of heterotrophic biomass under aerobic conditions and characterization of wastewater for activated sludge modeling. *Wat. Sci. Tech.*, **25**(6), 125-140.

Karahan-Gül, Ö., Artan, N., Orhon, D., Henze, M. and van Loosdrecht, M. C. M., 2002a. Respirometric assessment of storage yield for different substrates. *Wat. Sci. Tech.*, **46**(1-2), 345-352.

Karahan-Gül, Ö., van Loosdrecht, M. C. M. and Orhon, D., 2002b. Modification of activated sludge model No.3 considering direct growth on primary substrate. *Proceedings of IWA 3rd World Water Congress*, Melbourne, Australia, April 7-12.

Kaul, S. N. and Szpyrkowicz, L., 1996. Biological processes as a pretreatment for electrochemical oxidation- A case study for Clusterof Tanneries from a common effluent treatment plant. *2nd specialized conference on pretreatment of industrial wastewaters*. Athens, Greece, October 16-18.

Koch, G., Kühni, M., Gujer W. and Siegrist, H., 2000. Calibration and validation of activated sludge model No.3 for Swiss municipal wastewater. *Wat. Res.*, **34**(14), 3580-3590.

Kompala, D. S., Ramkrishna, D. and Tsao G. T., 1984. Cybernetic modeling of microbial growth on multiple substrates. *Biotech. Bioeng.* **26**, 1272-1281.

Krishna, C. and van Loosdrecht, M. C. M., 1999a. Effect of temperature on storage polymers and settleability of activated sludge. *Wat. Res.*, **33**(10), 2374-2382.

Krishna, C. and van Loosdrecht, M. C. M., 1999b. Substrate flux into storage and growth in relation to activated sludge modeling. *Wat. Res.*, **33**(14), 3149-3161.

Levenspiel, O., 1972. Chemical reaction engineering. John Wiley & Sons, Inc., Canada.

Liu, W. T., Mino, T., Nakamura, K. and Matsuo, T., 1994. Role of glycogen in acetate uptake and polyhydroxybutyrate synthesis in anaerobic aerobic activated sludge with minimized polyphosphate content. *J. Ferment. Bioeng.*, **77**, 535-540.

Majone, M., Massanisso, P., Carucci, A., Lindrea, K. and Tandoi, V., 1996. Influence of storage on kinetic selection to control aerobic filamenteous bulking. *Wat. Sci. Tech.*, **34**(5-6), 223-232.

Majone, M., Dircks, K. and Beun, J., J., 1999. Aerobic storage under dynamic conditions in activated sludge processes. The state of art. *Wat. Sci. Tech.*, **39**(1), 61-73.

Matsuzawa, Y. and Mino, T., 1991. Role of glycogen as an intracellular carbon reserve of activated sludge in the competitive growth of filamentous and non- filamentous bacteria. *Wat. Sci. Tech.*, **23**(4-6), 899-905.

Meijer, S C. F., van Loosdrecht, M. C. M. and Heijnen, J. J., 2001. Metabolic Modeling of full-scale biological nitrogen and phosphorus removing WWTP's. *Wat. Res.*, **35**(11), 2711-2723.

Moussa, M., S., Rojas, A., R., Hooijmans, C., M., van Loosdrecht, M. C .M. and Gijzen, H., J., 2001. Model-based evaluation of the upgrading of a full-scale industrial wastewater treatment plant. *Wat. Sci. Tech.*, (*submitted*).

Nemerow, N. L., Warne, D. and Falk, F., 1978. A new and effective solution for treatment of tannery wastewaters. *Proceedings of the 33rd Industrial Waste Conference*, Purdue University, IN USA, May 9-11, pp. 596-603.

Novak, L., Larrea, L. and Wanner, J., 1995. Mathematical model for soluble carbonaceous substrate biosorption. *Wat. Sci. Tech.*, **31**(2), 67-77.

O' Connor, J.T., 1972. Environmental engineering unit operations and unit process laboratory manual, Association of Environmental Engineering Professors.

Orhon, D. and Artan, N., 1994. Modelling of Activated Sludge Systems. Technomic Press, Lancester, PA.

Orhon, D. and Çokgör E. U., 1997. COD Fractionation in wastewater characterization- the state of art, *J. Chem. Tech. Biotechnol.*, **68**, 294-302.

Orhon, D., Ubay Çokgör, E. and Sözen, S., 1998. Dual hydrolysis model of the slowly biodegradable substrate in activated sludge systems. *Biotechnology Techniques*, **12**(10), 737-741.

Orhon, D., 1999. Aktif çamur sistemlerinde proses stokiyometrisi ve dönüşüm oranı kavramı. (*In Turkish*) *Su Kirlenmesi Kontrolü Dergisi*, **9** (1), 35-45.

Orhon, D., Ateş Genceli, E. and Ubay Çokgör, E., 1999. Characterization and Modeling of Activated Sludge for Tannery Wastewater. *Water Environment Research*, **71**(1), 50-63.

Orhon, D., Karahan, Ö. and Sözen, S., 1999. The effect of residual microbial products on the experimental assesment of the particulate inert COD in wastewaters. *Wat. Res.*, **33**(14), 3191-3203.

Orhon, D., Ubay Çokgör, E. and Sözen, S., 1999. Experimental basis for the hydrolysis of slowly biodegradable substrate in different wastewaters. *Wat. Sci. Tech.*, **39**(1), 87-95.

Padukone, N. and Andrews, G. F., 1989. A simple, conceptual mathematical model for the activated sludge process and its variants. *Wat. Res.* **23**(12), 1535-1543.

Parker, C. E., 1970. Biological treatment of spent vegetable tannins. *Proceedings of the 25th Industrial Waste Conference*, Purdue University, IN USA, pp. 678-686.

Pot, M., van Leeuwen, M. A., van Loosdrecht M. C. M. and Heijnen, J. J., 1996a. Kinetic modeling of polyhydroxybutyrate production and consumption by *Thiosphaera pantotropha* under dynamic substrate supply. *Biotech. Bioeng.* (*submitted*).

Pot, M., van Loosdrecht M. C. M. and Heijnen, J. J., 1996b. Effect of substrate addition on polymer storage in nitrification/denitrification SBR processes. *Wat. Res.* (*submitted*).

Reichert, P., Ruchti, J. and Simon, W., 1998. Aquasim 2.0 Swiss Federal Institute for Environmental Science and Technology (EAWAG), CH-8600 Duebendorf, Switzerland.

Roels, J., A., 1983. Energetics and kinetics in biotechnology. Elsevier Biomedical Press, Amsterdam.

Rojas, A., R., 2001. Computer modeling of an activated sludge wastewater treatment plant treating tannery wastewater. M.Sc. thesis, Delft University, The Netherlands.

Smolders, G. J. F., van Loosdrecht M. C. M. and Heijnen, J. J., 1995. A metabolic model for the biological phosphorus removal process. *Wat. Sci. Tech.*, **31**(2), 79-93.

Şengül, F. and Gürel, O., 1993. Pollution profile of leather ındustries waste characterization and pretreatment of pollutants. *Wat. Sci. Tech.*, **28**(2), 87-97.

Talınlı, İ., 1994. Pretreatment of tannery wastewaters. *Wat. Sci. Tech.*, **29**(9), 175-178.

Thackston, E. L., 1973. Secondary treatment of wastes from an alum tannery. *Proceedings of the 28th Industrial Waste Conference*, Purdue University, IN USA, pp. 881-893.

Turner, B. G. and Ramkrishna D., 1988. Revised enzyme synthesis rate expression in cybernetic models of bacterial growth. *Biotech. Bioeng.* **31**, 41-43.

Tünay, O., Orhon, D. and Kabdaşlı, I., 1994. Pretreatment requirements for leather tanning industry wastewaters. *Wat. Sci. Tech.*, **32**(12), 121-128

Ubay Çokgör, E., 1997. Respirometric evaluation of process kinetic and stoichiometry for aerobic systems. *Ph.D. thesis*, I.T.U. Institute of Science and Technology, Istanbul.

Ubay Çokgör, E., Sözen, S., Orhon, D. and Henze, M., 1998. Respirometric analysis of activated sludge behaviour I. Assessment of the readily biodegradable substrate. *Wat. Res.*, **32**(2), 461-475

van Aalst-van Leeuwen, M. A., Pot, M. A., van Loosdrecht, M. C. M. and Heijnen, J. J., 1997. Kinetic modeling of poly (ß-hydroxybutyrate) production and consumption by P. P. under dynamic substrate supply. *Biotech. Bioeng.*, **55**(5), 773-782.

van Loosdrecht, M. C .M., Pot, M. A. and Heijnen, J. J., 1997. Importance of bacterial storage polymers in bioprocesses. *Wat. Sci. Tech.*, **35**(1), 41-47.

van Loosdrecht, M. C .M., and Henze, M., 1999. Maintenance, endogenous respiration, lysis, decay and predation. *Wat. Sci. Tech.*, **39**, 107-118.

van Loosdrecht, M. C .M., and Heijnen, J. J., 2002. Modeling of activated sludge processes with structured biomass. *Wat. Sci. Tech.*, **45** (6), 13-23.

van den Eynde, E., Geerts, J., Maes, B. and Verachtert, H., 1983. Influence of the feeding pattern on the glucose metabolism of *Arthrobacter Sp.* and

Sphaerotilus Natans, growing in chemostat culture, simulating activated sludge bulking. *European J. Appl. Microbiol. Biotechnol.*, **17**, 35-43.

van den Eynde, E., Vriens, L., Wynants, M. and Verachtert, H., 1984. Transient behaviour and time aspects of intermittently and continuously fed bacterial cultures with regard to filamentous bulking of activated sludge. *Applied Microbiology Biotechnology,* **19**, 44-52.

Zevenhuizen, L., P., T., M. and Ebbink, A., G., 1974. Interrelations between glycogen, poly-β-hydroxybutyric acid and lipids during accumulation and subsequent utilization in a Pseudomonas. *Antonie van Leeuwenhoek*, **40**, 103-120.

APPENDIX A

Derivations of the rate equations

ASM3 adapted for tannery wastewater

$Y_H = Y_{H1} = Y_{H2}$

- $-r_{S,C} = \frac{1}{Y_{STO}} r_{STO,P}$

$$-r_{S,C} = \frac{1}{Y_{STO}} Y_{STO} k_{STO} \frac{S_O}{K_O + S_O} \frac{S_S}{K_S + S_S} X_H$$

$$-r_{S,C} = k_{STO} \frac{S_O}{K_O + S_O} \frac{S_S}{K_S + S_S} X_H$$

- $r_{STO,C} = \frac{1}{Y_H} r_{X,P}$

$$r_{STO,C} = \frac{1}{Y_H} \mu_H \frac{S_O}{K_O + S_O} \frac{X_{STO}/X_H}{K_{STO} + X_{STO}/X_H} X_H$$

- $r_{X,P} = Y_H r_{STO,C}$

$$r_{X,P} = Y_H \frac{\mu_H}{Y_H} \frac{S_O}{K_O + S_O} \frac{X_{STO}/X_H}{K_{STO} + X_{STO}/X_H} X_H$$

$$r_{X,P} = \mu_H \frac{S_O}{K_O + S_O} \frac{X_{STO}/X_H}{K_{STO} + X_{STO}/X_H} X_H$$

- $r_{STO,P} = Y_{STO}\, r_{S,C}$

$$r_{STO,P} = Y_{STO} k_{STO} \frac{S_O}{S_O + K_O} \frac{S_S}{K_S + S_S} X_H$$

ASM3 based model proposed by Krishna and van Loosdrecht (1999) adapted for tannery wastewater (Model A)

FEAST

- $$-r_{S,C} = \frac{1}{Y_{H1}} r_{X,P1} + \frac{1}{Y_{STO}} r_{STO,P}$$

$$-r_{S,C} = \frac{\mu_{H1}}{Y_{H1}} \frac{S_O}{K_O + S_O} \frac{S_S}{K_S + S_S} X_H + \frac{Y_{STO}}{Y_{STO}} k_{STO} \frac{S_O}{K_O + S_O} \frac{S_S}{K_S + S_S} X_H$$

$$r_{S,C} = \left[k_{STO} + \frac{\mu_{H1}}{Y_{H1}} \right] \frac{S_O}{K_O + S_O} \frac{S_S}{K_S + S_S} X_H$$

- $$r_{X,P1} = Y_{H1} r_{S,C} - \frac{Y_{H1}}{Y_{STO}} r_{STO,P}$$

$$r_{X,P1} = Y_{H1} \left(k_{STO} \frac{S_O}{K_O + S_O} \frac{S_S}{K_S + S_S} X_H + \frac{\mu_{H1}}{Y_{H1}} \frac{S_O}{K_O + S_O} \frac{S_S}{K_S + S_S} X_H \right)$$
$$- Y_{H1} \left(k_{STO} \frac{S_O}{K_O + S_O} \frac{S_S}{K_S + S_S} X_H \right)$$

$$r_{X,P1} = \mu_{H1} \frac{S_O}{S_O + K_O} \frac{S_S}{K_S + S_S} X_H$$

- $$r_{STO,P} = Y_{STO} r_{S,C} - \frac{Y_{STO}}{Y_{H1}} r_{X,P1}$$

$$r_{STO,P} = Y_{STO} \left(k_{STO} \frac{S_O}{K_O + S_O} \frac{S_S}{K_S + S_S} X_H + \frac{\mu_{H1}}{Y_{H1}} \frac{S_O}{K_O + S_O} \frac{S_S}{K_S + S_S} X_H \right)$$
$$- \frac{Y_{STO}}{Y_{H1}} \left(\mu_{H1} \frac{S_O}{K_O + S_O} \frac{S_S}{K_S + S_S} X_H \right)$$

$$r_{STO,P} = Y_{STO} k_{STO} \frac{S_O}{K_O + S_O} \frac{S_S}{K_S + S_S} X_H$$

FAMINE

- $$r_{X,P2} = Y_{H2} r_{STO,C}$$

$$r_{X,P2} = Y_{H2} \frac{\mu_{H2}}{Y_{H2}} \frac{S_O}{K_O + S_O} \frac{K_S}{K_S + S_S} \frac{X_{STO}/X_H}{K_{STO} + X_{STO}/X_H} X_H$$

$$r_{X,P2} = \mu_{H2} \frac{S_O}{K_O + S_O} \frac{K_S}{K_S + S_S} \frac{X_{STO}/X_H}{K_{STO} + X_{STO}/X_H} X_H$$

- $r_{STO,C} = -\frac{1}{Y_{H2}} r_{X,P2}$

$$r_{STO,C} = -\frac{1}{Y_{H2}} \mu_{H2} \frac{S_O}{K_O + S_O} \frac{K_S}{K_S + S_S} \frac{X_{STO}/X_H}{K_{STO} + X_{STO}/X_H} X_H$$

$$r_{STO,C} = \frac{\mu_{H2}}{Y_{H2}} \frac{S_O}{K_O + S_O} \frac{K_S}{K_S + S_S} \frac{X_{STO}/X_H}{K_{STO} + X_{STO}/X_H} X_H$$

ASM3 based model proposed by Karahan-Gül *et al.* (2002b) adapted for tannery wastewater (Model B)

FEAST

- $-r_{S,C} = \frac{1}{Y_{H1}} r_{X,P1} + \frac{1}{Y_{STO}} r_{STO,P}$

$$-r_{S,C} = \frac{1}{Y_{H1}} (\mu_{H1} \frac{S_O}{K_O + S_O} \frac{S_S}{K_S + S_S} X_H) + \frac{1}{Y_{STO}} (k_{STO} \frac{S_O}{K_O + S_O} \frac{S_S}{K_S + S_S} X_H)$$

$$r_{S,C} = \left[\frac{k_{STO}}{Y_{STO}} + \frac{\mu_{H1}}{Y_{H1}} \right] \frac{S_O}{K_O + S_O} \frac{S_S}{K_S + S_S} X_H$$

- $r_{X,P1} = Y_{H1} r_{S,C} - \frac{Y_{H1}}{Y_{STO}} r_{STO,P}$

$$r_{X,P1} = Y_{H1} (\frac{k_{STO}}{Y_{STO}} \frac{S_O}{K_O + S_O} \frac{S_S}{K_S + S_S} X_H + \frac{\mu_{H1}}{Y_{H1}} \frac{S_O}{K_O + S_O} \frac{S_S}{K_S + S_S} X_H)$$
$$- \frac{Y_{H1}}{Y_{STO}} (k_{STO} \frac{S_O}{K_O + S_O} \frac{S_S}{K_S + S_S} X_H)$$

$$r_{X,P1} = \mu_{H1} \frac{S_O}{S_O + K_O} \frac{S_S}{K_S + S_S} X_H$$

- $r_{STO,P} = Y_{STO} r_{S,C} - \frac{Y_{STO}}{Y_{H1}} r_{X,P1}$

$$r_{STO,P} = {}_{YSTO} (\frac{k_{STO}}{Y_{STO}} \frac{S_O}{K_O + S_O} \frac{S_S}{K_S + S_S} X_H + \frac{\mu_{H1}}{Y_{H1}} \frac{S_O}{K_O + S_O} \frac{S_S}{K_S + S_S} X_H)$$
$$- \frac{Y_{H1}}{Y_{STO}} (k_{STO} \frac{S_O}{K_O + S_O} \frac{S_S}{K_S + S_S} X_H)$$

$$r_{STO,P} = k_{STO} \frac{S_O}{K_O + S_O} \frac{S_S}{K_S + S_S} X_H$$

FAMINE

- $r_{X,P2} = Y_{H2}\, r_{STO,C}$

$$r_{X,P2} = Y_{H2} \frac{\mu_{H2}}{Y_{H2}} \frac{S_O}{K_O + S_O} \frac{K_S}{K_S + S_S} \frac{X_{STO}/X_H}{K_{STO} + X_{STO}/X_H} X_H$$

$$r_{X,P2} = \mu_{H2} \frac{S_O}{K_O + S_O} \frac{K_S}{K_S + S_S} \frac{X_{STO}/X_H}{K_{STO} + X_{STO}/X_H} X_H$$

- $r_{STO,C} = -\frac{1}{Y_{H2}} r_{X,P2}$

$$r_{STO,C} = -\frac{1}{Y_{H2}} \mu_{H2} \frac{S_O}{K_O + S_O} \frac{K_S}{K_S + S_S} \frac{X_{STO}/X_H}{K_{STO} + X_{STO}/X_H} X_H$$

$$r_{STO,C} = \frac{\mu_{H2}}{Y_{H2}} \frac{S_O}{K_O + S_O} \frac{K_S}{K_S + S_S} \frac{X_{STO}/X_H}{K_{STO} + X_{STO}/X_H} X_H$$

Model proposed by van Loosdrecht and Heijnen (2002) adapted for tannery wastewater in ASM3 terms (Model C)

FEAST

- $-r_{S,C} = \frac{1}{Y_{H1}} r_{X,P1} + \frac{1}{Y_{STO}} r_{STO,P}$

$$-r_{S,C} = \frac{1}{Y_{H1}} (\mu_H \frac{S_O}{K_O + S_O} \frac{S_S}{K_S + S_S} X_H) + \frac{1}{Y_{STO}} [\, Y_{STO} q_S \frac{S_O}{K_O + S_O} \frac{S_S}{K_S + S_S} X_H$$
$$- \frac{Y_{STO}}{Y_{H1}} \mu_H \frac{S_O}{K_O + S_O} \frac{S_S}{K_S + S_S} X_H \,]$$
$$r_{S,C} = q_S \frac{S_O}{K_O + S_O} \frac{S_S}{K_S + S_S} X_H$$

- $r_{X,P1} = Y_{H1} r_{S,C} - \frac{Y_{H1}}{Y_{STO}} r_{STO,P}$

$$-r_{X,P1} = Y_{H1} (q_S \frac{S_O}{K_O + S_O} \frac{S_S}{K_S + S_S} X_H) - \frac{Y_{H1}}{Y_{STO}} [\, Y_{STO} q_S \frac{S_O}{K_O + S_O} \frac{S_S}{K_S + S_S} X_H$$
$$- \frac{Y_{STO}}{Y_{H1}} \mu_H \frac{S_O}{K_O + S_O} \frac{S_S}{K_S + S_S} X_H \,]$$

$$r_{X,P1} = \mu_H \frac{S_O}{S_O + K_O} \frac{S_S}{K_S + S_S} X_H$$

- $$r_{STO,P} = Y_{STO} r_{S,C} - \frac{Y_{STO}}{Y_{H1}} r_{X,P1}$$

$$r_{STO,P} = Y_{STO}\left(q_S \frac{S_O}{K_O + S_O} \frac{S_S}{K_S + S_S} X_H \right) - \frac{Y_{STO}}{Y_{H1}}\left(\mu_H \frac{S_O}{K_O + S_O} \frac{S_S}{K_S + S_S} X_H \right)$$

$$r_{STO,P} = \left[q_S - \frac{\mu_H}{Y_{H1}} \right] Y_{STO} \frac{S_O}{S_O + K_O} \frac{S_S}{K_S + S_S} X_H$$

FAMINE

- $$r_{X,P2} = Y_{H2} r_{STO,C}$$

$$r_{X,P2} = Y_{H2} k_{X_{STO}} \frac{S_O}{K_O + S_O} \frac{K_S}{K_S + S_S} \frac{X_{STO}}{X_H} X_H$$

- $$r_{STO,C} = -\frac{1}{Y_{H2}} r_{X,P2}$$

$$r_{STO,C} = -\frac{1}{Y_{H2}} (Y_{H2} k_{X_{STO}} \frac{S_O}{K_O + S_O} \frac{K_S}{K_S + S_S} \frac{X_{STO}}{X_H} X_H)$$

$$r_{STO,C} = k_{X_{STO}} \frac{S_O}{K_O + S_O} \frac{K_S}{K_S + S_S} \frac{X_{STO}}{X_H} X_H$$

APPENDIX B

An Example of Aquasim System Definitions

ASM3 adapted for tannery wastewater

****
AQUASIM Version 2.0 (win/mfc) - Listing of System Definition
****
Date and time of listing: 04/14/2003 00:49:25
****
Variables
****

Aer_coef: Description: Aeration Coefficient
Type: Constant Variable
Unit:
Value: 1000
Standard Deviation: 1
Minimum: 0
Maximum: 1000
Sensitivity Analysis: inactive
Parameter Estimation: inactive

---

b_H: Description: Kin. par.
Type: Formula Variable
Unit: 1/d
Expression: 0.12

---

b_STO: Description: Kin. par.
Type: Formula Variable
Unit: 1/d
Expression: 0.2

---

f_e_s: Description: Stoic. par
Type: Constant Variable
Unit:
Value: 0.1
Standard Deviation: 1
Minimum: 0
Maximum: 10
Sensitivity Analysis: inactive
Parameter Estimation: inactive

f_e_x: Description: Stoic. par.
Type: Constant Variable
Unit:
Value: 0.2
Standard Deviation: 1
Minimum: 0
Maximum: 10
Sensitivity Analysis: inactive
Parameter Estimation: inactive

InCOD: Description: Inf. COD
Type: Formula Variable
Unit: mg/l
Expression: 2550

---

k_H: Description: Kinetic par.
Type: Formula Variable
Unit: 1/d
Expression: 0.8

K_O2: Description: Kin. par.
Type: Constant Variable
Unit: gO/m3
Value: 0.2
Standard Deviation: 1
Minimum: 0
Maximum: 10
Sensitivity Analysis: inactive
Parameter Estimation: inactive

K_S: Description: Kin.par.
Type: Constant Variable
Unit: mg/l
Value: 12
Standard Deviation: 1
Minimum: 0
Maximum: 40
Sensitivity Analysis: inactive
Parameter Estimation: inactive

K_STO: Description: Kin. par.
Type: Constant Variable
Unit:
Value: 0.3
Standard Deviation: 1
Minimum: 0
Maximum: 10
Sensitivity Analysis: inactive
Parameter Estimation: inactive

---

k_STO: Description: Kin. par.
Type: Formula Variable
Unit: 1/d
Expression: 7

K_X: Description: Kin. par.
Type: Formula Variable
Unit:
Expression: 0.01

---

mue_H: Description: Kin. par.
Type: Formula Variable
Unit: 1/d
Expression: 4

OUR: Description: Oxygen Uptake Rate
Type: Formula Variable
Unit: mg/l/h
Expression: (((1-Y_STO)*(k_STO*(S_O2/(K_O2+S_O2)))
*(S_S/(K_S+S_S))*X_H)+(((1-Y_H)/Y_H)
mue_H(S_O2/(K_O2+S_O2))
*((X_STO/X_H)/(K_STO+(X_STO/X_H)))*X_H)
+((1-f_e_s-f_e_x)*b_H*(S_O2/(K_O2+S_O2))*X_H)
+(b_STO*(S_O2/(K_O2+S_O2))*X_STO))/24

OURdata: Description:
Type: Real List Variable
Unit:
Argument: time
Standard Deviations: global
Rel. Stand. Deviat.: 0
Abs. Stand. Deviat.: 1
Minimum: 0
Maximum: 1e+009
Interpolation Method: linear interpolation
Sensitivity Analysis: inactive
Real Data Pairs (316 pairs):

-0.052083333	8.7648382
-0.051388889	7.9753085
-0.050694444	9.5543678
-0.05	8.647468
-0.049305556	8.5087707
.	.
.	.
0.16388889	5.9214722
0.16458333	5.2999825
0.16527778	5.9214722
0.16597222	6.1188547
0.16666667	5.4973649

OURenddec: Description: Oxygen Uptake Rate
Type: Formula Variable
Unit: mg/l/h
Expression: ((1-f_e_s-f_e_x)*b_H*(S_O2/(K_O2+S_O2))*X_H)/24

OURendPHA: Description: Oxygen Uptake Rate
Type: Formula Variable
Unit: mg/l/h
Expression: (b_STO*(S_O2/(K_O2+S_O2))*X_STO)/24

OURgrowth: Description: Oxygen Uptake Rate
Type: Formula Variable
Unit: mg/l/h
Expression: (((1-Y_H)/Y_H)*mue_H*(S_O2/(K_O2+S_O2))
*((X_STO/X_H)/(K_STO+(X_STO/X_H)))*X_H)/24

OURstorage: Description: Oxygen Uptake Rate
Type: Formula Variable
Unit: mg/l/h
Expression: (((1-Y_STO)*(k_STO*(S_O2/(K_O2+S_O2)))
*(S_S/(K_S+S_S))*X_H))/24

S_I: Description: Sol. inert COD
Type: Dyn. Volume State Var.
Unit: gCOD/m3
Relative Accuracy: 1e-006
Absolute Accuracy: 1e-006

S_O2: Description: Dis. oxygen
Type: Dyn. Volume State Var.
Unit: gO/m3
Relative Accuracy: 1e-006
Absolute Accuracy: 1e-006

S_O2SAT: Description: Sat.oxy.
Type: Constant Variable
Unit: mg/l
Value: 10
Standard Deviation: 1
Minimum: 0
Maximum: 10
Sensitivity Analysis: inactive
Parameter Estimation: inactive

S_P: Description: Conc.
Type: Dyn. Volume State Var.
Unit: gCOD/m3
Relative Accuracy: 1e-006
Absolute Accuracy: 1e-006

S_S: Description: Readily biodegr.COD
Type: Dyn. Volume State Var.
Unit: gCOD/m3
Relative Accuracy: 1e-006
Absolute Accuracy: 1e-006

Temparature: Description: Temp.
Type: Constant Variable
Unit: C
Value: 20
Standard Deviation: 1
Minimum: 0
Maximum: 20
Sensitivity Analysis: inactive
Parameter Estimation: inactive

---

time: Description: t
Type: Program Variable
Unit: d
Reference to: Time

X_H: Description: Het. biomass
Type: Dyn. Volume State Var.
Unit: gCOD/m3
Relative Accuracy: 1e-006
Absolute Accuracy: 1e-006

X_I: Description: Part. Inert COD
Type: Dyn. Volume State Var.
Unit: gCOD/m3
Relative Accuracy: 1e-006
Absolute Accuracy: 1e-006

X_P: Description: Conc.
Type: Dyn. Volume State Var.
Unit: gCOD/m3
Relative Accuracy: 1e-006
Absolute Accuracy: 1e-006

X_S: Description: Slow. Biodegr. COD
Type: Dyn. Volume State Var.
Unit: gCOD/m3
Relative Accuracy: 1e-006
Absolute Accuracy: 1e-006

X_STO: Description: X_storage
Type: Dyn. Volume State Var.
Unit: gCOD/m3
Relative Accuracy: 1e-006
Absolute Accuracy: 1e-006

Y_H: Description: Stoic. par.
Type: Constant Variable
Unit:
Value: 0.68
Standard Deviation: 1
Minimum: 0
Maximum: 10
Sensitivity Analysis: inactive
Parameter Estimation: active

Y_STO: Description: Stoic. par.
Type: Constant Variable
Unit:
Value: 0.83
Standard Deviation: 1
Minimum: 0
Maximum: 10
Sensitivity Analysis: inactive
Parameter Estimation: inactive

****

Processes

****

Aeration: Description: Aeration
Type: Dynamic Process
Rate: Aer_coef*(S_O2SAT-S_O2)
Stoichiometry:
Variable : Stoichiometric Coefficient
S_O2 : 1

EndogenResp: Description: Aerobic endogenous respiration
Type: Dynamic Process
Rate: b_H*(S_O2/(K_O2+S_O2))*X_H
Stoichiometry:
Variable : Stoichiometric Coefficient
X_H : -1
S_O2 : -(1-f_e_x-f_e_s)
X_P : f_e_x
S_P : f_e_s

Growth: Description: Aerobic growth
Type: Dynamic Process
Rate: mue_H*(S_O2/(K_O2+S_O2))
*((X_STO/X_H)/(K_STO+(X_STO/X_H)))*X_H
Stoichiometry:
Variable : Stoichiometric Coefficient
X_H : 1
X_STO : -(1/Y_H)
S_O2 : -(1-Y_H)/Y_H

Hydrolysis: Description: Hyd.
Type: Dynamic Process
Rate: if X_S>0 then k_H*((X_S/X_H)/(K_X+(X_S/X_H)))*X_H
else 0 endif
Stoichiometry:
Variable : Stoichiometric Coefficient
X_S : -1
S_S : 1

Resp_XSTO: Description: Aerobic resp.of X_STO
Type: Dynamic Process
Rate: b_STO*(S_O2/(K_O2+S_O2))*X_STO
Stoichiometry:
Variable : Stoichiometric Coefficient
S_O2 : -1
X_STO : -1

Storage: Description: Aerobic storage
Type: Dynamic Process
Rate: k_STO*(S_O2/(K_O2+S_O2))*(S_S/(K_S+S_S))*X_H
Stoichiometry:
Variable : Stoichiometric Coefficient
S_S : -1
S_O2 : -(1-Y_STO)
X_STO : Y_STO

****

Compartments

****

Reactor: Description: Batch reactor
Type: Mixed Reactor Compartment
Compartment Index: 0
Active Variables: S_S, S_O2, S_I, X_I, X_S, X_H, X_STO, X_P, S_P, OUR, OURenddec, OURendPHA, OURgrowth, OURstorage
Active Processes: Resp_XSTO, EndogenResp, Storage, Growth, Aeration, Hydrolysis
Initial Conditions:
Variable(Zone) : Initial Condition
S_O2(Bulk Volume) : 0
S_I(Bulk Volume) : 9
S_S(Bulk Volume) : 62
X_I(Bulk Volume) : 33
X_S(Bulk Volume) : 8
X_H(Bulk Volume) : 1900
X_STO(Bulk Volume) : 0
X_P(Bulk Volume) : 0
S_P(Bulk Volume) : 0
Inflow: 0
Loadings:

Volume: 2.1
Accuracies:
Rel. Acc. Q: 0.001
Abs. Acc. Q: 0.001
Rel. Acc. V: 0.001
Abs. Acc. V: 0.001
Abs. Acc. V: 0.001

****

Definitions of Calculations

****

calc1: Description:
Calculation Number: 0
Initial Time: 0
Initial State: given, made consistent
Step Size: 0.001
Num. Steps: 190
Status: active for simulation
inactive for sensitivity analysis

****

Plot Definitions

****

Conc: Description:
Abscissa: Time
Title: Conc
Abscissa Label: time(d)
Ordinate Label: Conc(mgCOD/l)
Curves:
Type : Variable [CalcNum,Comp.,Zone,Time/Space]
Value : X_S [0,Reactor,Bulk Volume,0]
Value : S_S [0,Reactor,Bulk Volume,0]
Value : S_I [0,Reactor,Bulk Volume,0]
Value : X_I [0,Reactor,Bulk Volume,0]
Value : X_H [0,Reactor,Bulk Volume,0]
Value : X_STO [0,Reactor,Bulk Volume,0]
Value : S_P [0,Reactor,Bulk Volume,0]
Value : X_P [0,Reactor,Bulk Volume,0]
Value : S_O2 [0,Reactor,Bulk Volume,0]

OUR: Description: Oxygen Uptake Rate
Abscissa: Time
Title: OUR (mg/l/h)
Abscissa Label: T (d)
Ordinate Label: OUR (mg/l/h)
Curves:
Type : Variable [CalcNum,Comp.,Zone,Time/Space]
Value : OUR [0,Reactor,Bulk Volume,0]
Value : OURdata [0,Reactor,Bulk Volume,0]

OUR2: Description: Oxygen Uptake Rate
Abscissa: Time
Title: OUR (mg/l/h)
Abscissa Label: T (d)
Ordinate Label: OUR (mg/l/h)
Curves:
Type : Variable [CalcNum,Comp.,Zone,Time/Space]
Value : OUR [0,Reactor,Bulk Volume,0]
Value : OURenddec [0,Reactor,Bulk Volume,0]
Value : OURdata [0,Reactor,Bulk Volume,0]
Value : OURendPHA [0,Reactor,Bulk Volume,0]
Value : OURgrowth [0,Reactor,Bulk Volume,0]
Value : OURstorage [0,Reactor,Bulk Volume,0]

S_I: Description:
Abscissa: Time
Title: S_I
Abscissa Label: Time(d)
Ordinate Label: S_I(mgCOD/l)
Curves:
Type : Variable [CalcNum,Comp.,Zone,Time/Space]
Value : S_I [0,Reactor,Bulk Volume,0]
Value : S_I [0,Reactor,Bulk Volume,0]

S_O2: Description:
Abscissa: Time
Title: S_O2
Abscissa Label: Time(d)
Ordinate Label: S_O2(mg/l)
Curves:
Type : Variable [CalcNum,Comp.,Zone,Time/Space]
Value : S_O2 [0,Reactor,Bulk Volume,0]

S_P: Description:
Abscissa: Time
Title: S_P
Abscissa Label: Time(d)
Ordinate Label: S_P(mgCOD/l)
Curves:
Type : Variable [CalcNum,Comp.,Zone,Time/Space]
Value : S_P [0,Reactor,Bulk Volume,0]

S_S: Description: S_S degr
Abscissa: Time
Title: S_S
Abscissa Label: Time(d)
Ordinate Label: S_S(mgCOD/l)
Curves:
Type : Variable [CalcNum,Comp.,Zone,Time/Space]
Value : S_S [0,Reactor,Bulk Volume,0]

X_H: Description:
Abscissa: Time
Title:
Abscissa Label: Time(d)
Ordinate Label: X_H[gCOD/l]
Curves:
Type : Variable [CalcNum,Comp.,Zone,Time/Space]
Value : X_H [0,Reactor,Bulk Volume,0]
Value : X_H [0,Reactor,Bulk Volume,0]

X_I: Description:
Abscissa: Time
Title: X_I
Abscissa Label: Time(d)
Ordinate Label: X_I
Curves:
Type : Variable [CalcNum,Comp.,Zone,Time/Space]
Value : X_I [0,Reactor,Bulk Volume,0]

X_P: Description:
Abscissa: Time
Title: X_P
Abscissa Label: Time(d)
Ordinate Label: X_P(mgCOD/l)
Curves:
Type : Variable [CalcNum,Comp.,Zone,Time/Space]
Value : X_P [0,Reactor,Bulk Volume,0]

X_S: Description:
Abscissa: Time
Title: X_S
Abscissa Label: Time(d)
Ordinate Label: X_S(mgCOD/l)
Curves:
Type : Variable [CalcNum,Comp.,Zone,Time/Space]
Value : X_S [0,Reactor,Bulk Volume,0]

X_STO: Description:
Abscissa: Time
Title: X_STO
Abscissa Label: Time(d)
Ordinate Label: X_STO(mgCOD/l)
Curves:
Type : Variable [CalcNum,Comp.,Zone,Time/Space]
Value : X_STO [0,Reactor,Bulk Volume,0]

****

Calculation Parameters

****

Numerical Parameters: Maximum Int. Step Size: 1
Maximum Integrat. Order: 5
Number of Codiagonals: 1000
Maximum Number of Steps: 1000

Fit Method: secant
Max. Number of Iterat.: 100

****

Calculated States

****

Calc. Num.	Num. States	Comments
0	191	Range of Times: 0 - 0.19

****

BIBLIOGRAPHY

Gülseda DİZDAROĞLU-RİŞVANOĞLU, was born in 1958 in Ankara. She completed high school in Mardin and graduated from Middle East Technical University as chemical engineer in 1982. She got her MSc. Degree with the thesis "Modification and Expansion of Computer Aided Design Package for Process Flow Sheet Development" at Bosphorous University, Chemical Engineering Department in 1986. She worked as production engineer at Pfizer Medicals-İstanbul in 1987. From 1993 to 1995, she worked as inspector and engineer at Ministry of Environment İstanbul Directorate. She is especially qualified in Turkish Environment Law, No:2872, Environmental Impact Assessment Regulations, Water Pollution Control Regulations, including Domestic, Industrial, Sanitary, Chemical, Toxic, Hazardous, Radioactive Waste Disposal Control Regulations and Noise Pollution Control Regulations. She started her PhD. study in 1994 at Istanbul Technical University. In 1998 she moved to The Netherlands and conducted a part of her study in Delft University of Technology.